Wide Area Power System Monitoring Device Design and Data Analysis

By

Kevin J.H. Khan

Thesis submitted to the faculty of the Virginia Polytechnic Institute and State University
in partial fulfillment of the requirements for the degree of

Master of Science
In
Electrical Engineering

Approved by:

Dr. Yilu Liu (Chair)
Dr. Virgilio Centeno (Co-Chair)
Dr. Richard Conners

13 July 2006
Blacksburg, Virginia

Keywords: Frequency Disturbance Recorder, FNET, Voltage Angle, Angle Difference, k-means

Wide Area Power System Monitoring Device Design and Data Analysis

By

Kevin J.H. Khan

Abstract

The frequency disturbance recorder (FDR) is a cost effective data acquisition device used to measure power system frequency at the distribution level. FDRs are time synchronized via the global positioning system (GPS) timing and data recorded by FDRs are time stamped to allow for comparative analysis between FDRs. The data is transmitted over the internet to a central server where the data is collected and stored for post mortem analysis. Currently, most of the analysis is done with power system frequency.

The purpose of this study is to take a first in depth look at the angle data collected by FDRs. Different data conditioning techniques are proposed and tested before one is chosen. The chosen technique is then used to extract useable angle data for angle analysis on eight generation trip events. The angle differences are then used to create surface plot angle difference movies for further analysis.

A new event detection algorithm, the k-means algorithm, is also presented in this paper. The algorithm is proposed as a simple and fast alternative to the current detection method. Next, this thesis examines several GPS modules and recommends one for a replacement of the current GPS chip, which is no longer in production. Finally, the manufacturing process for creating an FDR is documented.

This thesis may have raised more questions than it answers and it is hoped that this work will lay the foundation for further analysis of angles from FDR data.

Acknowledgements

I would like to express my deepest appreciation to my advisors, Dr. Yilu Liu and Dr. Virgilio Centeno for their patient guidance and encouragement throughout this study. I would also like to thank Dr. Richard Conners for serving on my committee. Also, I would like to thank every member of the FNET team for all their help, advice, and suggestions regarding my study.

I want to thank my friends and family for their encouragement, advice, and laughs over the years.

I'd like to thank my brothers, Justin and Jeffrey, for their support and for making life so fun. Finally, I would like to thank my parents, Akram and Faith Khan, for their unconditional love and support and for giving me the opportunity to get the best education possible.

Acronyms and Symbols

A/D: Analog to Digital

CPU: Central Processing Unit

DFT: Discrete Fourier Transform

ECAR: East Central Area Reliability Coordination Agreement

EI: Eastern (United States) Interconnected System

FDR: Frequency Disturbance Recorder

FNET: Frequency Monitoring Network

FRCC: Florida Reliability Coordinating Council

GPS: Global Positioning System

LCD: Liquid Crystal Display

MAIN: Mid-America Interconnected Network

MIOS: Modular Input Output Subsystem

NPCC: Northeast Power Coordinating Council

PMU: Phasor Measurement Unit

PPS: Pulse Per Second

PSS/E: Power System Simulator for Engineering

PWM: Pulse Width Modulation

SERC: Southeastern Electric Reliability Council

SV: Satellite Visible

TVA: Tennessee Valley Authority

UTC: Coordinated Universal Time

WECC: Western (United States) Electricity Coordinating Council

Table of Contents

List of Figures

List of Tables

Chapter 1: Introduction

1.1 FNET

With the development of the Global Positioning System (GPS), numerous projects have been created to measure power system parameters on a wide scale using the GPS to time synchronize measurement units [1-5]. Power system frequency is one of the most important parameters of the power system [6]. Virginia Tech has created the Frequency Monitoring Network (FNET) to measure the system frequency at the distribution level using a low cost frequency disturbance recorder (FDR) [6-8]. With the potential of being located all over the United States, these FDRs are time synchronized via GPS and provide ten frequency measurements per second. The data is collected at the central server on the Virginia Tech campus. In addition to power system frequency, FNET also collects voltage angle data. The voltage angles, angle differences between locations, and how they vary over time can provide very valuable information about the power system [3-4]. Furthermore, the stability of the system can be estimated by looking at the power angles of generators [5].

1.2 Problem Statement and Proposed Work

From the creation of FNET to now, not much work has been done with the angle information received from FDRs. Most of the work done with FDR data is centered on the power system frequency. The purpose of this thesis, then, is to develop an acceptable method to condition FNET data for in-depth angle analysis. In addition, the conditioned FNET angle data for eight generation trip events will be presented and analyzed.

Part of this thesis will also focus on power system event detection. The method currently used to detect events in FDR data requires the frequency data to be smoothed, which is a time consuming process. This thesis will propose a new event detection technique that doesn't require smoothed frequency data.

Finally, this paper will address some FDR hardware issues. The GPS unit used in the current generation FDR has been discontinued and will not be available by the time the next generation is completed. Several GPS units are examined in this thesis as possible replacements. A look at the FDR manufacturing process will follow and an FDR assembly guide will be presented.

1.3 Thesis Organization

Chapter 2 presents an overview of FDR frequency and voltage angle data and investigates the presence of several nuances in the data. A comparison is made between data collected with FDRs that have different firmware versions. Chapter 3 presents three different data processing techniques in an attempt to condition FDR data and produce angle plots sufficient for analysis. In Chapter 4, angle analysis is done on several generation trip events recorded by FNET. The k-means event detection algorithm is presented in Chapter 5. Chapter 6 focuses on FDR construction and GPS replacement. Conclusions and future work suggestions are presented in Chapter 7.

Chapter 2: FDR Data

The current generation FDR sends a wealth of information back to the central server. Every tenth of a second, the server receives time stamped frequency, voltage angle, and voltage magnitude from each operating FDR. This data is stored in a Microsoft Access file as shown in Figure 2.1.

FRURawData4 : Table

Index	UnitID	Sample_Date&Time	ConvNum	FirstFreq	FinalFreq	VoltageAng	VoltageMag	DateCreated
1	4	2/3/2006 4:59:51 AM	1	60.0425	60.0445	2.9561	120.0882	2/3/2006 12:00:02 AM
2	4	2/3/2006 4:59:51 AM	2	60.0463	60.0483	2.9829	120.0923	2/3/2006 12:00:02 AM
3	4	2/3/2006 4:59:51 AM	3	60.0452	60.0472	3.0096	120.0231	2/3/2006 12:00:02 AM
4	4	2/3/2006 4:59:51 AM	4	60.0384	60.0405	3.0357	120.0659	2/3/2006 12:00:02 AM
5	4	2/3/2006 4:59:51 AM	5	60.0436	60.0456	3.0612	120.0422	2/3/2006 12:00:02 AM
6	4	2/3/2006 4:59:51 AM	6	60.0436	60.0456	3.0867	119.9621	2/3/2006 12:00:02 AM
7	4	2/3/2006 4:59:51 AM	7	60.0393	60.0413	3.1109	119.9994	2/3/2006 12:00:02 AM
8	4	2/3/2006 4:59:51 AM	8	60.0407	60.0427	3.1371	119.966	2/3/2006 12:00:02 AM
9	4	2/3/2006 4:59:51 AM	9	60.0382	60.0403	3.1622	120.0274	2/3/2006 12:00:02 AM
10	4	2/3/2006 4:59:51 AM	10	60.0388	60.0409	3.1875	120.044	2/3/2006 12:00:03 AM
11	4	2/3/2006 4:59:52 AM	1	60.0419	60.044	3.2134	120.0344	2/3/2006 12:00:03 AM
12	4	2/3/2006 4:59:52 AM	2	60.0409	60.0429	3.2394	120.1155	2/3/2006 12:00:03 AM

Figure 2.1 Sample FDR data

Most of the system analysis is done with the frequency information; however, we would like to explore the analysis possibilities with the voltage angle information.

2.1 Frequency

We can tell a lot about a power system's behavior by looking at the frequency data gathered by the FDRs. However, the raw frequency data includes a fair amount of noise. Various methods have been developed to de-noise the frequency data, including the moving mean and moving median techniques [9-10]. The Virginia Tech (VT) unit, in particular, has a relatively high amount of noise in the frequency data. Figure 2.2 compares the VT frequency data with the VT Substation frequency data.

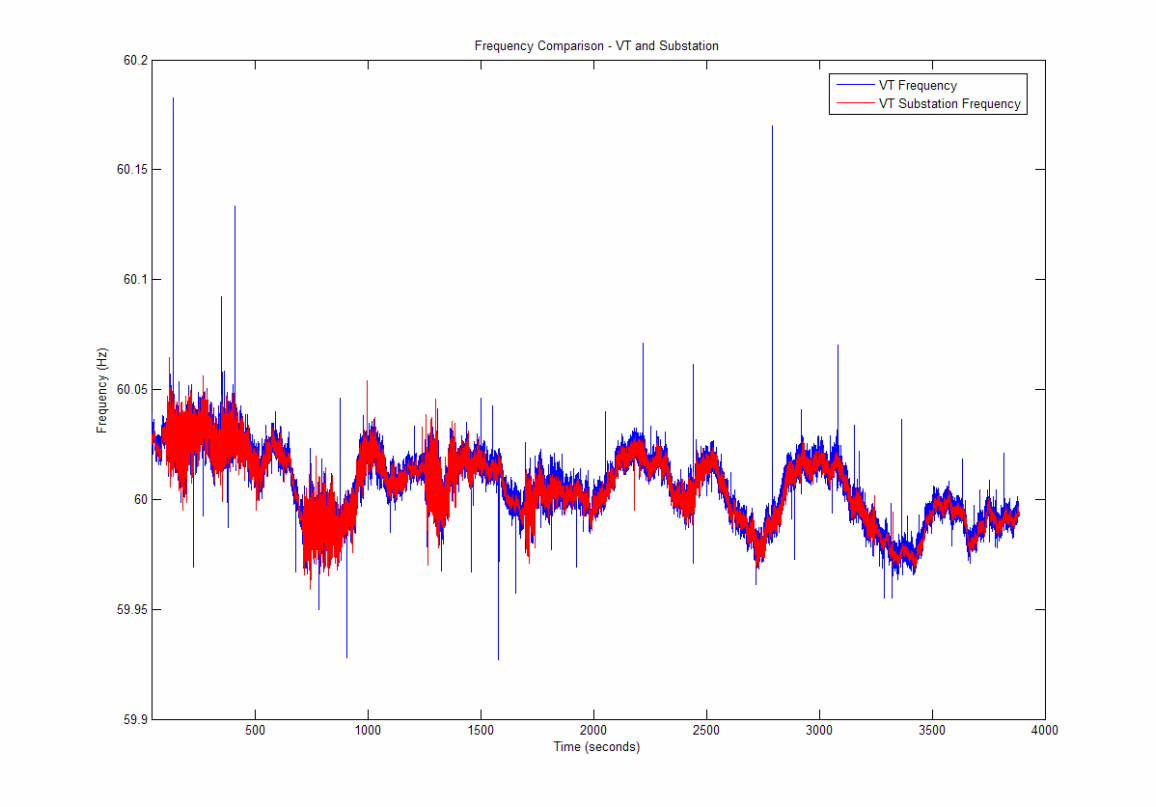

Figure 2.2 VT and VT Substation frequency comparison

It is clear that the VT unit contains more noise than the VT Substation unit, despite the two units being physically and electrically close together. The presence of noise on the VT unit is expected because the VT unit is located in a building where it is subjected to a constantly changing load. On the other hand, the VT substation unit is not. For further analysis and a clearer picture, the noise is extracted using a 21 point moving mean and then the noise data is plotted in a histogram. Once again, we can see that the VT unit has a relatively large amount of noise in its frequency data.

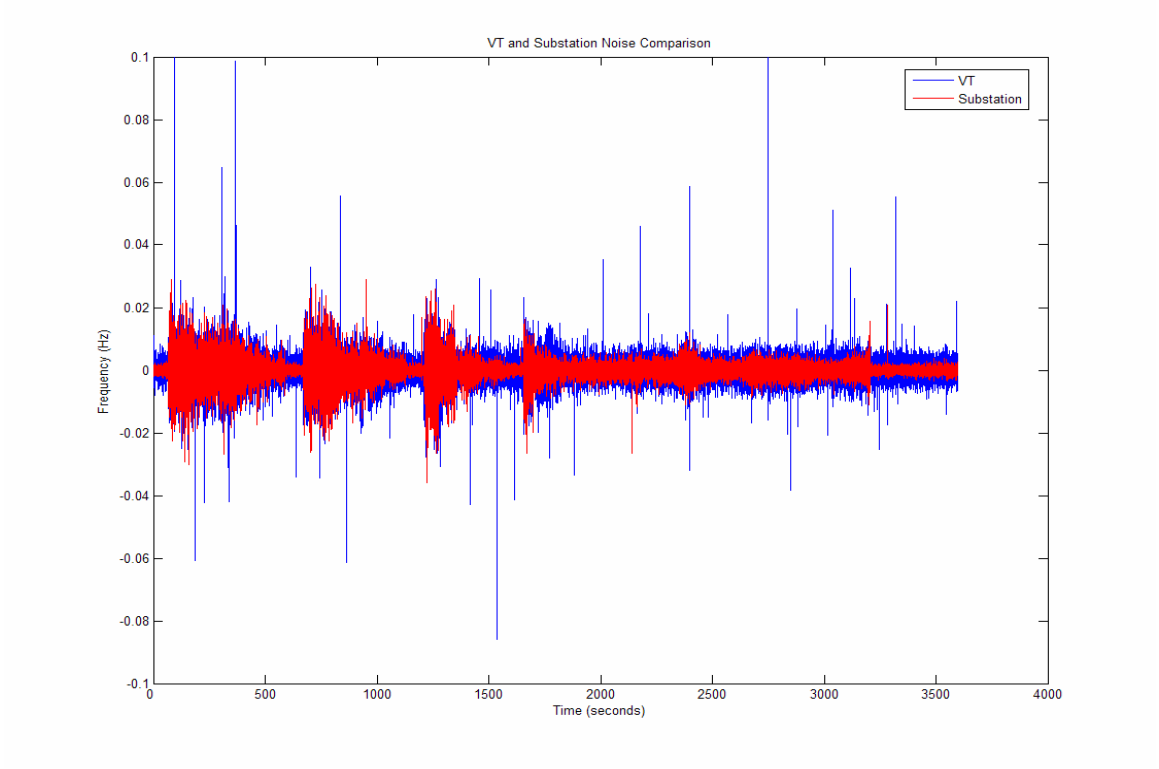

Figure 2.3 Extracted frequency noise

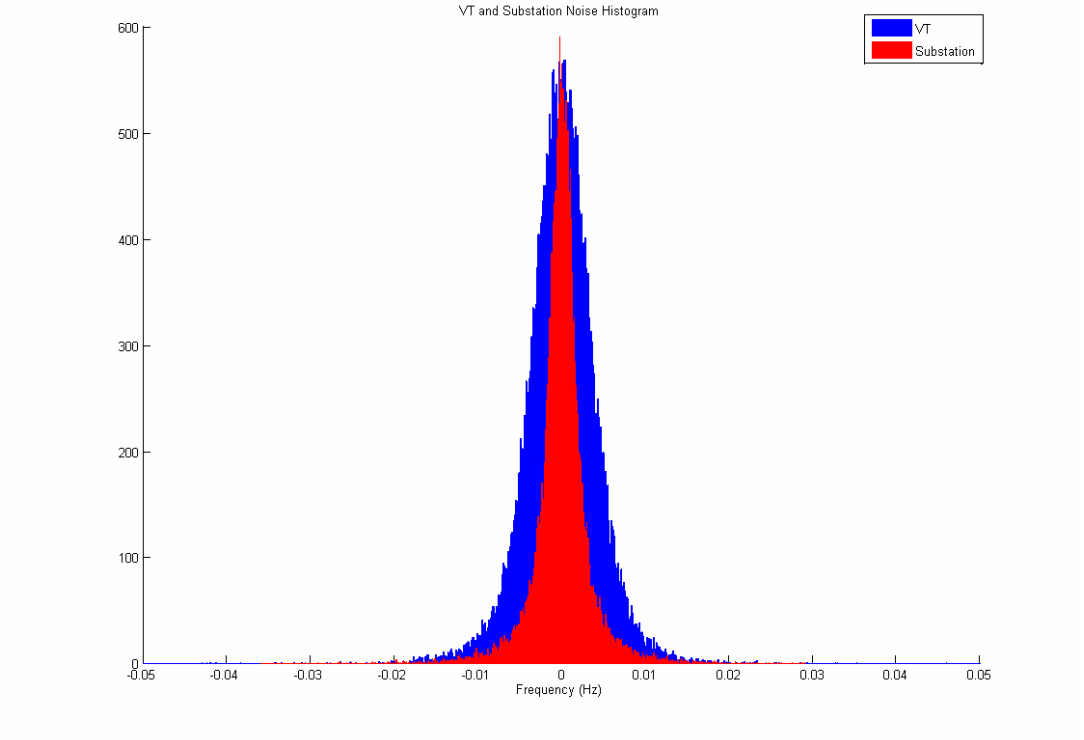

Figure 2.4 Frequency noise histogram

2.2 Voltage Angle

While numerous studies have been conducted using FDR frequency data, not much has been done using FDR angle data. As previously stated, the bulk of this thesis will explore the possibility of using angle data for power system analysis.

Figure 2.5 shows a sample of the raw FDR angle data. The FNET server receives an angle value, measured in radians, every tenth of a second. As shown in the graph, the angle data experiences wrap-around whenever the angle exceeds zero or 2π radians.

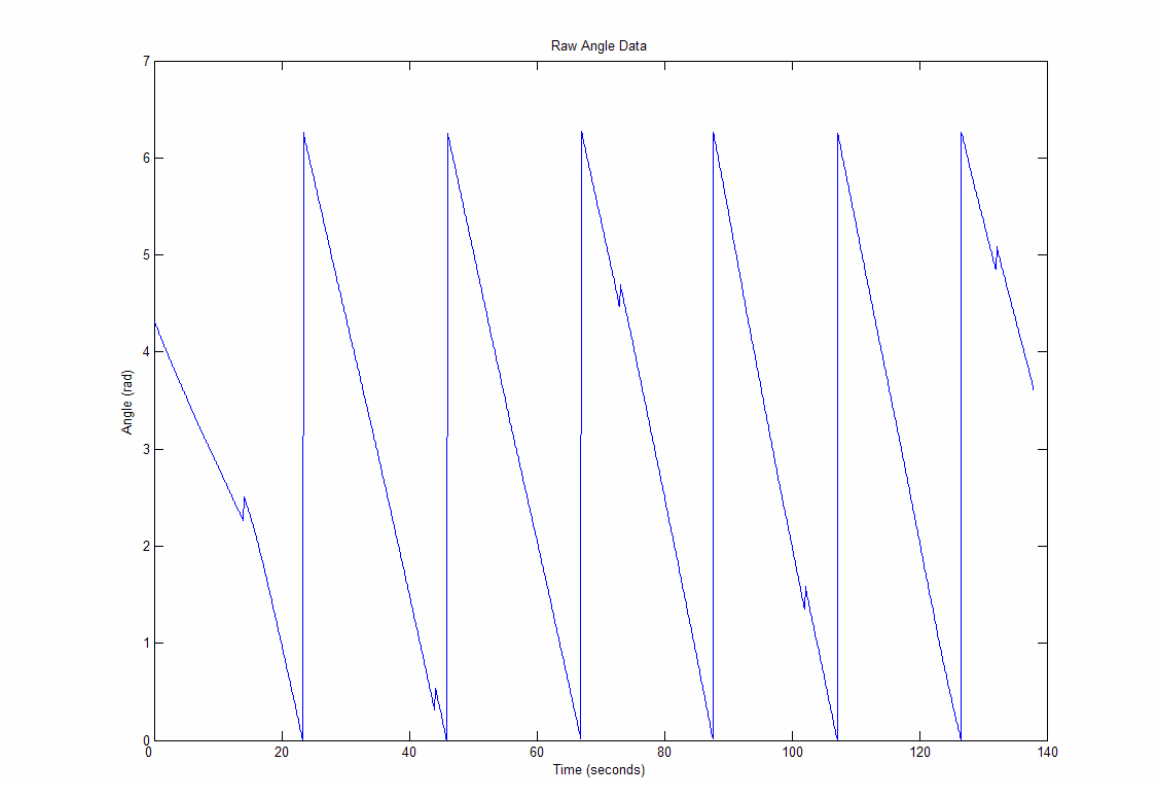

Figure 2.5 Raw FDR angle data

Taking a closer look at the raw angle data, we can see small discontinuities occurring periodically. The cause of these discontinuities will be discussed in further detail in the next section.

2.3 FDR Firmware Comparison

Recently, the FDR firmware has been updated to address the angle discontinuity problem. The angle discontinuities in the old firmware were attributed to the sampling frequency and algorithm [11, 13]. Since the actual power system frequency fluctuates around nominal frequency, there is occasionally one missing sample point in the frequency calculation using the old firmware code. This missing sample point creates a jump in the angle data, and a sharp spike in the frequency data. Furthermore, the time interval between discontinuities varies with each FDR. It is postulated that slight differences in the sampling oscillator frequency between FDRs (due to error or temperature differences) cause these interval differences. While the spike is eliminated in the frequency data, the angle data remains untouched in the old firmware. The new firmware addresses this issue and provides a smoother angle curve, as shown in Figure 2.6.

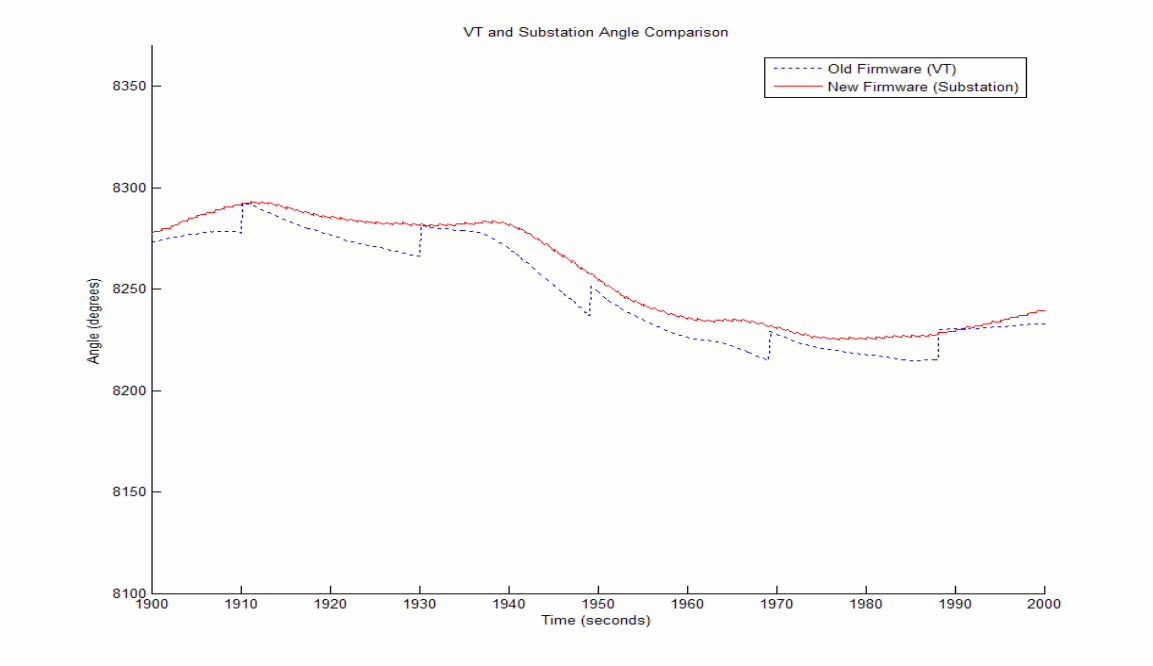

Figure 2.6 Old firmware and new firmware comparison

The smoother curve is achieved by strictly forcing the pulse width modulation (PWM) train to restart every second. It should be noted that despite having different firmware

versions, the VT and VT Substation angle data do not diverge. The figure below shows the VT and VT Substation angles, normalized at the start. There is a small difference between the two, but the difference remains fairly small and the two plots don't diverge over a long time interval. In the future, a comparison between the VT, VT Substation, and Roanoke units should be pursued.

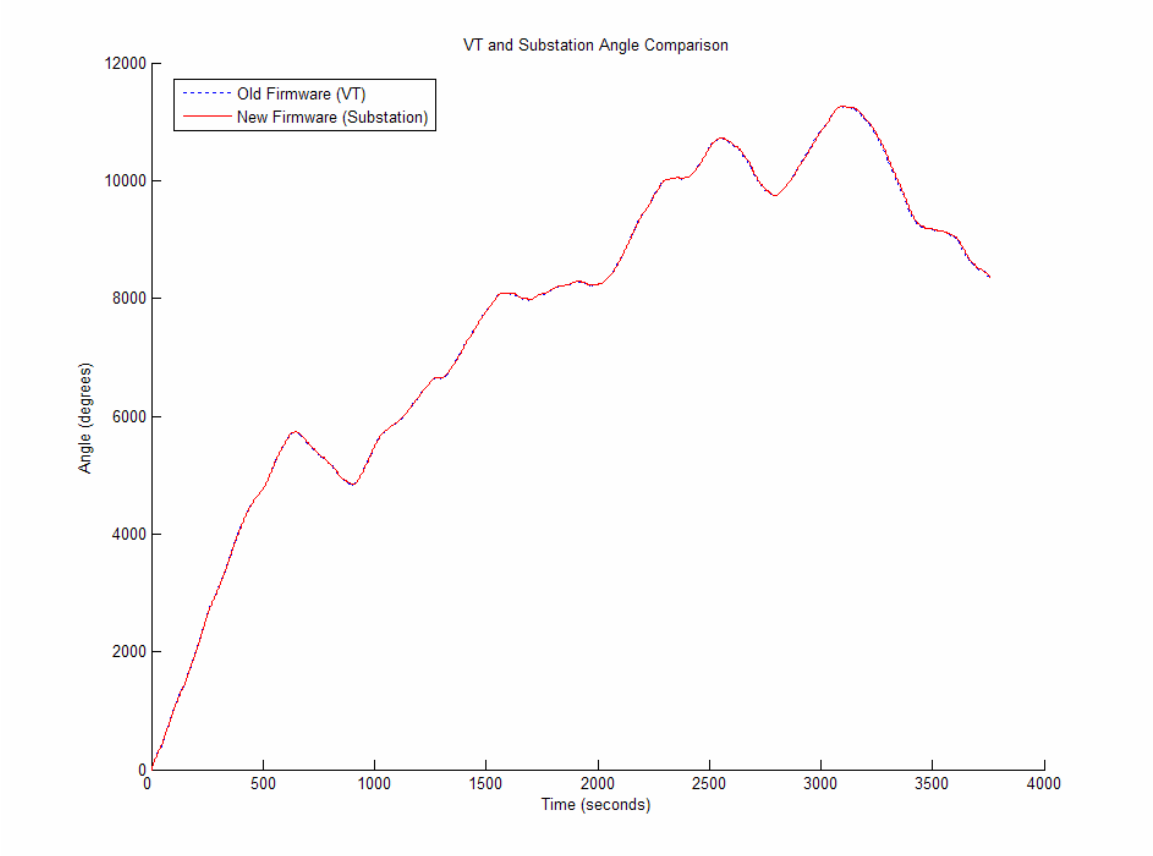

Figure 2.7 Old firmware and new firmware comparison over a long time interval

While the new firmware offers a smoother angle curve, which is more desirable for analysis, not all currently deployed FDRs have the update. Furthermore, most of the older angle data in our database contain the small discontinuities.

Chapter 3: Data Processing

Before any analysis can be done on FNET angle data, some data processing must be done. Three different data processing techniques were investigated in hopes of finding an effective and acceptable method of preparing the data for analysis.

3.1 Unwrapping

As we have previously seen, raw FDR angle data is wrapped. The first data processing technique we will investigate is to simply unwrap the angle data by adding or subtracting 2π radians wherever wraparound occurs. An example of the resulting waveform is shown in Figure 3.1.

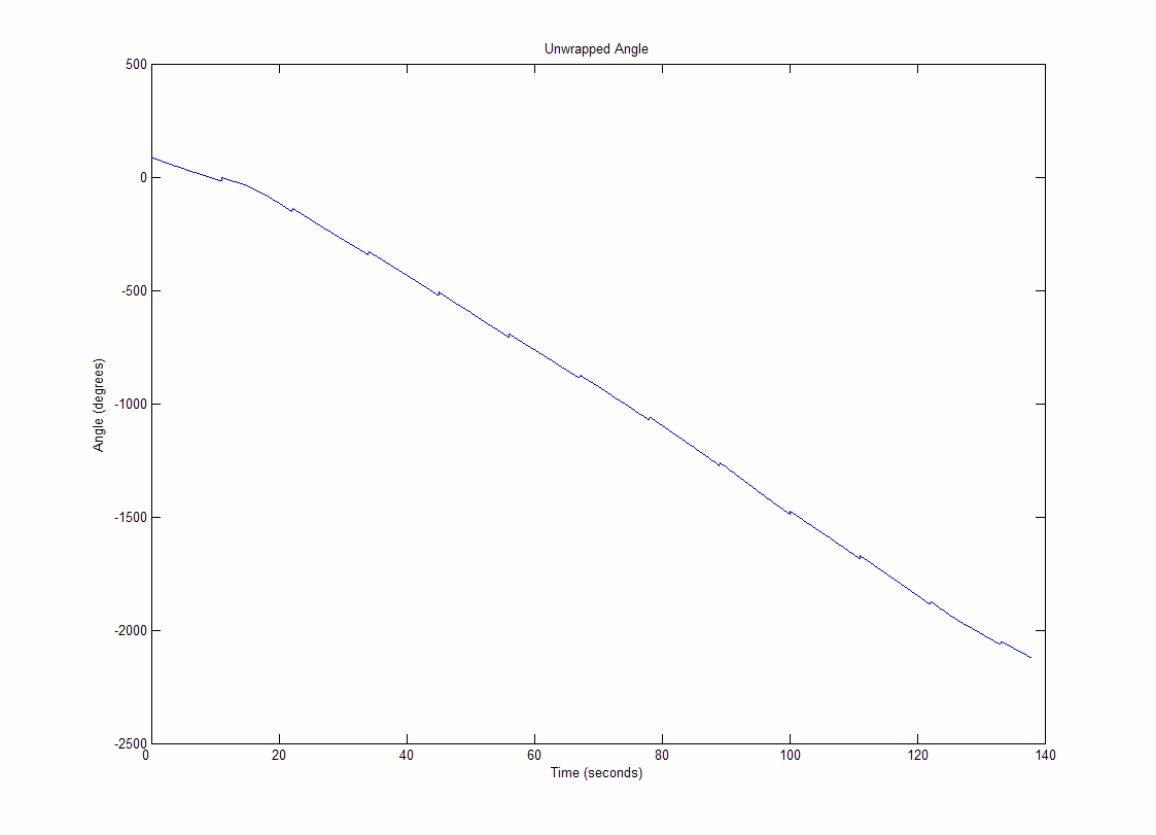

Figure 3.1 Unwrapped angle

After unwrapping, the angle data plots are easier to read. However, the small discontinuities are still present. While these discontinuities look relatively small, the angle jumps can actually be as high as 15 degrees. Figure 3.2 shows the difference between the unwrapped angles of two units. We can see that these jumps make any kind of angle difference analysis very difficult.

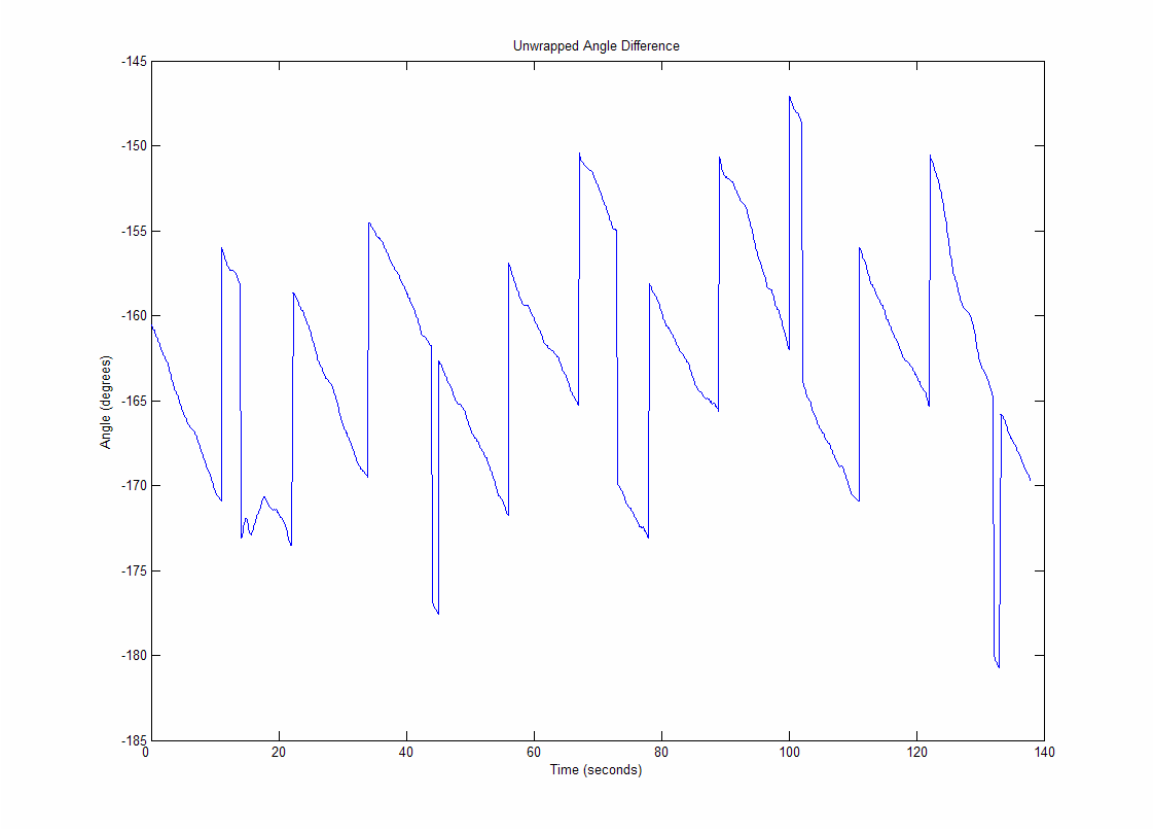

Figure 3.2 Typical angle difference plot using unwrapped angle data

Since most power system angle analysis involves looking at the difference between angles, it is obvious that simply unwrapping the FDR angle data is insufficient.

3.2 Small Shifts

To counter the effects of the angle discontinuities, we consider simply shifting each continuous piece of angle data to fit in with the previous piece. The smoothing algorithm scans unwrapped angle data for any discontinuities and whenever a discontinuity is detected, the two data points immediately before the discontinuity are used to calculate a projected line to which the next segment is attached.

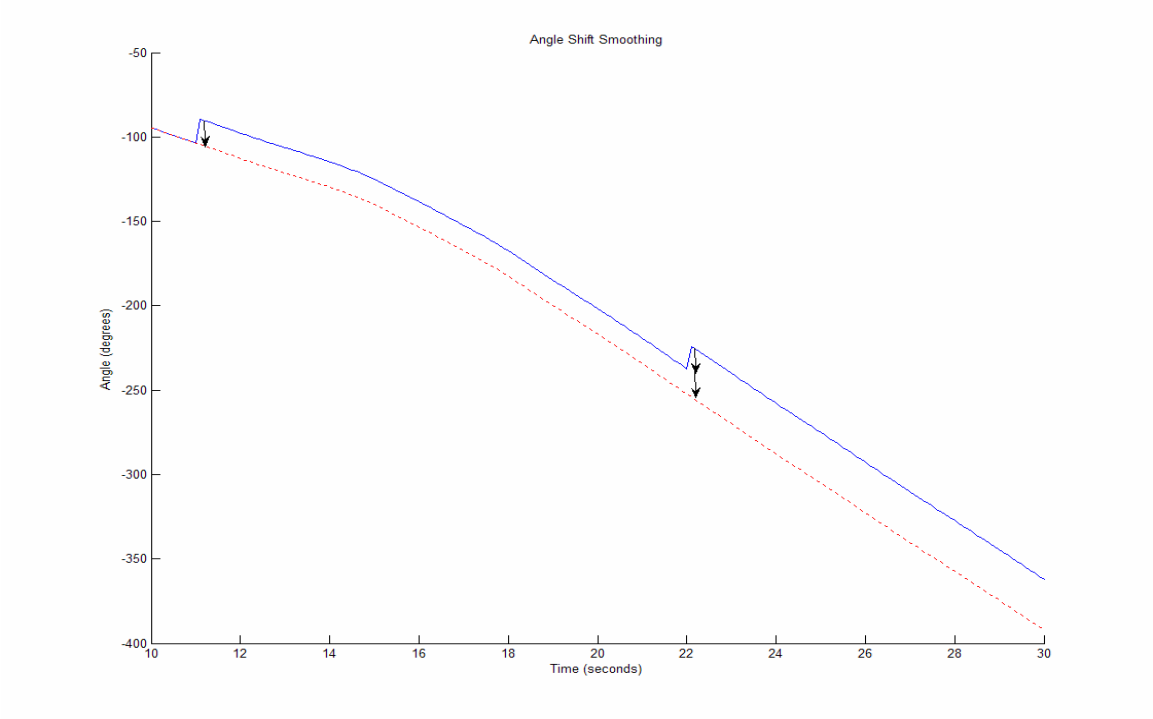

Figure 3.3 Angle shift smoothing technique

While this technique produces smooth angle plots as well as smooth angle difference plots, there is an issue we must first address: the frequency of occurrence of the angle discontinuities varies from FDR to FDR. For example, the Alexandria Research Institute (ARI) unit experiences discontinuities every 10-11 seconds while the University of Missouri-Rolla (UMR) unit experiences discontinuities every 26-30 seconds. As a result, the UMR unit angle gets shifted less often than the ARI unit over the same time interval. Figure 3.4 illustrates how this disparity causes the angle of the two units to diverge over time. Under normal circumstances, the voltage angles would not separate this much

during a generation trip event, indicating that the smoothing method is causing the divergence. Finally, Figure 3.5 shows that the raw unwrapped angle data doesn't diverge over the same interval.

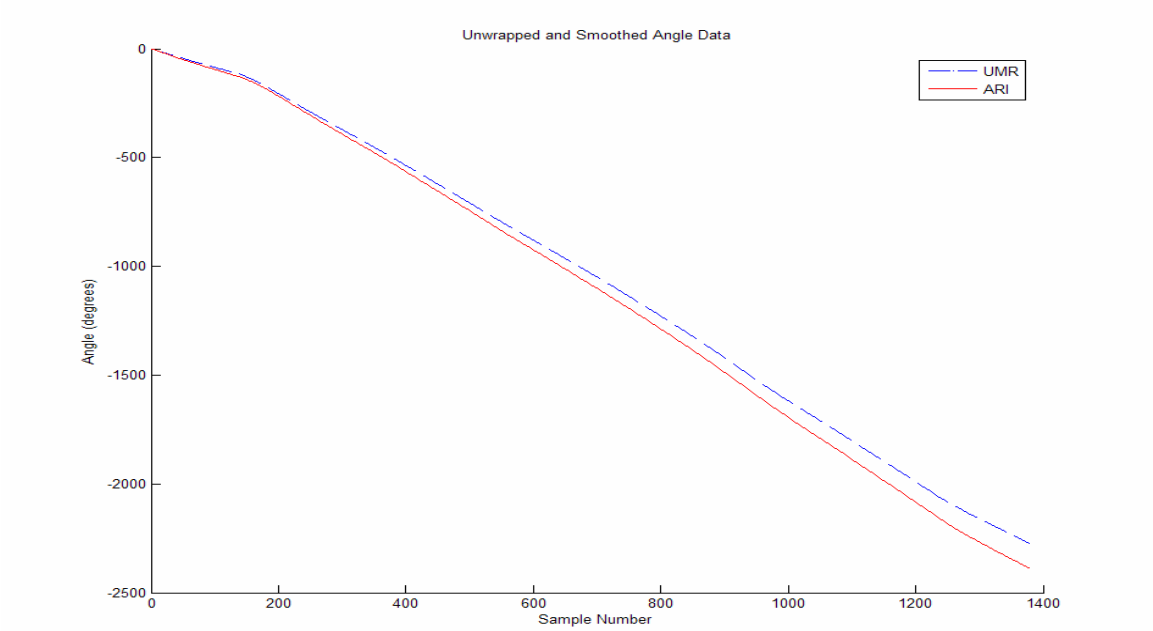

Figure 3.4 Divergence of smoothed angle data

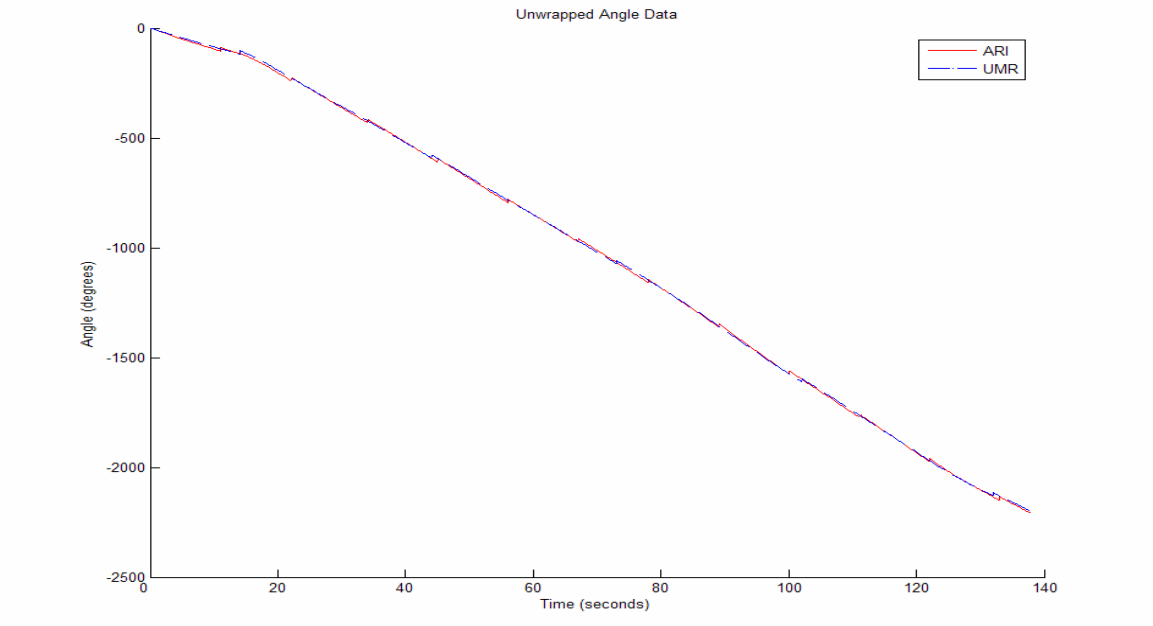

Figure 3.5 Unsmoothed angle data

3.3 Frequency Integration

Before we look at the final data processing technique, we must first investigate the theory behind the phasor angle analysis algorithm implemented in the FDR. Phasor angle analysis is a Discrete Fourier Transform (DFT) based algorithm and is the most widely used algorithm used in commercial Phasor Measurement Units (PMU) [11-13].

First, we consider a purely sinusoidal input signal

$$x(t) = \sqrt{2}X\sin(\omega t + \phi) \tag{3.1}$$

After sampling Equation (3.1) with a sampling frequency N times per cycle we can write

$$x_k = \sqrt{2}X\sin\left(\frac{2\pi}{N}k + \phi\right) \tag{3.2}$$

Then, taking the Discrete Fourier Transform of Equation (3.2) gives

$$\overline{X} = \frac{1}{\sqrt{2}}\left(X_c + jX_s\right) \tag{3.3}$$

where

$$X_c = \frac{2}{N}\sum_{0}^{N-1} X_k \cos\frac{2\pi}{N}k \tag{3.4}$$

and

$$X_s = -\frac{2}{N}\sum_{0}^{N-1} X_k \sin\frac{2\pi}{N}k \tag{3.5}$$

Next, using the recursive phasor computation technique we can obtain the rth phasor

$$\overline{X}^{(r)} = \overline{X}^{(r-1)} + j\frac{1}{\sqrt{2}}\frac{2}{N}\left(x_{N+r} - x_r\right)\exp\left(-j\frac{2\pi}{N}(r-1)\right) \tag{3.6}$$

Then from Equation (3.6), the phasor of a sinusoidal wave with frequency $f = f_0 + \Delta f$ can written as

$$\begin{aligned}\overset{\rho}{X}_{f_0+\Delta f}^{(r)} &= \overset{\rho}{X}_{f_0}^{(0)}\frac{\sin\left(\frac{N\Delta\omega\Delta t}{2}\right)}{N\sin\left(\frac{\Delta\omega\Delta t}{2}\right)}\exp\left(jr\Delta\omega\Delta t\right)\exp\left(j(N-1)\frac{\Delta\omega\Delta t}{2}\right) \\ &+ \overset{\rho}{X}_{f_0}^{*(0)}\frac{\sin\left(\frac{N\left(\omega+\omega_0\right)\Delta t}{2}\right)}{N\sin\left(\frac{\left(\omega+\omega_0\right)\Delta t}{2}\right)}\exp\left(-j\frac{(N-1)\left(\omega+\omega_0\right)\Delta t}{2}\right)\exp\left(-jr\left(\omega+\omega_0\right)\Delta t\right)\end{aligned} \tag{3.7}$$

where $\overset{\rho}{X}_{f_0}^{(0)}$ is the initial computation of the phasor at f_0 and Δt is the time interval between the sampled data.

If Δf is relatively small compared to f_0, the second term of Equation (3.7) will be approximately zero and the equation can be simplified as

$$\overset{\rho}{X}_{f_0+\Delta f}^{(r)} = \overset{\rho}{X}_{f_0}^{(0)}\frac{\sin\left(\frac{N\Delta\omega\Delta t}{2}\right)}{N\sin\left(\frac{\Delta\omega\Delta t}{2}\right)}\exp\left(jr\Delta\omega\Delta t\right)\exp\left((N-1)\frac{\Delta\omega\Delta t}{2}\right) \tag{3.8}$$

To examine the relationship between the phasor and the waveform frequency, we can break the computed phasor into its magnitude and angle parts. The product of the magnitude, phasor and a magnitude factor gives the magnitude of the new phasor

$$\left|\underset{f_0+\Delta f}{\rho_{X}^{(r)}}\right| = \left|\underset{f_0}{\rho_{X}^{(0)}}\right| \frac{\sin\left(\frac{N\Delta\omega\Delta t}{2}\right)}{N\sin\left(\frac{\Delta\omega\Delta t}{2}\right)} \tag{3.9}$$

Denoting the angle of the new phasor as ψ_r and the angle of the previous phasor as ψ_{r-1}, the new phasor angle can be approximated as

$$\psi_r = \frac{\Delta f}{f_0}\frac{2\pi}{N}r + \psi_{r-1} \tag{3.10}$$

Then, using the definition of derivatives, we get

$$\frac{d\psi}{dt} = \lim_{t\to 0}\frac{\psi_r - \psi_{r-1}}{t} \approx \frac{\psi_r - \psi_{r-1}}{1/Nf_0} = 2\pi\Delta f \tag{3.11}$$

Finally, we can compute the system frequency with

$$f = f_0 + \Delta f = f_0 + \frac{1}{2\pi}\frac{d\psi}{dt} \tag{3.12}$$

Using the relationship in Equation (3.12) we can use the frequency data to compute the voltage angle

$$f - f_0 = \frac{1}{2\pi}\frac{d\psi}{dt} \tag{3.13}$$

$$\int \frac{d\psi}{dt}dt = 2\pi\int (f - f_0)dt \tag{3.14}$$

$$\psi + C = 2\pi\int (f - f_0)dt \tag{3.15}$$

We cannot solve for the constant C in Equation (3.15) to obtain the absolute angle values. However, we can still gain useful information by integrating the FNET frequency data to calculate angles that are normalized at a single point in time. We are interested in the dynamics of the system, and the normalized angles will allow us to see the changes in the voltage angles over time.

Using the cumulative trapezoidal rule in MATLAB to integrate our frequency data, we get an angle plot similar to the one shown in Figure 3.6.

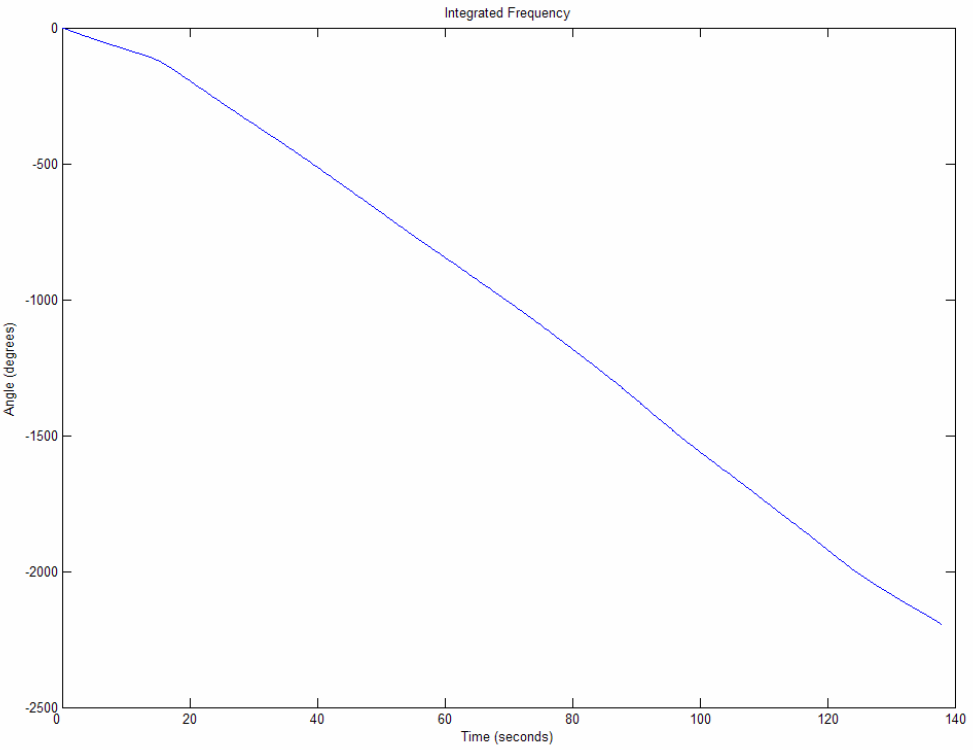

Figure 3.6 Integrated frequency

Current generation FDRs offer frequency readings with an accuracy within ±0.0005Hz [7, 13]. The angle accuracy, on the other hand, has not been determined. It makes sense, therefore, to use the information we are most confident in—frequency—to derive an angle estimation. It should be noted that due to the cumulative nature of integration, any error in the frequency will be additive when we calculate the angle, possibly pushing the

estimation further from the true value. Therefore we must be careful with the time durations of the windows of data we look at.

Another factor we must consider is the noise on the frequency data and how it affects the integration. By integrating the noise we extracted in Section 2.1 (Figure 2.3) we can tell whether or not the noise affects our angle calculation. If the resulting plot stays at an approximately constant value near zero, we can be confident that the noise has no effect on our angle derivation. Figure 3.7 shows that this is indeed the case for our FDR data.

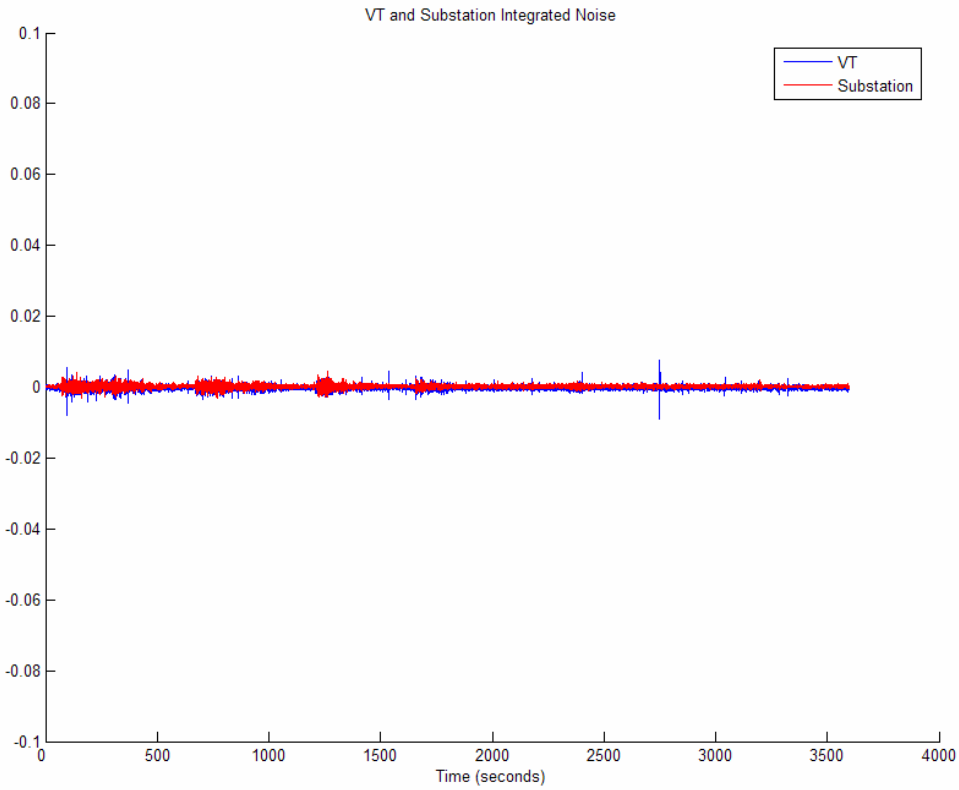

Figure 3.7 Integrated frequency noise

That being said, frequency integration is currently the best technique for obtaining a smooth angle curve suitable for angle difference analysis. Figure 3.8 compares the three data conditioning methods described in this chapter.

We can clearly see that the frequency integration curve is much closer to the raw unwrapped FDR angle data than the smoothed curve, further increasing our confidence in this method. Finally, Figures 3.9 and 3.10 compare raw unwrapped angles and calculated angles for an event. The calculated angles are very close to the raw data at the beginning.

While we would like to one day use raw FDR angle data in any angle analysis, the presence of discontinuities in the angle data of old firmware FDRs prevents us from using raw data. All angle analysis from this point on will be done with angle data derived from integrating the frequency.

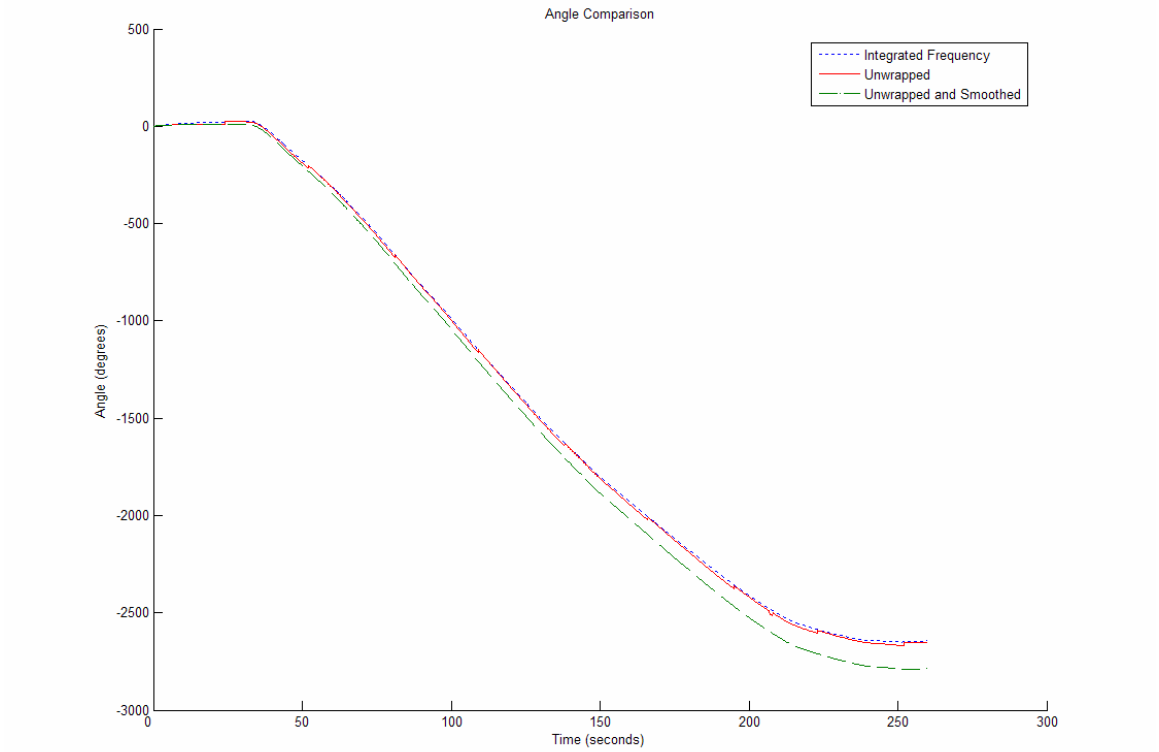

Figure 3.8 Data conditioning comparison

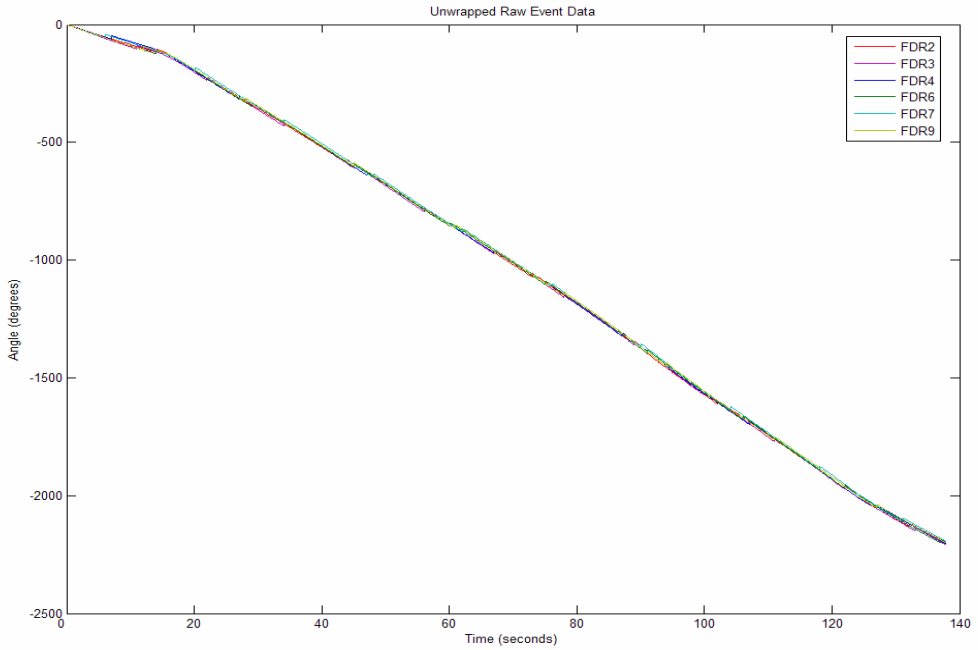

Figure 3.9 Unwrapped event data

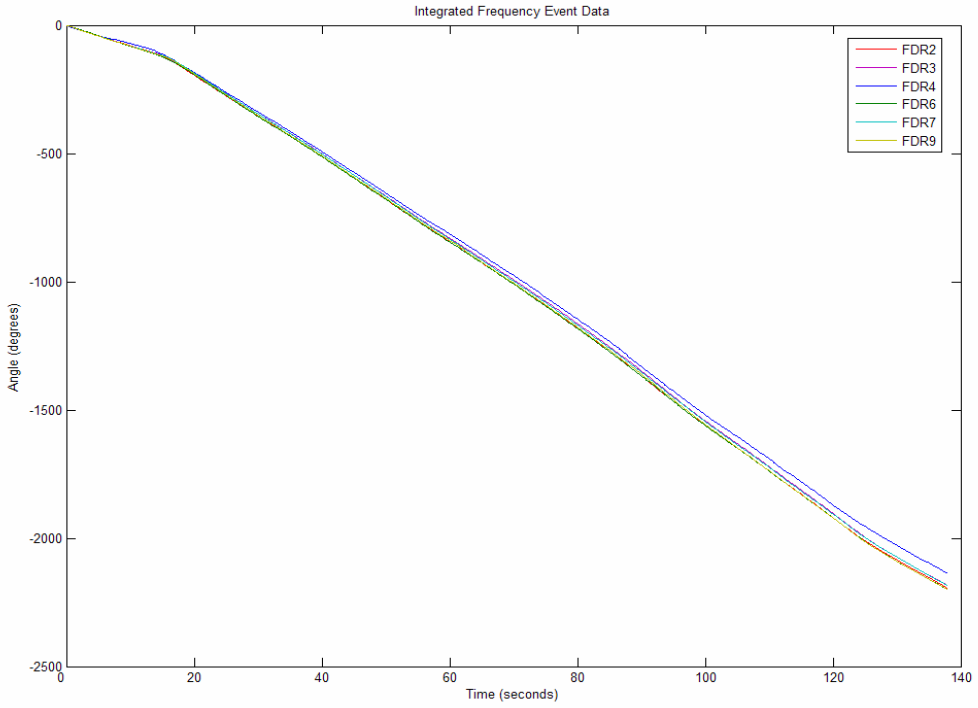

Figure 3.10 Integrated frequency event data

3.4 Frequency Integration Verification through PSS/E Simulation

To gauge the accuracy of our angle computation method, let us compare it with angles computed through PSS/E simulation*. The following figure shows the frequency readings from various points in the power system during a generation trip event. This is a 20 second simulation with a time step of 0.001s with the generation trip occurring at 1s.

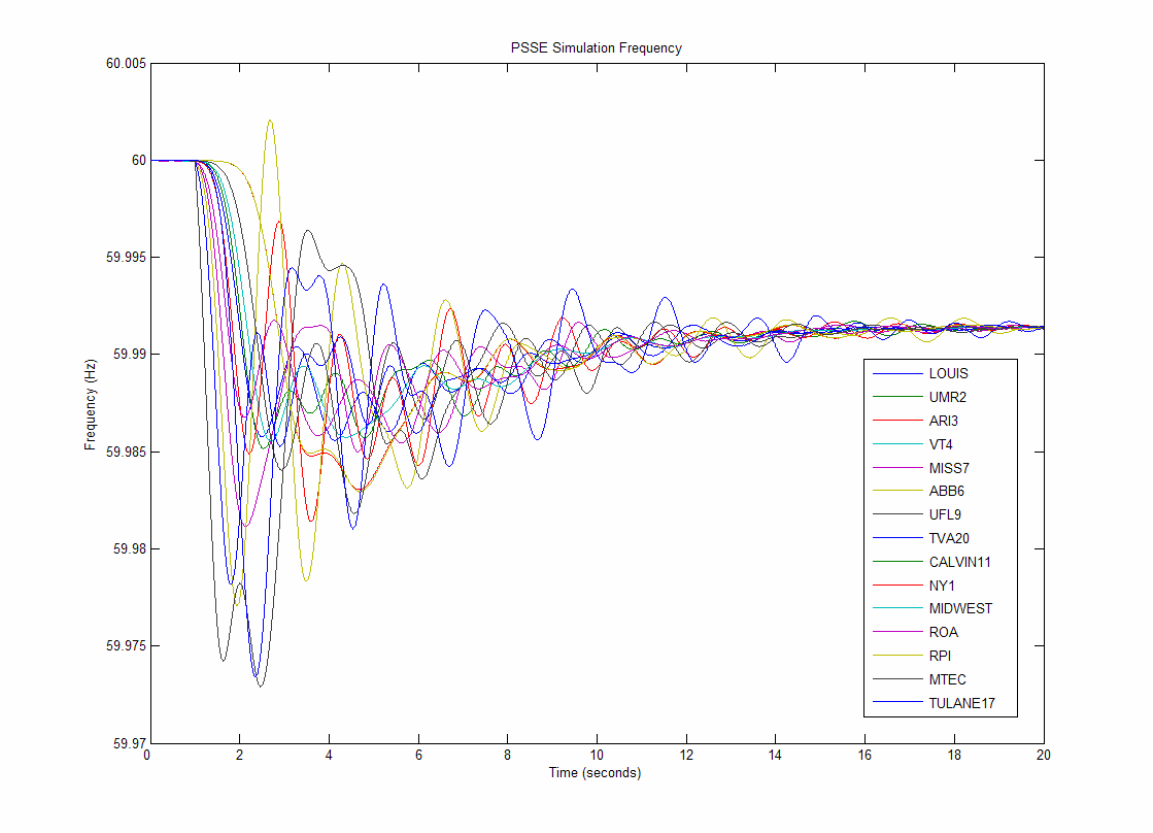

Figure 3.11 Simulated frequency

As we can see, the frequency drops quickly when the generation is lost. This is followed by a period of oscillation before the frequencies stabilize and reach a new operating point. On the following page, Figures 3.12 and 3.13 show the simulated angles and angles computed from simulated frequency through integration, respectively. By eye, these two graphs look identical.

* PSS/E data provided by Will Kook

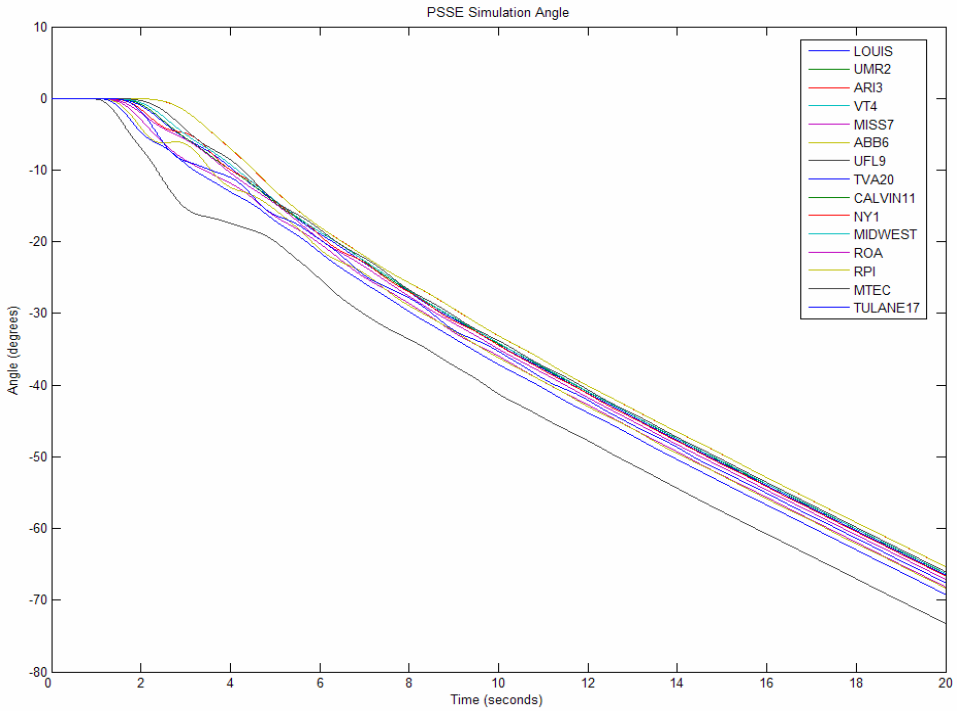

Figure 3.12 Simulated angles

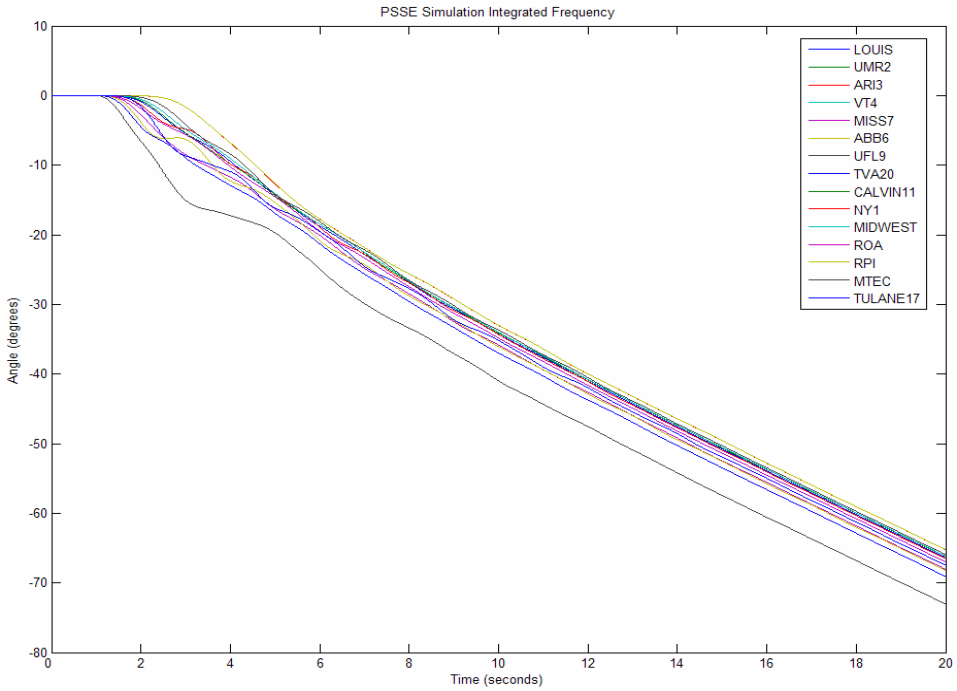

Figure 3.13 Computed angles

Laying the two previous figures on each other and zooming in, we get the graph shown below. We can see that there is a slight difference between the two (due to the approximations made in phasor angle analysis). However it is important to note that the computed angle does not diverge from the simulated angle. Instead, the difference between the computed angle and the simulated angle for each curve eventually settles to a constant. Furthermore, the difference between the two never exceeds half a degree.

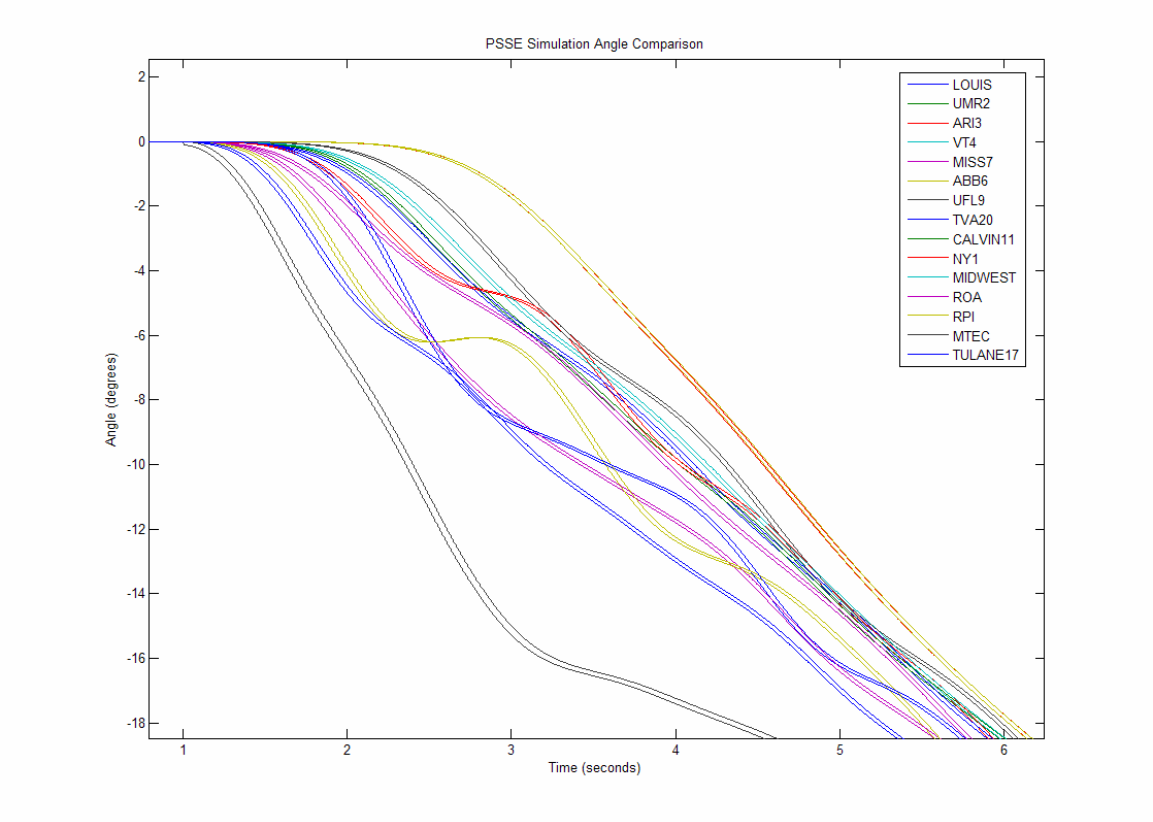

Figure 3.14 Comparison of simulated angles and angles computed through frequency integration

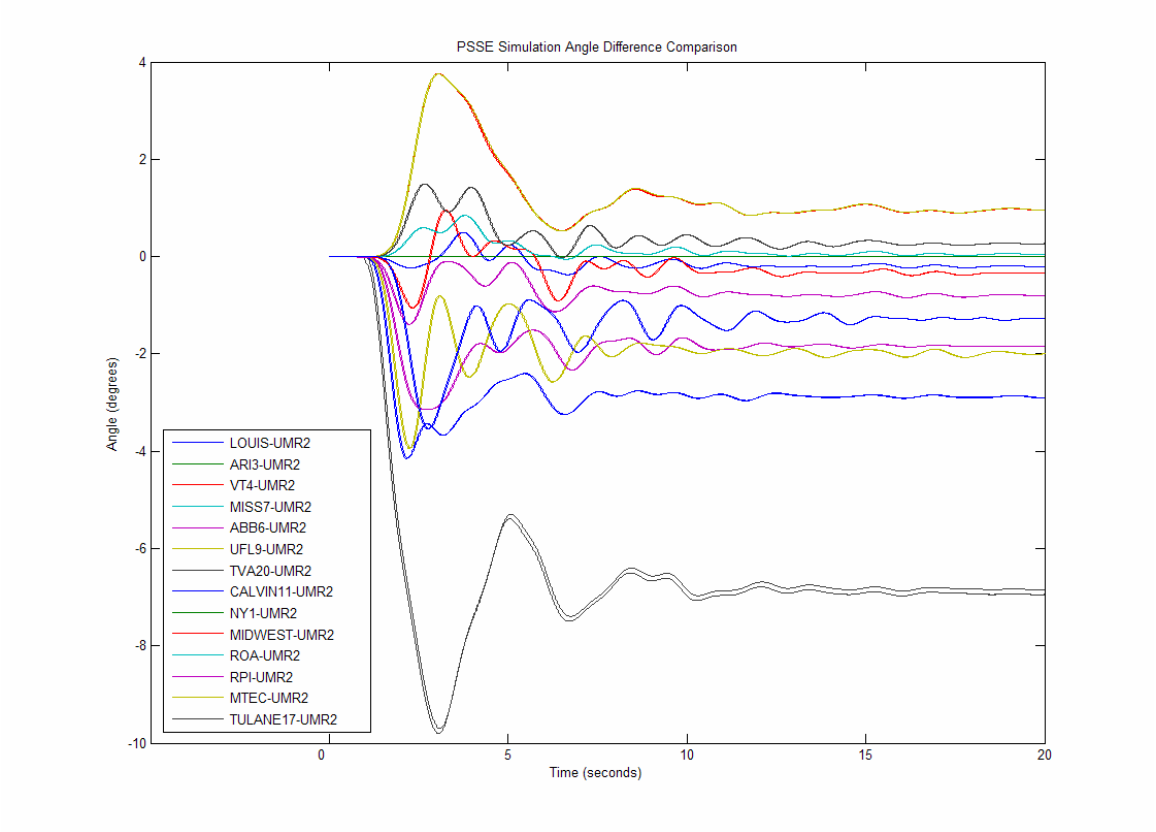

Figure 3.15 Comparison of simulated and computed angle differences

Most of our angle analysis will be done using the difference between each angle measurement and a common reference. Therefore, let's look at the angle differences between each measurement and the UMR angle. Once again, the results for the simulated data and computed data are placed on top of each other, as shown in Figure 3.15. We can see that there is only a very small difference between the two cases, which indicates that our method of calculating angles from the frequency is acceptable. Also, the angle difference graph gives us an idea of what to look for when we do angle analysis with FDR data.

3.5 Summary

In this chapter, we have explored three different methods of FDR angle data conditioning. The first method was to simply unwrap the raw angle data. We

discovered, however, that there were small periodic discontinuities in the angle data (due to sampling issues) that become a major problem when we take the angle differences between two unit measurements. Since most power system angle analysis is done with angle differences and how they change over time, we concluded that the unwrapping method did not condition the data enough for analysis. Next, we tried to smooth the data by shifting the angle data to counter the discontinuities and piece each continuous stretch of data head to tail. This method was quickly rejected, though, when we discovered that the frequency of occurrence of the discontinuities varied from FDR to FDR. Furthermore, we saw that the smoothed angles from different FDRs diverged after a fairly short period of time while the raw angles did not. The final method we looked at was to use the frequency data to calculate the angles using the frequency-angle relationship derived in phasor angle analysis. The result was much smoother angle curves that did not diverge nearly as much as they did with the angle shift technique. Finally, we tested the frequency integration method with simulated power system event data and saw that the angles derived from frequency were very close to the simulated angles. Therefore, frequency integration is the best method to obtain angle measurements from our FNET data. In the next chapter, we will use this method to analyze the voltage angles for several generation trip events.

Chapter 4: Event Angle Analysis

In power system frequency, a generator trip is marked by a sharp drop, followed by a slow, steady recovery to the system's normal operating frequency. Between August 2004 and April 2005, FNET captured several generator trip events in the Eastern Interconnected System (EI). Of these cases, we have confirmed the locations of the tripped generators for nine cases and ten FDRs placed in the EI recorded these events. However, each event was not recorded by every FDR – only a subset of the ten recorded the event and sent data back to our central server. Figure 4.1 shows the locations of the events as squares and the locations of our FDRs as dots. Tables 4.1 and 4.2 contain the FDR and event location details, respectively.

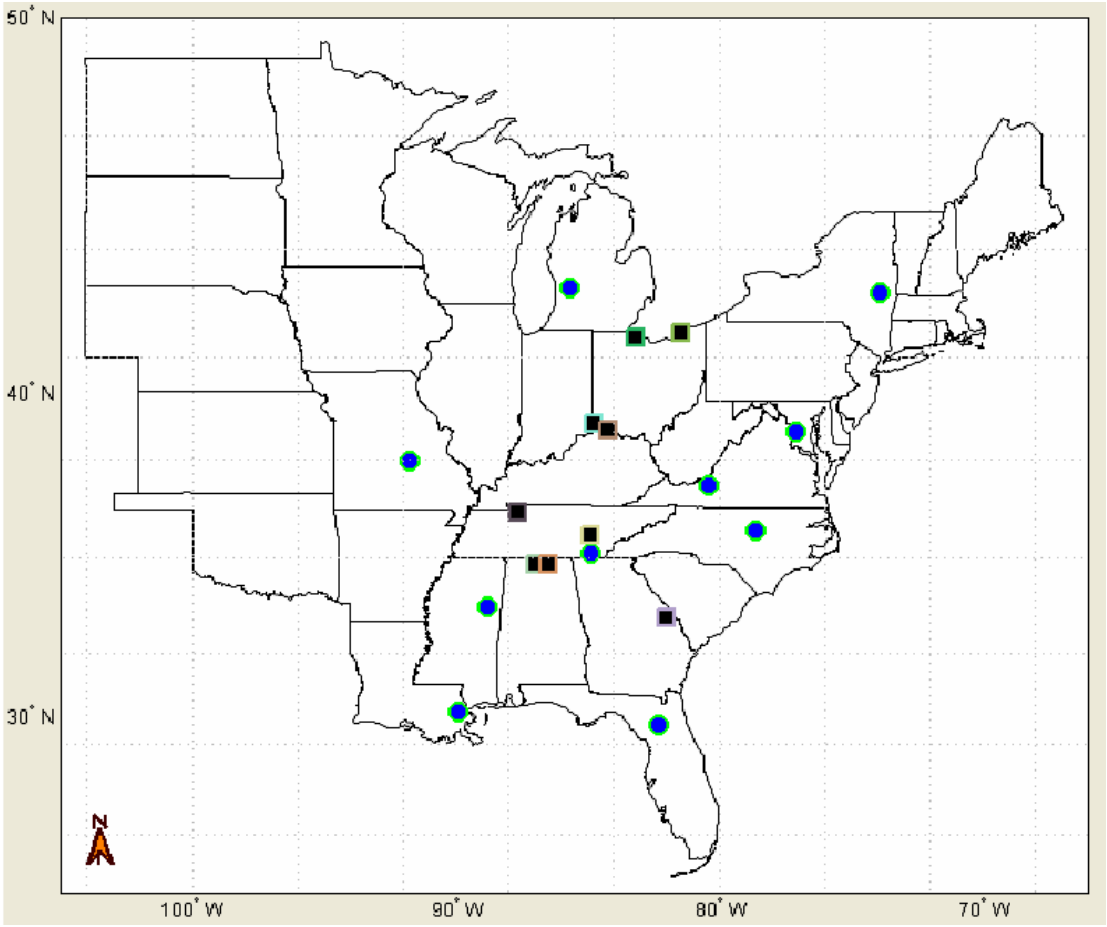

Figure 4.1 FDR and base case locations [9]. Permission granted by R. M. Gardner.

Table 4.1 FDR unit location data [9]. Permission granted by R. M. Gardner.

Unit Number	1	2	3	4	6	7	9	11	17	20
Unit Name	NY	UMR	ARI	VT	ABB	MISS	UFL	Calvin	Tulane	TVA1
NERC Region[1]	NPCC	MAIN/ SERC	SERC	ECAR/ SERC	SERC	SERC	FRCC	ECAR	SERC	SERC
Latitude[2]	42.8018	37.9487	38.8210	37.2327	35.8220	33.4567	29.6742	42.9613	30.0658	35.1313
Longitude[2]	-73.9281	-91.7658	-77.0862	-80.4284	-78.6587	-88.8222	-82.3363	-85.6557	-89.9313	-84.8750

[1] As determined by http://www.nerc.com

[2] As determined by the U.S. Gazetteer, http://www.census.gov/cgi-bin/gazetteer

Table 4.2 Base case location data [9]. Permission granted by R. M. Gardner.

Case Number	1	2	3	4	5	6	7	8	9
Date	8/4/2004	9/19/2004	11/23/2004	1/26/2005	2/11/2005	3/21/2005	4/2/2005	4/22/2005	4/29/2005
Plant Name	Davis Besse	Watts Bar	Browns Ferry	East Bend	Browns Ferry	Cumberland	Eastlake	Zimmer	Votgle-Wilson
Nearest Town	Oak Harbor	Spring City	Athens	Rabbit Hash	Athens	Cumberland City	Eastlake	Moscow	Waynesboro
State	Ohio	Tennessee	Alabama	Kentucky	Alabama	Tennessee	Ohio	Ohio	Georgia
NERC Region[3]	ECAR	SERC	SERC	ECAR	SERC	SERC	ECAR	ECAR	SERC
Latitude[4]	41.5116	35.6874	34.7860	30.0324	34.7860	36.3822	41.6596	38.8603	33.0900
Longitude[4]	-83.1467	-84.8641	-86.9599	-84.7414	-86.9599	-81.4306	-81.4306	-84.2285	-82.0136
FDR Set	2,3,4,6,7,9	1,2,3,4,6,7	2,3,4,6,7,11	2,3,4,6,7,11	2,3,4,6,7,9, 11	2,3,4,6,7,9, 11,17,20	2,3,4,6,7,9, 11,17,20	2,3,4,6,7,9, 11,20	2,3,4,6,7,9, 11,17,20

[3] As determined by http://www.nerc.com

[4] As determined by the U.S. Gazetteer, http://www.census.gov/cgi-bin/gazetteer

Due to missing data, Base Case 4 was eliminated from our angle analysis. Also, extended, continuous data windows could only be obtained for Base Cases 5, 6, 8, and 9. With the extended data window, we can look at the long term behavior of the system. Finally, all angles used in the analysis were derived from the frequency as discussed in Section 3.3.

4.1 PSS/E Simulation

Before delving into angle analysis with FDR data, let us first look at a simulated case*. While we would expect the real life data to differ from the simulation results, it is still beneficial to look at the simulation to give us an idea of what to look for. Simulation frequency data could only be obtained for an EI simulation of Base Case 8. There are 15 points of frequency measurement geographically, including the locations of our FDRs. Figure 4.2 shows the frequency plots for the simulation. Note that for this simulation, the time step between each sample point is 0.0001s.

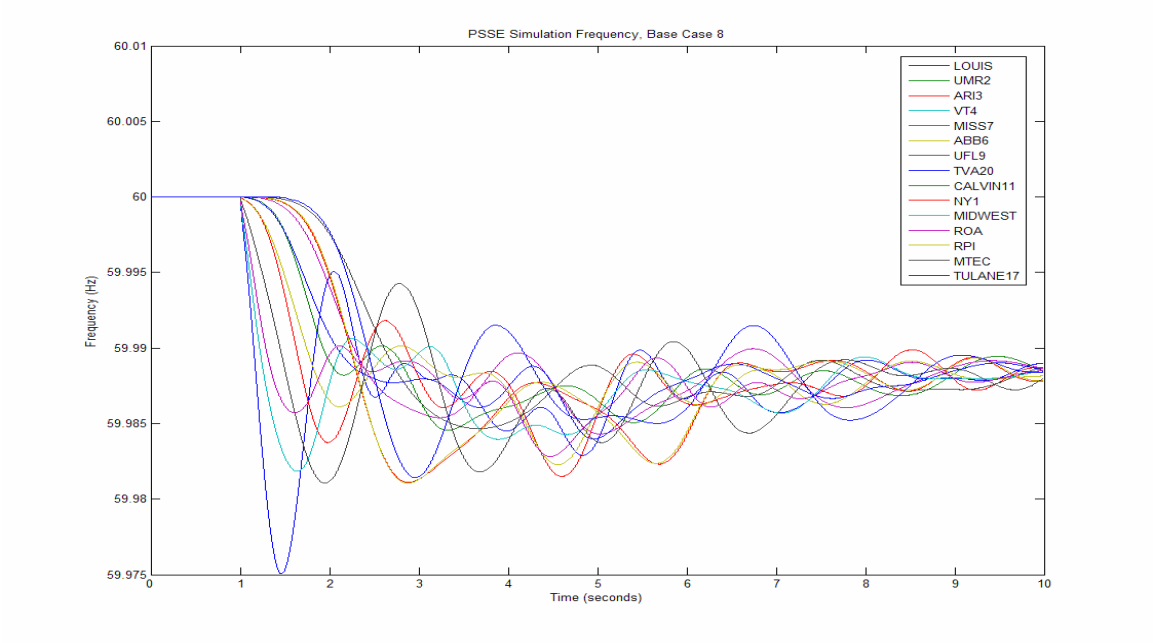

Figure 4.2 Frequency simulation results for Base Case 8

* PSS/E data provided by Will Kook

Unfortunately, angle information was not available for this simulation; so instead, the angle was calculated using the frequency-angle relationship in Section 3.3. As expected, the computed angles start to plummet when the frequency drops below 60Hz, as shown in Figure 4.3.

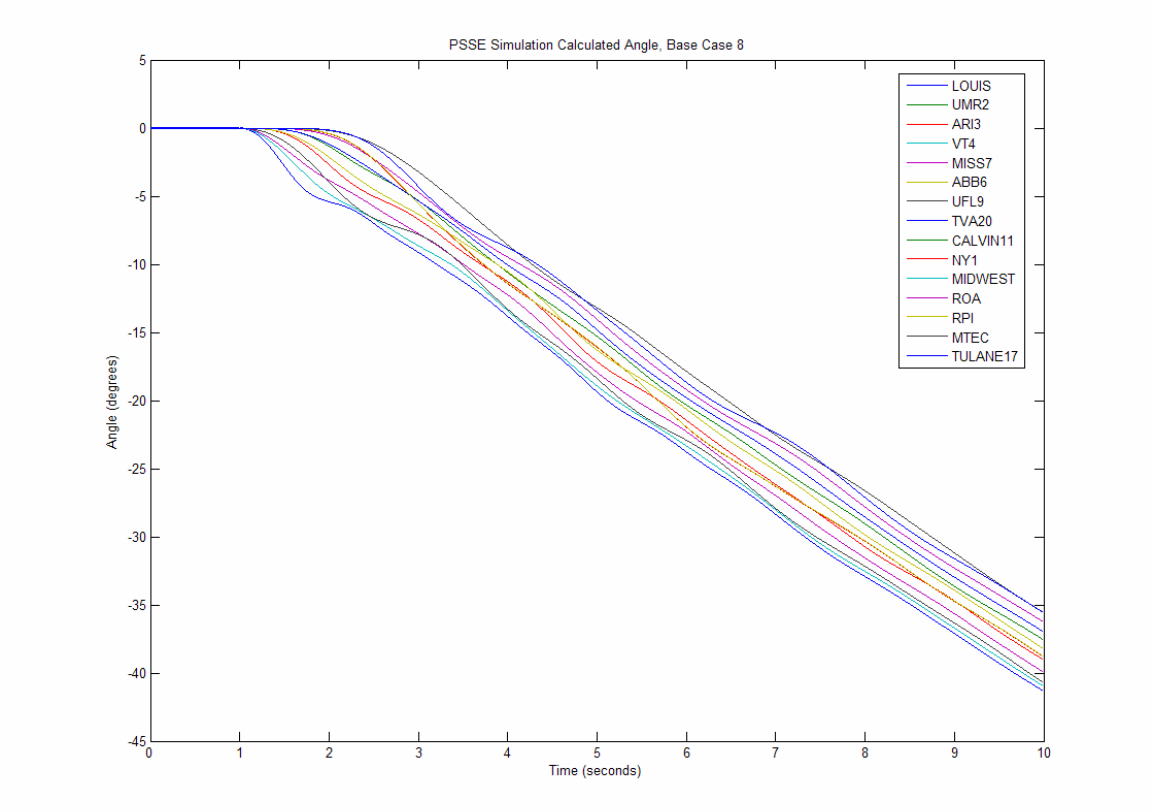

Figure 4.3 Calculated angles for Simulated Base Case 8

With limited information about the system parameters, it is not very useful to look at the phase angles directly because these angles can be directly shifted by an angular displacement at a wye-delta transformer. Furthermore, since our FDRs measure frequency at the distribution level, our data is more prone to transformer phase shifts. Varying phase angle and varying phase angle difference between two points, on the other hand, gives us very useful information. If the angle is increasing with time, the system frequency is above 60Hz; if the angle is decreasing with time, the system frequency is

below 60Hz. Any variation in the angle difference over time between two points indicates that the power flow has changed [3].

The UMR angle is used as a reference and subtracted from each of the other angles in the set. UMR was chosen as the reference for each base case because it was one of the first units deployed. Shown in Figure 4.4, the angle differences immediately jump with the onset of the event, followed by a relatively flat region, indicating that the system has reached a new operating point.

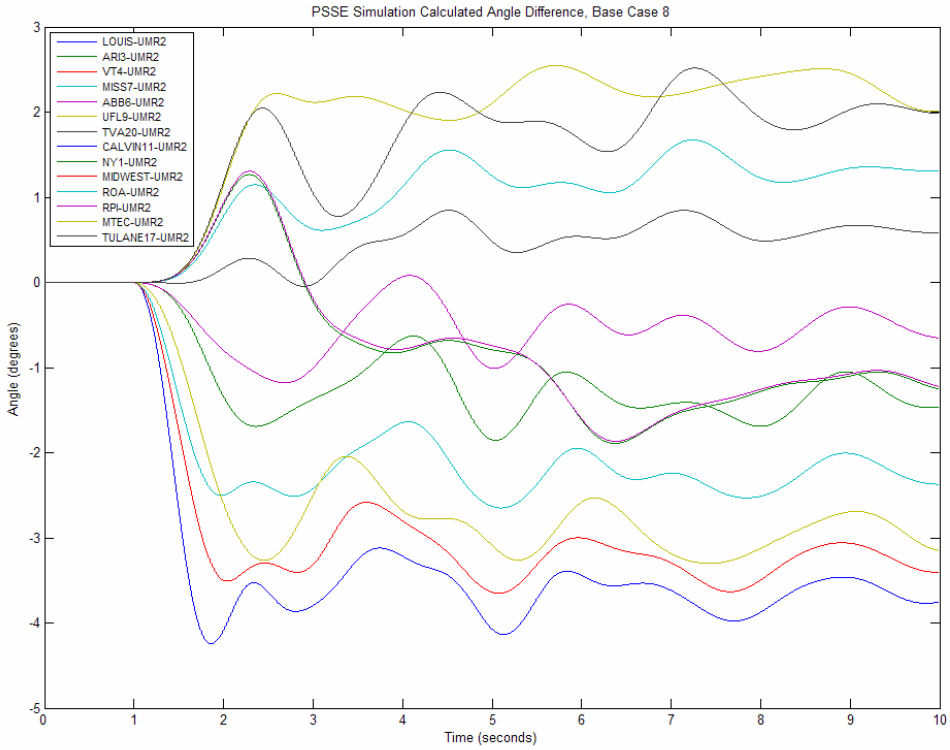

Figure 4.4 Calculated angle differences for Simulated Base Case 8

Though the simulation only represents a ten second window, it offers another representative case to which we can compare the measured EI base cases to.

4.2 Base Case 1

The first base case is a typical generation trip event originating at the Davis Besse plant located in Oak Harbor, Ohio. The frequency starts off slightly below 60Hz and then suddenly drops to about 59.95Hz just before the 20 second mark, as shown in Figure 4.5.

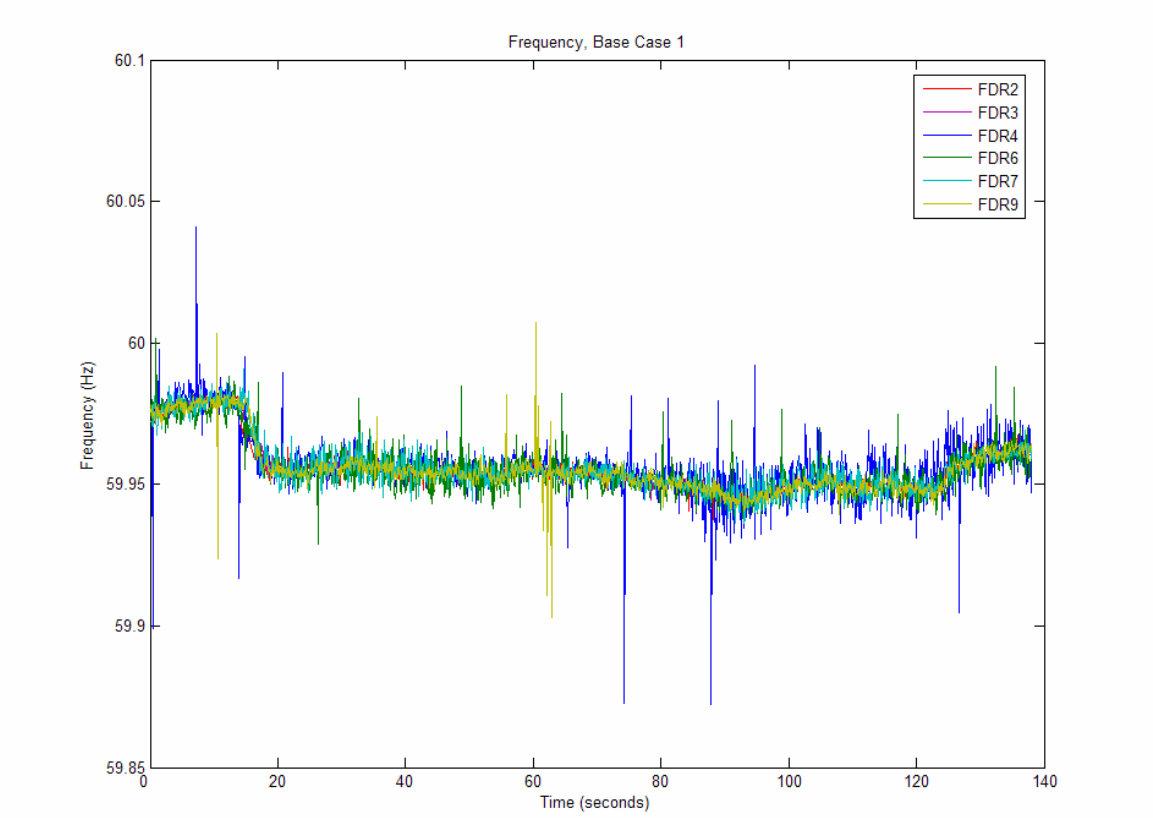

Figure 4.5 Base Case 1 raw frequency

For a better look, the noise is removed using a 21 point moving median, shown in Figure 4.6. The smoothed plot reveals some unusual behavior on the VT unit starting just after the 80 second mark. In the frequency plot, it is unclear whether this is an oscillation or just some noise (which often plagues the VT unit).

The angles are computed and plotted in, as shown in Figure 4.7, and the result is what we expect. Since the frequency starts below 60Hz, the angle initially has a negative slope. Then, the slope becomes even more negative as the event occurs.

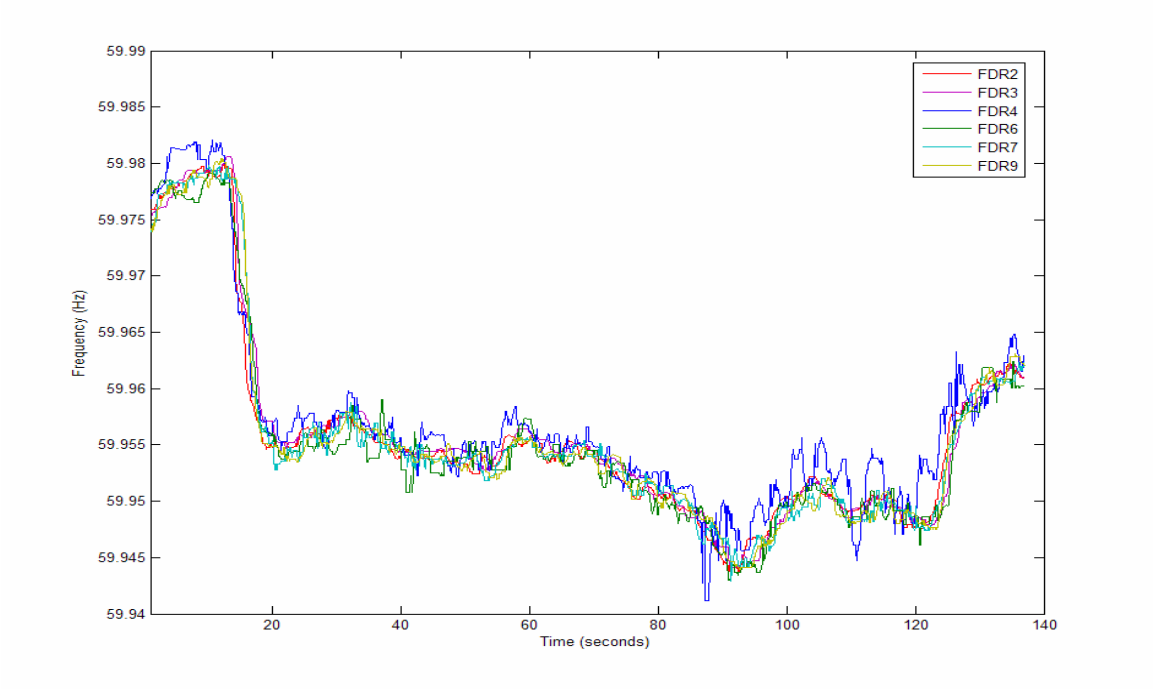

Figure 4.6 Base Case 1 frequency smoothed with a 21 point moving median

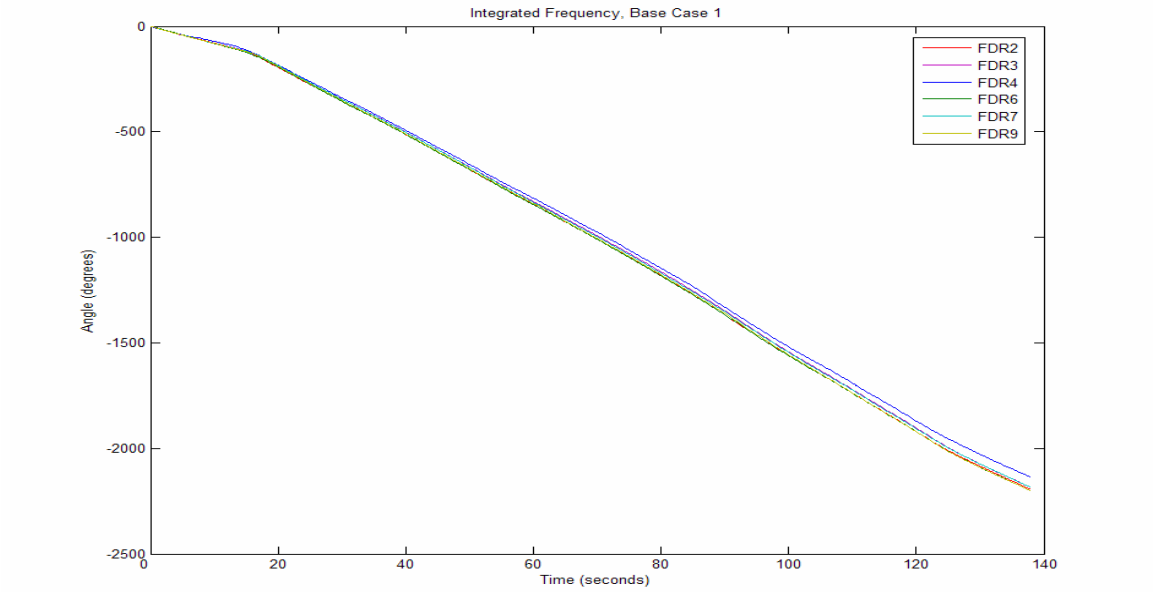

Figure 4.7 Base Case 1 angles

Using the UMR measurements as a reference point, the angle differences are computed and shown in Figure 4.8. With VT as an exception, the results are as we expect. ARI, ABB, MISS, and UFL units quickly jump when the event occurs, and then flatten out as the power flow in the system stabilizes. The VT unit, however, seems unaffected by the event and continues to increase linearly. It is suspected that there might be a hardware malfunction within the VT unit, possibly with the oscillator driving the sample pulses. Another possible cause is the "one second problem" that was recently discovered on some FDRs. The "one second problem" stems from a GPS malfunction that causes the FDR data to be skewed by one second. The same behavior on the VT angle difference is also present in other base cases.

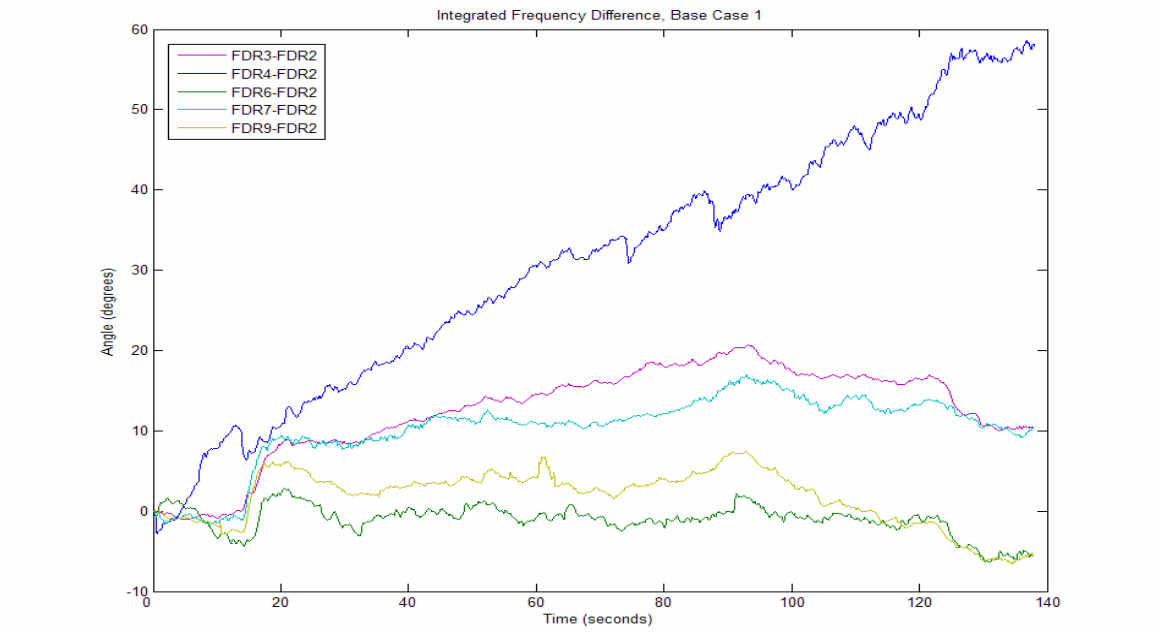

Figure 4.8 Base Case 1 angle differences

To gain a better perspective of how the system reacts to the event, each angle difference is normalized just prior to the event, as shown in Figure 4.9. Using this plot, we can see which units tend to group together during a generation trip event. In this case, it is clear that the ARI and MISS units form a group and the ABB and UFL units form another group. A color coordinated map of this grouping is shown in Figure 4.10.

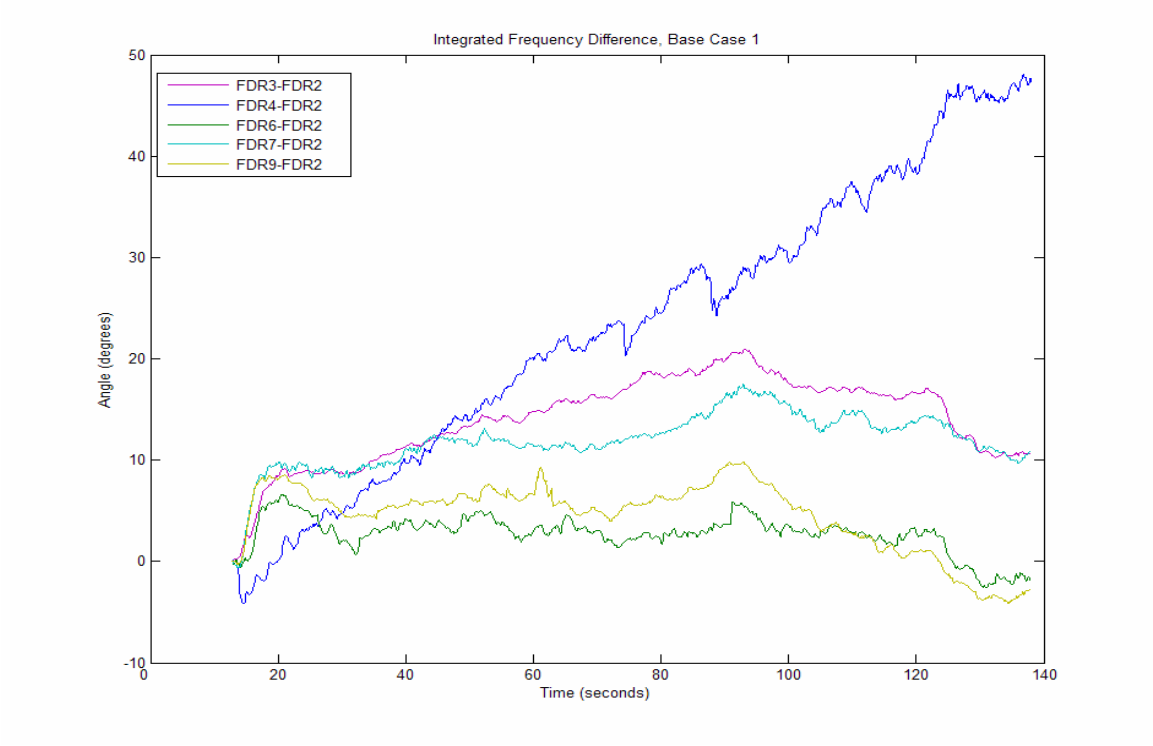

Figure 4.9 Base Case 1 angle differences, normalized prior to event

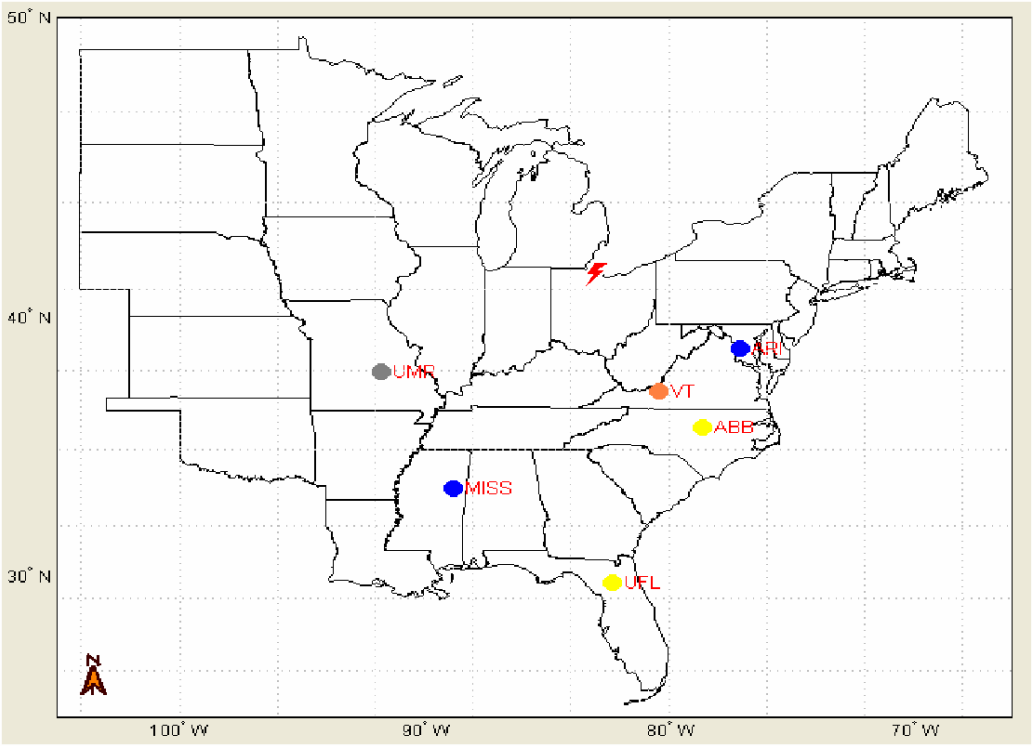

Figure 4.10 Base Case 1 possible unit grouping

4.3 Base Case 2

Base Case 2 is another typical generation trip event originating in the Watts Bar plant located in Spring City, Tennessee. In this case, the frequency starts at approximately 60Hz and then drops to about 59.95Hz at around the 60 second mark. A slow recovery follows the event.

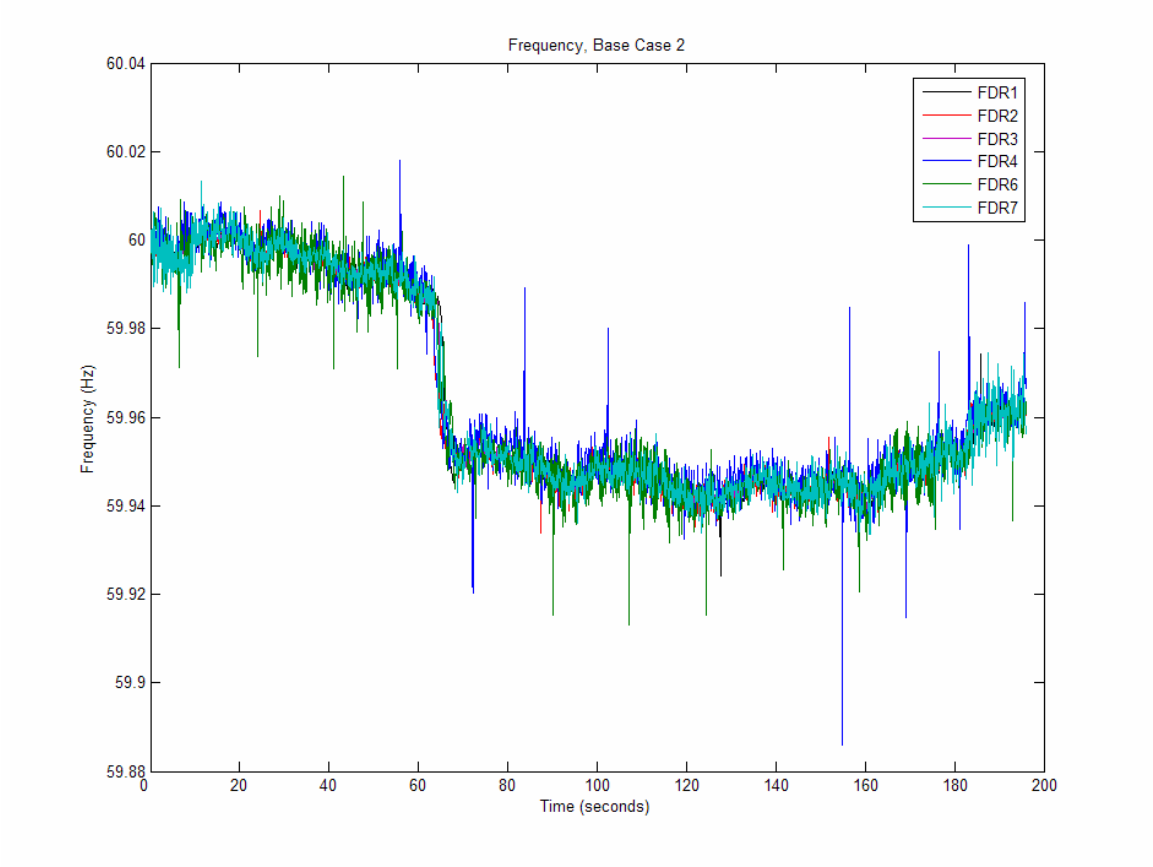

Figure 4.11 Base Case 2 raw frequency

The smoothed plot is shown in Figure 4.12. There is nothing obviously abnormal about the frequency behavior during this event. However, upon closer inspection, the VT unit does tend to deviate slightly from the rest of the measurements.

Using the raw frequency data, the angle is computed and plotted in Figure 4.13. Since the initial frequency is very close to 60Hz, the angle plot starts off fairly flat. When the frequency drops, the slope of the angle plot becomes negative and the angles plummet. Finally, we notice that the VT unit angle diverges from the pack toward the end of the angle plot.

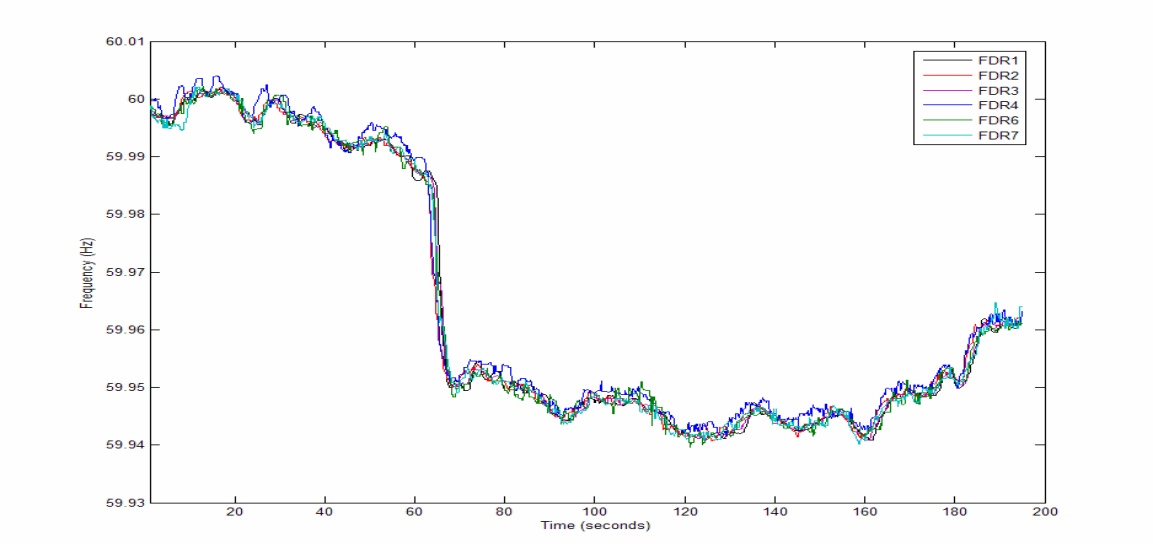

Figure 4.12 Base Case 2 frequency smoothed with a 21 point moving median

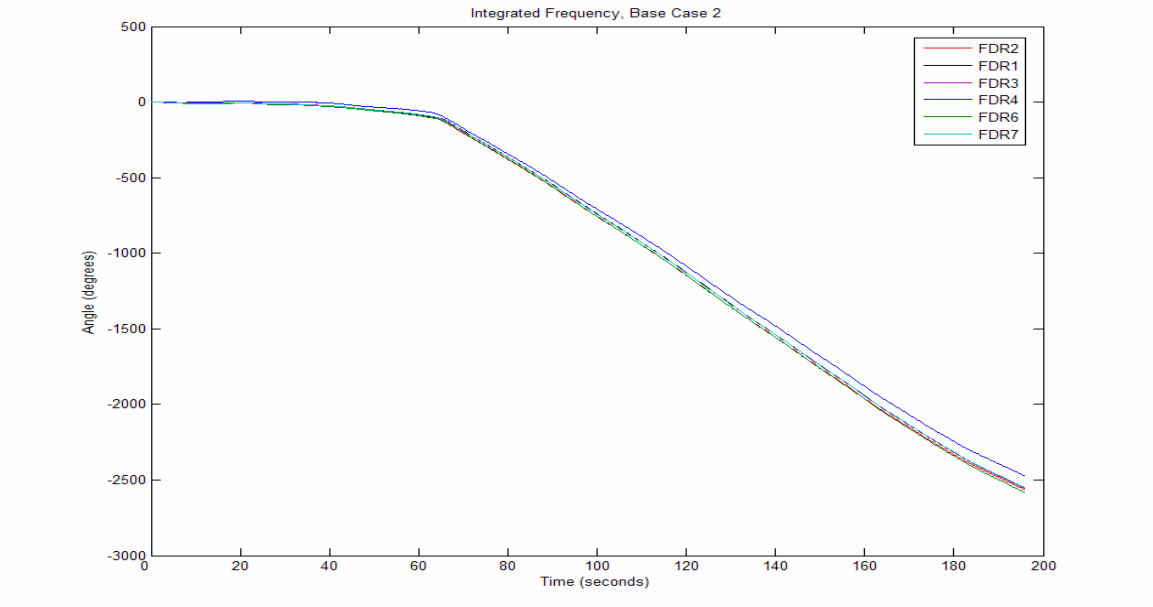

Figure 4.13 Base Case 2 angles

Once again using the UMR unit as a reference, the angle differences are computed and plotted. Remember, we are not plotting the actual angle differences because each unit has been normalized. Instead, we are looking at the changes in the angle differences as a result of the event. The NY, ARI, and MISS units exhibit the type of behavior that we expect. The ABB unit also behaves as expected initially, but then starts to drift as time passes.

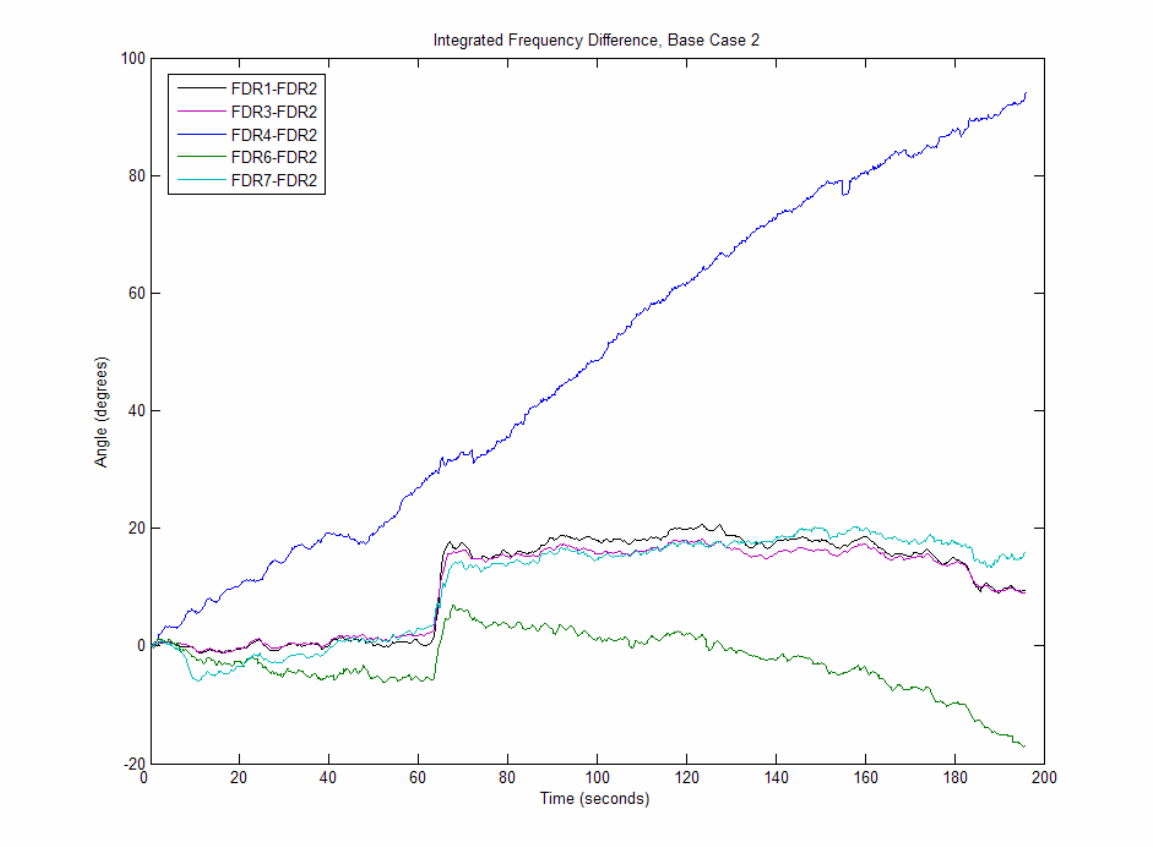

Figure 4.14 Base Case 2 angle differences

The angle difference plots are again shown in Figure 4.15, and normalized just before the event. Clearly, the NY, ARI, and MISS units have a grouped response to the event. The VT and ABB units each form their own groups. Figure 4.16 shows a color coordinated grouping map.

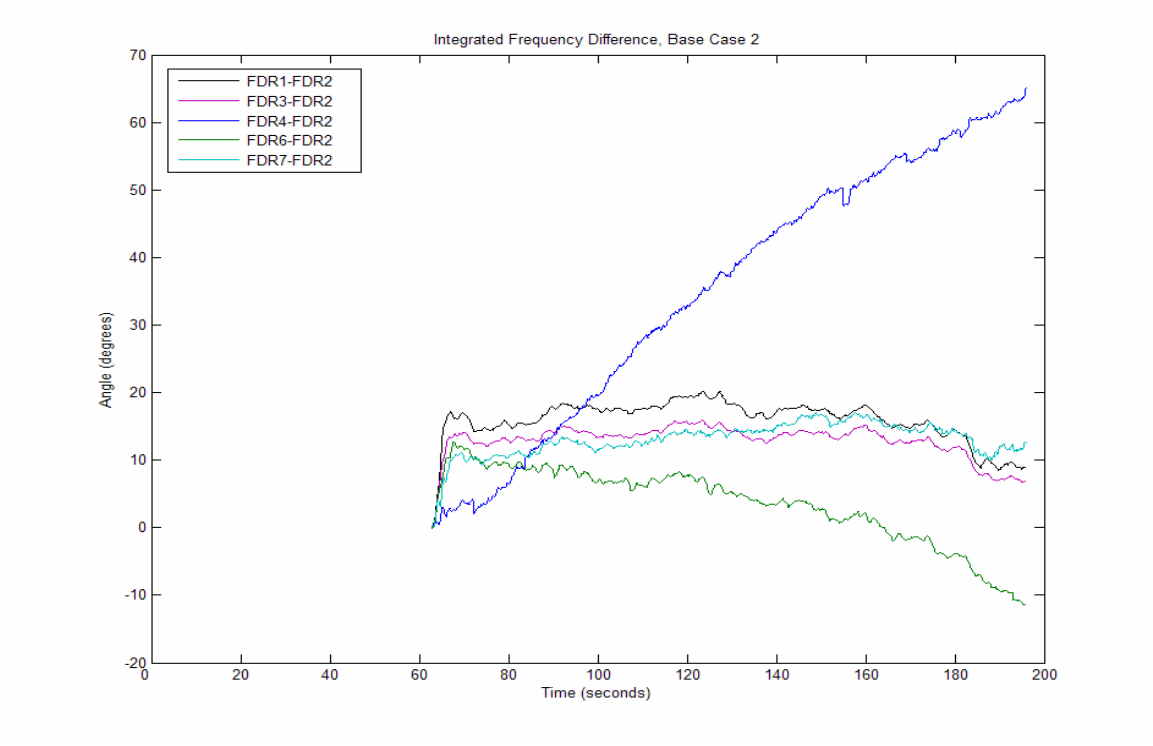

Figure 4.15 Base Case 2 angle differences, normalized prior to event

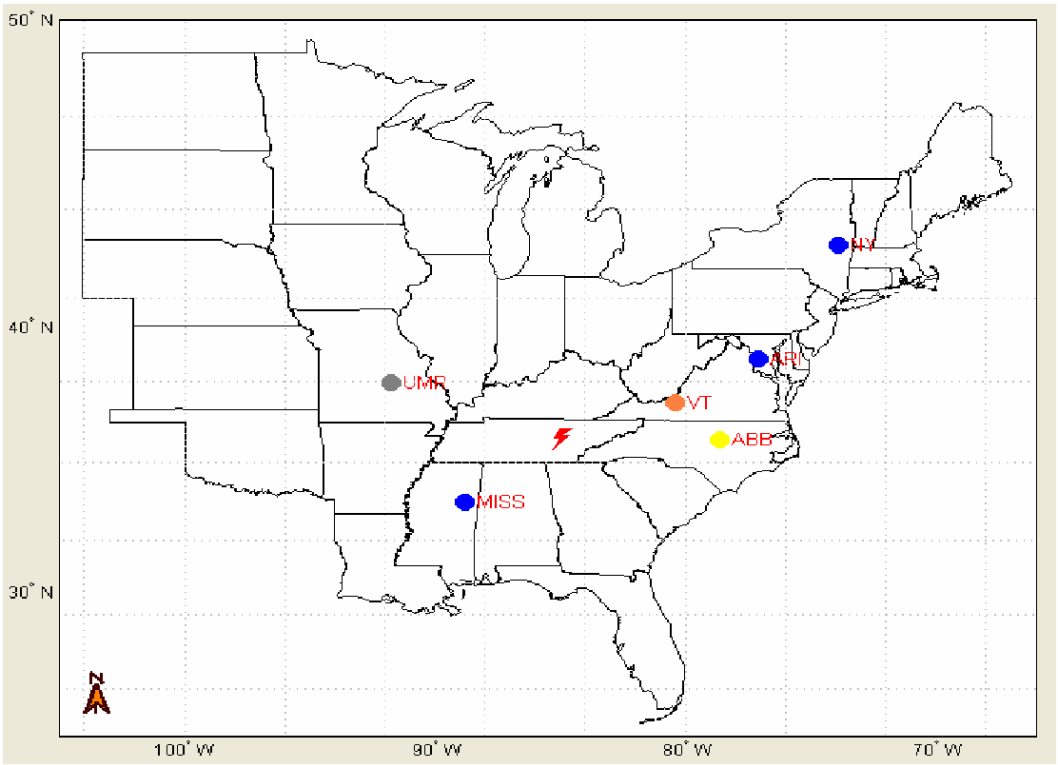

Figure 4.16 Base Case 2 possible unit grouping

4.4 Base Case 3

Base Case 3 is a generation trip event originating from the Browns Ferry power plant located in Athens, Alabama. Similar to Base Case 2, the frequency starts at about 60Hz and then drops dramatically as generation is lost. A slightly longer time duration is available for this case, so we can see the frequency slowly recover to pre-fault levels.

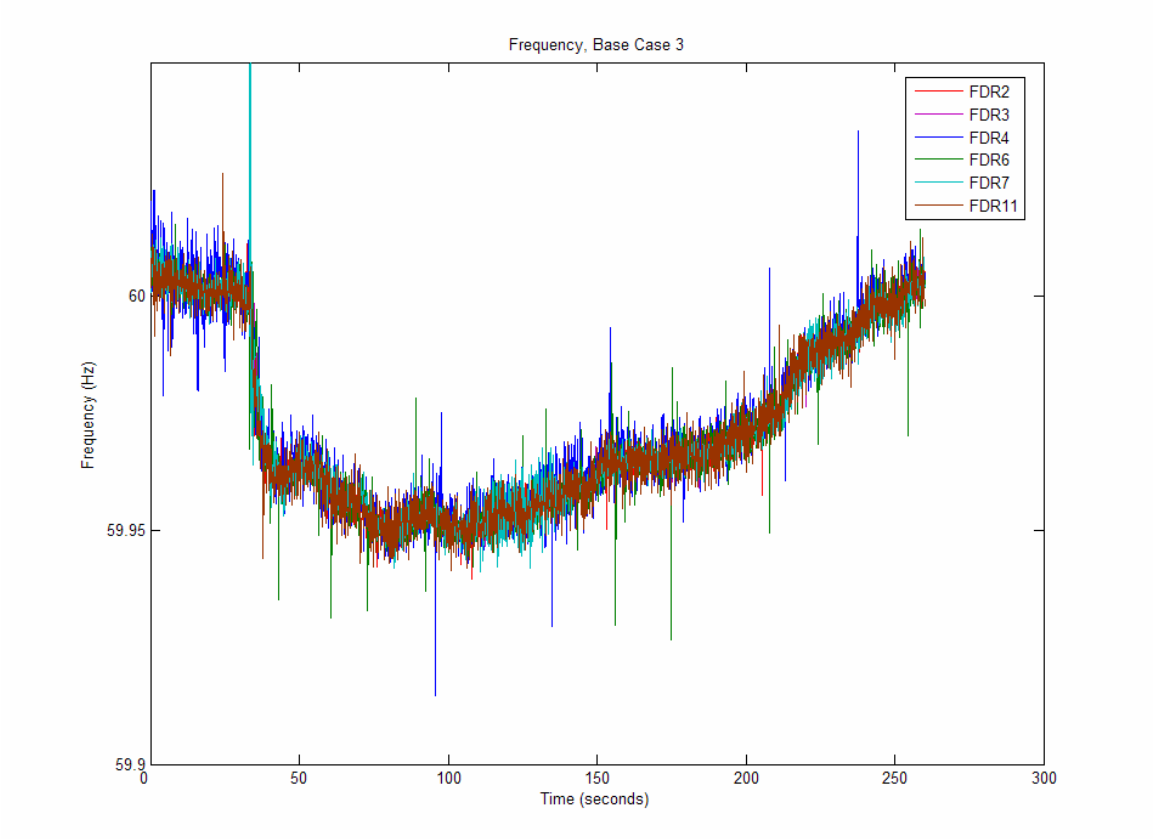

Figure 4.17 Base Case 3 raw frequency

Shown in Figure 4.18, the smoothed frequency looks very much like the plot for the previous case. Again, the VT unit frequency tends to be slightly higher than the rest of the FDR measurements which once again leads to a slightly divergent angle plot for the VT unit, as shown in Figure 4.19. The rest of the angle plots stay close together over the duration of the event.

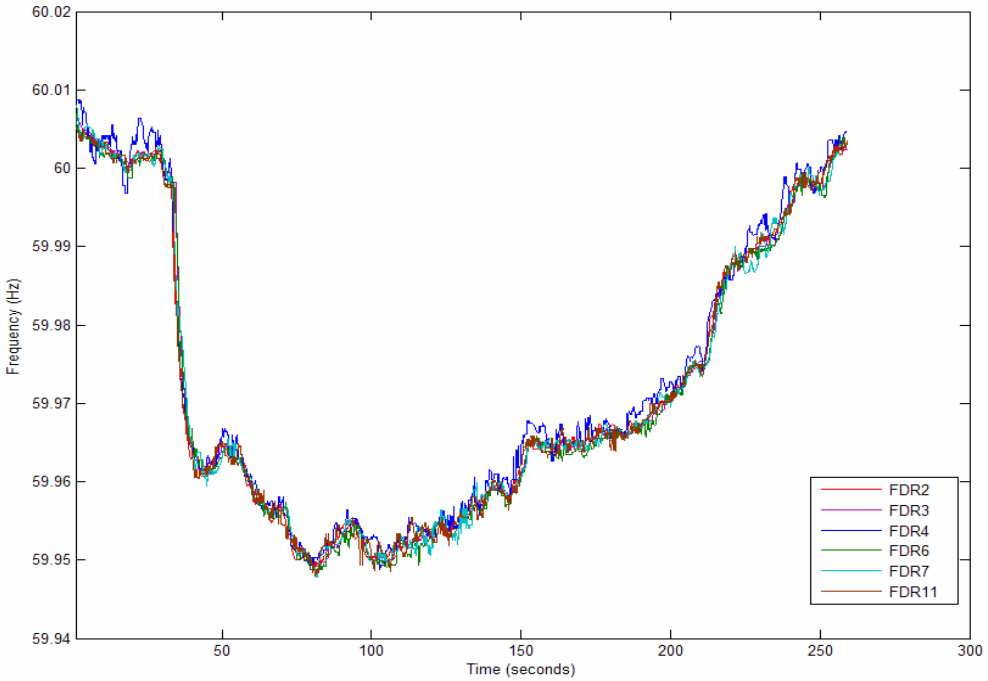

Figure 4.18 Base Case 3 frequency smoothed with a 21 point moving median

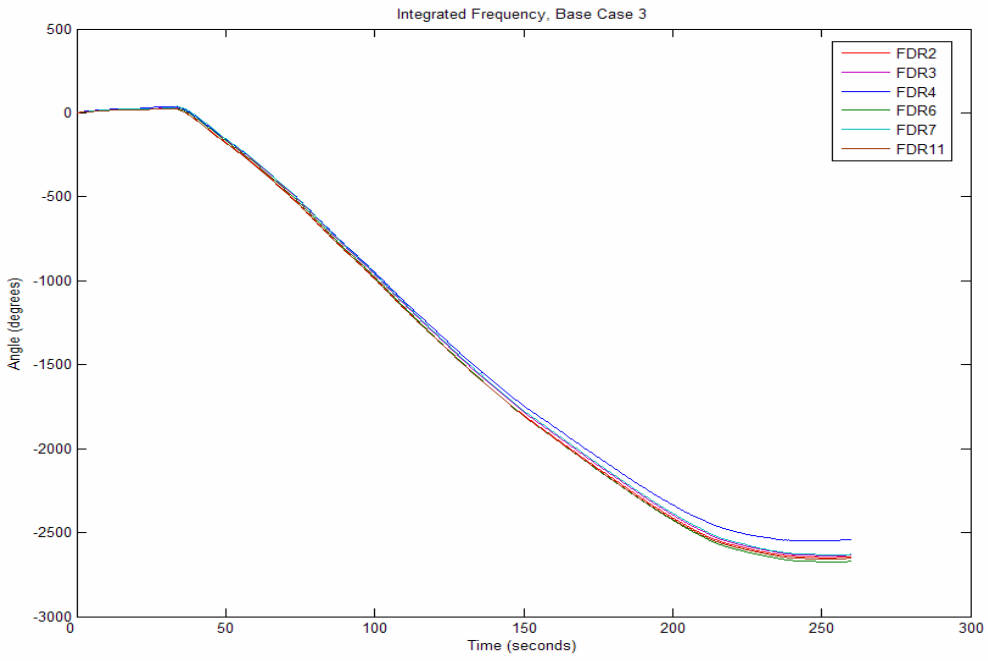

Figure 4.19 Base Case 3 angles

Looking at the angle difference plots, the ARI and MISS units once again react as expected to the event. Furthermore, the ABB unit tends to drift again, similar to the previous case. The Calvin unit remains fairly flat and close to zero throughout the plot revealing that its reaction is very close to that of the reference unit, UMR.

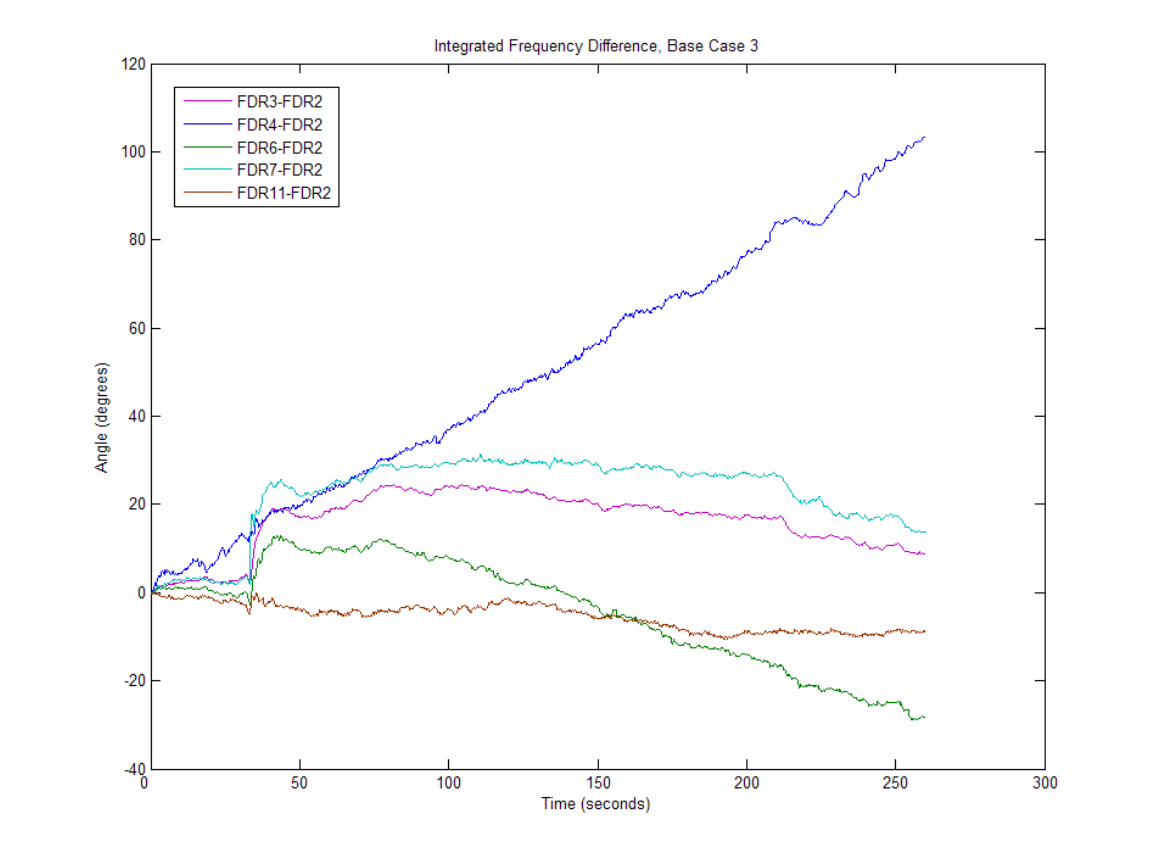

Figure 4.20 Base Case 3 angle differences

Normalizing the angle differences prior to the event yields the plot shown in Figure 4.21. The ARI and MISS units appear to be grouped, as they were in both of the previous cases. The flat plot of the Calvin unit indicates that it is grouped with the UMR unit. Figure 4.22 illustrates the unit grouping.

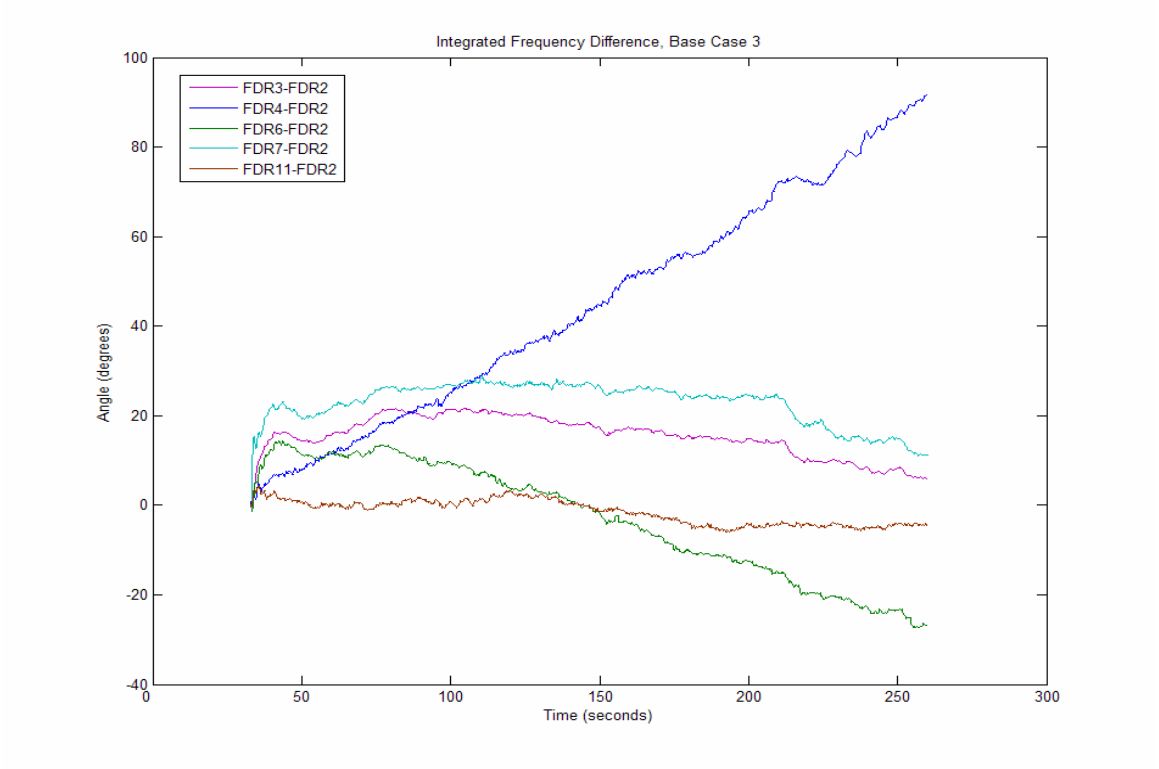

Figure 4.21 Base Case 3 angle differences, normalized prior to event

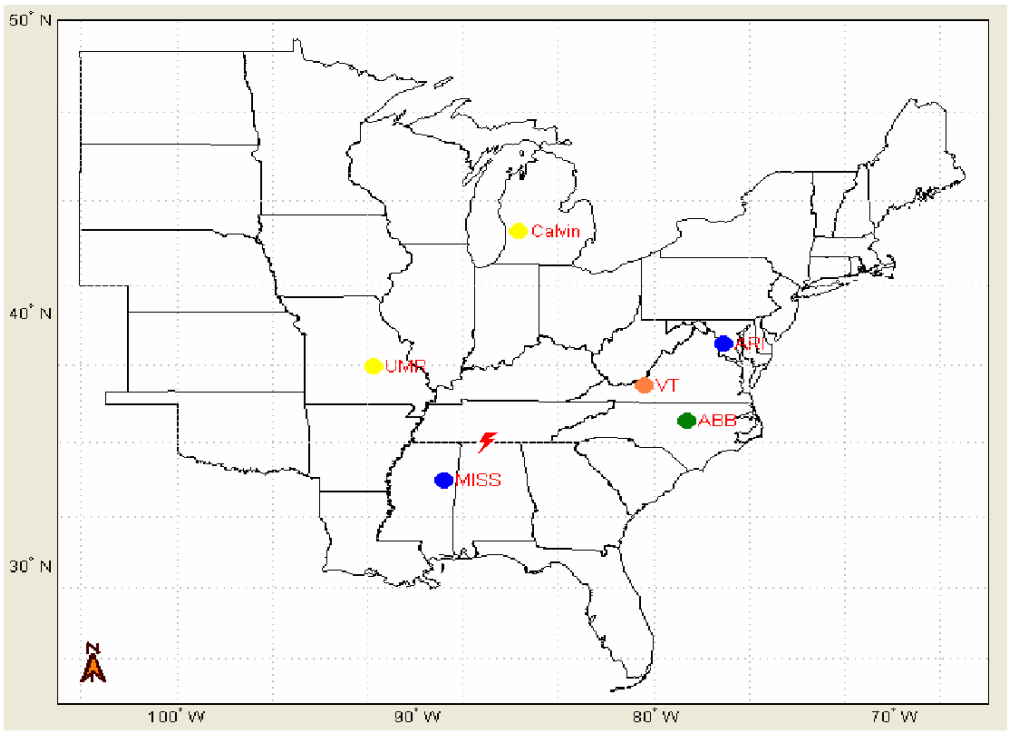

Figure 4.22 Base Case 3 possible unit grouping

4.5 Base Case 5

Base Case 5, also originating at the Browns Ferry plant, is a unique case in our set because it appears that more than one event is present. As shown in Figure 4.23, the initial generation trip event occurs prior to the 50 second mark. The frequency stays low for a while and then quickly recovers to pre-fault levels. It is unknown why this occurs, but it is likely due to a load rejection.

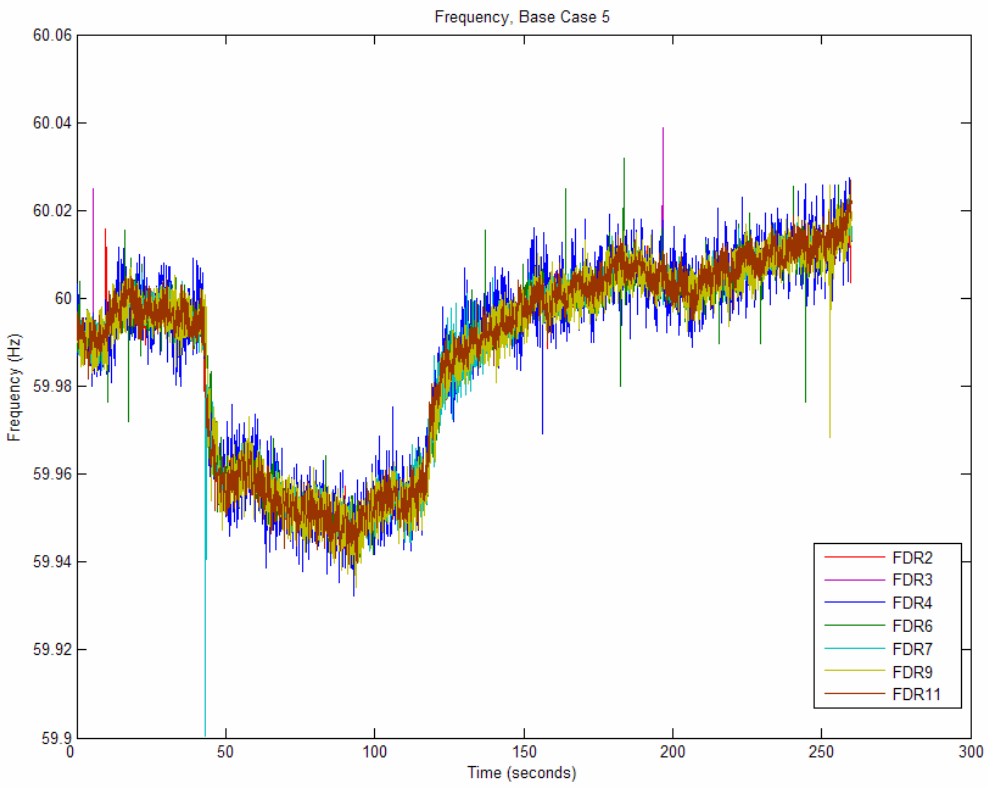

Figure 4.23 Base Case 5 raw frequency

The smoothed plot gives us a better view of the frequency data, and once again, we see that the VT unit frequency slightly differs from the rest of the data, especially just before the generation trip, and just after the load rejection. Toward the end, the noise on the VT unit dies down. As Figure 4.25 shows, the angle starts to drop when the frequency drops, and then flattens out when the system frequency recovers.

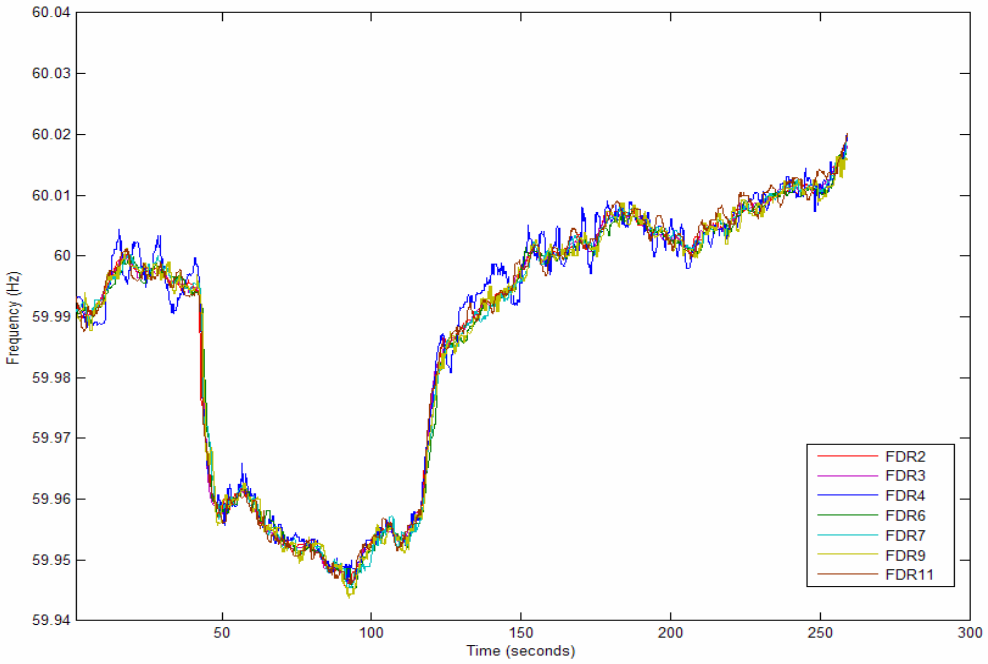

Figure 4.24 Base Case 5 frequency smoothed with a 21 point moving median

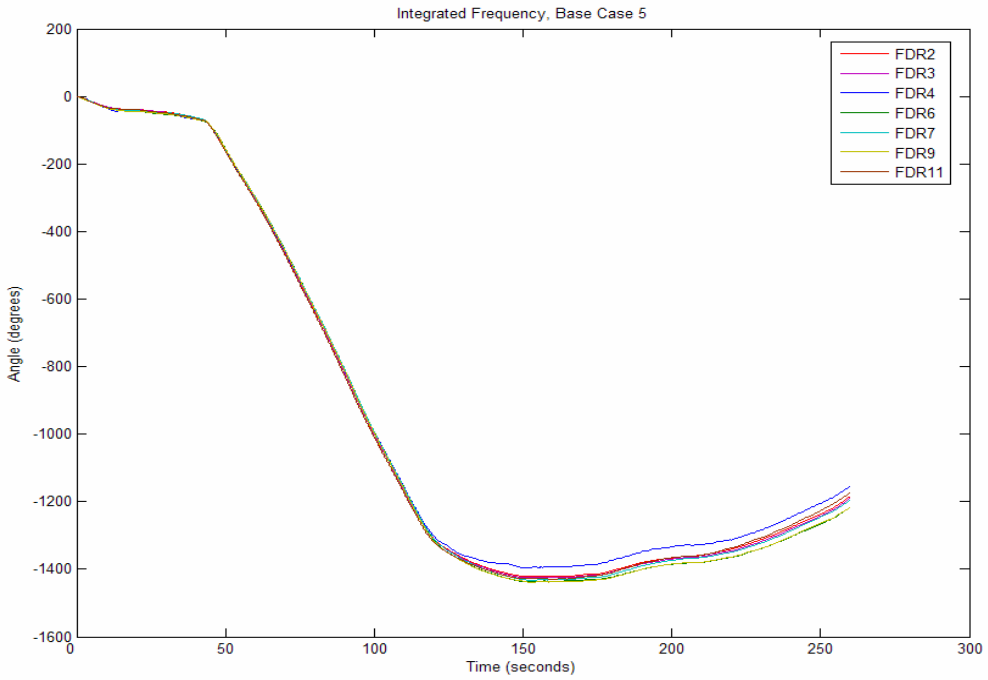

Figure 4.25 Base Case 5 angles

The angle difference plot presents some interesting results. Both the generation trip and load rejection events can be clearly seen on the ABB, MISS, and UFL units. The ARI unit shows a relatively small reaction to the generation trip and then flattens out—showing no visible response to the load rejection. Similarly, the Calvin unit also shows a slight jump with the generation trip and no reaction to the load rejection. However, instead of flattening out, it starts to drift. Finally, the VT unit has a fair amount of oscillation both before and after the events.

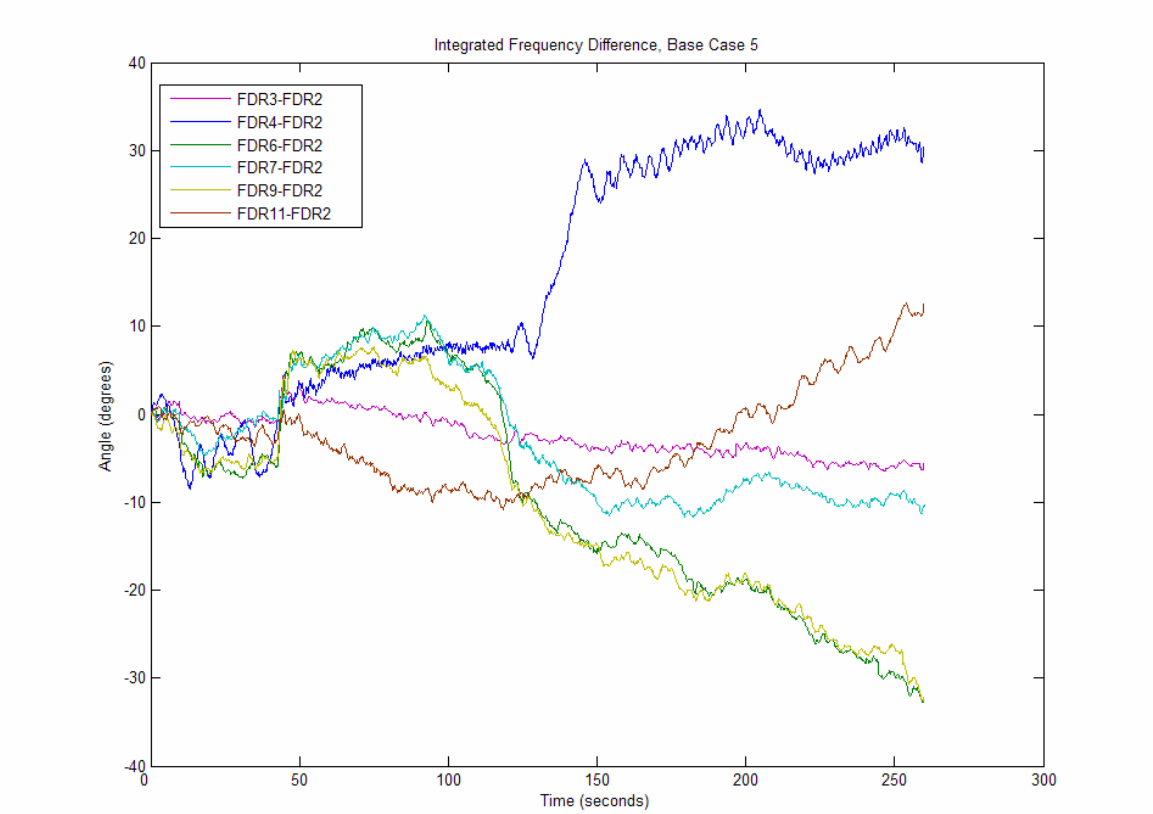

Figure 4.26 Base Case 5 angle differences

Looking at the angle difference plots normalized prior to the generation trip event, shown in Figure 4.27, only one unit group can be formed—ABB and UFL. The MISS unit does follow those two for a while, but then diverges later on. Also, the ARI and UMR units appear to be grouped, as the ARI angle difference remains relatively flat and close to zero. The remaining units, VT and Calvin, do not emulate the behavior of any other units. A map of the possible grouping for this event is shown in Figure 4.28.

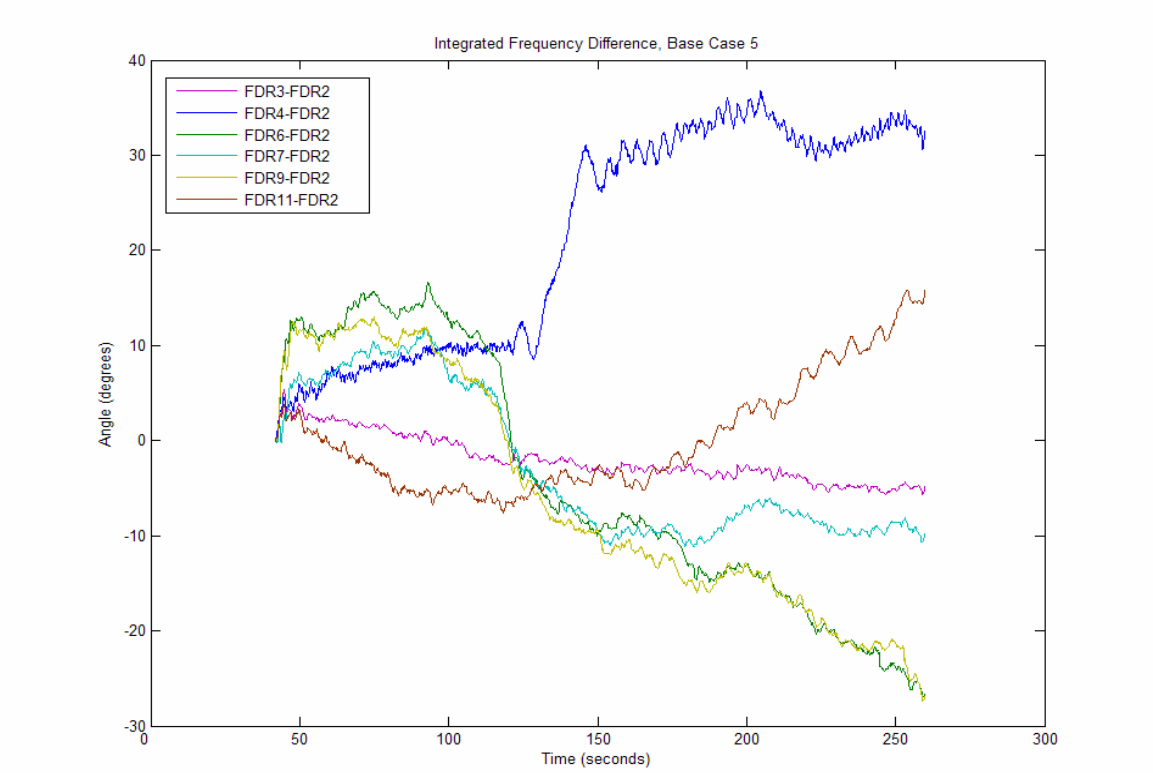

Figure 4.27 Base Case 5 angle differences, normalized prior to event

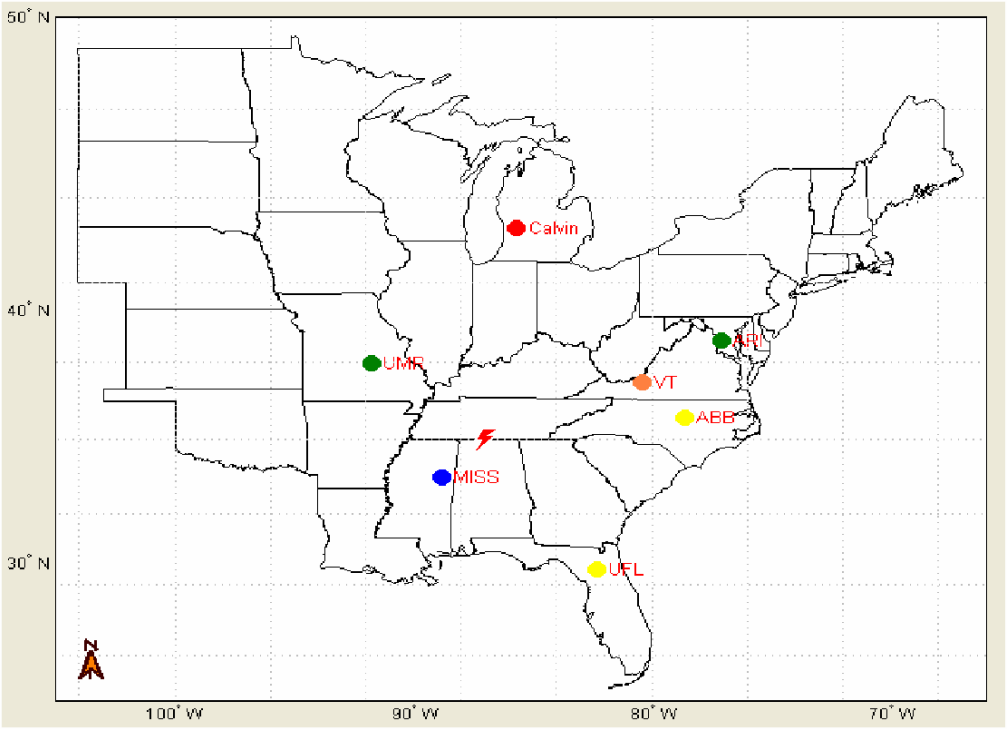

Figure 4.28 Base Case 5 possible unit grouping

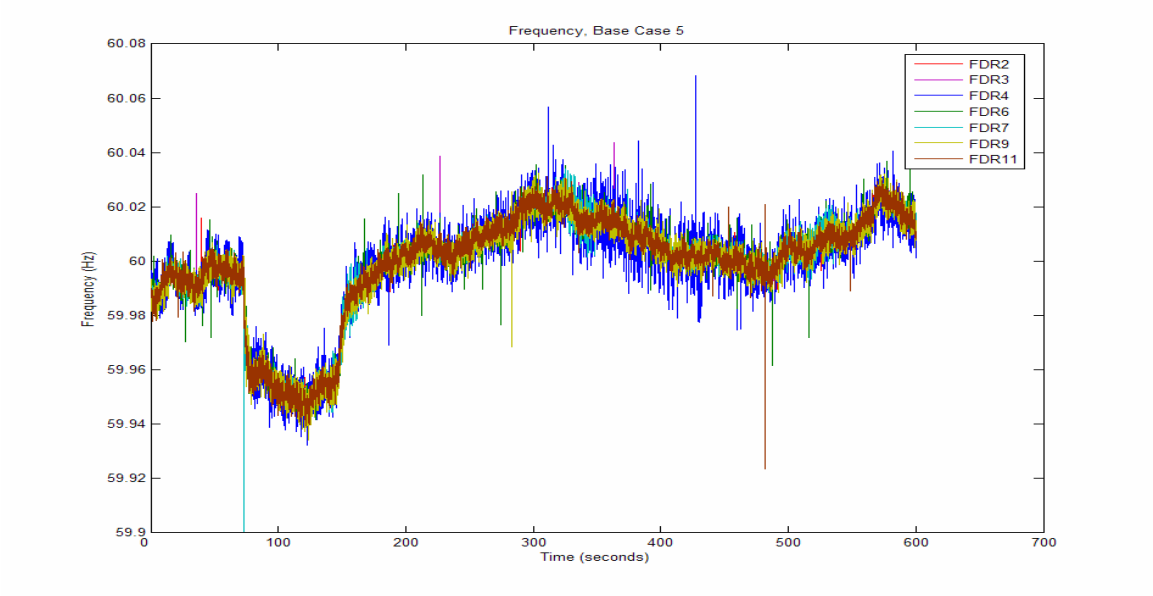

Figure 4.29 Base Case 5 raw frequency, long term

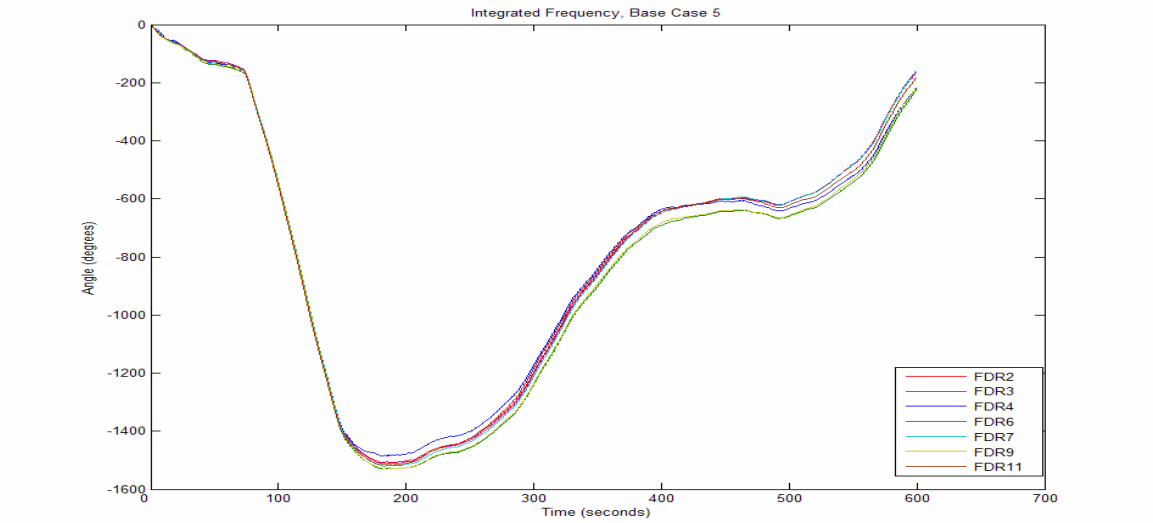

Figure 4.30 Base Case 5 angles, long term

Extended frequency and angle plots for Base Case 5 are shown above to get a better idea of the long term effects of the events. We can see that the frequency stabilizes and remains stable after the load rejection. This is reflected in the angle plot, as we can see that there are no sudden changes in the angle slope.

The extended angle difference plot gives us a mixed bag of results because some units exhibit the type of long term stability we expect. The ARI and MISS units eventually flatten out, indicating that the power flow has reached a new, stable operating point. The ABB and UFL units also flatten out briefly, starting at the 300 second mark, before dropping further.

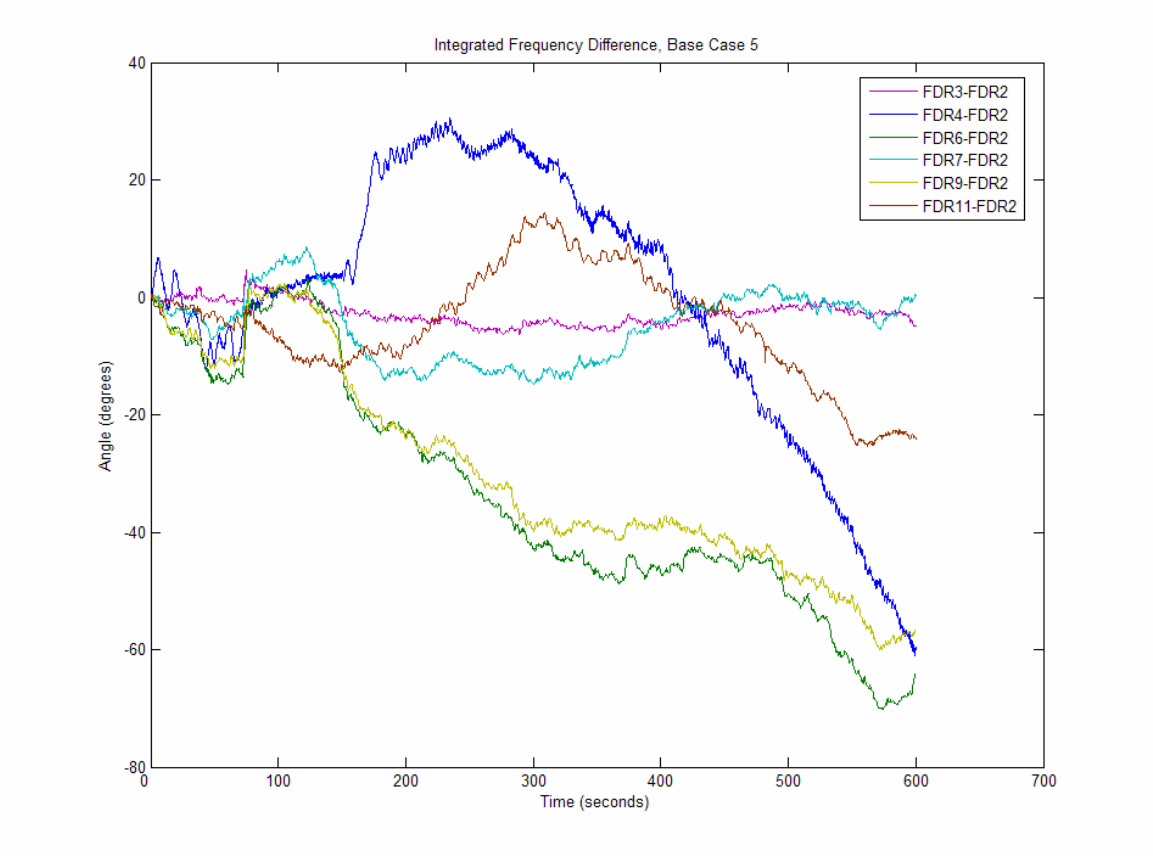

Figure 4.31 Base Case 5 angle differences, long term

4.6 Base Case 6

Base Case 6 is a typical generation trip event originating from the Cumberland plant in Cumberland City, Tennessee. The frequency plot, shown below, reveals that the operating frequency is initially higher than 60Hz before it drops to about 59.95Hz when generation is lost. Following the trip, the frequency continues to decrease until around the 130 second mark before it starts to slowly recover to pre-fault levels.

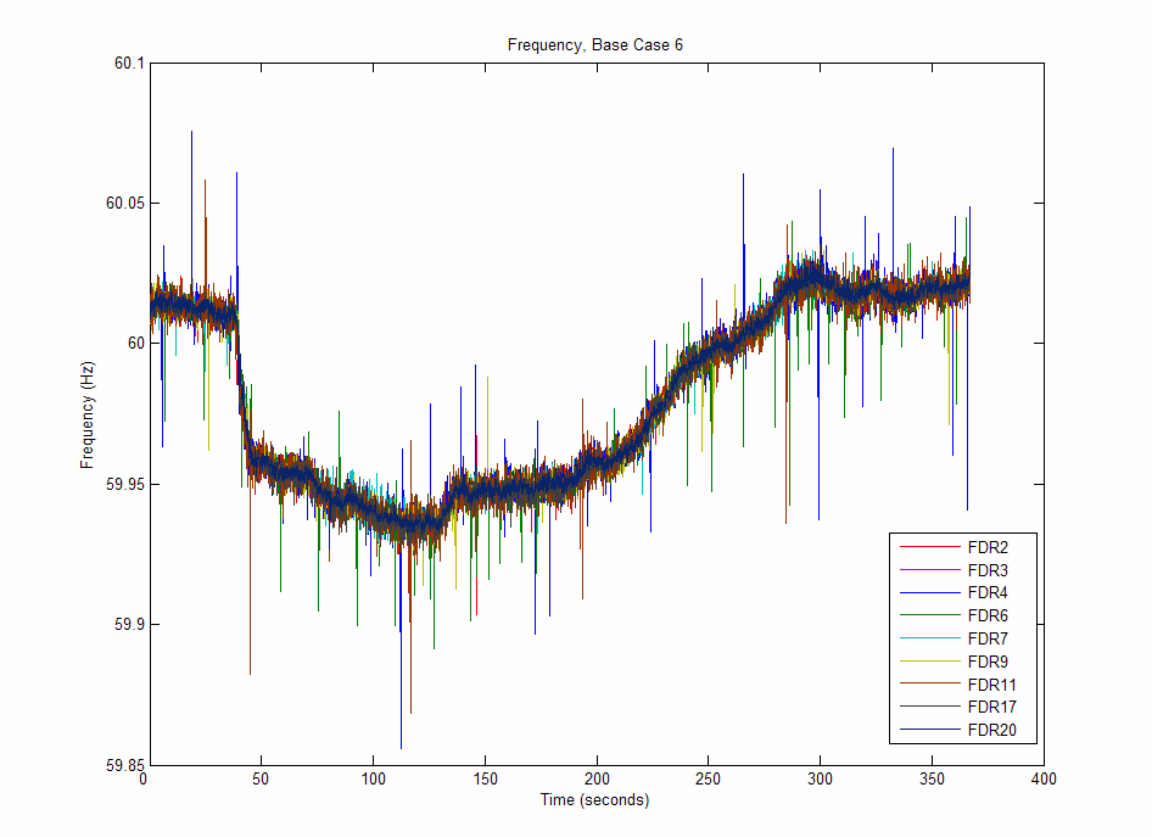

Figure 4.32 Base Case 6 raw frequency

The smoothed frequency data is shown in Figure 4.33. The frequency measurements from all units are very tightly packed throughout the event. The computed angles are also tightly packed. However, the ABB and TVA1 angles do diverge from the rest toward the end of the plot, as shown in Figure 4.34.

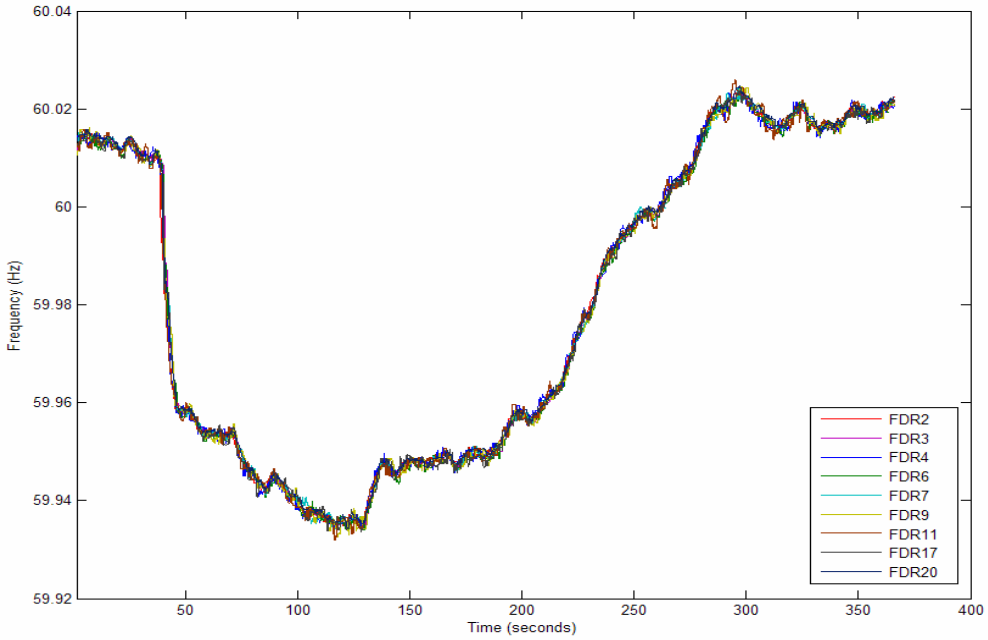

Figure 4.33 Base Case 6 frequency smoothed with a 21 point moving median

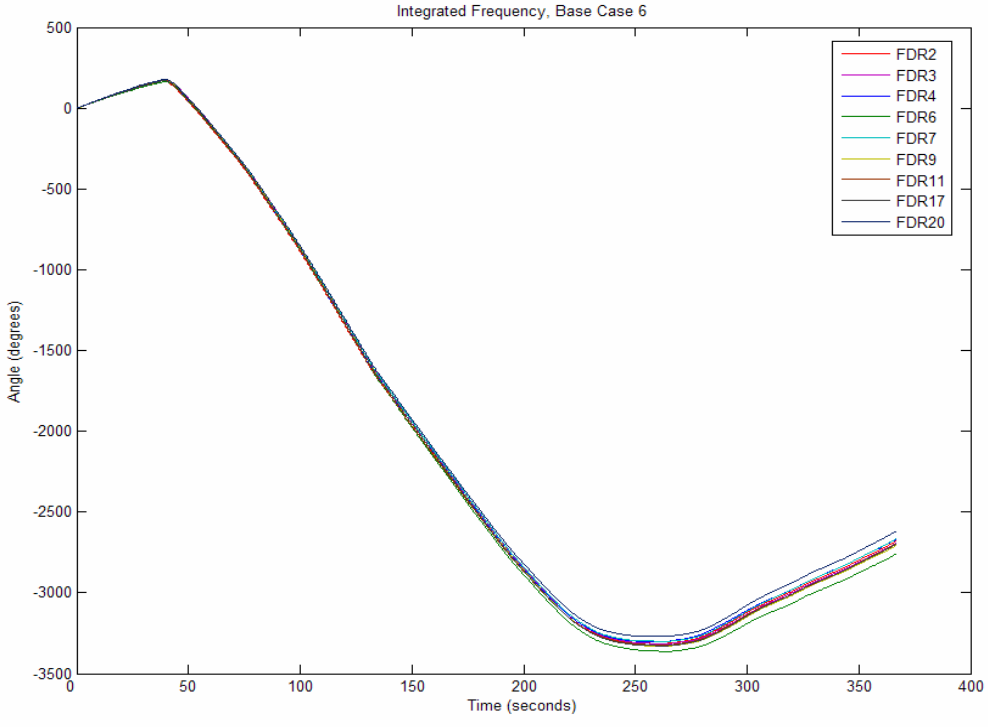

Figure 4.34 Base Case 6 angles

The angle difference plot looks very promising for this particular case. With ABB and TVA1 as exceptions, the angle differences shift when the event occurs and then quickly flatten out as the power system reaches a new operating point.

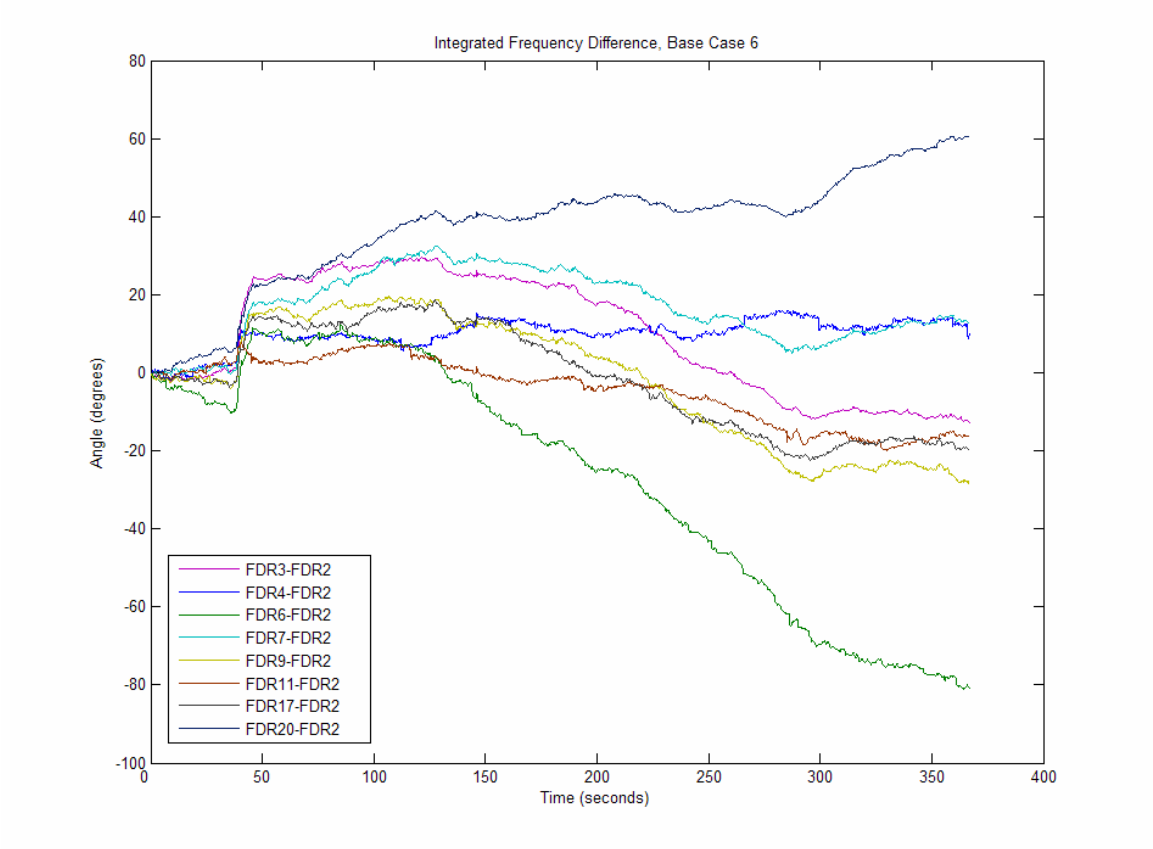

Figure 4.35 Base Case 6 angle differences

Although the angle difference plot for this case looks much better compared to the previous cases, determining the Case 6 grouping is difficult. The Tulane, UFL, and ARI units seem to be grouped because all three have similar behavior and stay fairly close to one another. Two other units, MISS and TVA1, could also possibly be grouped with those three because as Figure 4.36 shows, the same dip in angle can be seen on these two units at around the 300 second mark that is present on Tulane, UFL and ARI. Finally, the ABB, VT, and Calvin units appear to have no groups.

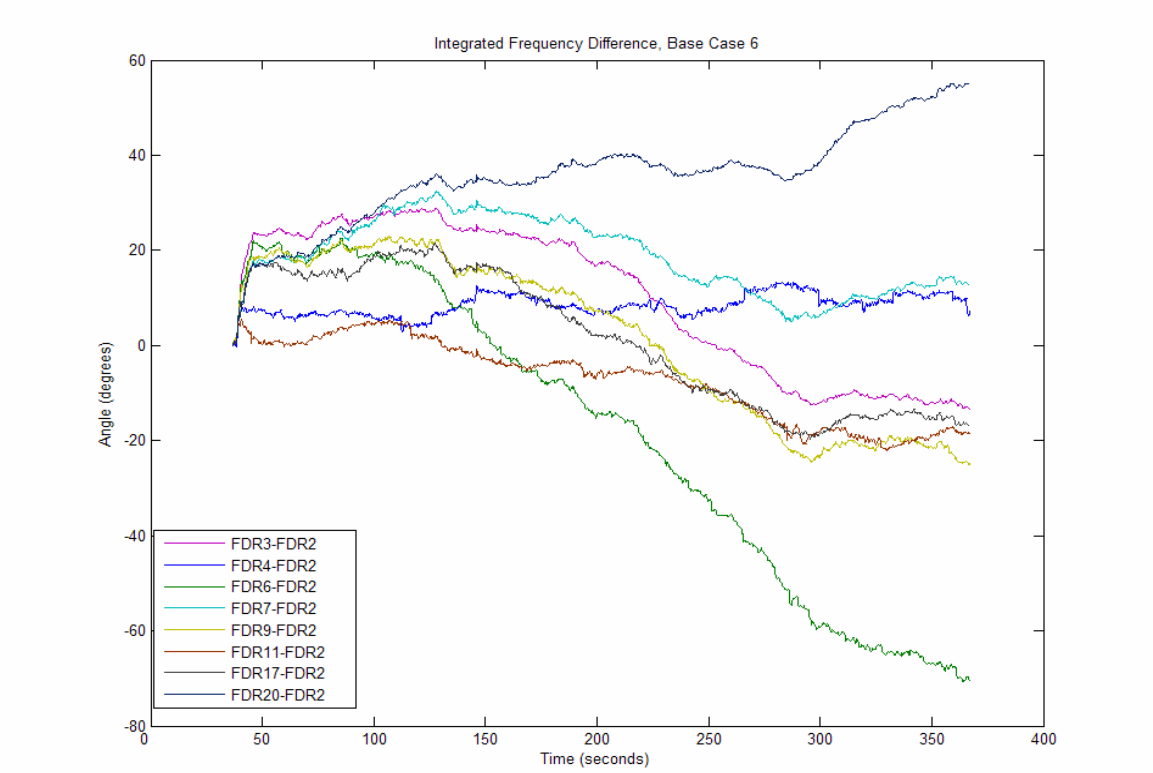

Figure 4.36 Base Case 6 angle differences, normalized prior to event

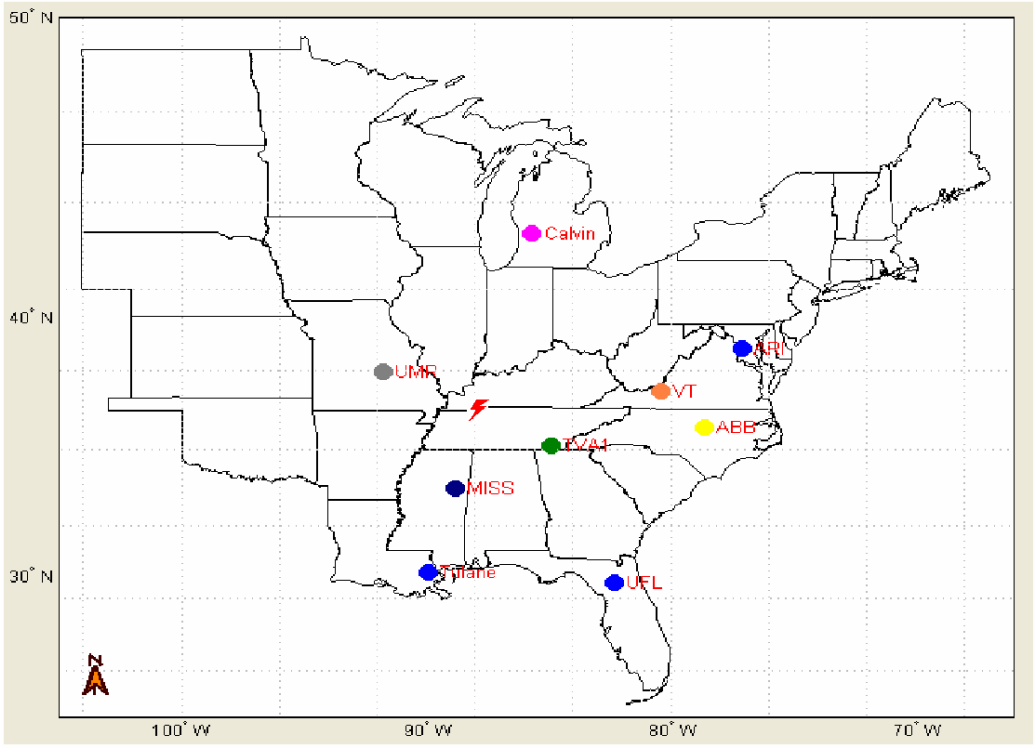

Figure 4.37 Base Case 6 possible unit grouping

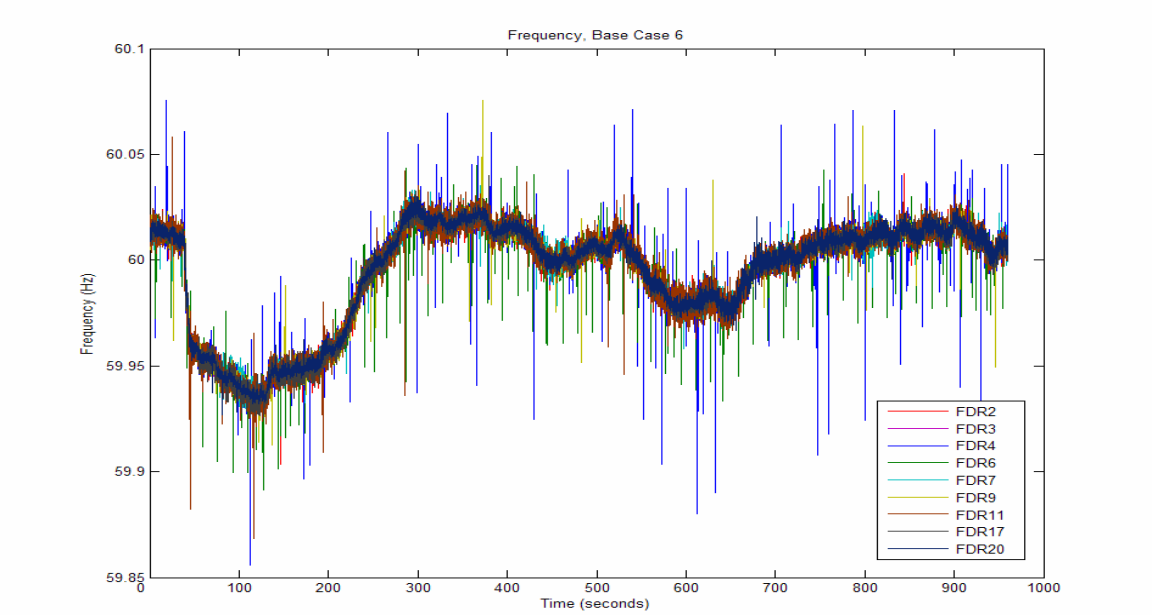

Figure 4.38 Base Case 6 raw frequency, long term

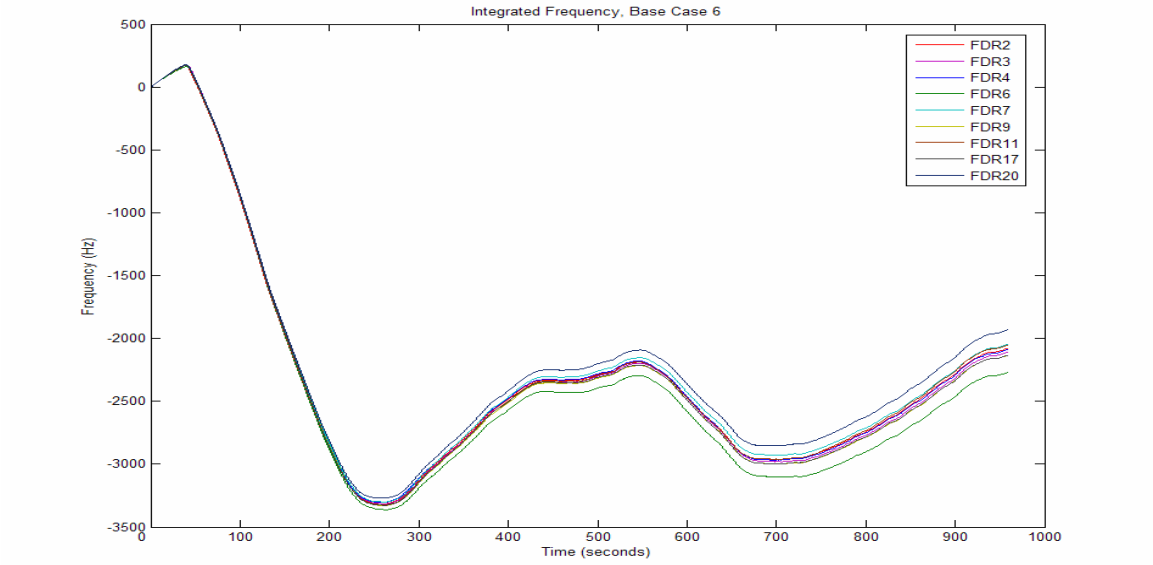

Figure 4.39 Base Case 6 angles, long term

Shown above, the long term frequency plot reveals that the frequency stabilizes after the event as does the angle. However, we notice that the TVA1 and ABB angles continue to diverge, gradually moving further from the pack. The long term angle difference plot,

shown below, reflects the TVA1 and ABB angle divergence, as the angle difference for these two units continue to separate from the rest. If we look closely, however, we can see that the shape of these two angle curves bear a slight resemblance to the flatter curves. But in the end, we cannot ignore the fact that the ABB and TVA1 units diverge tremendously.

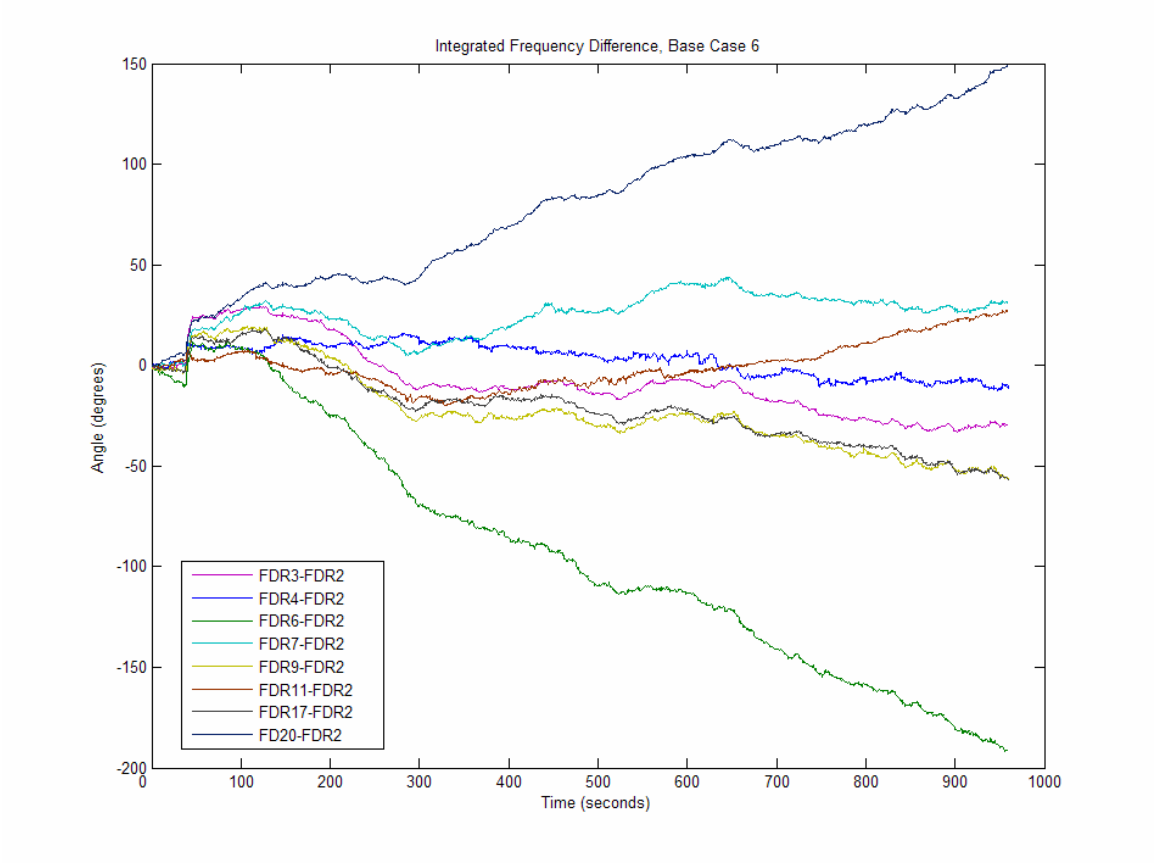

Figure 4.40 Base Case 6 angle differences, long term

4.7 Base Case 7

Base Case 7, originating at the Eastlake plant in Eastlake, Ohio, is an interesting case. Unlike the other cases, the frequency in Case 7 barely drops below 60Hz. As shown in Figure 4.41, the frequency starts at approximately 60.02Hz and then drops down to 60Hz. Unfortunately, due to missing data we only have a short time window for this case.

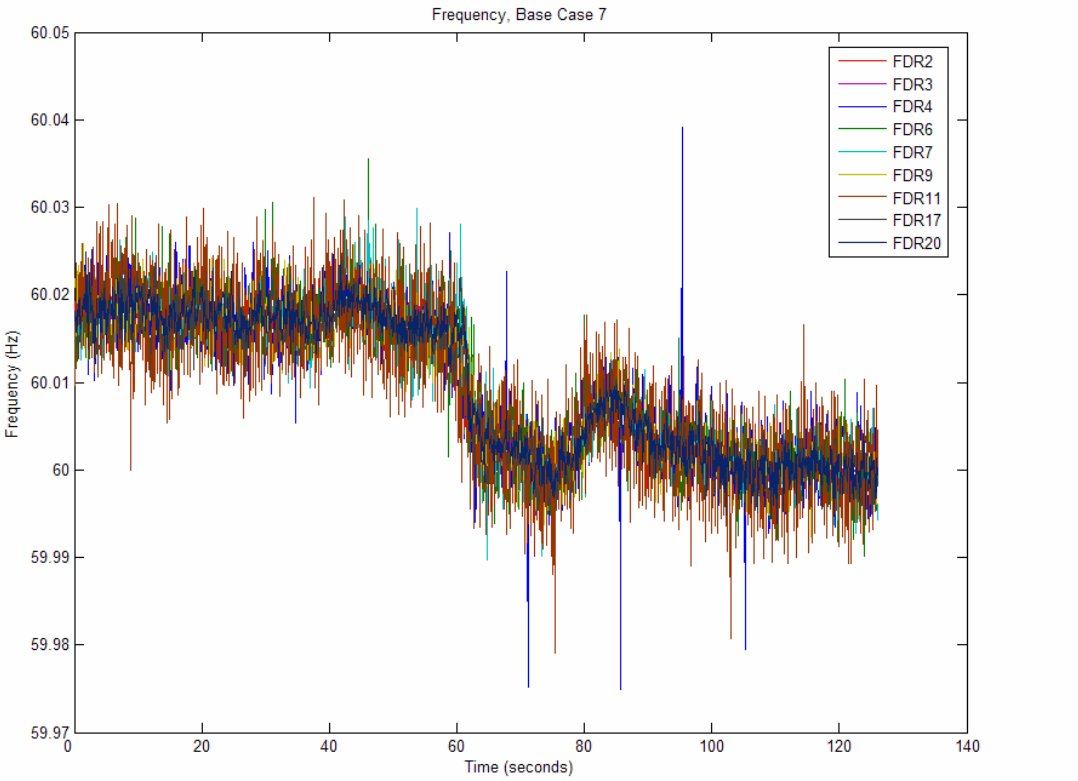

Figure 4.41 Base Case 7 raw frequency

The smoothed frequency gives us a better picture of the event, but even after smoothing, the Calvin unit still has a fair amount of noise on the signal. This noise does not cause the Calvin angle to diverge from the rest, as we can see in Figure 4.43. Since the frequency is above 60Hz most of the time, the angle increases and then flattens as the frequency drops closer to 60Hz.

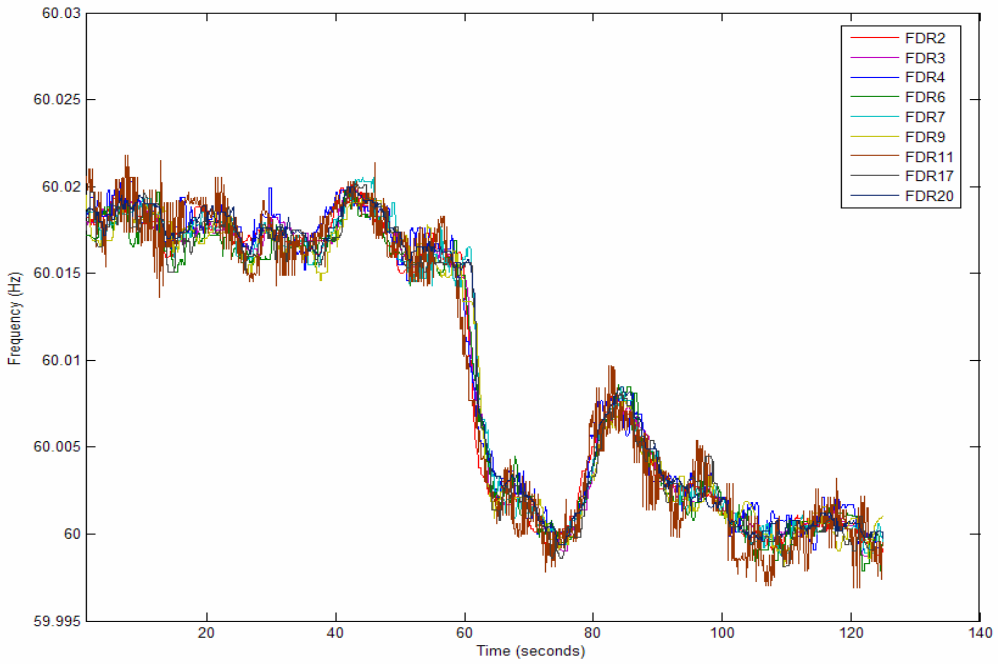

Figure 4.42 Base Case 7 frequency smoothed with a 21 point moving median

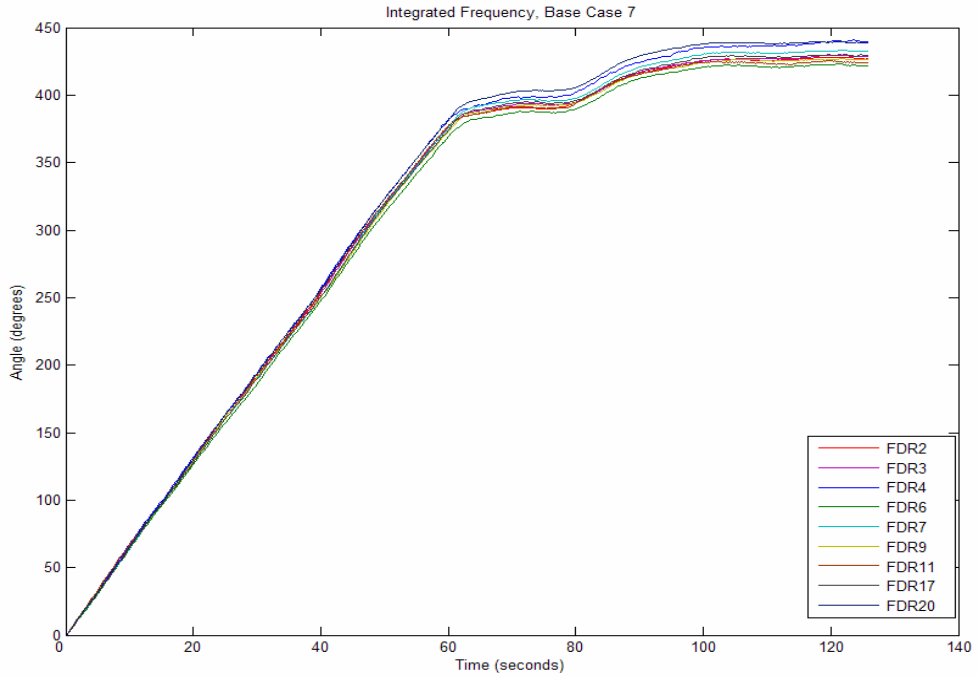

Figure 4.43 Base Case 7 angles

Upon initial inspection, the angle difference plot is hard to interpret. The Calvin unit looks unusual compared to the rest of the curves, as it appears to be more 'jagged' than the rest. This is a result of the large amount of noise in its frequency plot. Most of the remaining angle differences, however, look fairly normal, as they each jump to a new operating point when the event occurs and then flatten out. Unfortunately, our data is limited and we cannot see whether they remain flat as time passes.

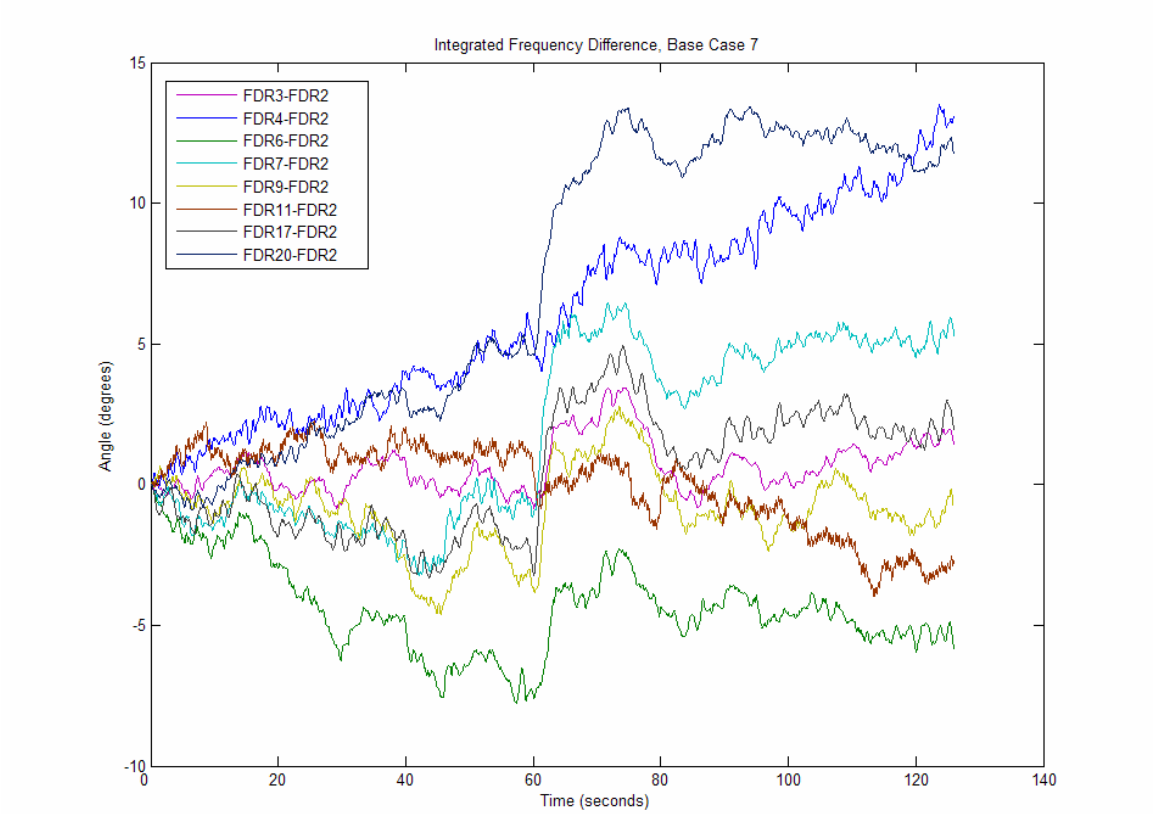

Figure 4.44 Base Case 7 angle differences

Normalizing the angle differences prior to the event, it becomes clearer that the VT and Calvin units do not follow the trend of the rest of the units. There are similarities between the remaining units, which suggest that they are possibly grouped.

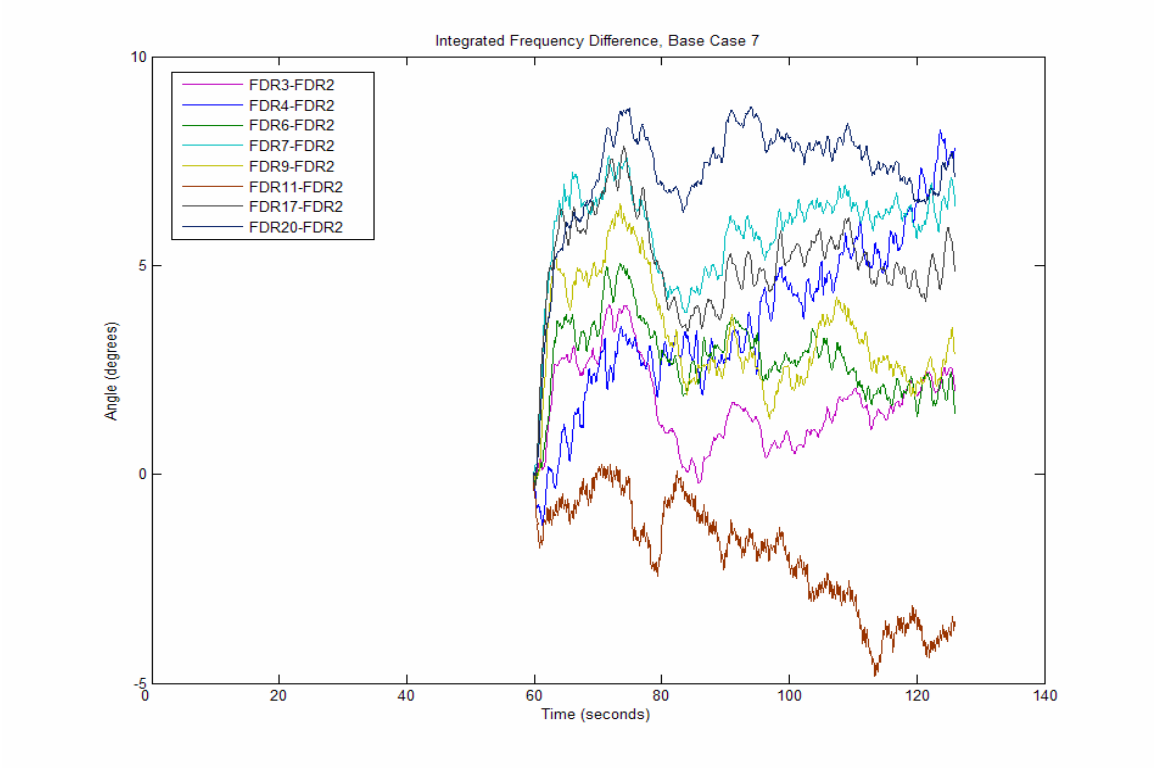

Figure 4.45 Base Case 7 angle differences, normalized prior to event

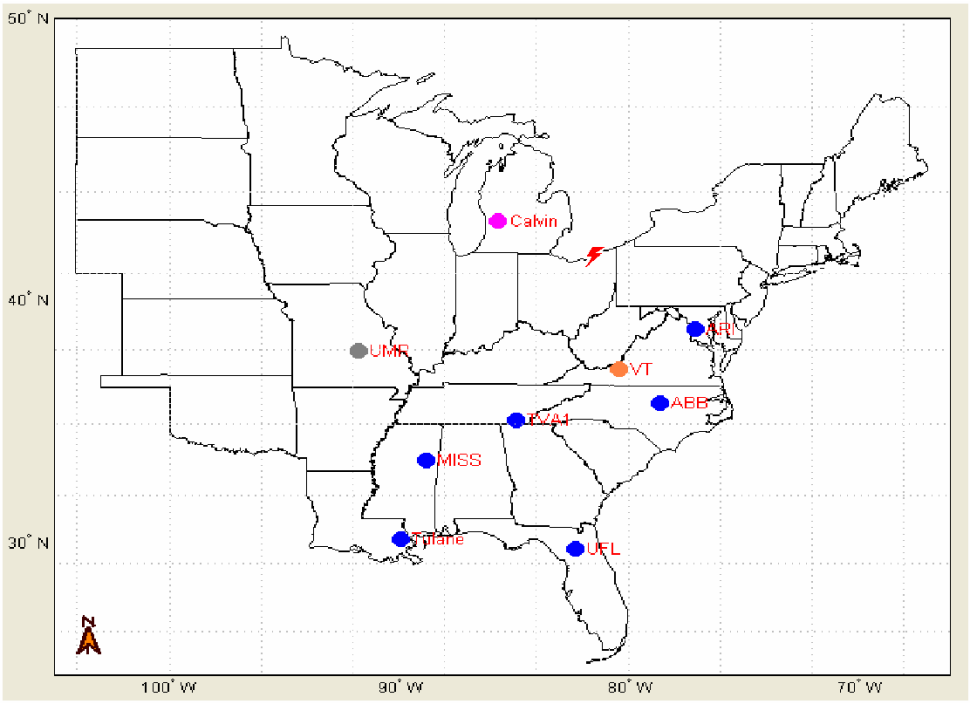

Figure 4.46 Base Case 7 possible unit grouping

4.8 Base Case 8

Base Case 8 is the result of a generation trip at the Zimmer power plant located in Moscow, Ohio. Prior to the fault, there is a brief increase in frequency, due to a load rejection. This is followed by a sharp drop in frequency, as shown in Figure 4.47. Then, the frequency continues to drop slowly for close to 90 seconds. Finally, the frequency begins a slow recovery starting just before the 150 second mark.

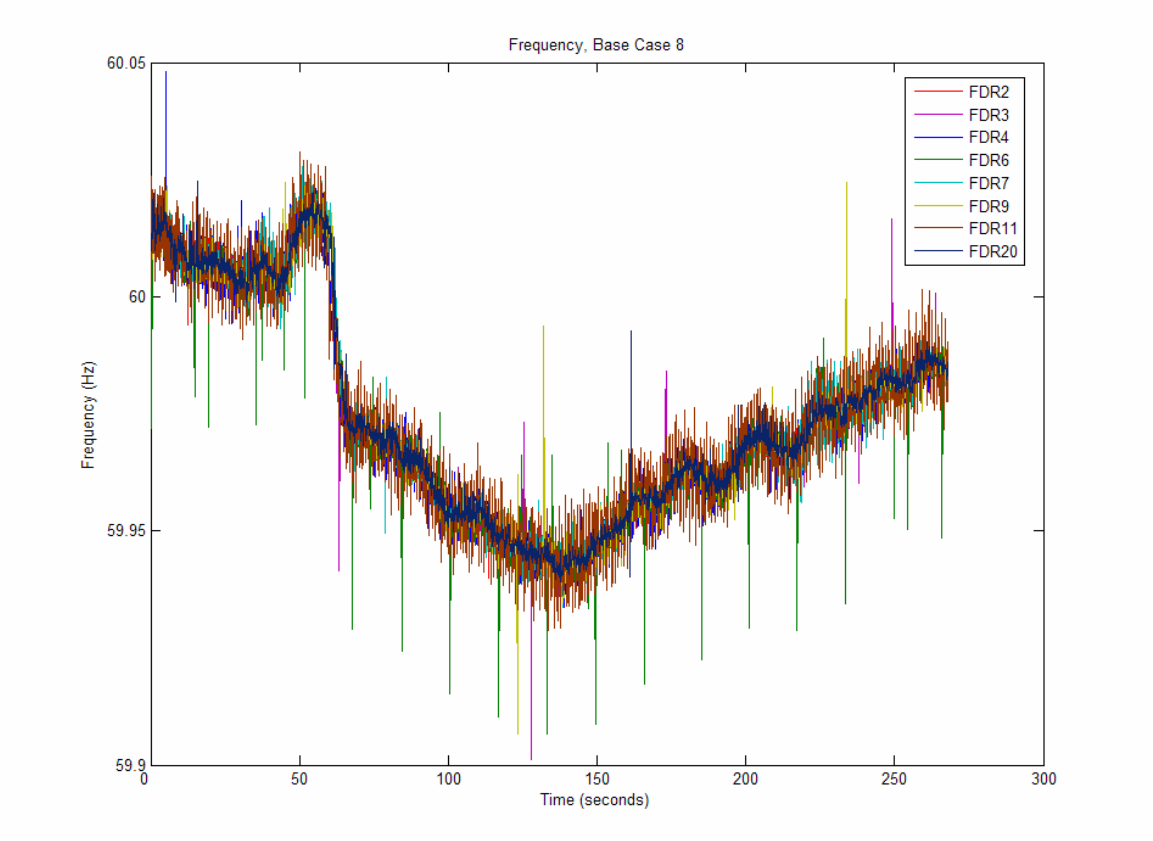

Figure 4.47 Base Case 8 raw frequency

The smoothed frequency data is shown below. The frequency measurements from each FDR are grouped tightly and no unit stands out, unlike some of the previous base cases. The calculated angles, shown in Figure 4.49, reveal that there is slight divergence toward the end of the time frame.

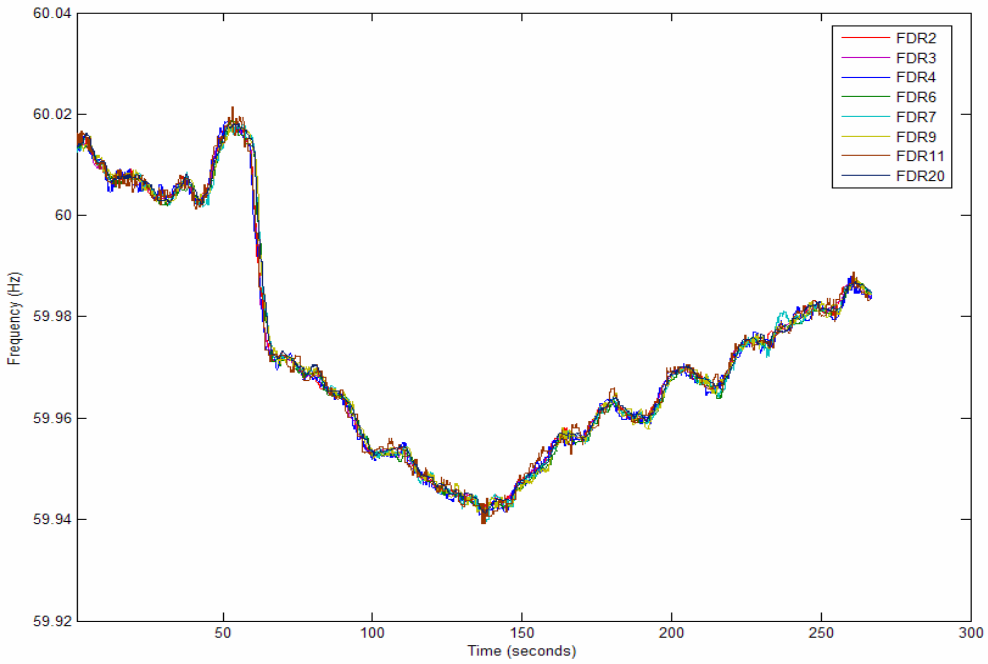

Figure 4.48 Base Case 8 frequency smoothed with a 21 point moving median

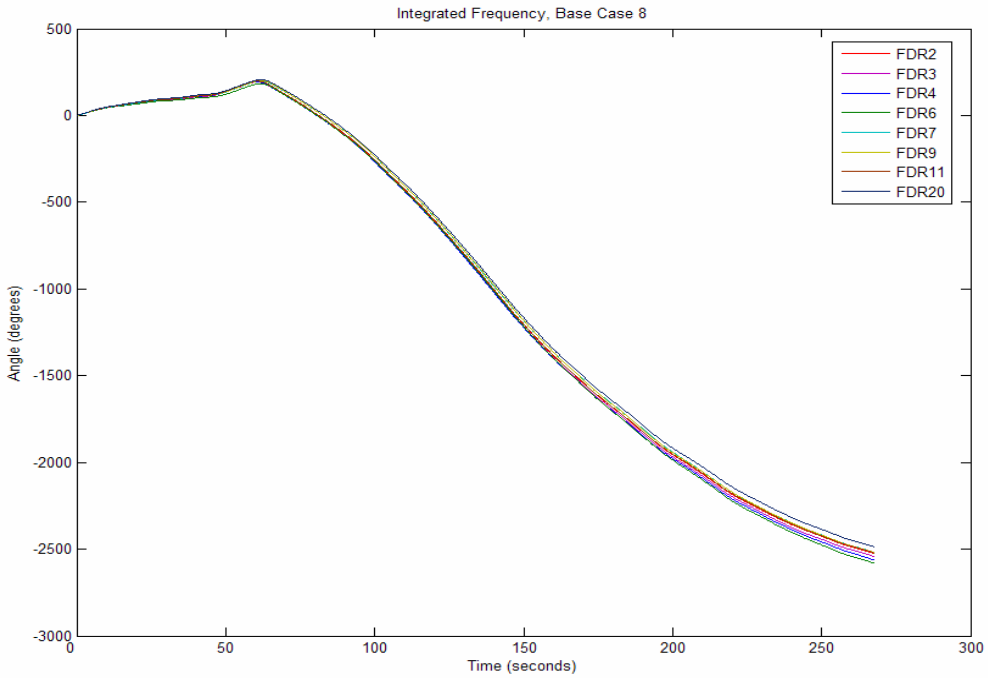

Figure 4.49 Base Case 8 angles

Looking at the angle difference plot, the Calvin unit once again appears unusually jagged compared to the other units. The ARI, VT, and ABB units all tend to drift, which is something we've seen several times already. Finally, the MISS, UFL, and TVA1 units behave the way we would expect for a generation trip event, jumping to a new operating point when the event occurs and then flattening out, indicating that the power flow to these units has stabilized.

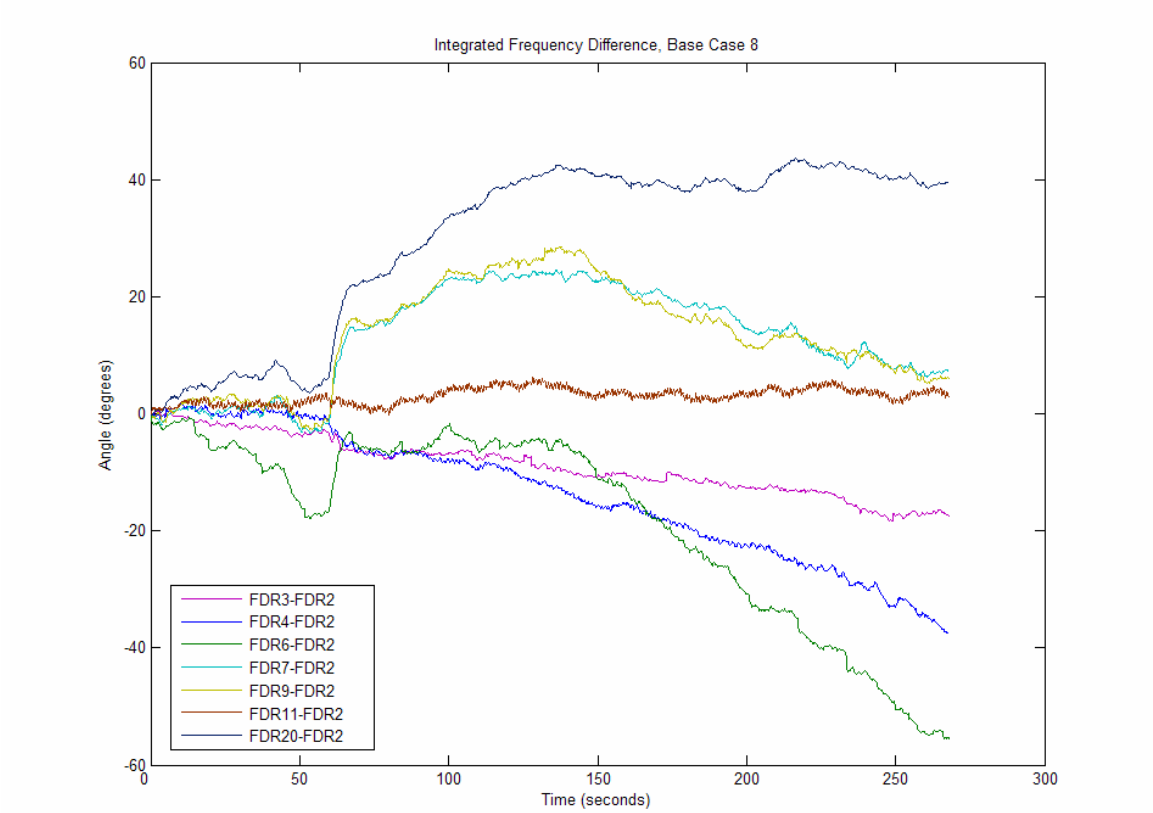

Figure 4.50 Base Case 8 angle differences

Normalizing before the event, we can focus on how the angle differences compare with each other as a result of the generation trip. It is clear that the MISS and UFL units are grouped, as they follow each other closely throughout the event. Furthermore, the Calvin and UMR units are possibly grouped because the Calvin curve remains relatively flat and close to zero, as shown below in Figure 4.51. The remaining units—TVA1, VT, ABB, and ARI—appear to be ungrouped.

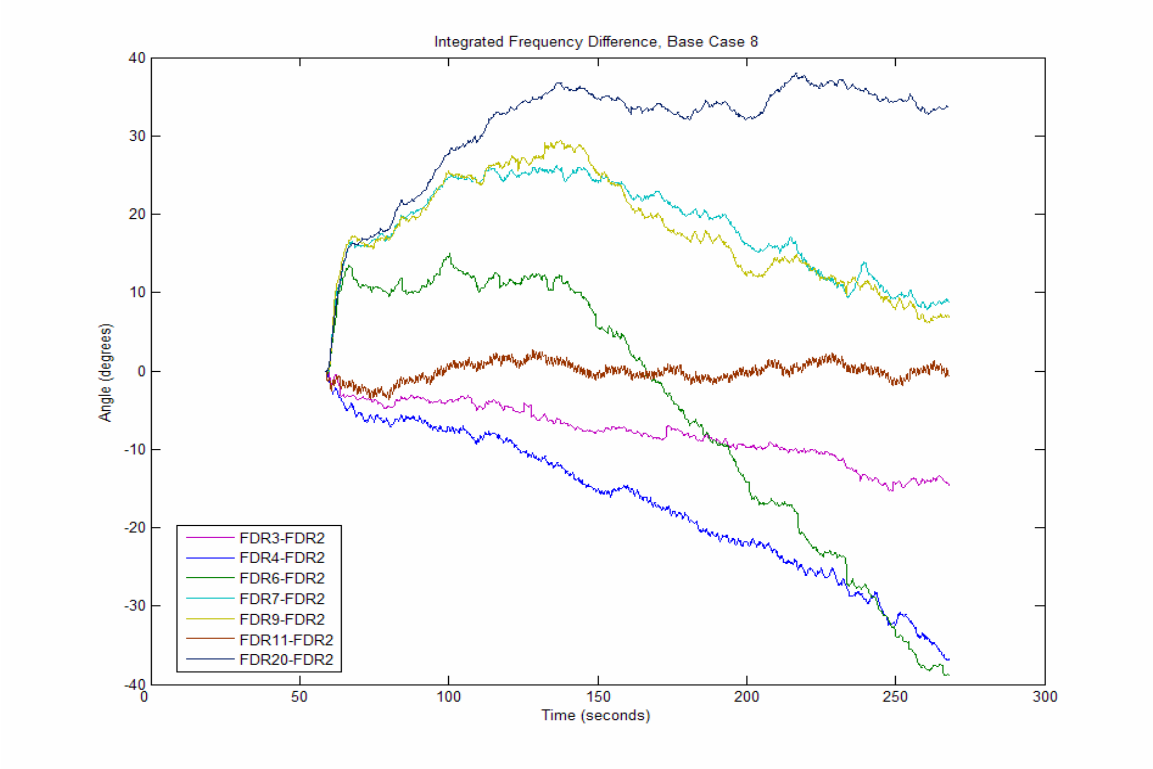

Figure 4.51 Base Case 8 angle differences, normalized prior to event

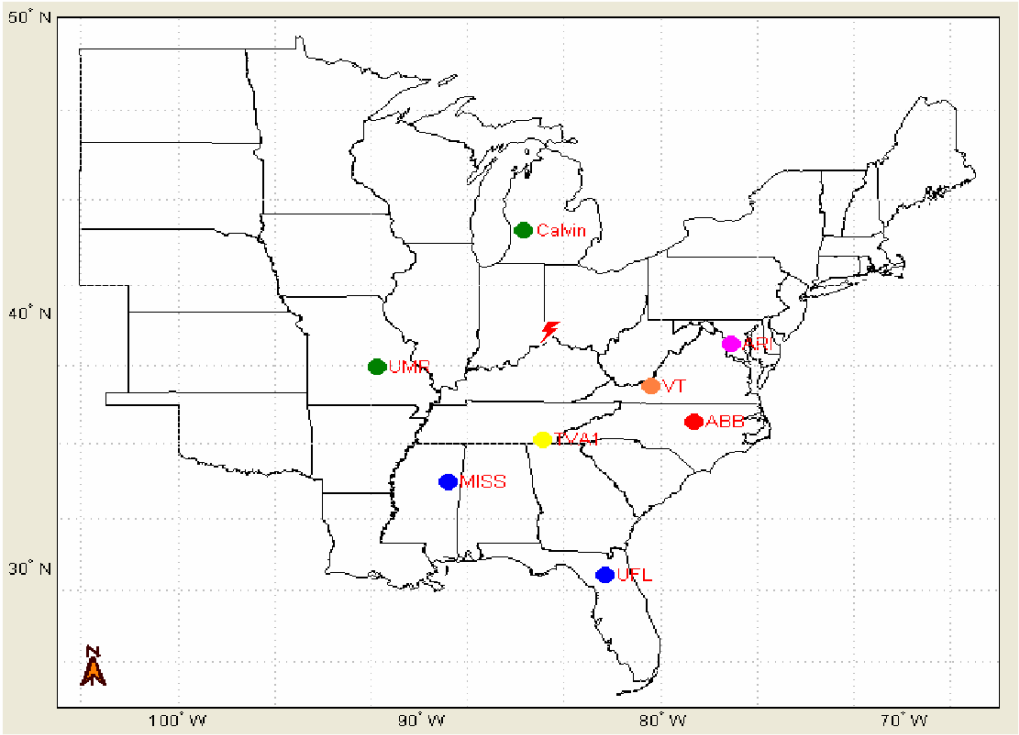

Figure 4.52 Base Case 8 possible unit grouping

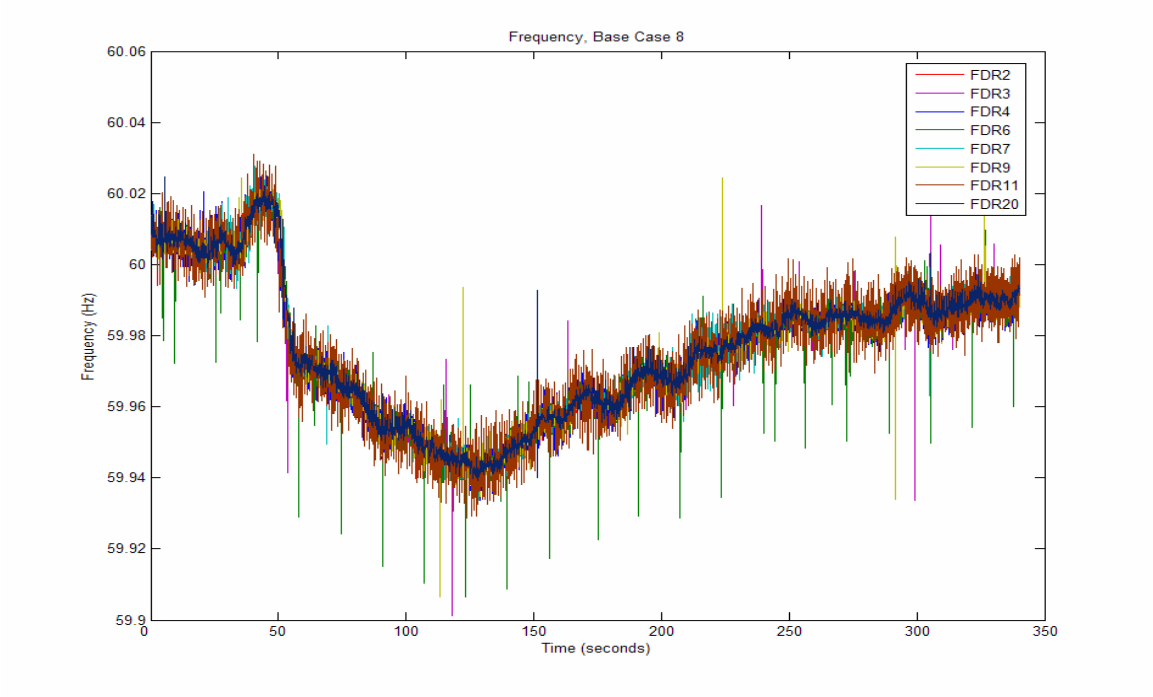

Figure 4.53 Base Case 8 raw frequency, long term

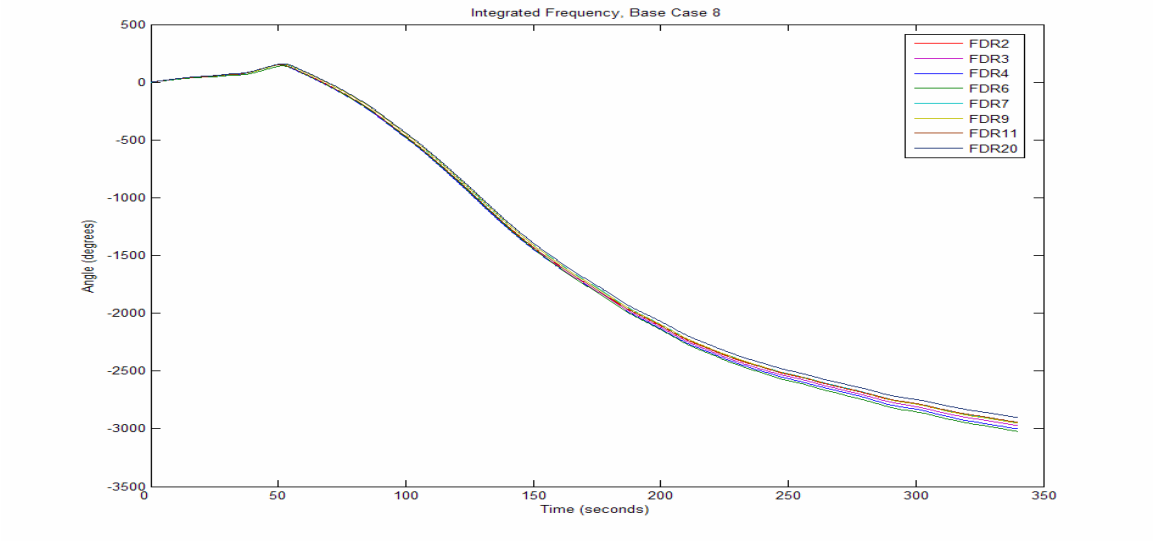

Figure 4.54 Base Case 8 angles, long term

Over a longer time period, we can see that the frequency eventually recovers and stabilizes just below 60Hz. The angle plot reflects this, though we can see that the angles continue to diverge. The long term angle differences, below, also continue the trend

we've seen earlier, with the ARI, VT, and ABB units maintaining their drift. Finally, the Calvin, MISS, UFL, and TVA1 angle differences continue to be fairly stable.

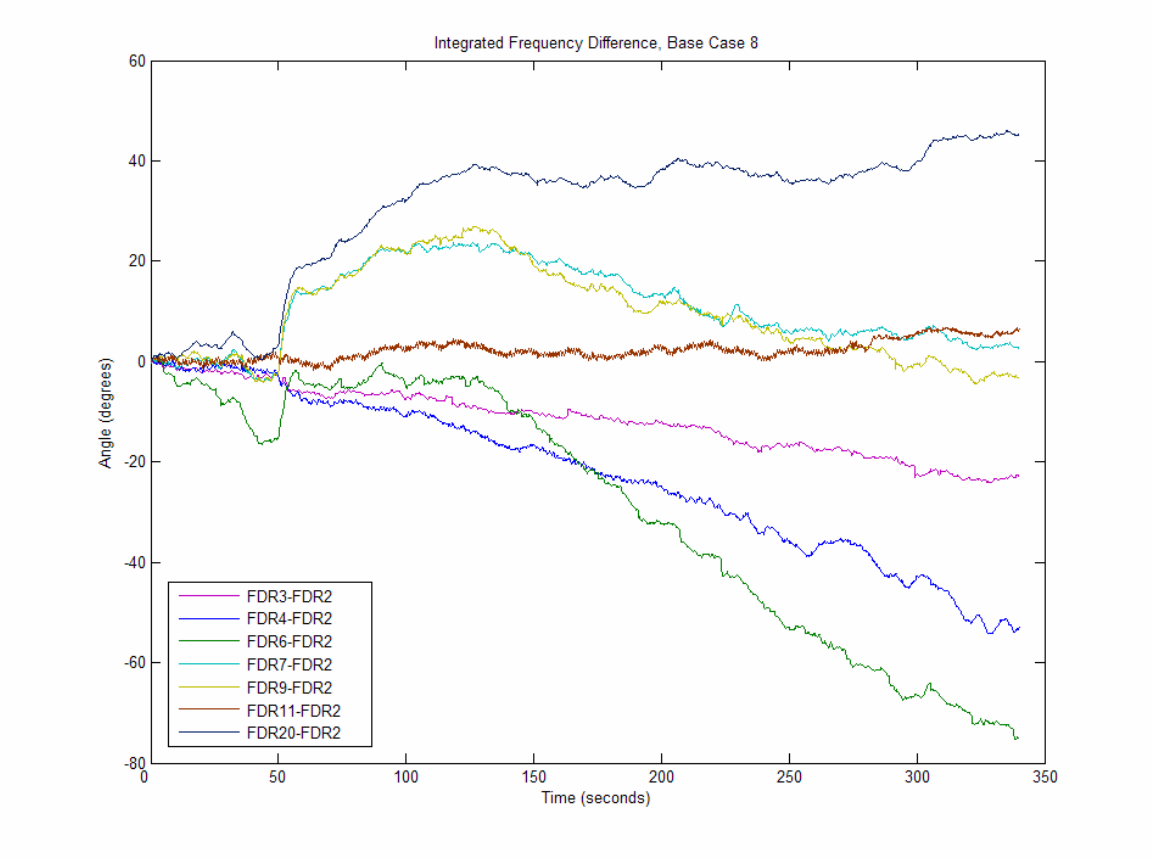

Figure 4.55 Base Case 8 angle differences, long term

4.9 Base Case 9

The final base case in our set, Base Case 9, is a fairly large generation trip originating at the Votgle-Wilson plant in Waynesboro, Georgia. As we can see in Figure 4.56, the generation trip causes the frequency to drop all the way down to around 59.94Hz. The frequency remains at that level for the rest of the window. Eventually, the frequency recovers, as we will see in the long term plots.

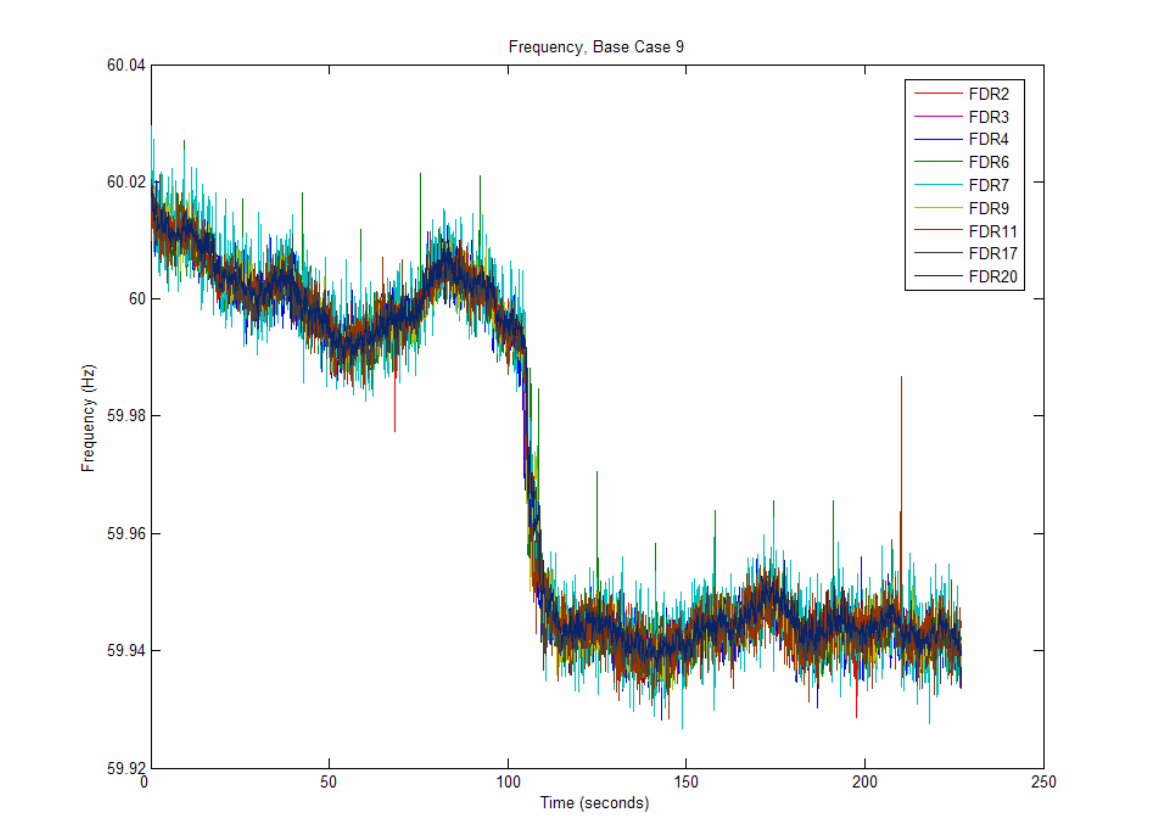

Figure 4.56 Base Case 9 raw frequency

The smoothed frequency, in Figure 4.57, looks normal for a generation trip event. Frequency measurements for all nine FDRs are tightly packed throughout the event, which results in the angle plot shown in Figure 4.58. Unlike some of the previous cases, the angles remain tightly grouped and there is minimal divergence toward the end of the plot.

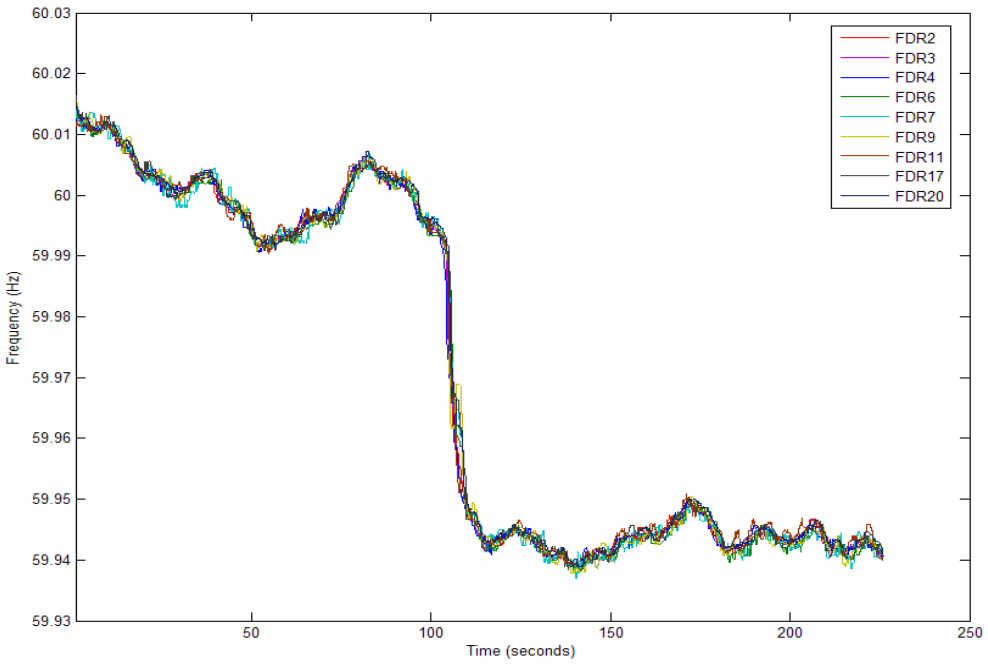

Figure 4.57 Base Case 9 frequency smoothed with a 21 point moving median

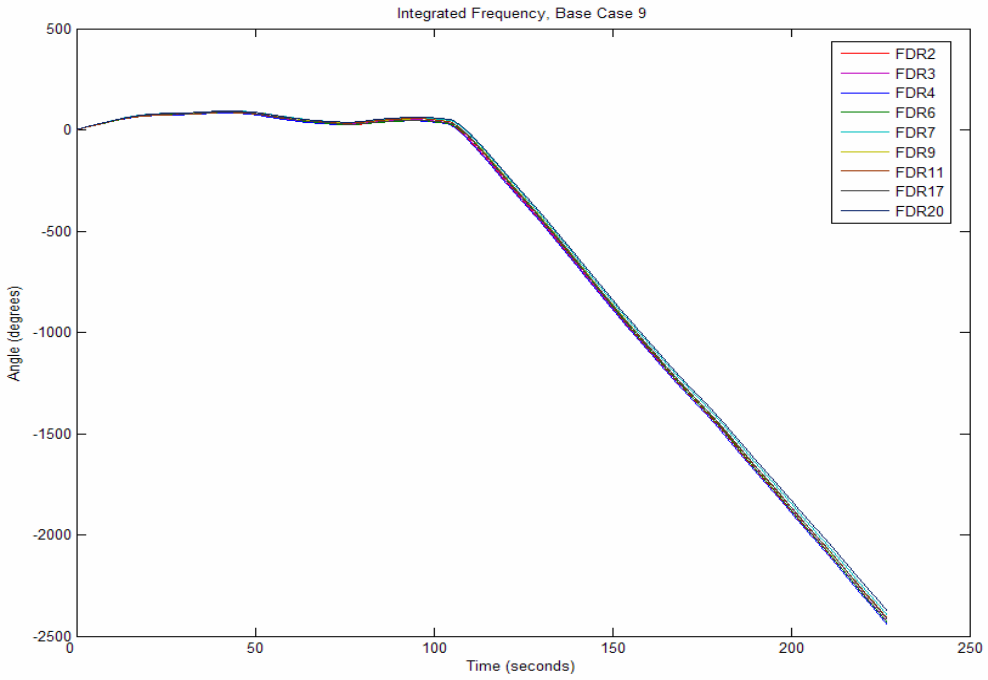

Figure 4.58 Base Case 9 angles

Base Case 9 produces the best angle difference plot in the entire set of base cases. As shown below, the angle difference plot for this case resembles the plot for the simulated case in Section 4.1. It is encouraging that none of the units show any substantial drift, which is something that has plagued us in other base cases.

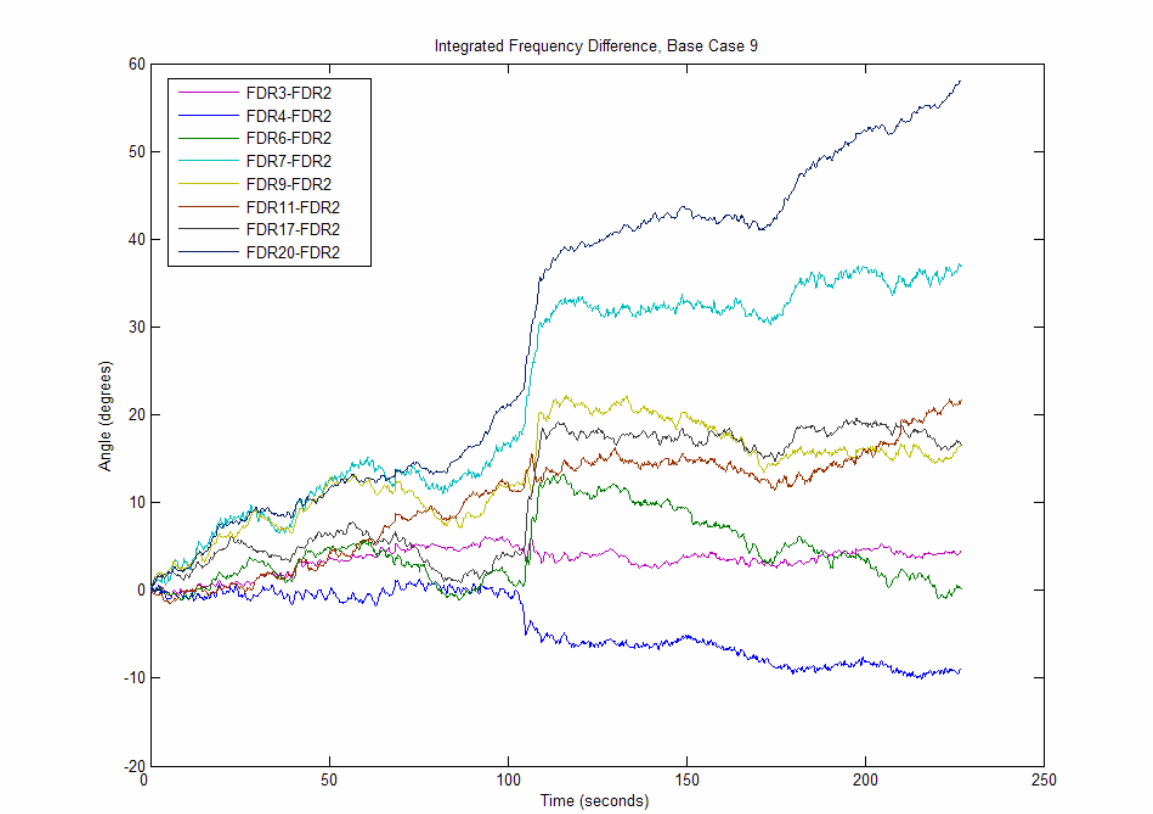

Figure 4.59 Base Case 9 angle differences

Normalizing the angle differences prior to the event, we get the plot shown in Figure 4.60. Based on the plot, we can determine three possible FDR groups: UMR and ARI, ABB and UFL, MISS and Tulane. The Calvin, TVA1, and VT units appear to be ungrouped. A map of the possible grouping for this case is illustrated in Figure 4.61. The grouping seems logical from a geographical point of view, as the FDRs in each group have relatively close distances to the location of the event.

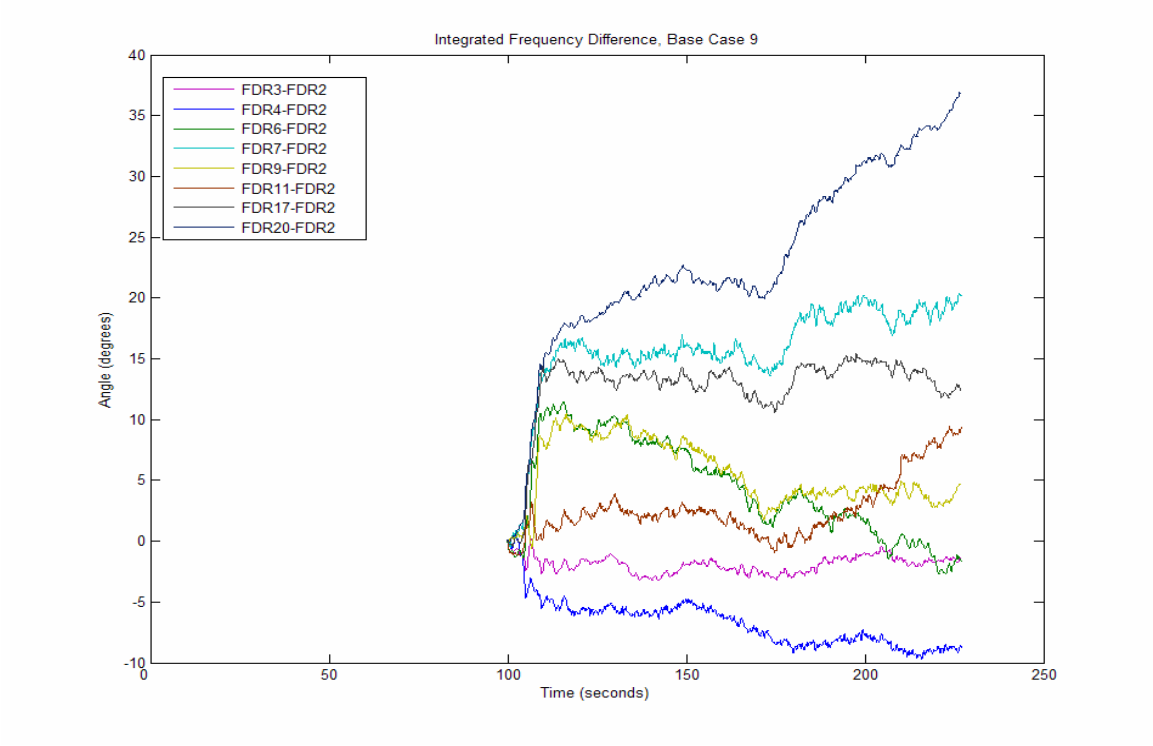

Figure 4.60 Base Case 9 angle differences, normalized prior to event

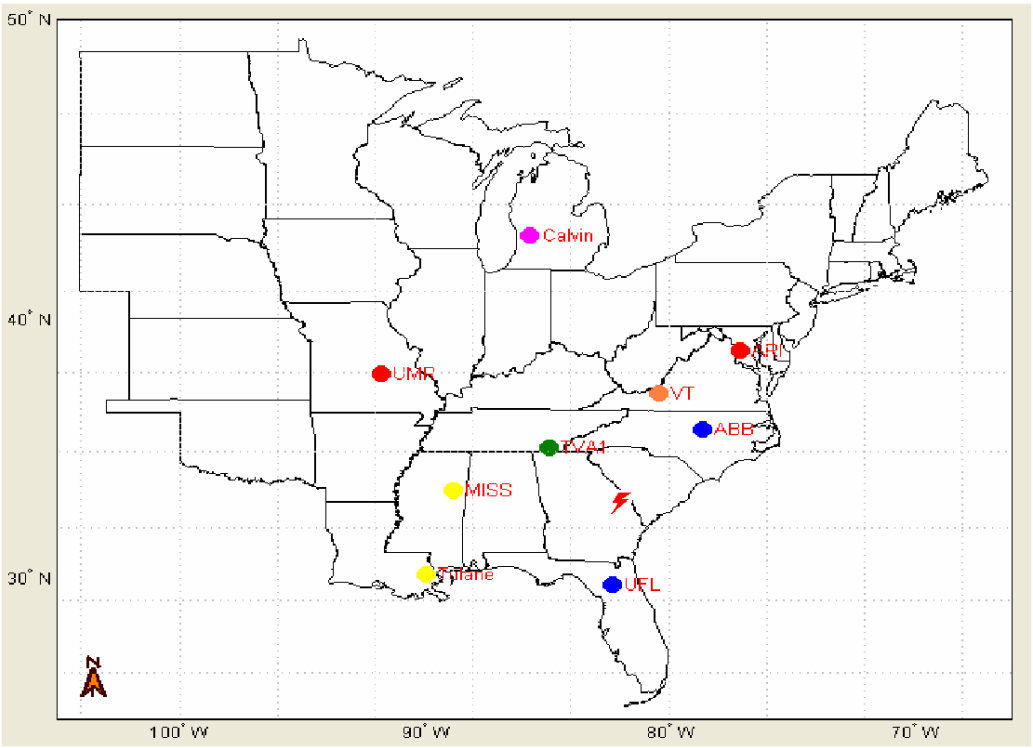

Figure 4.61 Base Case 9 possible unit grouping

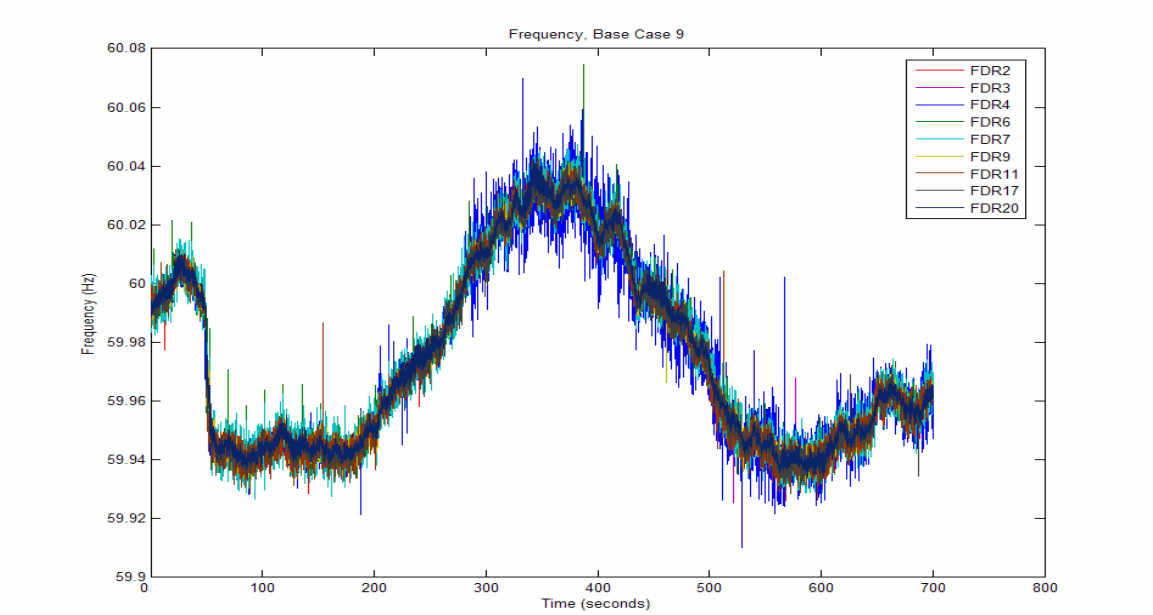

Figure 4.62 Base Case 9 raw frequency, long term

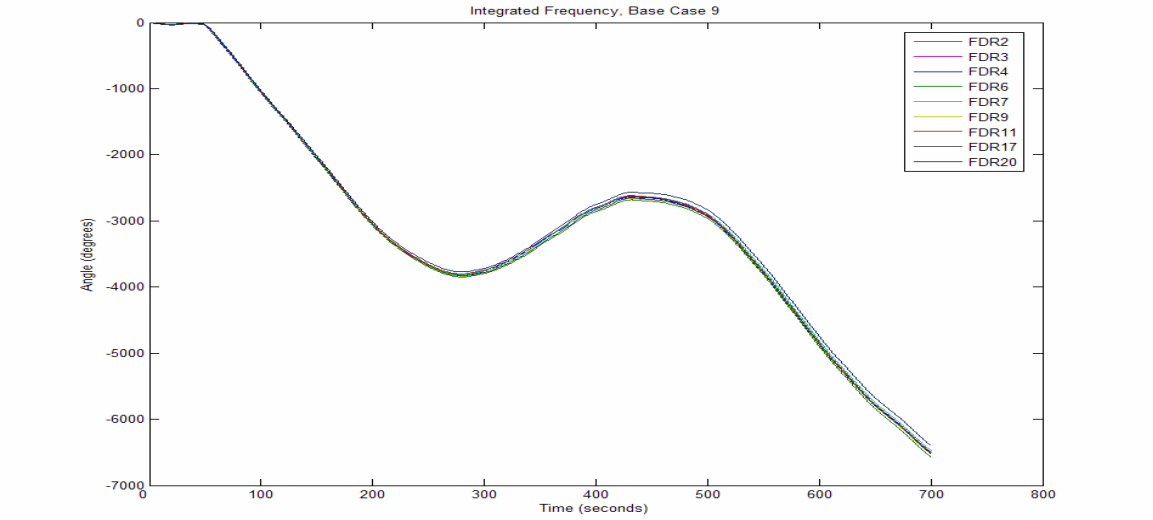

Figure 4.63 Base Case 9 angles, long term

Long term frequency and angle plots, shown above, reveal that the frequency recovers but doesn't necessarily stabilize. Instead, the frequency reaches a point above 60Hz, then slowly drifts to a point well below normal power system operating frequency, and finally starts to increase slowly.

Below, the long term angle difference plot shows that after a brief period of stability, the angle differences start to diverge over time. The TVA1, MISS, UFL, Tulane, and ABB curves all have a similar shape and are all the closest units surrounding the event.

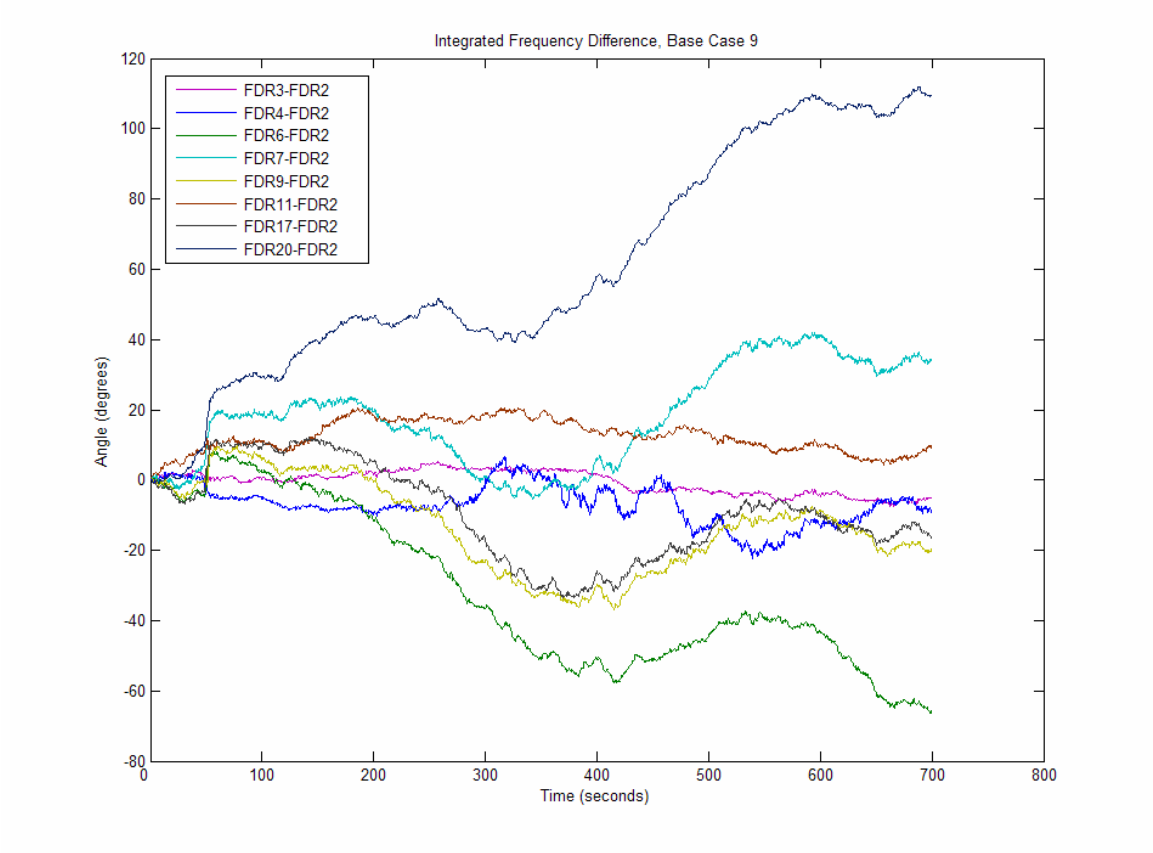

Figure 4.64 Base Case 9 angle differences, long term

4.10 Angle Movies

While the angle difference plots give us a good view of the angle separation during an event, we would like to find a way to visualize the data geographically. The figures on the following pages are snapshots of angle difference movies created for each base case. Each frame of each video is composed of a cubic fit surface plot of the angle differences computed for each FDR with respect to the UMR unit. The snapshots chosen for each case are selected at particular time stamps to show the contrast between before and after the event. Finally, note that the VT unit is not present in cases 1, 2, 3, and 7 due to the unusual angle difference behavior in each of those cases.

With the exclusion of the VT unit in Case 1, only five units remain, with each unit at the boundary of the surface, as shown in Figure 4.65. The first two snapshots show the angle differences before the event occurs and the surface is fairly flat. Then the third snapshot shows how the angles shift as a result of the event. The surface plots would indicate that power is flowing from the ARI and MISS areas to the rest of the system (since power flows from areas with a leading angle to areas with a lagging angle) if we were measuring the angles at the transmission level and if the angles were not normalized. However, this is not the case for our study, and we cannot make such claims. The movies do show us, though, which areas have an increase or decrease in power generation.

Base Case 2 is similar to Case 1 because the units are at the perimeter of the surface plot. The first three screenshots show that the angle differences stay pretty close to zero before the event occurs. Then, the next three screenshots show that when the event occurs in Tennessee, the angles in the Northeast and in Mississippi start to lead. Eventually, they start to fade while the ABB unit lags more and more. This is a plausible scenario given the amount of generation in the Northeast and around Mississippi.

Base Case 3 again has FDRs at the boundaries of the surface plot. The first two screenshots show the angle difference activity before the event, while the last four show the activity after the event. We can see a noticeable shift when the event occurs. It is

surprising that the MISS unit angle starts to lead after the event given that it is the closest unit to the power plant with the tripped generation. This could, however, be due to the fact that our FDR set for this case is very limited. Another thing we notice is that the ABB unit angle again starts to lag behind as time passes.

The event location for Base Case 5 is the same power plant that is responsible for Base Case 3. Yet, the angle difference surface plots paint a very different picture, as shown in Figure 4.68. This is probably due to the fact in Base Case 5 the generation trip is immediately followed by a possible load rejection. Furthermore, the VT unit is plotted for this case and tends to dominate the surface. The first two snapshots show the angles before the event and we can see that there is not much activity. The third and fourth snapshots illustrate the activity after the generation is lost. The last two show the angles after the load rejection. We can see that there is not much difference between the pre- and post-generation trip surface plots. After the load rejection, the VT unit angle starts to lead and the ABB and UFL units begin to lag. It was stated earlier, though, that the VT unit data is unusual for this particular case and possibly the result of a malfunctioning device.

The movie snapshots for Base Case 6 are shown in Figure 4.69. The first two frames depict the angle difference behavior before the event and the rest of the frames show the angle difference surface plots after the event occurs in Tennessee. Prior to the event, the angle differences are fairly constant and close to zero. Immediately after the event, we can see that the angles near the TVA1 unit and the ARI unit start to lead. Eventually, the angles in the TVA1 area start to dominate and the ABB angle starts to lag tremendously. So far, the ABB unit has shown this behavior in each case. Also, it is interesting to see that the TVA1 angle starts to lead even though is very close to the event.

Figure 4.70 shows the movie screenshots for Base Case 7. The first three frames show the surface plots before the event and the rest show the surface plots after the event. We can see that even before the event occurs, the TVA1 angle starts to lead and the ABB unit

starts to fall behind. When the event occurs, the TVA1 angle increases and the ABB and Calvin units fall behind.

Base Case 8 is shown in Figure 4.71 with the first two frames showing pre-event angle behavior and the last four showing post-event angle behavior. Prior to the event, we can see that the angles are fairly even with the drifting ABB unit as the exception. When the generation is lost, we can see a contrast between the eastern half of the surface plot and the western half. Once again the TVA1 unit leads all FDRs and the ABB unit falls behind.

The angle differences for Base Case 9 produced the best looking plot out of all the cases and also produce an interesting surface plot video. The first three frames show the surfaces before the event occurs and we can see that the TVA1 and MISS angles start to pull ahead. Then, when the event occurs in Georgia, the plotted area becomes partitioned. The areas surrounding the VT, ABB, ARI, and UMR units stay fairly close to zero while the rest of the units lead. Once again, the TVA1 and MISS units pull ahead the furthest.

The angle difference surface plot movies do give a new way to look at FNET data. Once again, this is our first real look at the voltage angles in the EI and a great deal of development and refinement must be done before we can do further analysis.

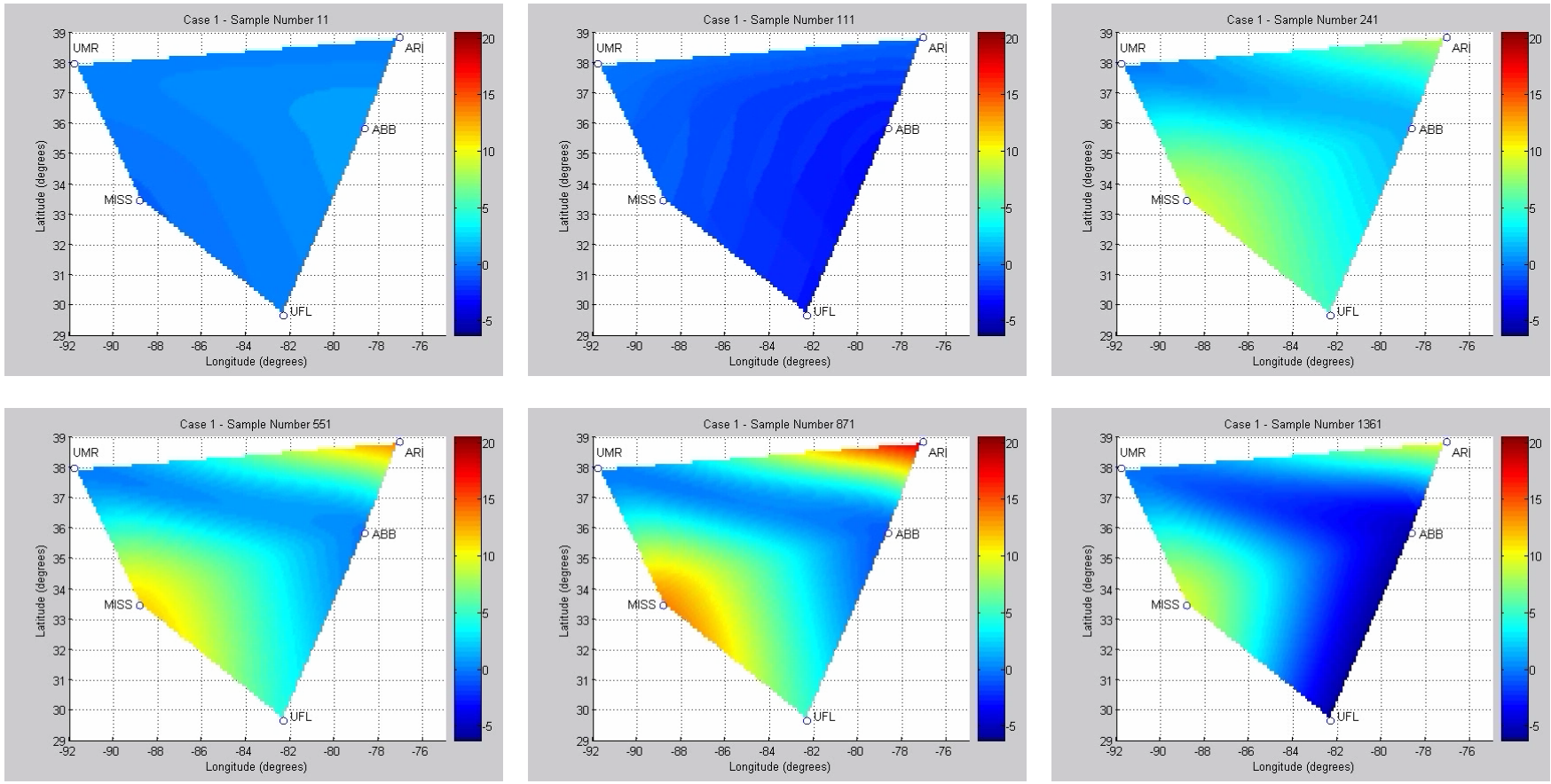

Figure 4.65 Base Case 1 video screenshots

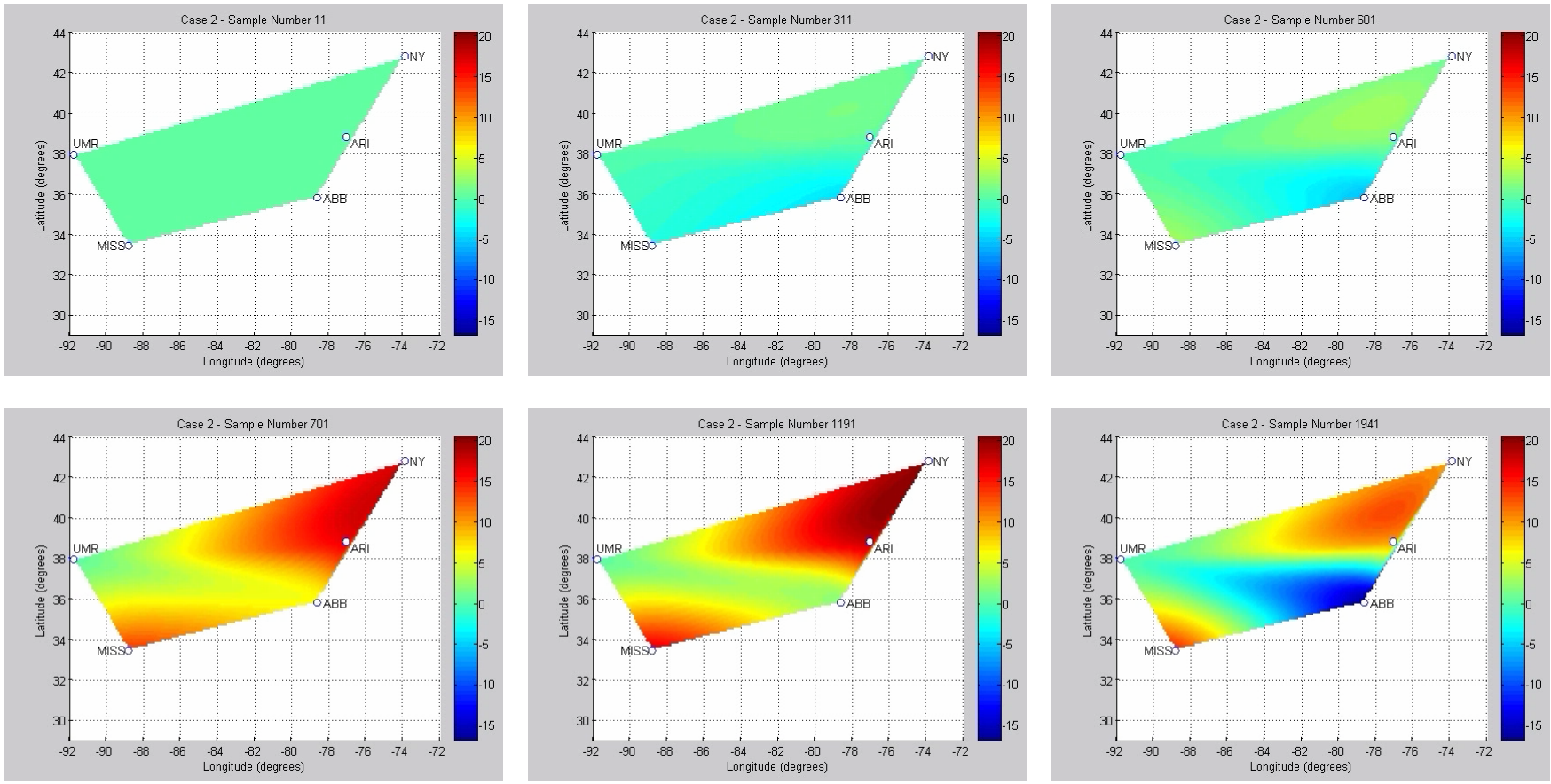

Figure 4.66 Base Case 2 video screenshots

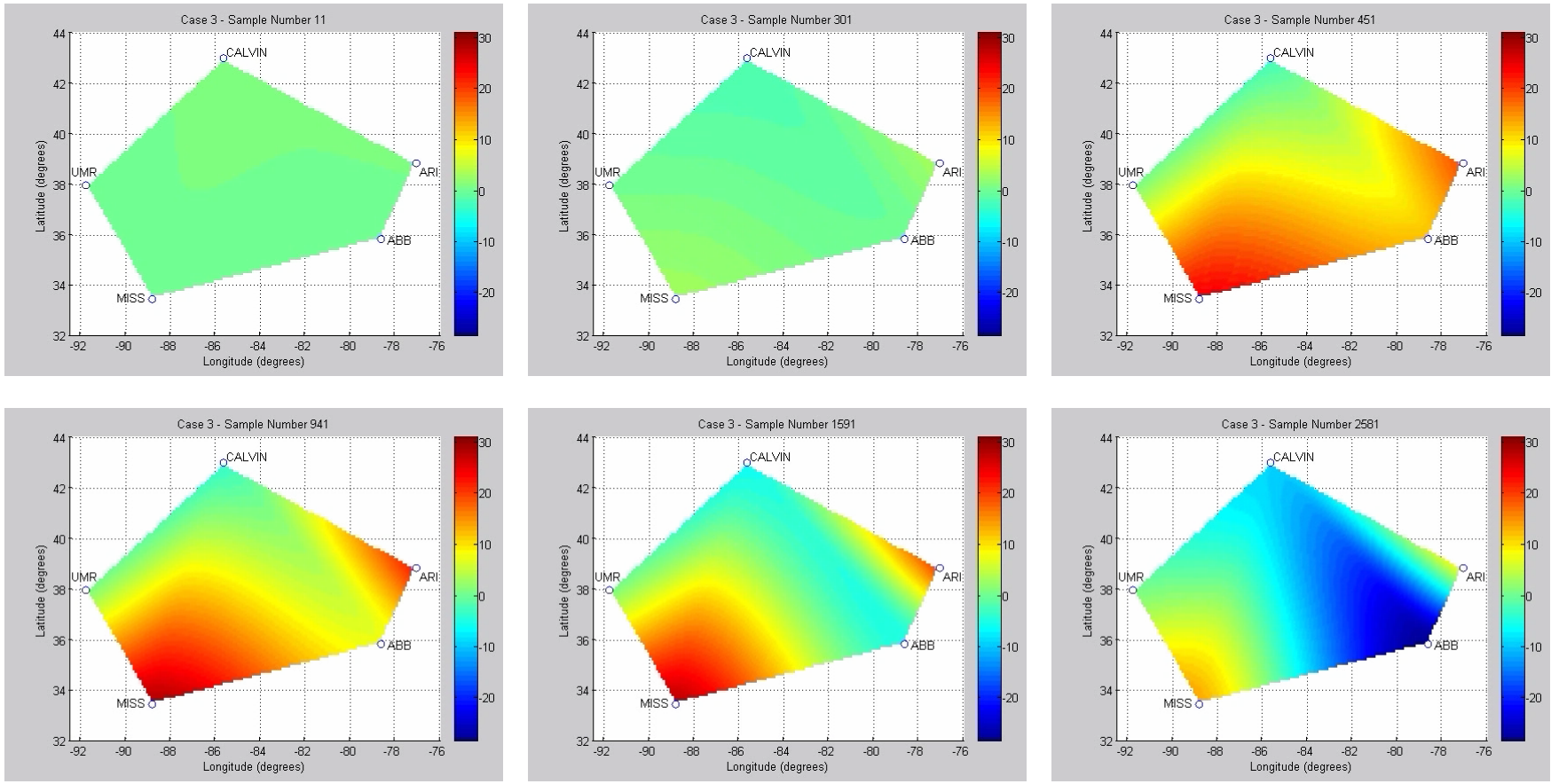

Figure 4.67 Base Case 3 video screenshots

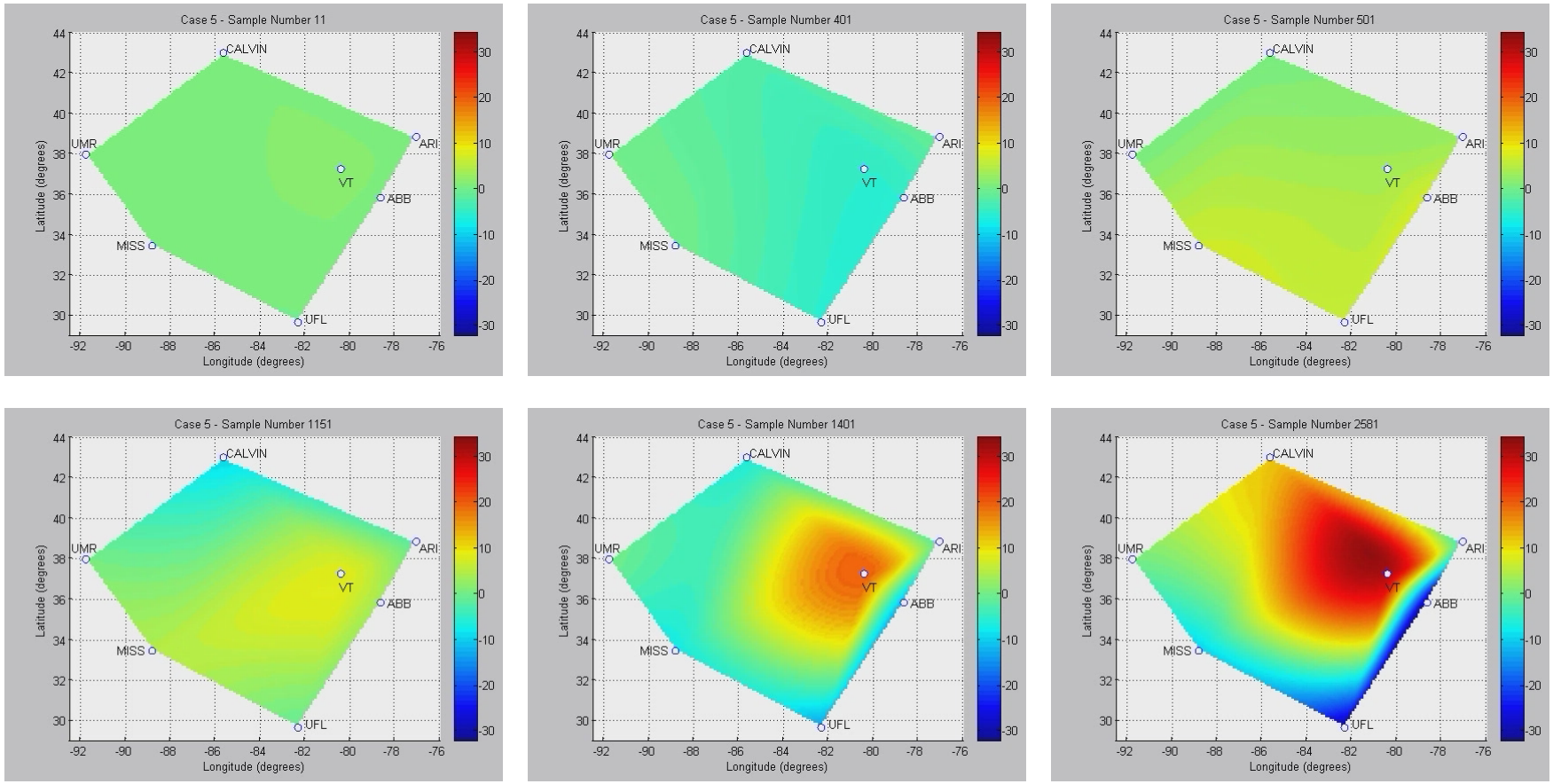

Figure 4.68 Base Case 5 video screenshots

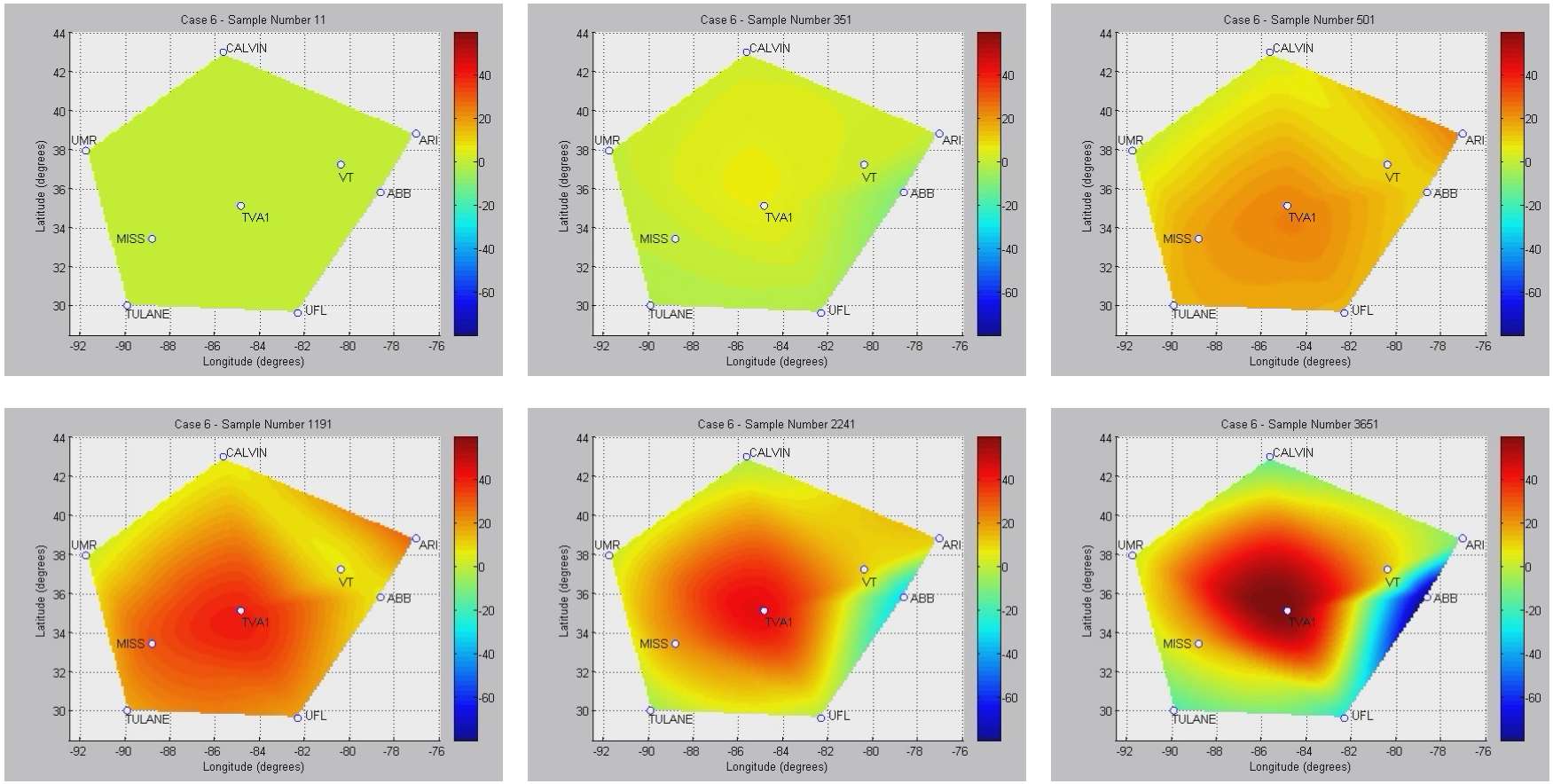

Figure 4.69 Base Case 6 video screenshots

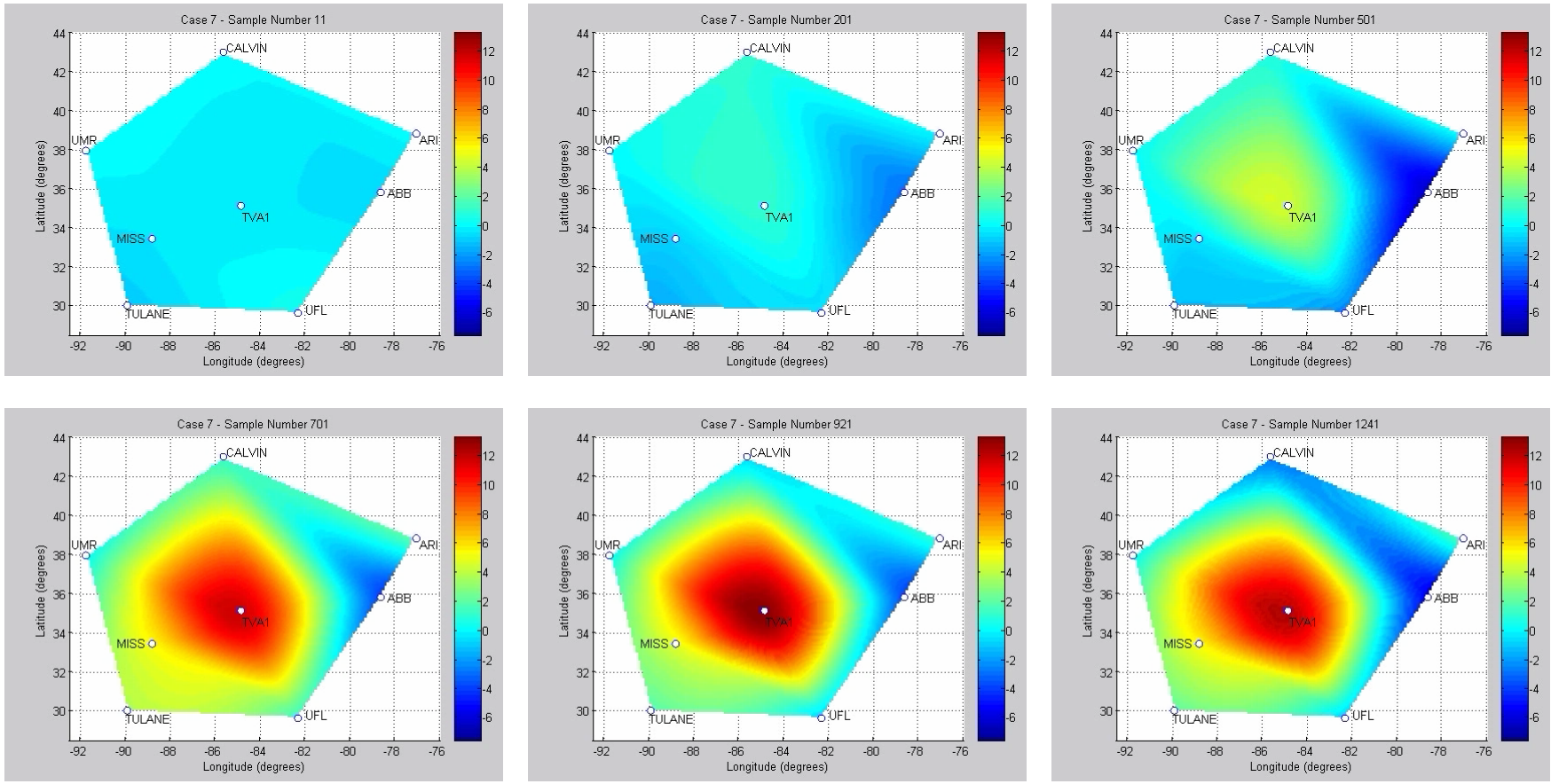

Figure 4.70 Base Case 7 video screenshots

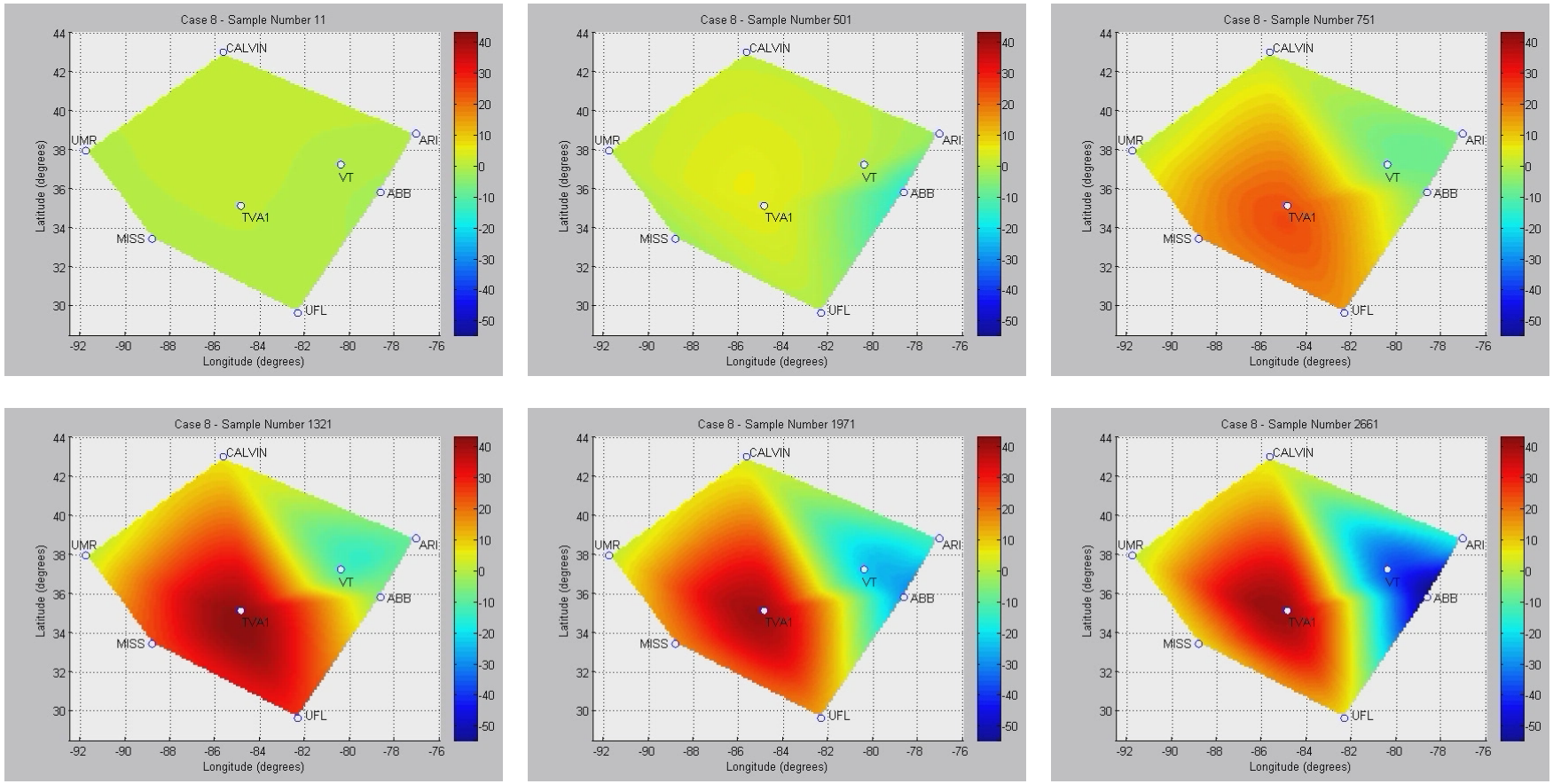

Figure 4.71 Base Case 8 video screenshots

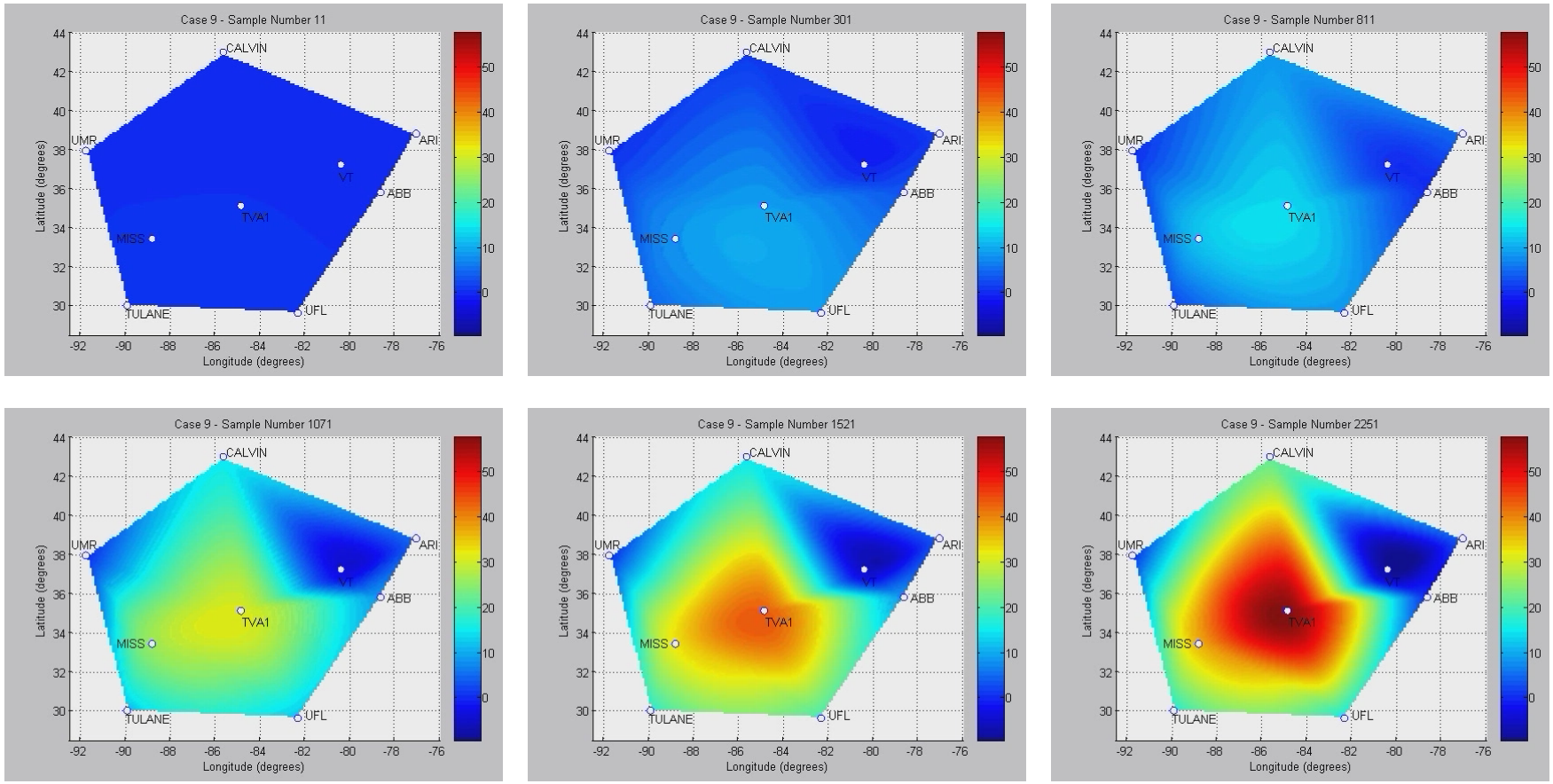

Figure 4.72 Base Case 9 video screenshots

4.11 Jackson Unit Noise

On May 4, 2006, FNET recorded an unusual amount of noise from the unit located in Jackson, TN. A hardware malfunction is ruled out because PMU data from a unit close by also contains the same noise at the same time intervals. Unusually, the noise flares up suddenly and then dies down, as shown in Figure 4.73. The PMU frequency data is shown in Figure 4.74 courtesy of the Tennessee Valley Authority (TVA).

A zoomed in frequency plot is shown in Figure 4.75. As shown, the frequency is fairly normal until the 80 second point. From that point on, the noise suddenly increases. However, looking at the angle plot in Figure 4.75, there is no visible difference in the angle plot when comparing the data before and after the noise starts. Zooming in further does not reveal any difference either.

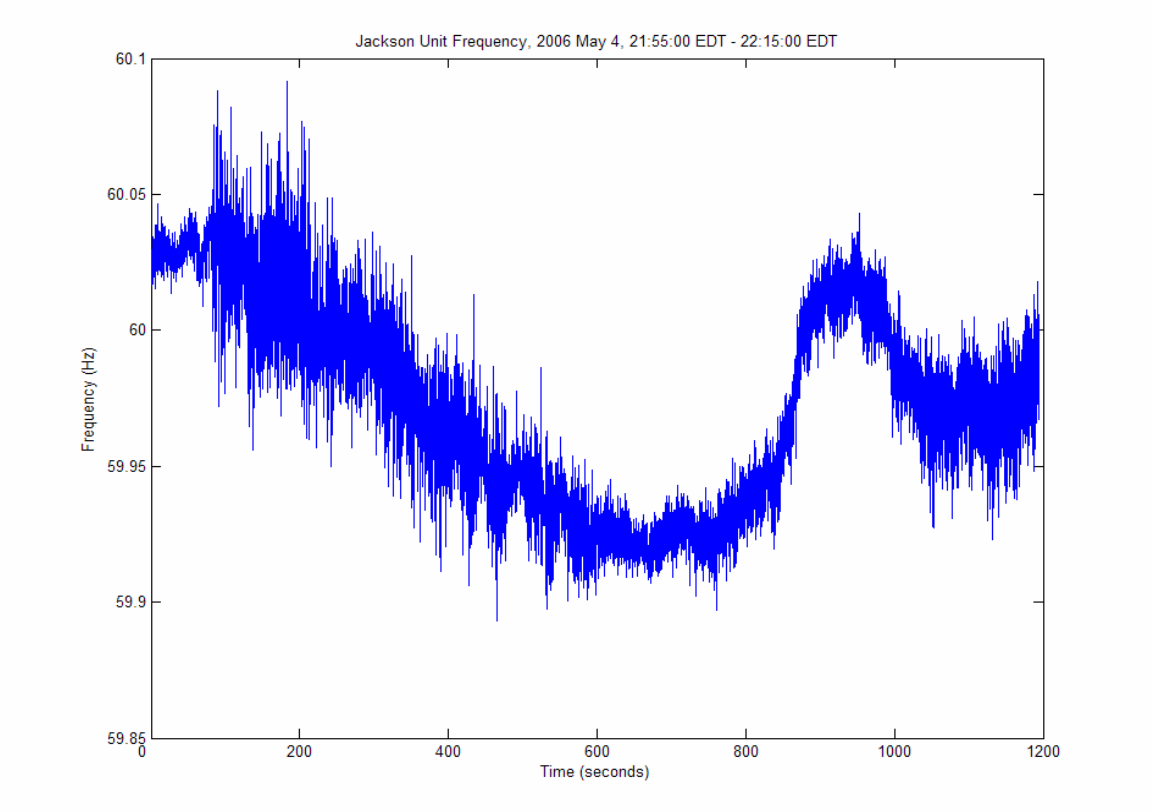

Figure 4.73 Noise recorded on FDR located in Jackson

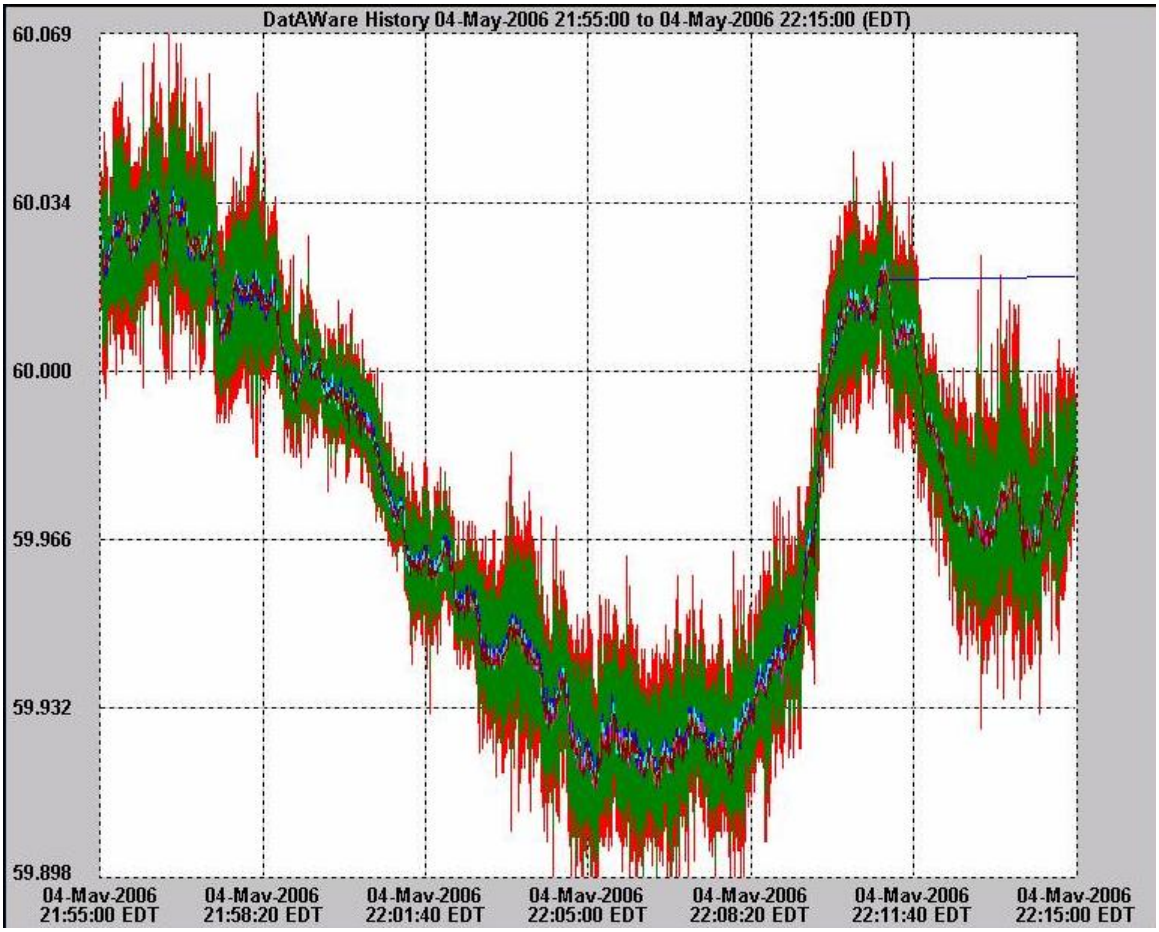

Figure 4.74 Frequency recorded on PMU (courtesy of TVA)

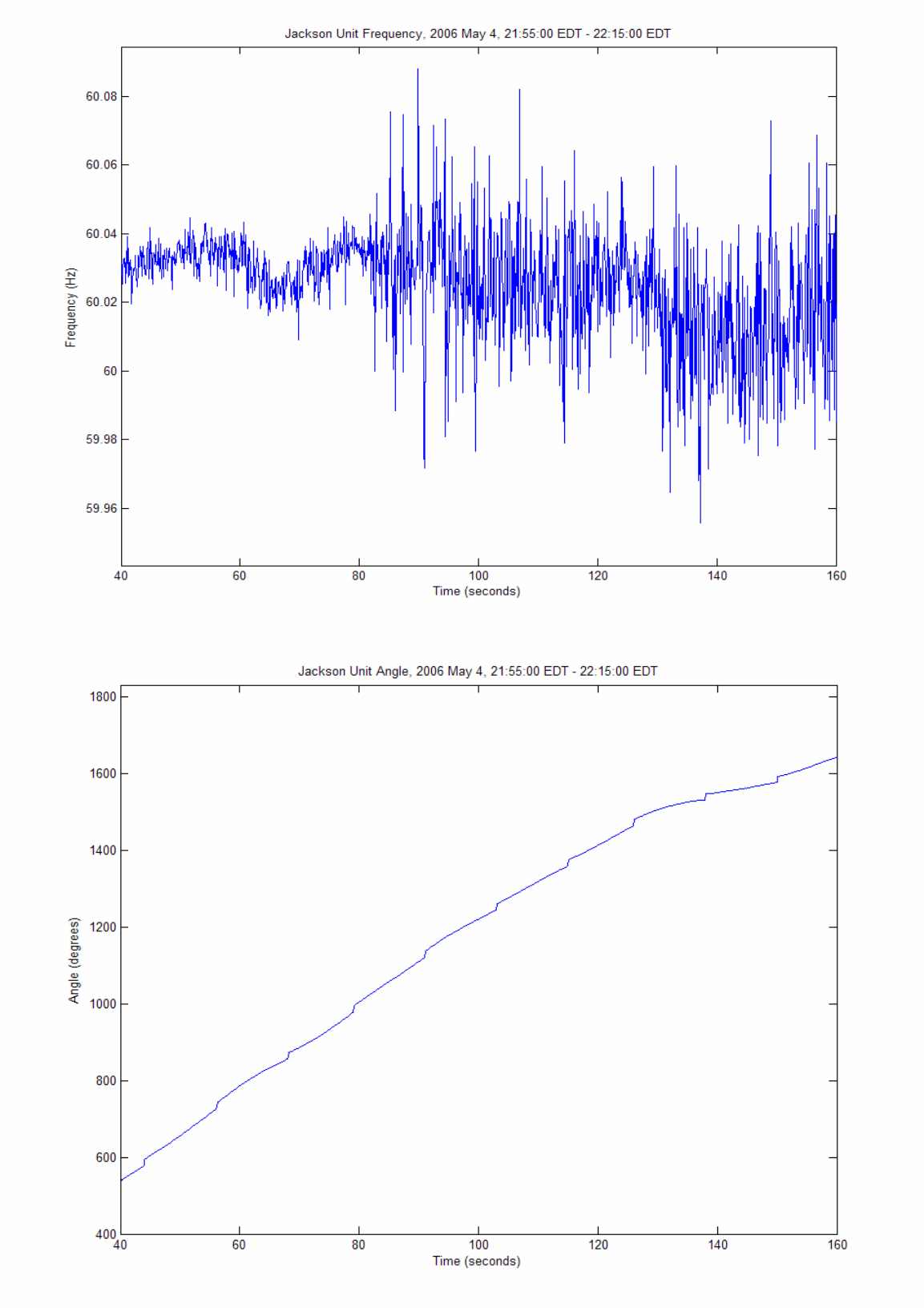

Figure 4.75 Noisy frequency and raw unwrapped angle

Figure 4.76 shows a comparison of the FDR output frequency and the frequency calculated from the FDR angle data using the relationship in Equation 3.12. The large, periodic blue spikes are due to the small discontinuities present in the angle data. FDRs use the same angle data to calculate the frequency but use a much more robust algorithm that eliminates the spikes. Ignoring the spikes, we can clearly see that the unusual noise flare-up is also present on the calculated frequency.

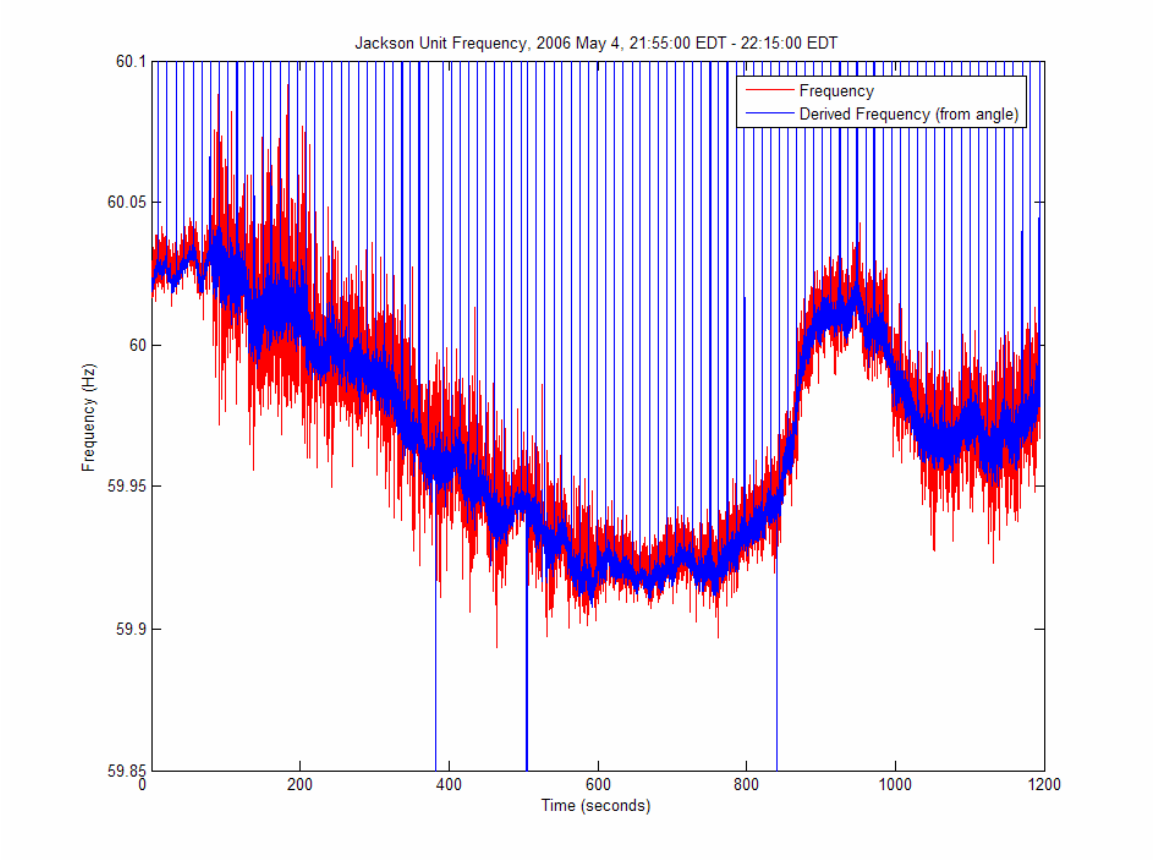

Figure 4.76 Comparison of raw frequency and calculated frequency

As a comparison, Figure 4.77 shows frequency and angle plots for the same unit on the same day during a period in which the unusual noise is absent. Once again, the angle looks normal. While a hardware malfunction has been ruled out, the cause of the unusual increase in noise on the Jackson Unit is still under investigation at the time of this thesis.

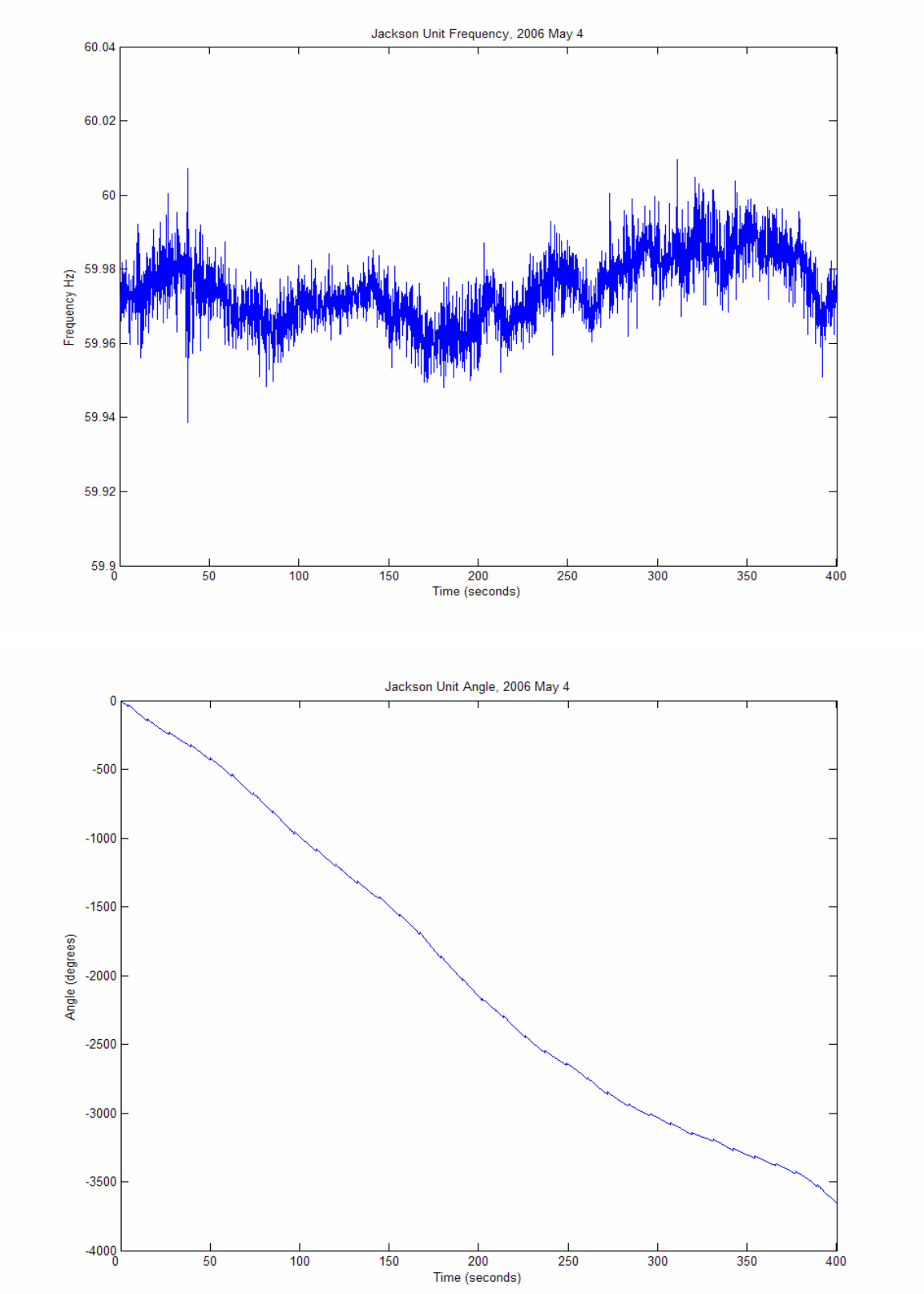

Figure 4.77 Frequency and raw unwrapped angle, normal operation

4.12 Summary

In this chapter, we looked at the voltage angles for several generation trip events in the EI. First, we looked at a computer simulated event to see how the angles and angle differences behaved during a generation trip event under ideal conditions. We showed that the angle differences diverged when the generation was lost and each jumped to a new operating point before flattening out.

Next, we looked at the angles and angle differences for eight EI generation trip events recorded by FNET. The results varied widely between cases, with some angle difference plots resembling the simulated case and some looking nothing like it. This indicates that the current simulation model for the EI does not match the overwhelming complexity of the real system, which is expected since simulation models are often simplified by combining similar devices and through equivalency reductions [8]. Furthermore, we noticed that certain units (VT, ABB, and Calvin) exhibited rather strange behavior on more than one occasion prompting us to question whether or not these FDRs were operating properly. It is possible that these units were affected by the "one second problem" (discussed in Section 4.2) or have a problem with the oscillator driving the sampling pulses. Finally, it should be noted that although the angle plots for these units were questionable, the frequency data from these FDRs were very close to the measurements made by other units.

The angle difference surface plot videos helped us to visualize the data geographically. Here, we noticed that the TVA1 unit tends to lead while the ABB unit tends to lag. In the future, these videos could give us some insight on the power generation within the system. But first, we need to deploy more FDRs to get more accurate surface plots.

Finally, we explored the unusual noise recorded on the Jackson unit. We found that the raw angle showed no visible change when the noise flared up in the frequency. We also saw that the raw angle measured during normal operation looked just like the raw angle measured during the noisy period.

Chapter 5: Event Detection Using K-Means Clustering

The k-means algorithm is a simple and effective pattern recognition technique used to classify unlabeled sample points. Clustering is used to separate a data set into a user defined number of groups. The Euclidean distance is often used to determine the similarity between data points. Furthermore, the k-means algorithm can adapt to changing characteristics [14]. The k-means clustering algorithm is shown below.

```
Algorithm: k-means clustering
Goal:  Find k mean vectors, each representing a cluster
    center
Given: k, n training samples, initial estimate for
    cluster centers
Repeat {
    Assign each training sample to the nearest cluster
        center (typically Euclidean distance)
    Re-compute cluster centers based on new
        classification
} until no change in cluster center
Return cluster centers and data classification
```

Basically, k-means takes a group of data points and chooses k points as initial cluster center guesses. Then, using the initial guesses, each data point is assigned a class based on which cluster center is closest. Once all of the points have been assigned, the mean of each class is computed and used as the new class center. Using the new class centers, the data points are again classified based on shortest distance. This process is repeated until there are no changes in class centers.

A variation of the k-means algorithm is used for FNET event detection. The main difference between the algorithm above and the variation used for event detection is that

the difference between class centers is computed and used as a measure to determine whether an event has been detected. Section 5.1 investigates the characteristics of power system events, Section 5.2 presents details about the k-means detection algorithm, and Section 5.3 discusses the performance results.

5.1 FNET Event Characteristics

Looking at a scatter plot of the frequency data and the point by point derivative of the frequency, shown in Figures 5.1 and 5.2, we can clearly see a separation between normal operation and an event. However, since the frequency data is so noisy, we cannot perceive any trends in the point by point derivative of the frequency and it was decided that the frequency derivative is not necessary to perform event detection.

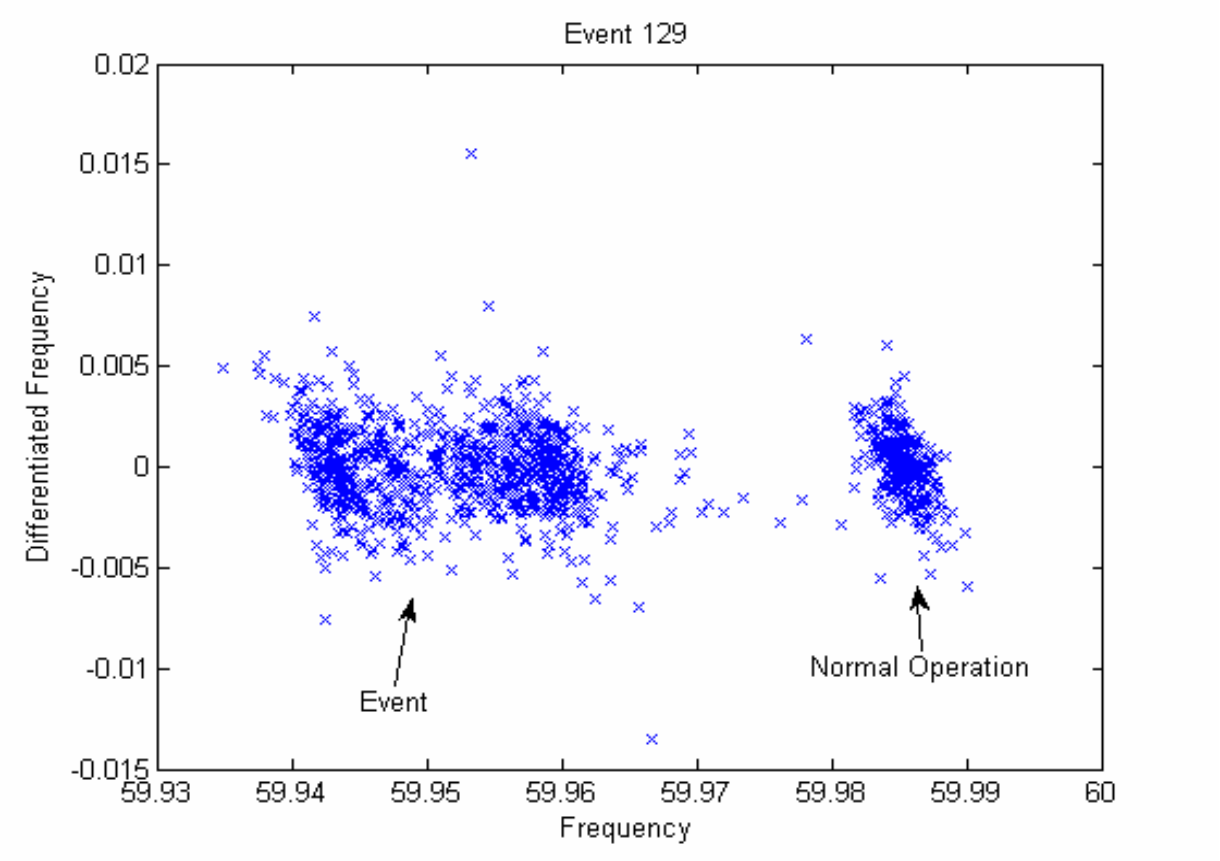

Figure 5.1 Scatter plot during a power system event in the eastern power system

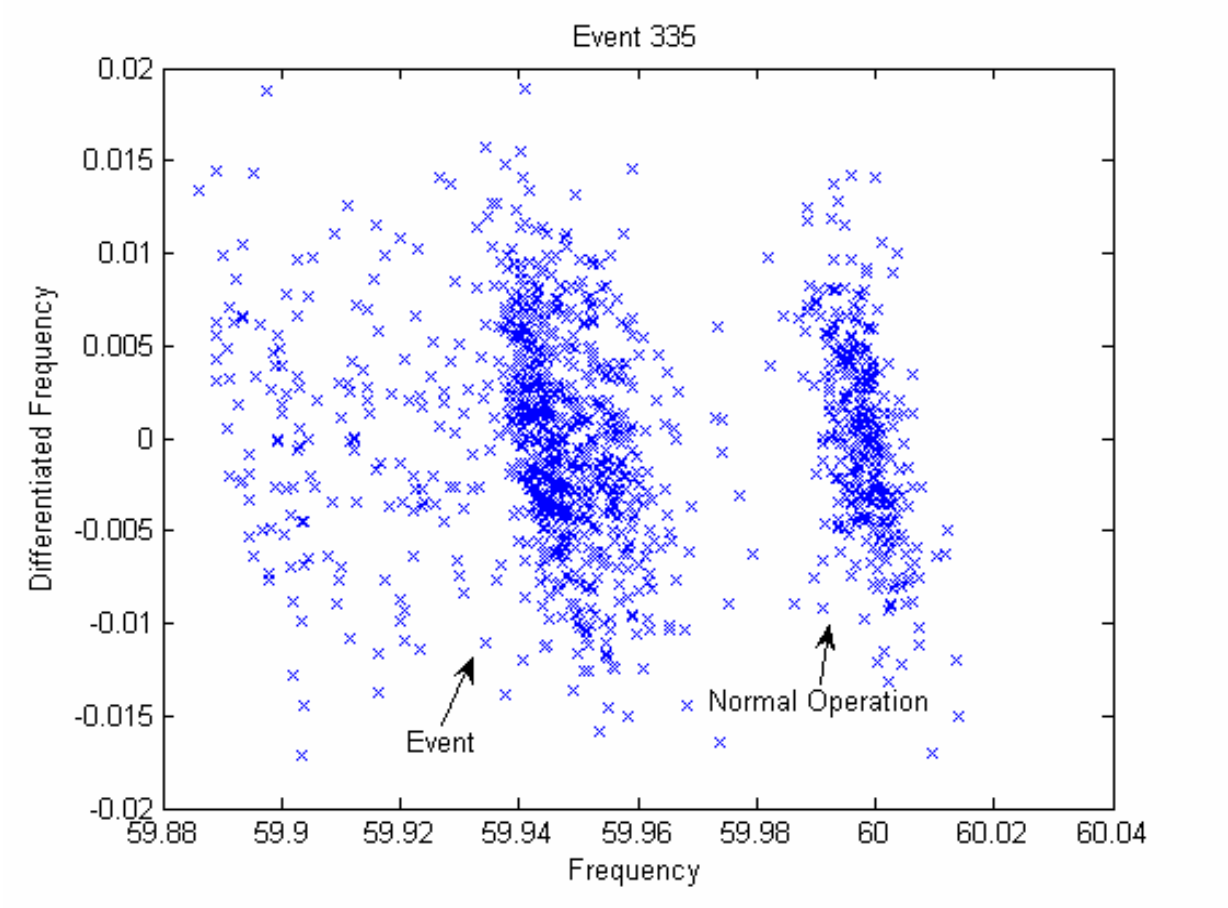

Figure 5.2 Scatter plot during a power system event in the western power system

Figures 5.3 and 5.4 show histograms for the frequency readings from an FDR during events in the EI and Western Electricity Coordinating Council (WECC) systems. Once again, we can clearly see separation between the normal operation distribution and the event distribution. The histograms indicate that we can easily reduce the k-means event detection algorithm to one dimension.

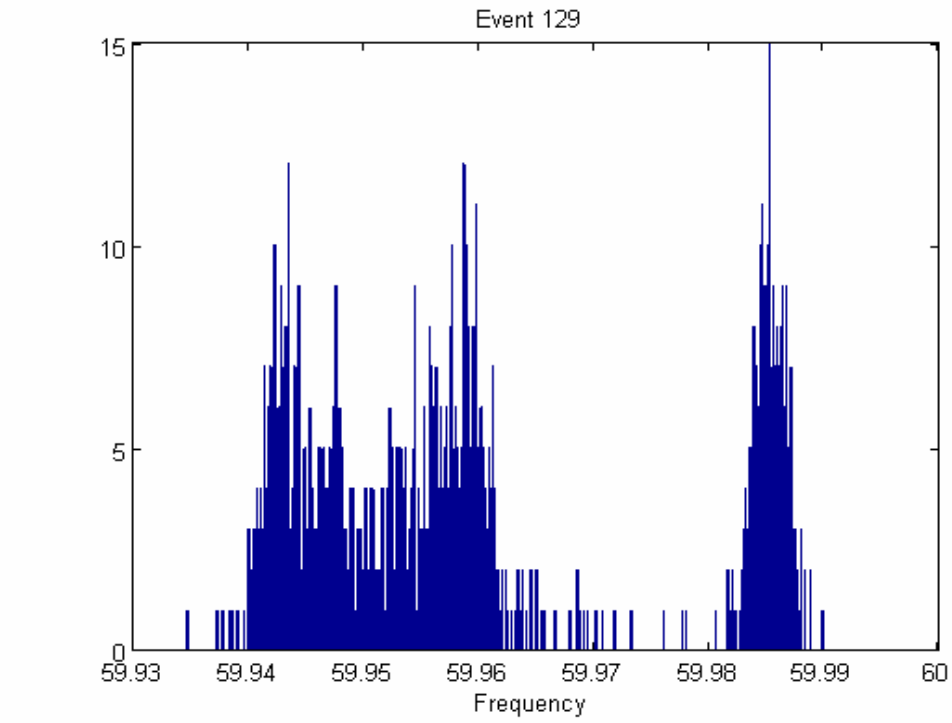

Figure 5.3 Frequency histogram for event 129 (EI)

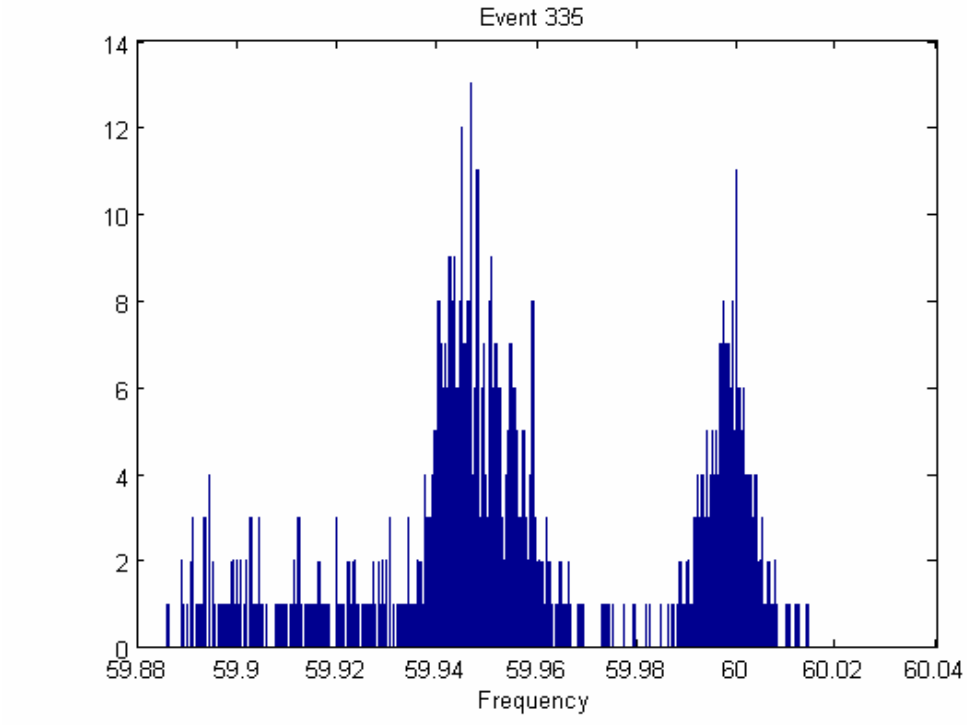

Figure 5.4 Frequency histogram for event 335 (WECC)

Initially it would seem that a static frequency threshold would do the job, but it is not only the frequency level we are looking at. We are more interested in sudden frequency drops. Furthermore, not all events behave the same way—different events start and end at different frequency levels. Also, since the frequency data is so noisy, a large spike could trigger a static threshold and create a false alarm. Finally, frequency drift is common in the power grid and considered normal behavior. It is plausible that the frequency might drift below the static threshold and trigger a false alarm.

Power system generation trip events are identified as sudden drops in frequency, and a moving window k-means algorithm would be able to detect this. To do this we would pass a moving window of a fixed size over the frequency data and perform two class k-means classification on the data contained within. As shown in Figure 5.5, the two k-means classes and class centers (shown as stars) are extremely close to one another during normal operation over a 10 second interval.

As the moving window shifts over to encompass an event, the classes and class centers drift further apart, as shown in Figure 5.6. Using the distance between class centers, we can determine whether or not the moving window contains an event.

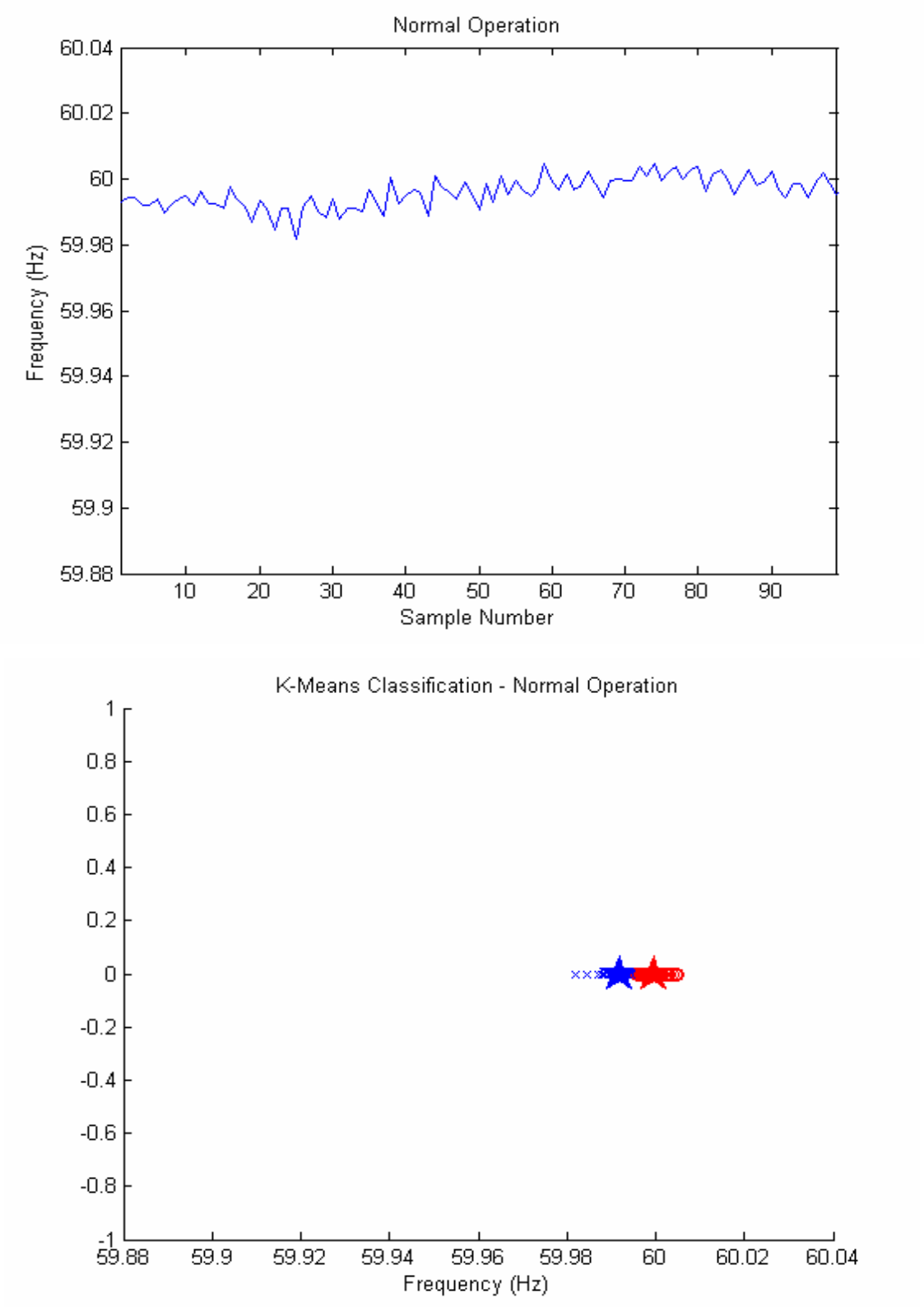

Figure 5.5 Frequency and k-means clustering plots for normal power system operation

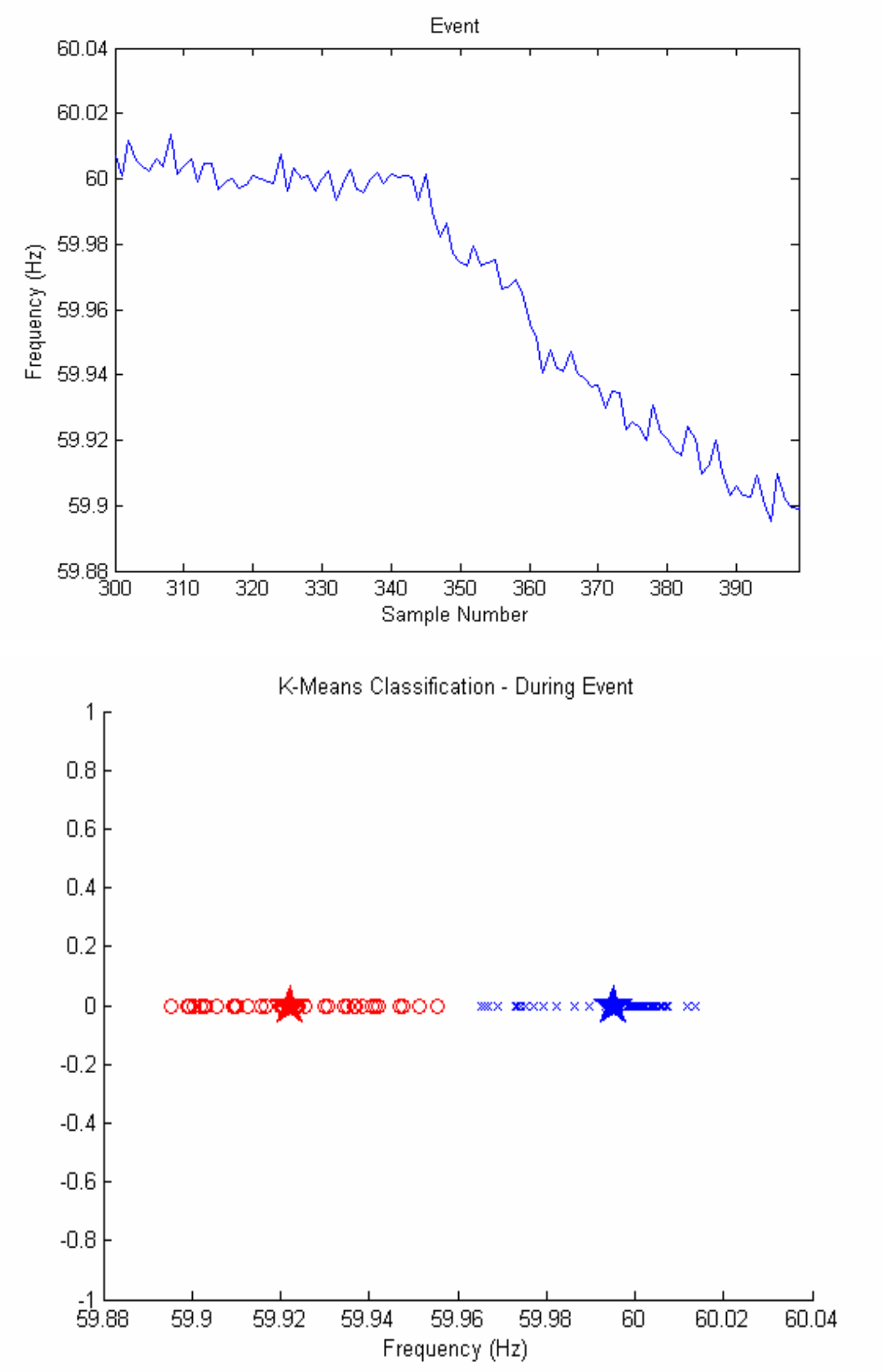

Figure 5.6 Frequency and k-means clustering plots during a power system event

5.2 K-Means Event Detection Algorithm

The k-means event detection consists of two parts—the main program, 'event_detector.m' and the k-means classification program, 'proj_kmeans.m'.

The event_detector function accepts a data structure containing the frequency data from the FDRs . Before the actual k-means classification takes place, the main program does some preprocessing. First, it determines whether all of the data points are present. If not, a message is printed to the screen alerting the user. Then, it continually passes 100 point windows of frequency data to the k-means function. The window slides over the entire set of data points in 50 point increments. While it may seem inefficient to allow the windows to overlap, it ensures that events will not be missed. For example, if the window happens to land so that the edge of the window cuts the event in half, the event might be overlooked.

The k-means classification function accepts a vector of numerical values and performs one dimensional, two class k-means classification on it. First, the k-means algorithm chooses the first and last entries in the input vector as initial class mean guesses. Before it continues, it makes sure that the two initial guesses are not equal. This is a necessary step because our data range is limited and duplicate frequency readings are very common. Next, the data is separated into two classes with the k-means clustering algorithm. Once the points are classified, the function returns the distance between the two class centers, because, for our application, we are only interested in the amount of frequency dropped, regardless of the starting point. To counter some of the effects of spikes in the frequency data, the program checks that more than ten points are in each class. If this requirement is met, the distance between class centers is returned. If not, the program returns zero.

Finally, the main program receives the class center distance and determines whether an event is contained in the window. If so, an alert is printed to the screen. To determine the mean distance threshold, the distances calculated by the k-means algorithm were plotted as a function of the window starting points. As shown in Figures 5.7 and 5.8,

there is a definite spike in the mean distances during events. The lines that don't spike represent FDRs in a different interconnect where no event is taking place. Using all of the training data, it was determined that separate thresholds were required for the east and west FDR data since the two power systems behave differently during an event. After inspecting mean distance plots for all the events, a distance threshold of 0.15 was chosen for the east, and a threshold of 0.25 was chosen for the west.

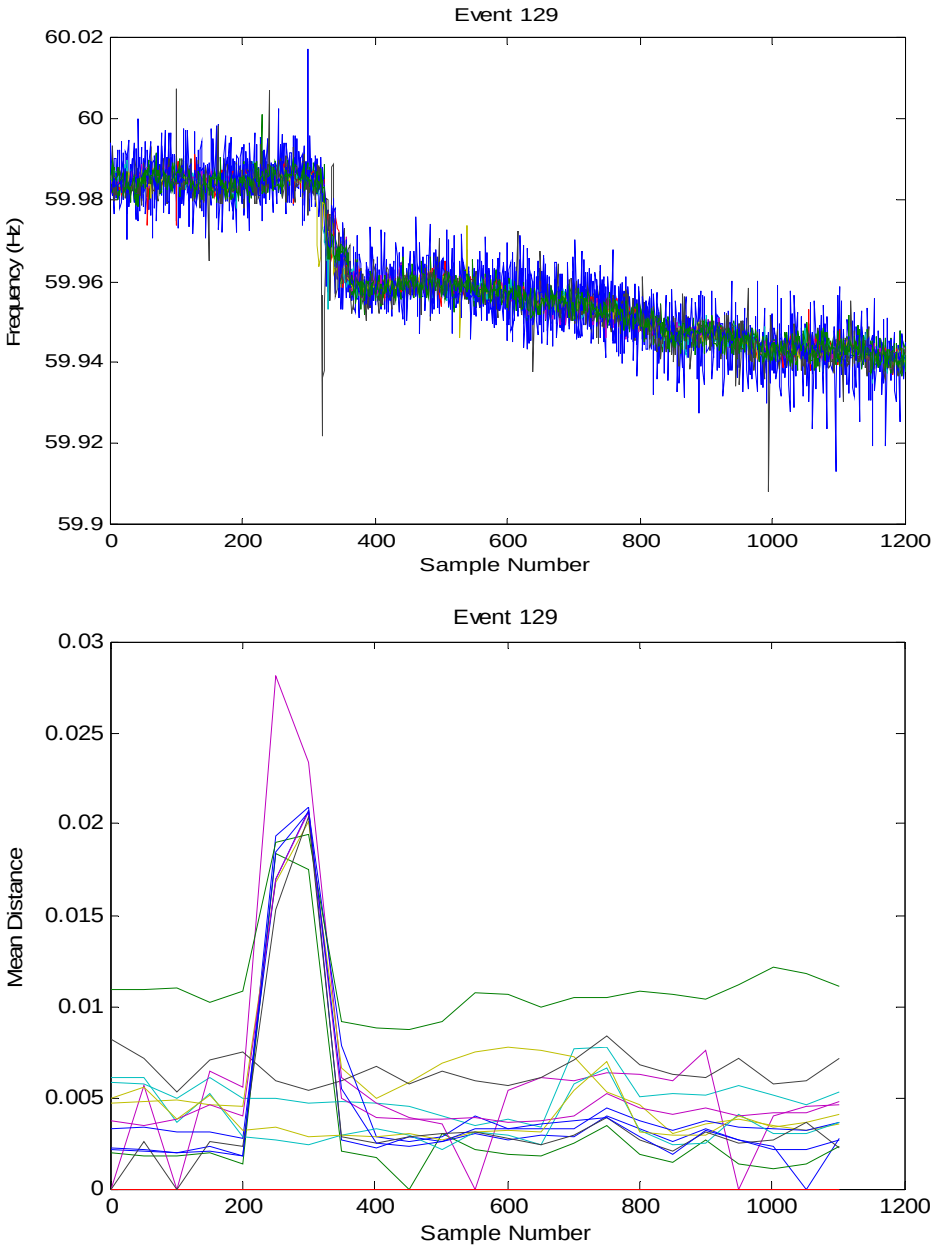

Figure 5.7 Frequency and k-means class center distances for Event 129 (EI)

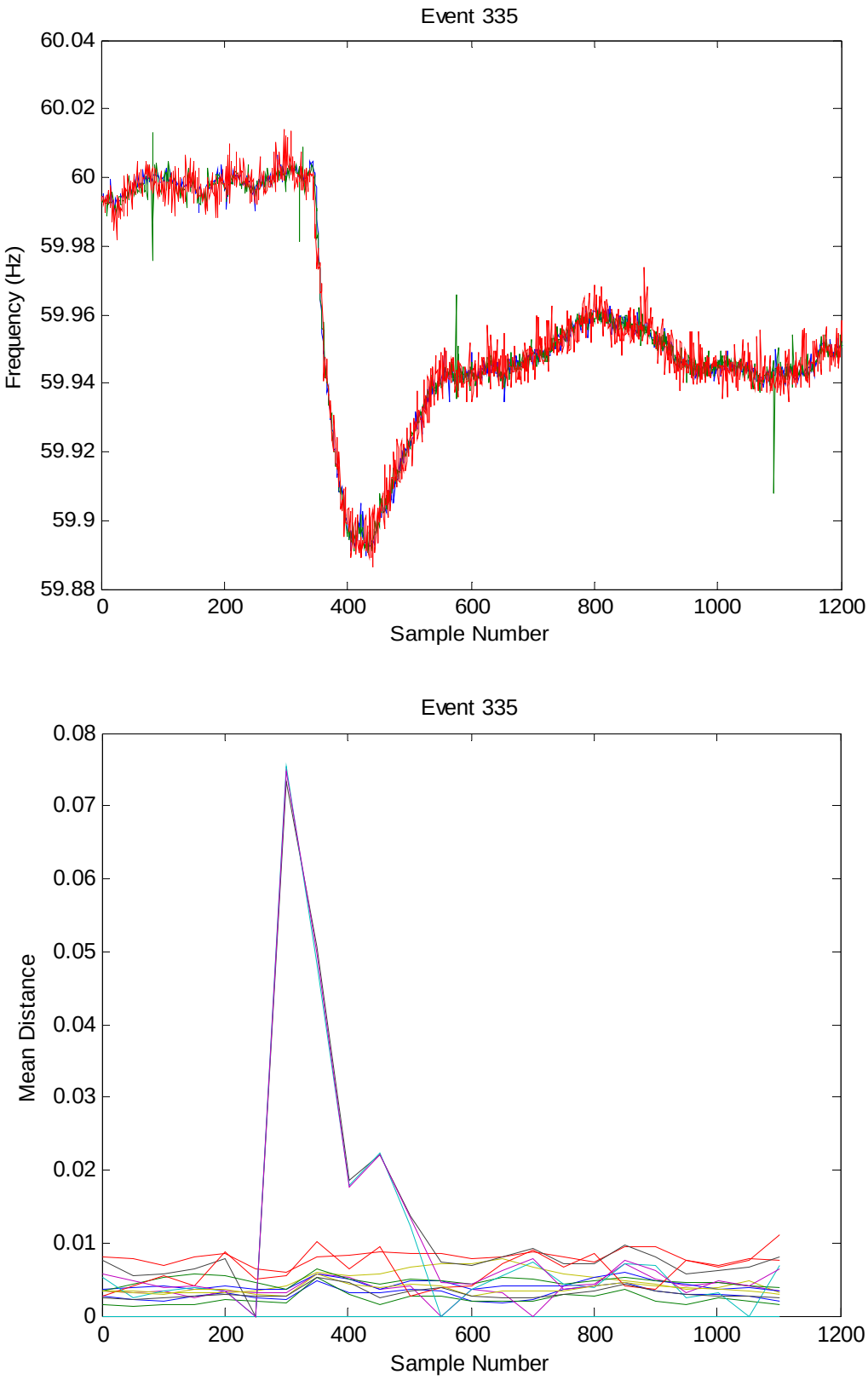

Figure 5.8 Frequency and k-means class center distances for Event 335 (WECC)

5.3 K-Means Event Detection Performance

The k-means event detection scheme worked very well for our sample data and the algorithm was able to detect and provide an approximate time window for 377 events out of a possible 377. (For the purposes of this test, each FDR's data was scanned separately. If we consider that each event is recorded by multiple FDRs, it can be seen that the same event will be detected several times.) However, the algorithm did not perform as well with unusually noisy data. There were several false alarms due to high noise on the input frequency data. The VT unit accounted for 96% of the false alarms, and in Figure 5.9, we can clearly see a large amount of noise on the VT unit (FDR4) when compared to the UMR (FDR2) unit.

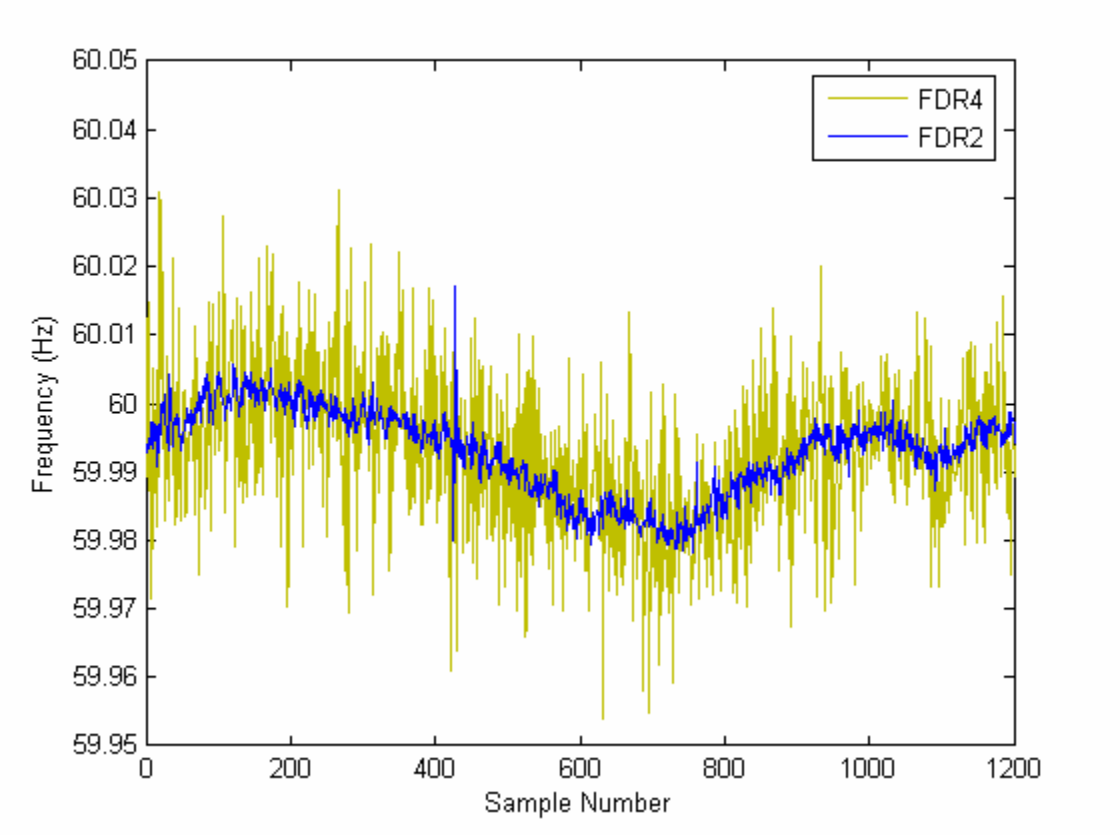

Figure 5.9 Frequency noise comparison between VT (FDR4) and UMR (FDR2)

Because we get mixed results for noisy frequency data, it would probably be advantageous to smooth the data before feeding it to the event detection program. Or, since smoothing the data takes time, we could simply disregard the noisy units and use the event times obtained for other units in the same interconnect (since an event will be reflected in the frequency data for all units in the same network).

An important note is that the algorithm is very quick—able to scan a 2 minute window in less than a second—which is advantageous given the massive amount of data we collect. Given the speed and accuracy of the k-means detection algorithm, it would be beneficial to consider it as a replacement for the current detection algorithm.

Chapter 6: FDR Hardware Design

6.1 GPS Replacement

The Global Positioning System, developed and operated by the United States Department of Defense, is a satellite based radio navigation system. The system consists of a network of 24 satellites to provide a minimum worldwide visibility of 4 satellites at all times. In addition to providing position and velocity information to users, GPS units also provide accurate timing by synchronizing with a ground based Cesium clock which is referenced to the world standard time Coordinated Universal Time (UTC). Time stamps provided via GPS allow us to synchronize FDR data for comparative analysis.

The Motorola M12+ timing receiver was selected as the best candidate for our application when the current generation FDRs were designed. However, since then, the M12+ has been discontinued. Before looking at possible M12+ replacements for the current and next generation FDRs, let us review the main requirements [13]:

- The GPS unit must provide the pulse-per-second (PPS) to the MIOS of the CPU to trigger each analog to digital (A/D) conversion with a stability of at least 1μs
- The GPS unit must provide a timestamp to the CPU for each second of time
- The GPS shall poll its own locations: latitude, longitude, and altitude, which is essential for FNET applications, such as the event location triangulation.

Furthermore, it would be advantageous for FNET if the GPS module is able to provide timing with only one satellite visible (1SV) after the FDR location has been fixed. Listed below are the main features of the Motorola M12+ and several other GPS units that were considered for its replacement at the time of this study [15-30].

Motorola M12+

- Timing receiver
- Operating voltage: 2.85-3.15V
- Time to first fix: 25s hot, 50s warm, 200s cold
- Backup battery support (retains the real-time-clock, position, satellite data, user commanded operating modes, and message formatting)
- Serial communication port
- 40mm x 60mm x 7.6mm
- Timing accuracy: 1PPS accuracy less than 25ns

Sony GXB5005

- Time to first fix: 2-3s hot, 33s warm, 40s cold
- Operating voltage: 3.1-3.7V (3.4V typical)
- Backup battery support
- Serial communication port
- Timing accuracy : 1PPS accuracy of 100ns, estimated accuracy of 200-300ns with 1SV
- 22.4mm x 23.5mm x 3.2mm
- Shielded

Sony GXB5210

- Based on same chip as Sony GXB5005
- Time to first fix: 2-4s hot, 35s warm, 50s cold
- Operating voltage: 3.1-3.7V (3.3V typical)
- Backup battery support
- Serial communication port
- 34.5mm x 35mm x 7.5mm
- Timing accuracy: 1PPS accuracy less than 50ns
- Built in ceramic patch antenna

Navman Jupiter 12

- Time to first fix: 18s hot, 48s warm
- Operating voltage: 3.3-3.5V
- 71.1mm x 40.6mm x 11.4mm
- Backup battery support
- Two serial communication ports
- Timing accuracy: 1PPS accuracy of less than 100ns

Fastrax iTrax 02/uTracker 02

- Time to first fix: 3s quick start, 8s hot, 35s warm, 50s cold
- Operating voltage: 2.7-3.3V
- 26mm x 26mm x 4.7mm
- Flash memory to save configuration
- Two serial communication ports
- 1PPS output
- Timing accuracy: less than 20ns

Fastrax iTrax 03/iTrax 03-S

- Time to first fix: 3s quick start, 8s hot, 35s warm, 40s cold
- Operating voltage: 2.7-3.3V
- 22mm x 23mm x 2.9mm
- Flash memory to save configuration
- Two serial communication ports
- 1PPS output
- Timing accuracy: less than 20ns

Fastrax iTrax100

- Time to first fix: 8s hot, 35s warm, 45s cold
- Operating voltage: 3.0-3.6V
- Battery backup support

- 16.2mm x 18.8mm x 3mm
- Serial communication port
- 1PPS output
- Timing accuracy: less than 50ns

Navman Pico-T

- Timing receiver
- Time to first fix: 24s hot, 45s warm, 120s cold
- Operating voltage: 3.15-3.45V
- Battery backup support
- 24.5mm x 31.5mm x 8.6mm
- Two serial communication ports
- Needs a valid 3D fix for 24hrs to have accurate 1PPS timing
- Emulated Motorola Binary support
- Timing accuracy: less than 100ns, 1PPS accuracy less than 25ns

Trimble Resolution T

- Timing receiver
- Operating voltage: 3.0-3.6V
- Battery backup support
- 66.3mm x 32.1mm x 8.5mm
- Serial communication port
- Time to first fix: 14s hot, 41s warm, 46s cold
- Timing accuracy: 1PPS accuracy less than 15ns

iLotus M12M

- Backward compatible with M12+
- Time to first fix: 1s internal reacquisition, 15s hot, 40s warm, 60s cold
- Battery backup support
- Serial communication port

- 40mm x 60mm x 13mm
- Operating voltage: 2.8-3.3V
- Timing accuracy: 1PPS accuracy less than 500ns

Because the iLotus M12M is fully backward compatible with the M12+, it is the best choice for FNET. However, the preliminary specifications for the M12M show a fairly high figure for timing accuracy. If the finished product does not meet our requirements for timing accuracy, the Trimble Resolution T, Navman Jupiter Pico-T, Fastrax iTrax100, and Sony GXB5005 should all be considered. In particular, the Resolution T, and Pico-T should be considered because they are both timing units (like the M12+) and are built primarily to provide accurate timing.

Based on the above information and advice from GPS vendors, the Sony GXB5210, Navman Jupiter 12, Fastrax iTrax 02, and Fastrax iTrax 03/iTrax 03-S units should not be considered for future FDRs. The Sony GXB5210 has a built in antenna which would create problems when trying to place an FDR so that it receives a satellite signal. The Navman Jupiter 12 was not recommended for our application by a Navman representative. Instead he recommended the Navman Jupiter Pico-T, which is better suited for our timing intensive application. Finally, none of the Fastrax modules are recommended; the iTrax 02 is an older model which is likely to be discontinued and the iTrax 03 doesn't provide 1PPS timing with only one satellite visible. Table 6.1 on the next page summarizes the features of each GPS module.

Table 6.1 GPS module summary [15-30]

	Number of Connection Pins	Number of Serial Ports	Timing Accuracy	Backup Support	1PPS with 1SV Capable
iLotus M12M	10	1	500ns*	Battery	Unknown
Trimble Resolution T	8	1	15ns*	Battery	Unknown
Navman Jupiter Pico-T	20	2	25ns*	Battery	Yes
Fastrax iTrax100	18	1	50ns	Battery	Yes
Sony GXB 5005	19	1	100ns*	Battery	Yes
Sony GXB 5210	10	1	50ns*	Battery	Unknown
Navman Jupiter 12	20	1	100ns	Battery	Unknown
Fastrax iTrax 02	40	2	20ns	Flash	Unknown
Fastrax iTrax 03	37	2	20ns	Flash	No
Fastrax iTrax 03-S	30	2	20ns	Flash	No
Motorola M12+	10	1	25ns*	Battery	Yes

* Timing accuracy value for 1PPS signal

6.2 FDR Assembly

FNET FDRs are constructed by hand in the Virginia Tech Power IT Laboratory. Each unit requires many hours of work to assemble the various components, which include the CME555 board, signal filter, Motorola M12+ GPS unit, A/D converter, liquid crystal display (LCD), and the step-down transformer. Additionally, numerous wiring connections, soldered connections, and jumper settings must be made to create a functioning FDR.

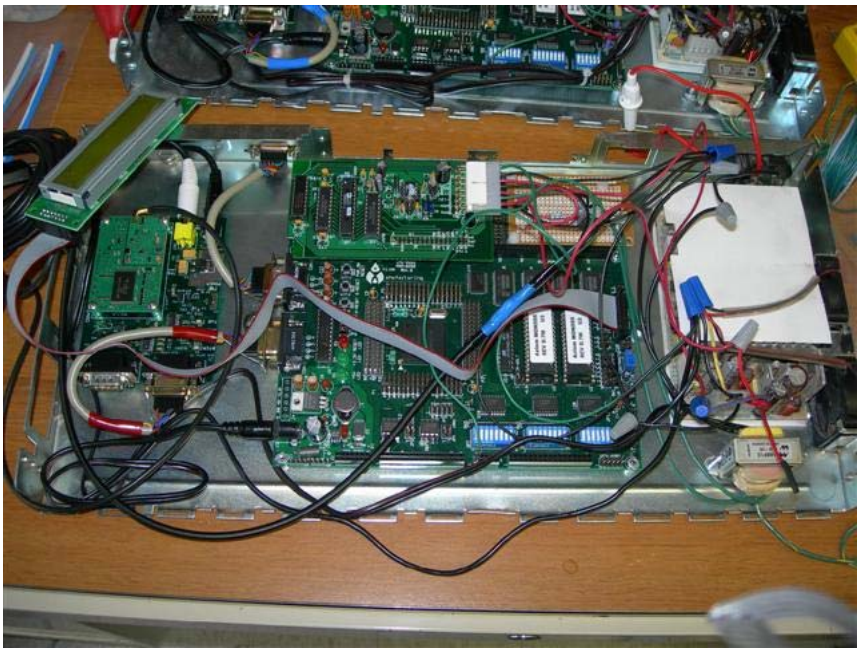

Figure 6.1 Fully wired and functioning FDR

FDR assembly can be broken into several steps:

- Manufacture serial cables
- Mount signal filter
- Mount GPS
- Mount transformer
- Mount A/D converter

- Wire components
- Attach LCD
- Configure jumper and switch settings

In the past, FDRs were assembled with only the help of another student (who had gone through the process), and an example unit to copy from. To help future students, an FDR assembly guide has been created (see Appendix IV). The guide provides step by step instructions, along with pictures and illustrations, to mount and wire each component. In addition, the guide documents switch and jumper settings and offers helpful tips for FDR construction.

6.3 Summary

In this chapter, we looked at several GPS modules to find a possible replacement for the discontinued Motorola M12+ chip that is used in the current generation of FDRs. In the end, the iLotus M12M was the highest recommended because of its backward compatibility with the M12+. The Trimble Resolution T, Navman Jupiter Pico-T, Fastrax iTrax100, and Sony GXB5005 modules were also recommended as alternatives to the M12M. Finally, we briefly looked at what steps are required to construct an FDR.

Chapter 7: Conclusions and Future Work

7.1 Conclusions

In this thesis, several aspects of FNET were touched upon. The main objective of this thesis was to take the first in depth look at voltage angles in the EI. First, we looked at the nuances of FDR data and found that the raw voltage angle data contained discontinuities that made it difficult to do any angle analysis. Next, three data conditioning techniques were proposed to attempt to extract usable angle data for analysis. In the end, extracting angle data by integrating the frequency was chosen and the technique was verified to be effective through tests on PSS/E simulation data. Then, we looked at the angle and angle difference plots of eight generation trip events recorded in the EI. The FDR data produced inconsistent, somewhat mixed results. For some cases, the angle difference plots looked like something we would expect. For other cases, the angle difference plots had little resemblance to the PSS/E simulated cases. At the very least, we discovered that certain units produce strange angle difference plots that prompted us to question whether or not they were operating properly. Finally, the angle difference surface plot movies provided a new interesting way to visualize the data.

This thesis has laid the groundwork for future angle analysis using FNET data. It has provided a method to extract usable angle data from FDRs and also given us our first look at the behavior of the voltage angles during a generation trip event in the EI. The techniques and results presented in this work could be used as a launch pad for future research.

This thesis also presented a new event detection technique. It was shown that the k-means event detection algorithm is fairly effective and efficient in detecting sudden deviations in frequency data. With further development, the k-means detection scheme could be used in the future to detect generation trip and load rejection events recorded by FDRs.

Finally, this paper touched on some FNET hardware issues. Several GPS modules were presented and compared in hopes of selecting one to replace the Motorola M12+ used in the current generation of FDRs. Furthermore, it was discovered that timing GPS modules provide the most accurate timing and are ideal for our application. Then we took a brief look at the procedure to manufacture an FDR. An illustrated FDR assembly guide designed to aid future students has been created and is included in Appendix IV.

7.2 Future Work

There are several areas that I feel future work is necessary for angle analysis:

- A few FDRs had unusual angle difference curves. These units must be inspected to ensure that they are functioning properly.
- More cases need to be plotted and analyzed, especially events involving more FDRs.
- More FDRs need to be deployed.
- Upon completion of this thesis, the FNET team discovered a one second time skew in some FDR units. The problem has been corrected, but some of the older data will still have this time skew. The data should be corrected before any further angle analysis.

More development is also necessary for the k-means event detection algorithm:

- Experiments must be done to optimize the window size and thresholds for better performance.
- A study must be done to compare the accuracy and speed of the current event detection algorithm with the k-means algorithm accuracy and speed.
- Finally, it might be beneficial to test the algorithm with smoothed FDR data to see whether the accuracy can be increased.

References

1. Ota, Y., et al., *PMU based Midterm Stability Evaluation of Wide-area Power System*. Transmission and Distribution Conference and Exhibition 2002: Asia Pacific. 2002. pp. 1676-1680.
2. Toyoda, J., et al., *Monitoring of Wide Area Dynamics in Power Network through Home Power-Outlet Signal by GPS-Internet Based Devices*. IEEE/PES Transmission and Distribution Conference and Exhibition 2002: Asia Pacific. 2002. pp. 769-774.
3. Hojo, M., et al., *Analysis of Load Frequency Control Dynamics Based on Multiple Synchronized Phasor Measurements*. 15th PSSC. August 2005.
4. Hashiguchi, T., et al., *Oscillation Mode Analysis in Power Systems Based on Data Acquired by Distributed Phasor Measurement Units*. Proceedings of the 2003 International Symposium on Circuits and Systems, 2003. pp. 367-370.
5. Chen, Y., et al., *A new Approach to Real Time Measurement of Power Angles of Generators at Different Locations for Stability Control*. IEEE Power Engineering Society Winter Meeting. 2000. pp. 1237-1242.
6. Qiu, B., et al., *Internet based frequency monitoring network (FNET)*. IEEE Power Engineering Society Winter Meeting. 2001. pp. 1166-1171.
7. Zhong, Z., et al., *Power System Frequency Monitoring Network (FNET) Implementation*. IEEE Transactions on Power Systems. 2005. pp. 1914-1921.
8. Tsai, S.S., et al., *Study of Global Frequency Dynamic Behavior of Large Power Systems*. IEEE PES Power Systems Conference and Exposition. 2004.
9. Gardner, R.M., *Conditioning of FNET Data and Triangulation of Generator Trips in the Eastern Interconnected System.* Master's Thesis, Electrical and Computer Engineering, Virginia Tech, Blacksburg, 2005.
10. Tsai, S.S., *Study of Global Power System Frequency Behavior Based on Simulations and FNET Measurements*. PhD Dissertation, Electrical and Computer Engineering, Virginia Tech, Blacksburg, 2005.

11. Zhang, X., *High Precision Dynamic Power System Frequency Estimation Algorithm Based on Phasor Approach*. Master's Thesis, Electrical and Computer Engineering, Virginia Tech, Blacksburg, 2004.
12. Chen, J., *Accurate Frequency Estimation with Phasor Angles*. Master's Thesis, Electrical and Computer Engineering, Virginia Tech, Blacksburg, 1994.
13. Xu, C., *High Accuracy Real-time GPS Synchronized Frequency Measurement Device for Wide-area Power Grid Monitoring*. PhD Dissertation, Electrical and Computer Engineering, Virginia Tech, Blacksburg,2006.
14. Duda, Richard O., Peter Hart, David Stork, *Pattern Classification*, 2nd ed. 2001, New York: Wiley.
15. Synergy Systems LLC, San Diego, California, *M12+ GPS Receiver User's Guide*, http://www.synergy-gps.com, 2004, pp. 20-21.
16. Synergy Systems LLC, San Diego, California, *Sony GXB5005 GPS Receiver Data*, http://oem-gps.com/images/stories/pdf/sony%20gxb5005%20gps%20receiver%20data.pdf, September 19, 2005.
17. Synergy Systems LLC, San Diego, California, *Sony GXB5210 GPS Receiver Data*, http://oem-gps.com/images/stories/pdf/sony%20gxb5210%20gps%20receiver%20data.pdf, August 26, 2005.
18. Navman NZ Ltd., USA. *Jupiter 12 GPS Receiver Module Datasheet*, www.navman.com/, 2005, pp. 4-15.
19. Fastrax Ltd., Vantaa, Finland. *iTrax02 GPS Receiver Module Brochure*, http://www.fastrax.fi/, September 3, 2002.
20. Fastrax Ltd., Vantaa, Finland. *iTrax02 GPS Receiver Interface Description*, http://www.fastrax.fi/, December 11, 2002, pp. 5-6.
21. Fastrax Ltd., Vantaa, Finland. *uTracker02 rev C Product Description*, http://www.fastrax.fi/, October 19, 2001.
22. Fastrax Ltd., Vantaa, Finland. *iTrax03 OEM GPS Receiver Module Brochure*, http://www.fastrax.fi/, August, 2004.

23. Fastrax Ltd., Vantaa, Finland. *iTrax03 GPS Receiver Technical Description*, http://www.fastrax.fi/, September 6, 2005, pp. 9-10.
24. Fastrax Ltd., Vantaa, Finland. *iTrax03-S GPS Receiver Technical Description*, http://www.fastrax.fi/, September 6, 2005, pp. 8-9.
25. Fastrax Ltd., Vantaa, Finland. *iTrax100 OEM GPS Receiver Module Datasheet*, http://www.fastrax.fi/, June 7, 2005.
26. Fastrax Ltd., Vantaa, Finland. *iTrax100 GPS Receiver Technical Interface Description*, http://www.fastrax.fi/, June 7, 2005, pp. 6-7.
27. Navman NZ Ltd., USA. *Jupiter Pico 12-Channel GPS Receiver Module Product Brief*, http://www.navman.com/, 2005.
28. Navman NZ Ltd., USA. *Jupiter Pico T GPS Receiver Module Datasheet*, http://www.navman.com/, 2005, pp. 5-15.
29. Trimble Navigation Ltd., Sunnyvale, California, *Resolution T Brochure*, http://www.trimble.com, 2004.
30. i-Lotus Corporation Pte Ltd, Singapore, Singapore, *M12M Navigation Oncore Receiver Preliminary Specification*, http://www.synergy-gps.com/images/stories/pdf/m12m%20timing%20prelim%20v11.pdf, 2006.

Appendix I

Data Conditioning Scripts

discontinuity_interval.m

```
0001 %*****************************************************************************
0002 % This program calculates the interval between discontinuities in unwrapped
0003 % FDR angle data.
0004 % Input: wrapped angle data in variable 'data'
0005 % Output: Variables 'disc' and 'gap' which contain information about the
0006 % angle jump magnitude and interval between discontinuities, respectively.
0007 %*****************************************************************************
0008
0009 angle=unwrap(data);
0010 k=1;
0011 for n=1:size(data,2)
0012     for i=2:size(data,1)
0013         if (angle(i,n)-angle(i-1,n))>0.1 | (angle(i,n)-angle(i-1,n))<-0.1
0014             disc(k,n)=i;
0015             gap(k,n)=angle(i,n)-angle(i-1,n);
0016             k=k+1;
0017         end
0018     end
0019     k=1;
0020 end
0021 disc
0022 gap
```

moving_median.m

```
0001 %*****************************************************************************
0002 % This program performs 21 point moving median smoothing on FDR frequency
0003 % data.
0004 % Input: raw frequency data stored in variable 'data'
0005 % Output: variable 'mov_median' which contains the smoothed data.
0006 %*****************************************************************************
0007
0008 half_window=10;
0009 num_samples=length(freq);
0010
0011 for k=1:size(freq,2)
0012     for i=half_window+1:num_samples-half_window
0013         x=freq(i-half_window:i+half_window,k);
0014         mov_median(i,k)=median(x);
0015     end
0016 end
```

moving_mean.m

```
0001 %*****************************************************************************
0002 % This program performs 21 point moving mean smoothing on FDR frequency
0003 % data.
0004 % Input: raw frequency data stored in variable 'data'
0005 % Output: variable 'mov_mean' which contains the smoothed data.
0006 %*****************************************************************************
0007
0008 half_window=10;
0009 num_samples=size(vtfreq,2);
0010
0011 for i=half_window+1:num_samples-half_window
0012     x=vtfreq(i-half_window:i+half_window);
0013     mov_mean_vt(i)=mean(x);
0014 end
```

Appendix II

MATLAB Angle Difference Video Code

```
0001 %*************************************************************************
0002 % This program creates an angle difference video for Base Case 1 using a
0003 % cubic fit surface plot.  UMR is used as the reference point.  VT has been
0004 % eliminated due to unusual data.
0005 %
0006 % Input: ang_diff matrix containing angle difference data measured in
0007 % degrees.  Each column is a different FDR.  The column order is ARI, ABB,
0008 % MISS, UFL.
0009 %
0010 % Output: Surface plot video.  Every 10th sample is plotted.
0011 %*************************************************************************
0012
0013 % Initialize grid and video parameters
0014 [X,Y]=meshgrid(-92:0.1:-75,29:0.1:39);
0015 avifilename='case1_noVT';
0016 aviobj = avifile(avifilename);
0017 aviobj.compression = 'indeo5';
0018 aviobj.fps = 10;
0019 aviobj.quality = 100;
0020 feature('usegenericopengl',1)
0021
0022 % Specify FDR locations (latitude and longitude)
0023 x=[-91.7658 -77.0862 -78.6587 -88.8222 -82.3363];
0024 y=[37.9487 38.8210 35.8220 33.4567 29.6742];
0025
0026 % This loop creates a surface plot for every 10th sample and adds it to the
0027 % video
0028 for i=1:10:length(ang_diff)
0029     hold off;
0030     z=[0 ang_diff(i,1:4)];
0031     [X,Y,Z] = griddata(x,y,z,X,Y,'cubic');
0032     surf(X,Y,Z);
0033     caxis([-6.5317 20.6838])
0034     colorbar
0035     shading interp
0036     drawnow
0037     axis([-92 -75 29 39 -6.5317 200])
0038     view(2);
0039     hold on
0040
0041     % Plot FDR locations and labels, label axis, add title
0042     plot3(x,y,[200 200 200 200 200],'o','MarkerFaceColor','w')
0043     title(['Case 1 - Sample Number ', int2str(i)])
0044     xlabel('Longitude (degrees)')
0045     ylabel('Latitude (degrees)')
0046     text(-91.8,38.5,200,'UMR')
0047     text(-90.4,33.5,200,'MISS')
0048     text(-82,29.8,200,'UFL')
0049     text(-78.3,35.8,200,'ABB')
0050     text(-76.8,38.5,200,'ARI')
0051
0052     % Add frame to video
0053     frame = getframe(gcf);
0054     aviobj = addframe(aviobj,frame);
0055 end
0056
0057 % Close video
0058 aviobj = close(aviobj);
0059 save(avifilename,'aviobj');
```

```
0001 %*************************************************************************
0002 % This program creates an angle difference video for Base Case 2 using a
0003 % cubic fit surface plot.  UMR is used as the reference point.  VT has been
0004 % eliminated due to unusual data.
0005 %
0006 % Input: ang_diff matrix containing angle difference data measured in
0007 % degrees.  Each column is a different FDR.  The column order is NY, ARI,
0008 % ABB, MISS.
0009 %
0010 % Output: Surface plot video.  Every 10th sample is plotted.
0011 %*************************************************************************
0012
0013 % Initialize grid and video parameters
0014 [X,Y]=meshgrid(-92:0.1:-72,29:0.1:44);
0015 avifilename='case2_noVT';
0016 aviobj = avifile(avifilename);
0017 aviobj.compression = 'indeo5';
0018 aviobj.fps = 10;
0019 aviobj.quality = 100;
0020 feature('usegenericopengl',1)
0021
0022 % Specify FDR locations (latitude and longitude)
0023 x=[-91.7658 -73.9281 -77.0862 -78.6587 -88.8222];
0024 y=[37.9487 42.8018 38.8210 35.8220 33.4567];
0025
0026 % This loop creates a surface plot for every 10th sample and adds it to the
0027 % video
0028 for i=1:10:length(ang_diff)
0029     hold off;
0030     z=[0 ang_diff(i,1:4)];
0031     [X,Y,Z] = griddata(x,y,z,X,Y,'cubic');
0032     surf(X,Y,Z);
0033     caxis([-17.1887 20.6838])
0034     colorbar
0035     shading interp
0036     drawnow
0037     axis([-92 -72 29 44 -20 200])
0038     view(2);
0039     hold on
0040
0041     % Plot FDR locations and labels, label axis, add title
0042     plot3(x,y,[200 200 200 200 200],'o','MarkerFaceColor','w')
0043     title(['Case 2 - Sample Number ', int2str(i)])
0044     xlabel('Longitude (degrees)')
0045     ylabel('Latitude (degrees)')
0046     text(-91.8,38.5,200,'UMR')
0047     text(-90.5,33.5,200,'MISS')
0048     text(-73.6,42.8,200,'NY')
0049     text(-78.3,35.8,200,'ABB')
0050     text(-76.8,38.5,200,'ARI')
0051
0052     % Add frame to video
0053     frame = getframe(gcf);
0054     aviobj = addframe(aviobj,frame);
0055 end
0056
0057 % Close video
0058 aviobj = close(aviobj);
0059 save(avifilename,'aviobj');
```

```
0001 %*************************************************************************
0002 % This program creates an angle difference video for Base Case 3 using a
0003 % cubic fit surface plot.  UMR is used as the reference point.  VT has been
0004 % eliminated due to unusual data.
0005 %
0006 % Input: ang_diff matrix containing angle difference data measured in
0007 % degrees.  Each column is a different FDR.  The column order is ARI, ABB,
0008 % MISS, Calvin.
0009 %
0010 % Output: Surface plot video.  Every 10th sample is plotted.
0011 %*************************************************************************
0012
0013 % Initialize grid and video parameters
0014 [X,Y]=meshgrid(-92:0.1:-76,29:0.1:44);
0015 avifilename='case3_noVT';
0016 aviobj = avifile(avifilename);
0017 aviobj.compression = 'indeo5';
0018 aviobj.fps = 10;
0019 aviobj.quality = 100;
0020 feature('usegenericopengl',1)
0021
0022 % Specify FDR locations (latitude and longitude)
0023 x=[-91.7658 -77.0862 -78.6587 -88.8222 -85.6557];
0024 y=[37.9487 38.8210 35.8220 33.4567 42.9613];
0025
0026 % This loop creates a surface plot for every 10th sample and adds it to the
0027 % video
0028 for i=1:10:length(ang_diff)
0029     hold off;
0030     z=[0 ang_diff(i,1:4)];
0031     [X,Y,Z] = griddata(x,y,z,X,Y,'cubic');
0032     surf(X,Y,Z);
0033     caxis([-28.8771 31.3408])
0034     colorbar
0035     shading interp
0036     drawnow
0037     axis([-92.5 -76 32 44 -29 200])
0038     view(2);
0039     hold on
0040
0041     % Plot FDR locations and labels, label axis, add title
0042     plot3(x,y,[200 200 200 200 200],'o','MarkerFaceColor','w')
0043     title(['Case 3 - Sample Number ', int2str(i)])
0044     xlabel('Longitude (degrees)')
0045     ylabel('Latitude (degrees)')
0046     text(-92.4,38.5,200,'UMR')
0047     text(-90.4,33.5,200,'MISS')
0048     text(-85.5,43.2,200,'CALVIN')
0049     text(-78.3,35.8,200,'ABB')
0050     text(-76.9,38.5,200,'ARI')
0051
0052     % Add frame to video
0053     frame = getframe(gcf);
0054     aviobj = addframe(aviobj,frame);
0055 end
0056
0057 % Close video
0058 aviobj = close(aviobj);
0059 save(avifilename,'aviobj');
```

```
0001 %************************************************************************
0002 % This program creates an angle difference video for Base Case 5 using a
0003 % cubic fit surface plot.  UMR is used as the reference point.
0004 %
0005 % Input: ang_diff matrix containing angle difference data measured in
0006 % degrees.  Each column is a different FDR.  The column order is ARI, VT,
0007 % ABB, MISS, UFL, Calvin.
0008 %
0009 % Output: Surface plot video.  Every 10th sample is plotted.
0010 %************************************************************************
0011
0012 % Initialize grid and video parameters
0013 [X,Y]=meshgrid(-92:0.1:-76,29:0.1:44);
0014 avifilename='case5';
0015 aviobj = avifile(avifilename);
0016 aviobj.compression = 'indeo5';
0017 aviobj.fps = 10;
0018 aviobj.quality = 100;
0019 feature('usegenericopengl',1)
0020
0021 % Specify FDR locations (latitude and longitude)
0022 x=[-91.7658 -77.0862 -80.4284 -78.6587 -88.8222 -82.3363 -85.6557];
0023 y=[37.9487 38.8210 37.2327 35.8220 33.4567 29.6742 42.9613];
0024
0025 % This loop creates a surface plot for every 10th sample and adds it to the
0026 % video
0027 for i=1:10:length(ang_diff)
0028     hold off;
0029     z=[0 ang_diff(i,1:6)];
0030     [X,Y,Z] = griddata(x,y,z,X,Y,'cubic');
0031     surf(X,Y,Z);
0032     caxis([-32.7159 34.6067])
0033     colorbar
0034     shading interp
0035     drawnow
0036     axis([-92.5 -76 29 44 -35 2000])
0037     view(2);
0038     hold on
0039
0040     % Plot FDR locations and labels, label axis, add title
0041     plot3(x,y,[200 200 200 200 200 200 200],'o','MarkerFaceColor','w')
0042     title(['Case 5 - Sample Number ', int2str(i)])
0043     xlabel('Longitude (degrees)')
0044     ylabel('Latitude (degrees)')
0045     text(-92.4,38.5,200,'UMR')
0046     text(-90.4,33.5,200,'MISS')
0047     text(-85.5,43.2,200,'CALVIN')
0048     text(-78.3,35.8,200,'ABB')
0049     text(-76.9,38.5,200,'ARI')
0050     text(-80.5,36.6,200,'VT')
0051     text(-82,29.8,200,'UFL')
0052
0053     % Add frame to video
0054     frame = getframe(gcf);
0055     aviobj = addframe(aviobj,frame);
0056 end
0057
0058 % Close video
0059 aviobj = close(aviobj);
0060 save(avifilename,'aviobj');
```

```
0001 %************************************************************************
0002 % This program creates an angle difference video for Base Case 6 using a
0003 % cubic fit surface plot.  UMR is used as the reference point.
0004 %
0005 % Input: ang_diff matrix containing angle difference data measured in
0006 % degrees.  Each column is a different FDR.  The column order is ARI, VT,
0007 % ABB, MISS, UFL, Calvin, Tulane, TVA1.
0008 %
0009 % Output: Surface plot video.  Every 10th sample is plotted.
0010 %************************************************************************
0011
0012 % Initialize grid and video parameters
0013 [X,Y]=meshgrid(-92:0.1:-76,29:0.1:44);
0014 avifilename='case6';
0015 aviobj = avifile(avifilename);
0016 aviobj.compression = 'indeo5';
0017 aviobj.fps = 10;
0018 aviobj.quality = 100;
0019 feature('usegenericopengl',1)
0020
0021 % Specify FDR locations (latitude and longitude)
0022 x=[-91.7658 -77.0862 -80.4284 -78.6587 -88.8222 -82.3363 -85.6557 -89.9313 -
84.8750];
0023 y=[37.9487 38.8210 37.2327 35.8220 33.4567 29.6742 42.9613 30.0658 35.1313];
0024
0025 % This loop creates a surface plot for every 10th sample and adds it to the
0026 % video
0027 for i=1:10:length(ang_diff)
0028     hold off;
0029     z=[0 ang_diff(i,1:8)];
0030     [X,Y,Z] = griddata(x,y,z,X,Y,'cubic');
0031     surf(X,Y,Z);
0032     caxis([-81.0735 60.5616])
0033     colorbar
0034     shading interp
0035     drawnow
0036     axis([-92.5 -76 28.5 44 -82 2000])
0037     view(2);
0038     hold on
0039
0040     % Plot FDR locations and labels, label axis, add title
0041     plot3(x,y,[200 200 200 200 200 200 200 200 200],'o','MarkerFaceColor','w')
0042     title(['Case 6 - Sample Number ', int2str(i)])
0043     xlabel('Longitude (degrees)')
0044     ylabel('Latitude (degrees)')
0045     text(-92.4,38.5,200,'UMR')
0046     text(-90.4,33.5,200,'MISS')
0047     text(-85.5,43.2,200,'CALVIN')
0048     text(-78.3,35.8,200,'ABB')
0049     text(-76.9,38.5,200,'ARI')
0050     text(-80.5,36.6,200,'VT')
0051     text(-82,29.8,200,'UFL')
0052     text(-90,29.6,200,'TULANE')
0053     text(-84.8,34.6,200,'TVA1')
0054
0055     % Add frame to video
0056     frame = getframe(gcf);
0057     aviobj = addframe(aviobj,frame);
0058 end
0059
0060 % Close video
0061 aviobj = close(aviobj);
0062 save(avifilename,'aviobj');
```

```
0001 %*************************************************************************
0002 % This program creates an angle difference video for Base Case 7 using a
0003 % cubic fit surface plot.  UMR is used as the reference point.  VT has been
0004 % eliminated due to unusual data.
0005 %
0006 % Input: ang_diff matrix containing angle difference data measured in
0007 % degrees.  Each column is a different FDR.  The column order is ARI, ABB,
0008 % MISS, UFL, Calvin, Tulane, TVA1.
0009 %
0010 % Output: Surface plot video.  Every 10th sample is plotted.
0011 %*************************************************************************
0012
0013 % Initialize grid and video parameters
0014 [X,Y]=meshgrid(-92:0.1:-76,29:0.1:44);
0015 avifilename='case7_noVT';
0016 aviobj = avifile(avifilename);
0017 aviobj.compression = 'indeo5';
0018 aviobj.fps = 10;
0019 aviobj.quality = 100;
0020 feature('usegenericopengl',1)
0021
0022 % Specify FDR locations (latitude and longitude)
0023 x=[-91.7658 -77.0862 -78.6587 -88.8222 -82.3363 -85.6557 -89.9313 -84.8750];
0024 y=[37.9487 38.8210 35.8220 33.4567 29.6742 42.9613 30.0658 35.1313];
0025
0026 % This loop creates a surface plot for every 10th sample and adds it to the
0027 % video
0028 for i=1:10:length(ang_diff)
0029     hold off;
0030     z=[0 ang_diff(i,1:7)];
0031     [X,Y,Z] = griddata(x,y,z,X,Y,'cubic');
0032     surf(X,Y,Z);
0033     caxis([-7.7578 13.4187])
0034     colorbar
0035     shading interp
0036     drawnow
0037     axis([-92.5 -76 28.5 44 -10 2000])
0038     view(2);
0039     hold on
0040
0041     % Plot FDR locations and labels, label axis, add title
0042     plot3(x,y,[200 200 200 200 200 200 200 200],'o','MarkerFaceColor','w')
0043     title(['Case 7 - Sample Number ', int2str(i)])
0044     xlabel('Longitude (degrees)')
0045     ylabel('Latitude (degrees)')
0046     text(-92.4,38.5,200,'UMR')
0047     text(-90.4,33.5,200,'MISS')
0048     text(-85.5,43.2,200,'CALVIN')
0049     text(-78.3,35.8,200,'ABB')
0050     text(-76.9,38.5,200,'ARI')
0051     text(-82,29.8,200,'UFL')
0052     text(-90,29.6,200,'TULANE')
0053     text(-84.8,34.6,200,'TVA1')
0054
0055     % Add frame to video
0056     frame = getframe(gcf);
0057     aviobj = addframe(aviobj,frame);
0058 end
0059
0060 % Close video
0061 aviobj = close(aviobj);
0062 save(avifilename,'aviobj');
```

```
0001 %************************************************************************
0002 % This program creates an angle difference video for Base Case 8 using a
0003 % cubic fit surface plot.  UMR is used as the reference point.
0004 %
0005 % Input: ang_diff matrix containing angle difference data measured in
0006 % degrees.  Each column is a different FDR.  The column order is ARI, VT,
0007 % ABB, MISS, UFL, Calvin, TVA1.
0008 %
0009 % Output: Surface plot video.  Every 10th sample is plotted.
0010 %************************************************************************
0011
0012 % Initialize grid and video parameters
0013 [X,Y]=meshgrid(-92:0.1:-76,29:0.1:44);
0014 avifilename='case8';
0015 aviobj = avifile(avifilename);
0016 aviobj.compression = 'indeo5';
0017 aviobj.fps = 10;
0018 aviobj.quality = 100;
0019 feature('usegenericopengl',1)
0020
0021 % Specify FDR locations (latitude and longitude)
0022 x=[-91.7658 -77.0862 -80.4284 -78.6587 -88.8222 -82.3363 -85.6557 -84.8750];
0023 y=[37.9487 38.8210 37.2327 35.8220 33.4567 29.6742 42.9613 35.1313];
0024
0025 % This loop creates a surface plot for every 10th sample and adds it to the
0026 % video
0027 for i=1:10:length(ang_diff)
0028     hold off;
0029     z=[0 ang_diff(i,1:7)];
0030     [X,Y,Z] = griddata(x,y,z,X,Y,'cubic');
0031     surf(X,Y,Z);
0032     caxis([-55.5769 43.7167])
0033     colorbar
0034     shading interp
0035     drawnow
0036     axis([-92.5 -76 28.5 44 -56 2000])
0037     view(2);
0038     hold on
0039
0040     % Plot FDR locations and labels, label axis, add title
0041     plot3(x,y,[200 200 200 200 200 200 200 200],'o','MarkerFaceColor','w')
0042     title(['Case 8 - Sample Number ', int2str(i)])
0043     xlabel('Longitude (degrees)')
0044     ylabel('Latitude (degrees)')
0045     text(-92.4,38.5,200,'UMR')
0046     text(-90.4,33.5,200,'MISS')
0047     text(-85.5,43.2,200,'CALVIN')
0048     text(-78.3,35.8,200,'ABB')
0049     text(-76.9,38.5,200,'ARI')
0050     text(-80.5,36.6,200,'VT')
0051     text(-82,29.8,200,'UFL')
0052     text(-84.8,34.6,200,'TVA1')
0053
0054     % Add frame to video
0055     frame = getframe(gcf);
0056     aviobj = addframe(aviobj,frame);
0057 end
0058
0059 % Close video
0060 aviobj = close(aviobj);
0061 save(avifilename,'aviobj');
```

```
0001 %************************************************************************
0002 % This program creates an angle difference video for Base Case 9 using a
0003 % cubic fit surface plot.  UMR is used as the reference point.
0004 %
0005 % Input: ang_diff matrix containing angle difference data measured in
0006 % degrees.  Each column is a different FDR.  The column order is ARI, VT,
0007 % ABB, MISS, UFL, Calvin, Tulane, TVA1.
0008 %
0009 % Output: Surface plot video.  Every 10th sample is plotted.
0010 %************************************************************************
0011
0012 % Initialize grid and video parameters
0013 [X,Y]=meshgrid(-92:0.1:-76,29:0.1:44);
0014 avifilename='case9';
0015 aviobj = avifile(avifilename);
0016 aviobj.compression = 'indeo5';
0017 aviobj.fps = 10;
0018 aviobj.quality = 100;
0019 feature('usegenericopengl',1)
0020
0021 % Specify FDR locations (latitude and longitude)
0022 x=[-91.7658 -77.0862 -80.4284 -78.6587 -88.8222 -82.3363 -85.6557 -89.9313 -
84.8750];
0023 y=[37.9487 38.8210 37.2327 35.8220 33.4567 29.6742 42.9613 30.0658 35.1313];
0024
0025 % This loop creates a surface plot for every 10th sample and adds it to the
0026 % video
0027 for i=1:10:length(ang_diff)
0028     hold off;
0029     z=[0 ang_diff(i,1:8)];
0030     [X,Y,Z] = griddata(x,y,z,X,Y,'cubic');
0031     surf(X,Y,Z);
0032     caxis([-10.0268 58.0406])
0033     colorbar
0034     shading interp
0035     drawnow
0036     axis([-92.5 -76 28.5 44 -15 2000])
0037     view(2);
0038     hold on
0039
0040     % Plot FDR locations and labels, label axis, add title
0041     plot3(x,y,[200 200 200 200 200 200 200 200 200],'o','MarkerFaceColor','w')
0042     title(['Case 9 - Sample Number ', int2str(i)])
0043     xlabel('Longitude (degrees)')
0044     ylabel('Latitude (degrees)')
0045     text(-92.4,38.5,200,'UMR')
0046     text(-90.4,33.5,200,'MISS')
0047     text(-85.5,43.2,200,'CALVIN')
0048     text(-78.3,35.8,200,'ABB')
0049     text(-76.9,38.5,200,'ARI')
0050     text(-80.5,36.6,200,'VT')
0051     text(-82,29.8,200,'UFL')
0052     text(-90,29.6,200,'TULANE')
0053     text(-84.8,34.6,200,'TVA1')
0054
0055     % Add frame to video
0056     frame = getframe(gcf);
0057     aviobj = addframe(aviobj,frame);
0058 end
0059
0060 % Close video
0061 aviobj = close(aviobj);
0062 save(avifilename,'aviobj');
```

Appendix III

K-Means Matlab Code

event_detector.m

```
0001 %************************************************************************
0002 % Function: event_detector.m - Scans FDR frequency data for possible power
0003 % system events.
0004 %
0005 % Input: Data structure containing FDR frequency data
0006 %
0007 % Output: Prints a time range where an event possibly exists for each FDR.
0008 %
0009 % Authors: Kevin Khan, Jon Burgett
0010 %************************************************************************
0011
0012 function [] = event_detector(EVENT_Data)
0013 format long;
0014 names=fieldnames(EVENT_Data);
0015 windowsize=100;
0016 step=50;
0017 fdrNMS = [];
0018
0019 % For each FDR, this block checks that all data is present.  Then it passes
0020 % a 100 point window to proj_kmeans.m.  Based on the returned value, it is
0021 % determined whether there is an event.
0022 for k=5:length(names)
0023     if max(isnan(EVENT_Data.(char(names(k))).freq))==0
0024         %fdrNMS = [fdrNMS EVENT_Data.(char(names(k))).name ','];
0025         for i=1:step:length(EVENT_Data.(char(names(k))).freq)-windowsize
0026             distance=proj_kmeans(EVENT_Data.(char(names(k))).freq(i:i+windowsize));
0027             % Print results based on distance and FDR location
0028             if distance > 0.015 & length(EVENT_Data.(char(names(k))).net) == 2
0029                 fprintf('Event found between %1.0f and %1.0f on %s
                     \n',i,i+windowsize,(char(names(k))))
0030             elseif distance > 0.025 & length(EVENT_Data.(char(names(k))).net) == 4
0031                 fprintf('Event found between %1.0f and %1.0f on %s
                    \n',i,i+windowsize,(char(names(k))))
0032             end
0033         end
0034     else
0035         fprintf('Data missing for %s \n',(char(names(k))))
0036     end
0037 end
```

proj_kmeans.m

```
0001 %************************************************************************
0002 % Function: proj_kmeans.m - Performs one dimensional k-means classification
0003 % on a set of points and returns the distance between class centers.
0004 %
0005 % Input: Vector containing data points
0006 %
0007 % Output: Returns distance between class centers.  If a class contains less
0008 % than 10 points, returns 0.
0009 %
0010 % Authors: Kevin Khan, Jon Burgett
0011 %************************************************************************
0012
0013 function [center_dist] = proj_kmeans(training)
0014 format long;
```

```
0015
0016 % Store input data
0017 num_samples=length(training);
0018
0019 % Choose first and last data points as initial mean guesses
0020 % Reject 2nd mean guess if it is equal to the 1st mean guess
0021 centers(1)=training(1);
0022 centers(2)=training(num_samples);
0023 i=1;
0024 while centers(1)==centers(2)
0025     centers(2)=training(num_samples-i);
0026     i=i+1;
0027 end
0028
0029 delta_centers=1;
0030
0031 % Run until the change in class centers is zero
0032 while max(abs(delta_centers))~=0
0033     class1=[0];
0034     class2=[0];
0035     class1_length=0;
0036     class2_length=0;
0037     % Assign classes for each sample
0038     for i=1:num_samples
0039         dist1=abs(training(i)-centers(1));
0040         dist2=abs(training(i)-centers(2));
0041         if dist2<dist1
0042             class2_length=class2_length+1;
0043             class2(class2_length)=training(i);
0044         else
0045             class1_length=class1_length+1;
0046             class1(class1_length)=training(i);
0047         end
0048     end
0049
0050     % Calculate new means and compare to old means
0051     new_mean(1)=mean(class1);
0052     new_mean(2)=mean(class2);
0053     delta_centers=centers-new_mean;
0054     centers=new_mean;
0055 end
0056
0057 % Return distance between class means
0058 % If a class contains less than 10 data points, return 0
0059 if class1_length<10 | class2_length<10
0060     center_dist=0;
0061 else
0062     center_dist=norm(centers(1)-centers(2));
0063 end
```

Appendix IV

FDR Assembly Guide

1) Serial Cables

- GPS to CME555 (~ 5.5 inches)

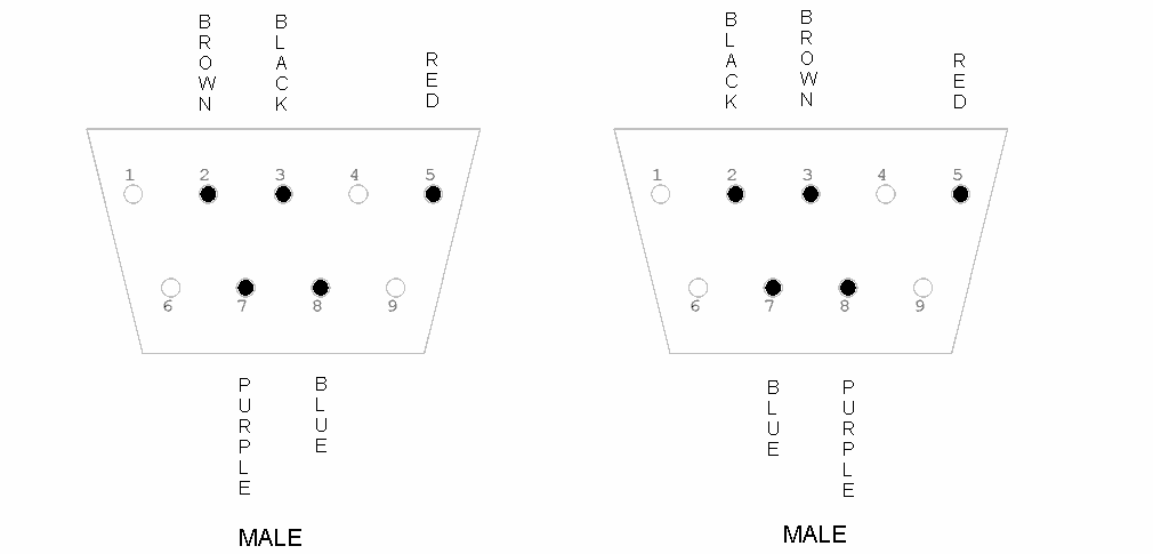

- CME555 to Ethernet (~ 5.5 inches)

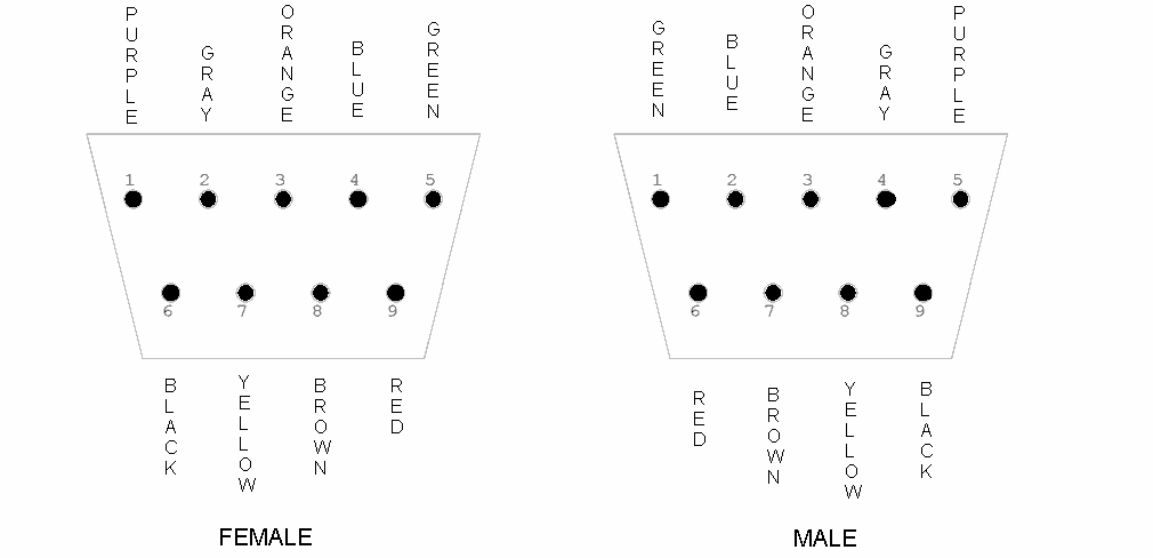

*Note: Plug does not fit through hole in the case; must put cable through hole before attaching plug (male end of CME555 to Ethernet cable).
*Solder shield wire to plug

2) Mount Filter

- Drill holes in CME555 and filter board
- Fasten with nylon screws, nuts, and spacers

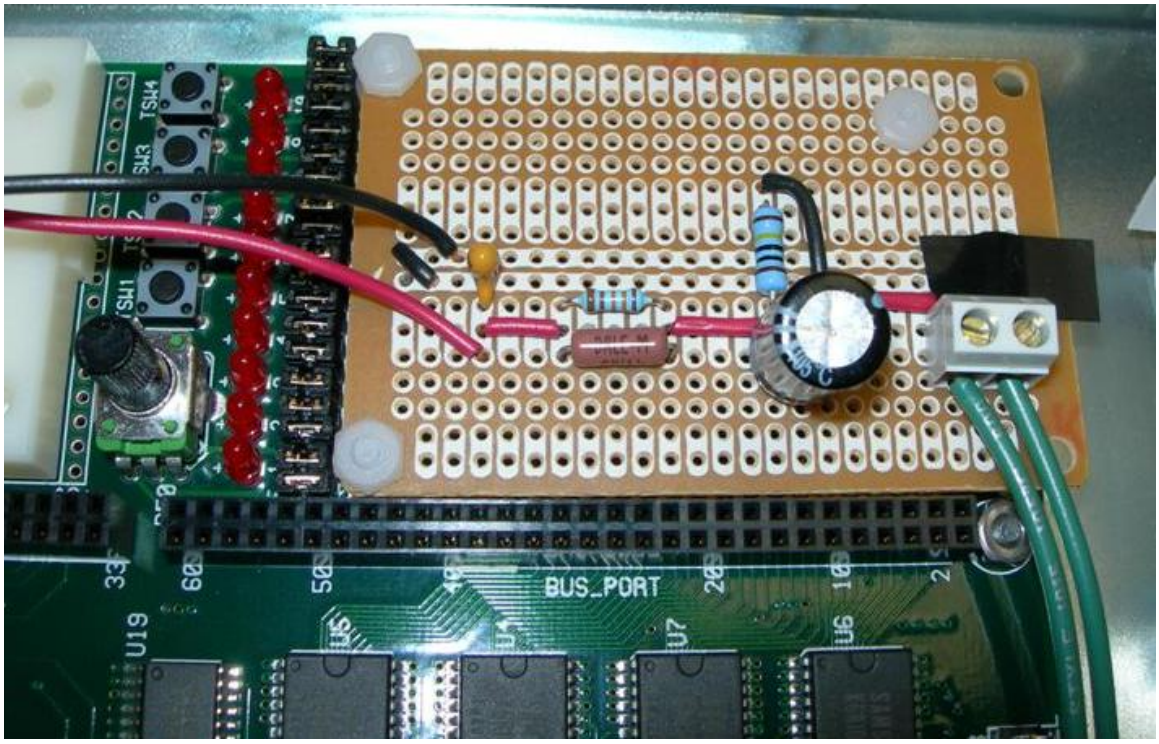

*Be careful not to drill the CME555 board near any circuits or jumpers

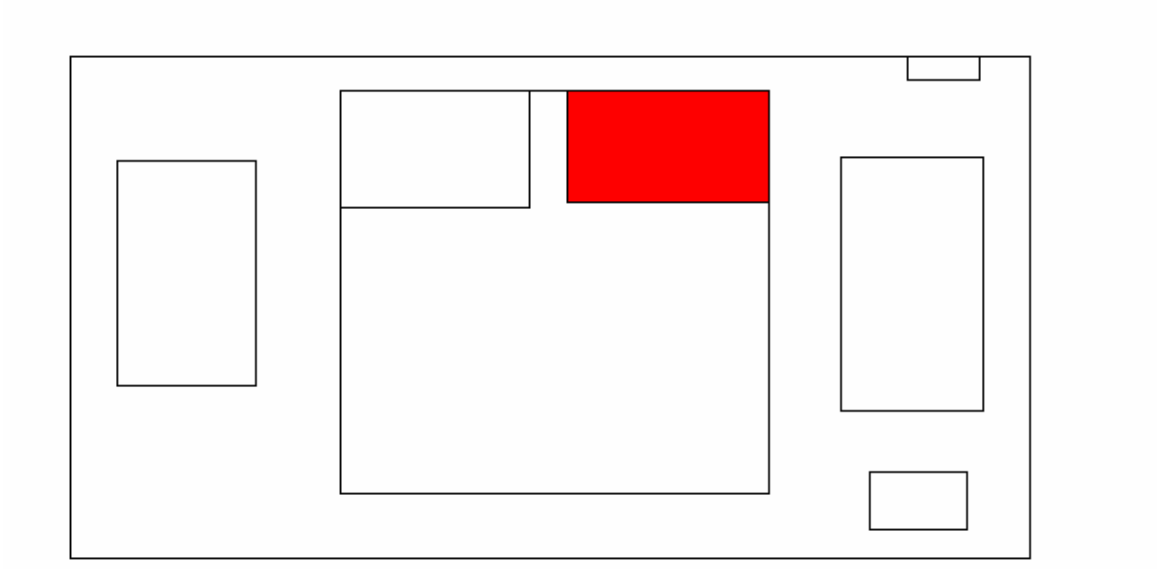

3) Fasten GPS and CME555 to Case

- Drill holes in case
- Fasten with metal screws, nuts, and nylon spacers

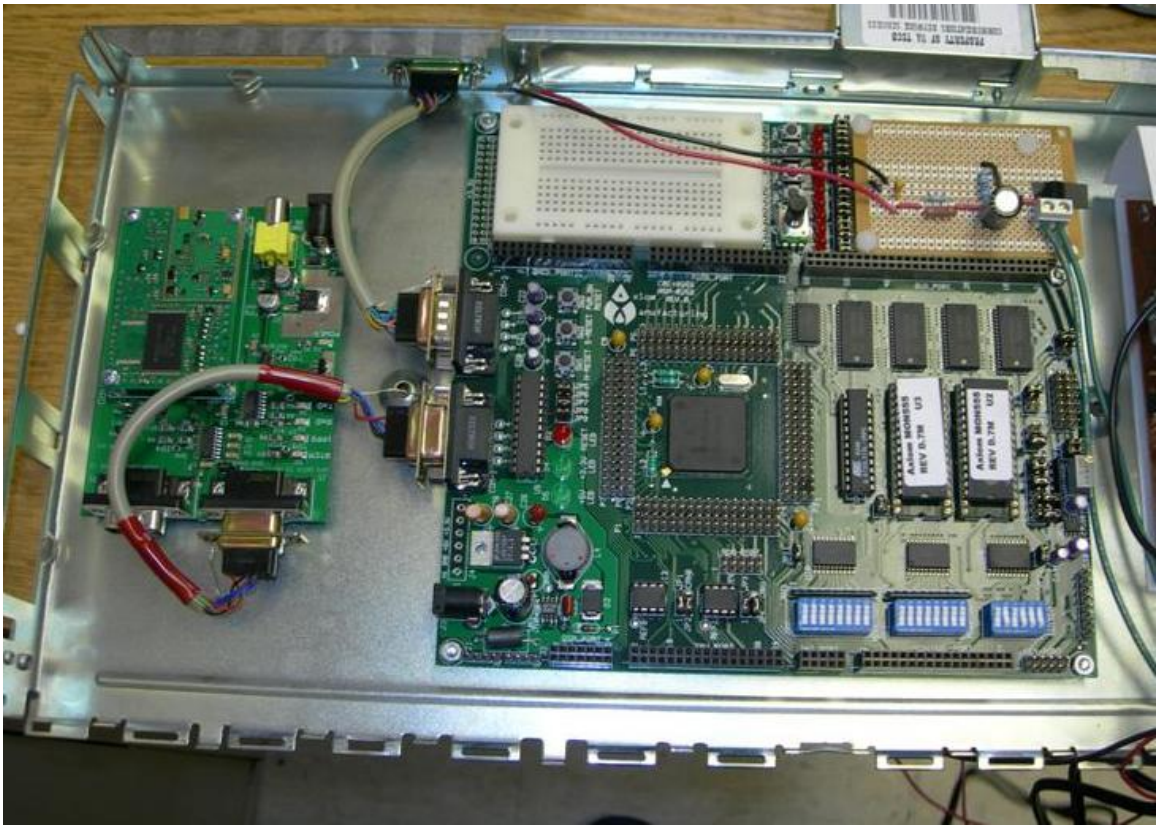

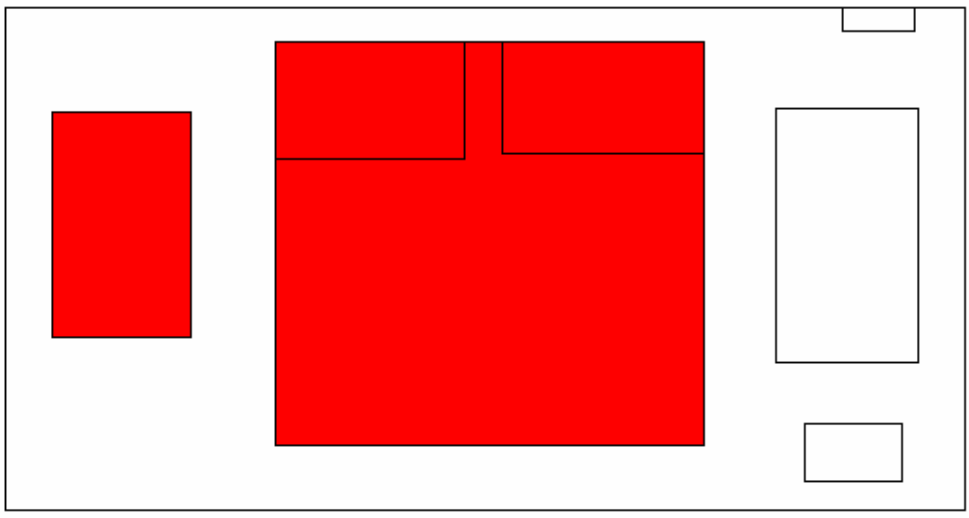

4) Mount Transformer

- Drill two holes and mount with metal screws and nuts

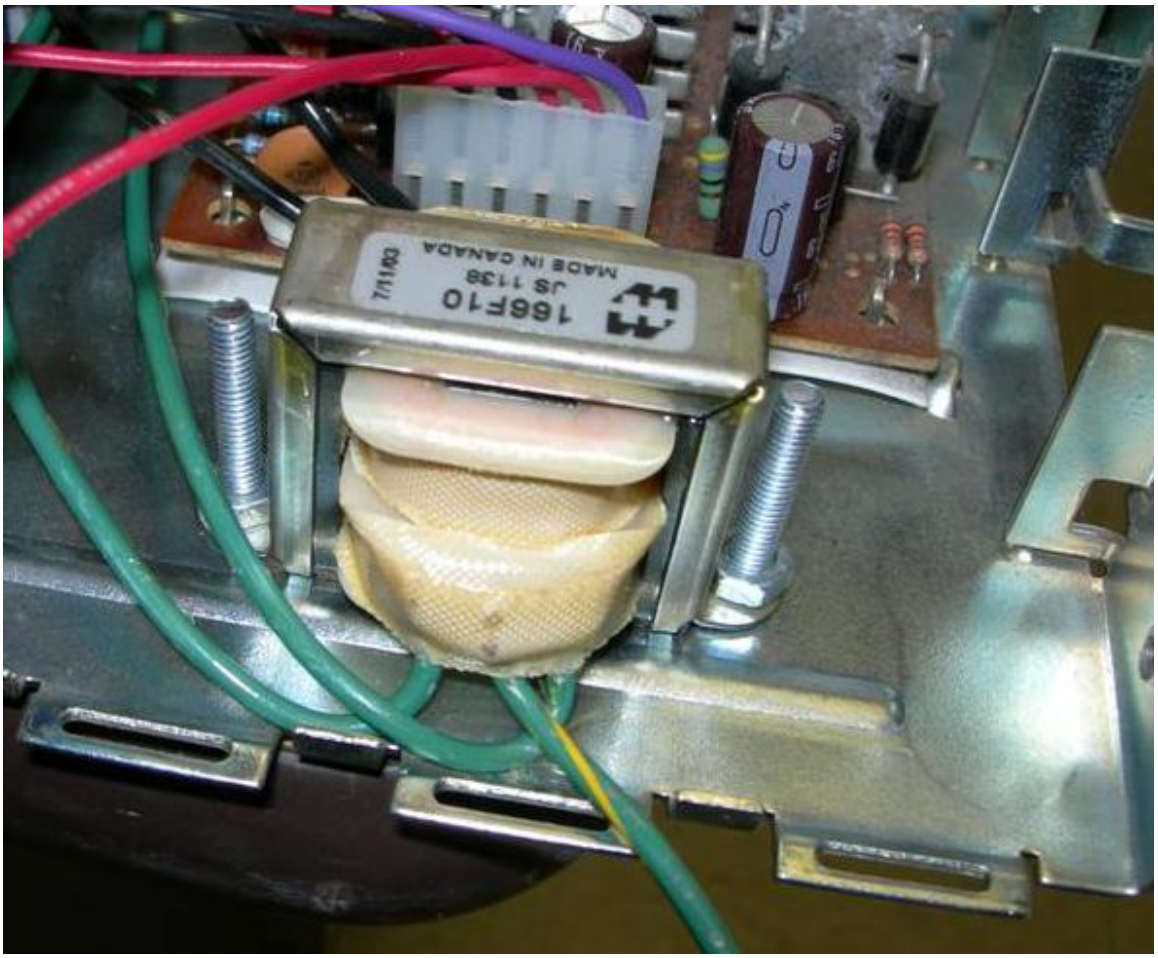

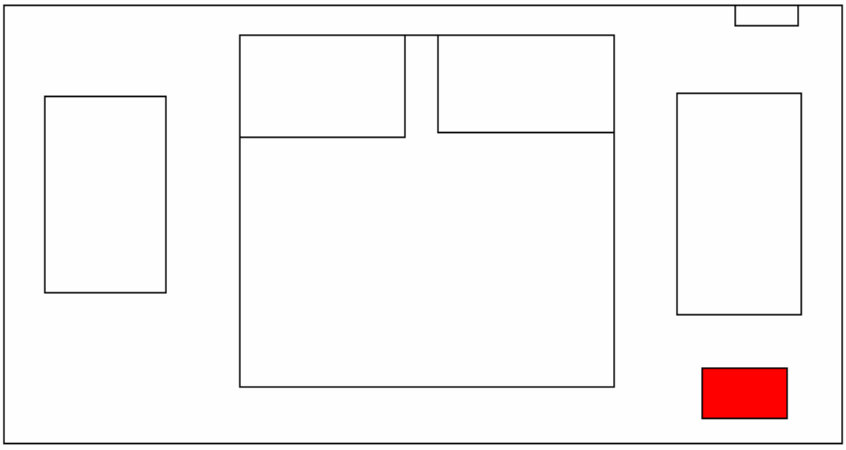

5) Mount A/D Converter

- Plugs into CME555

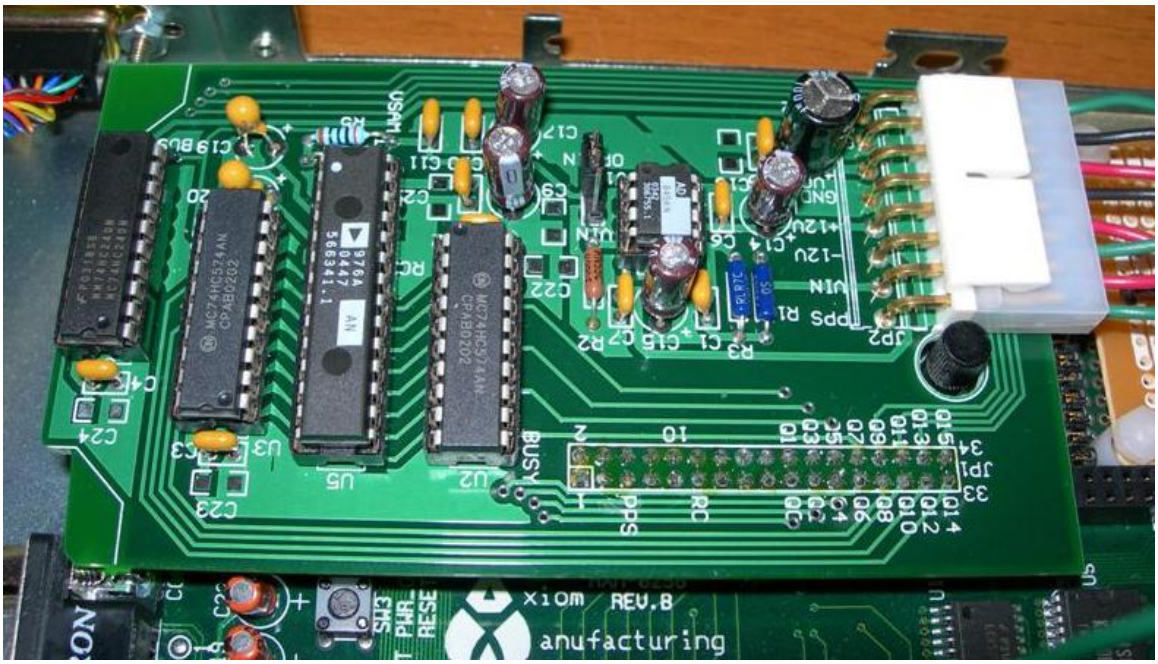

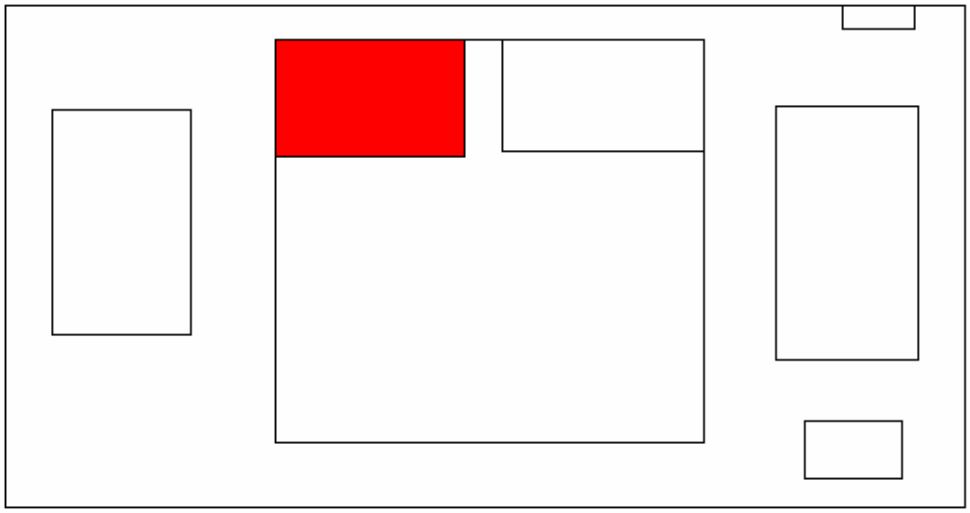

6) Wiring

- See wiring diagram
- Use wire nuts to connect wires
- Use RCA cable to connect 1PPS signal to A/D converter
- Install fuse between transformer and power input
- Insulate ends of unused wires

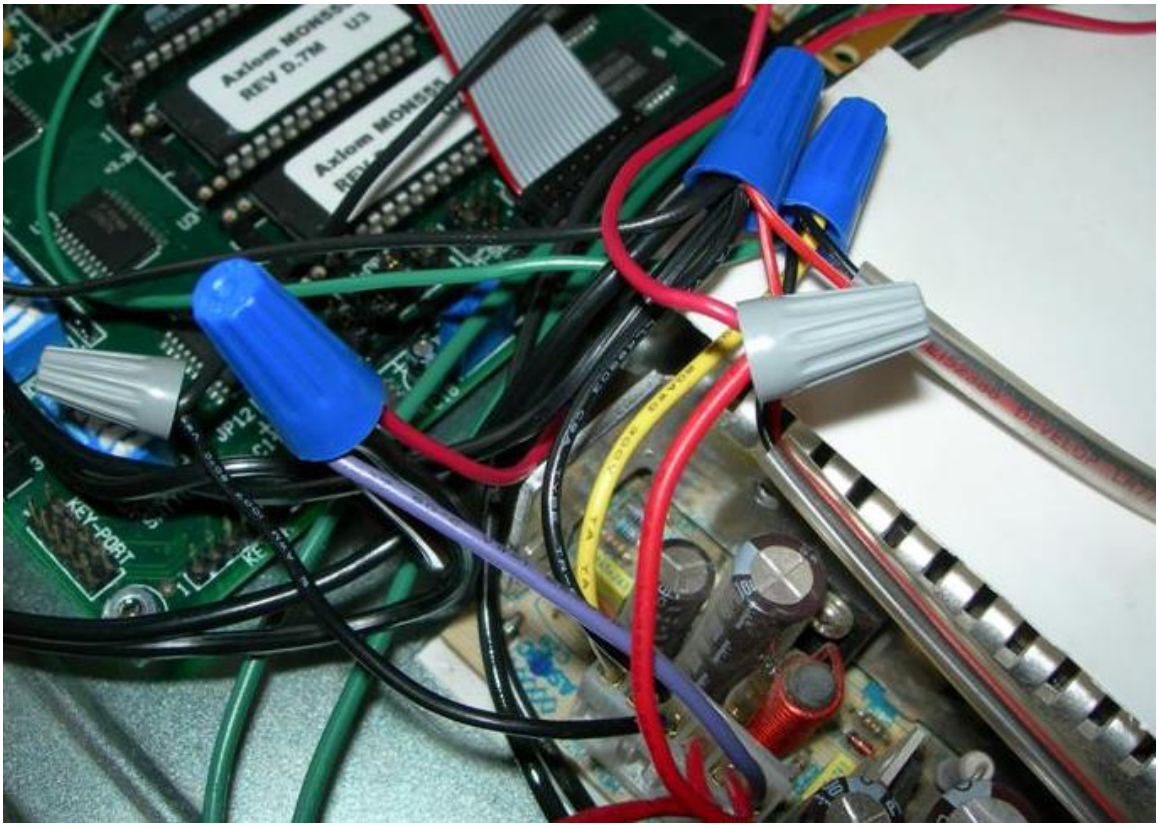

7) Soldering

- Solder transformer input wires to power input

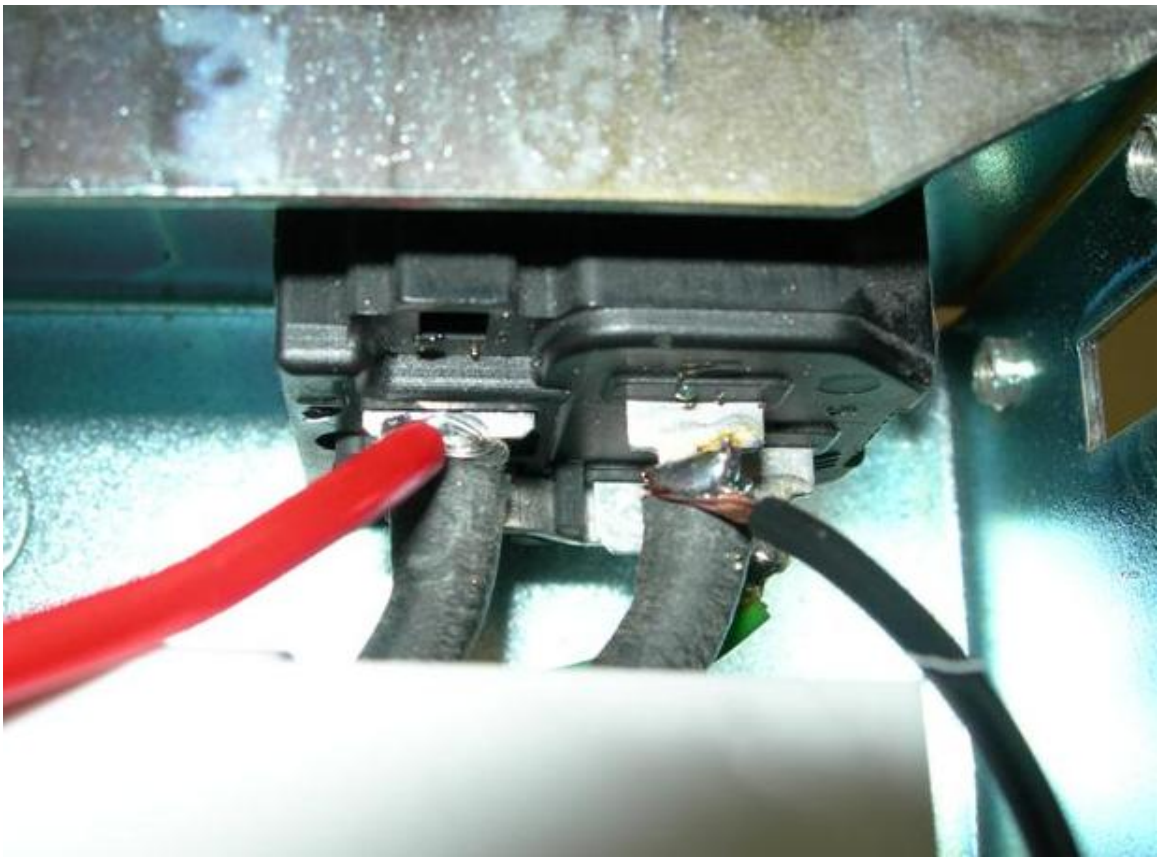

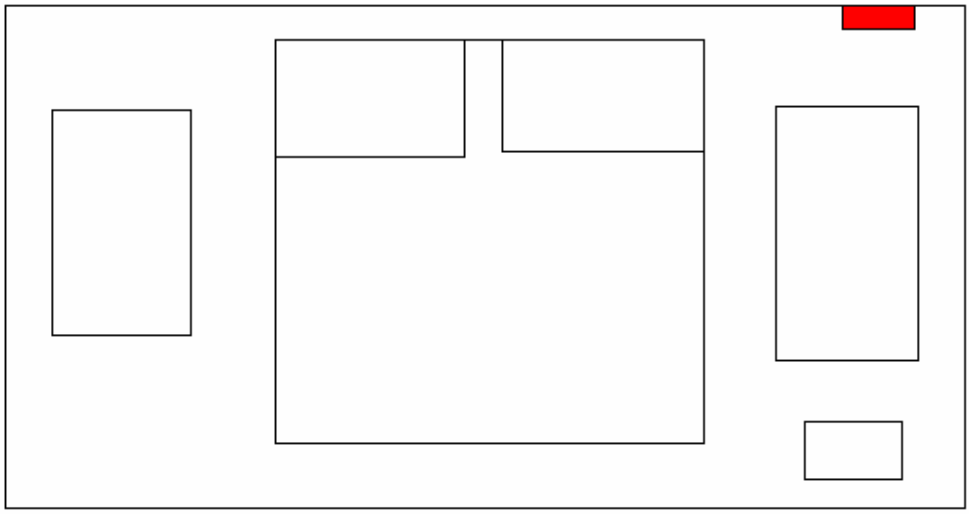

- Solder pins to the LCD

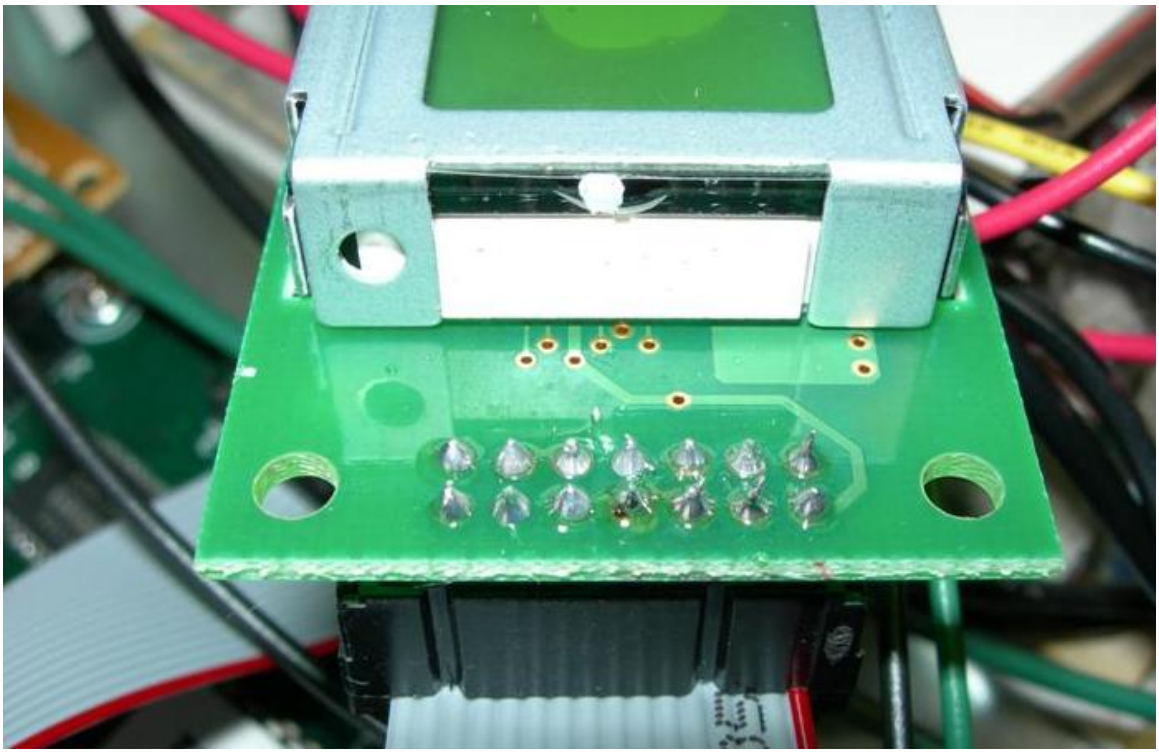

8) Jumper and Switch Positions

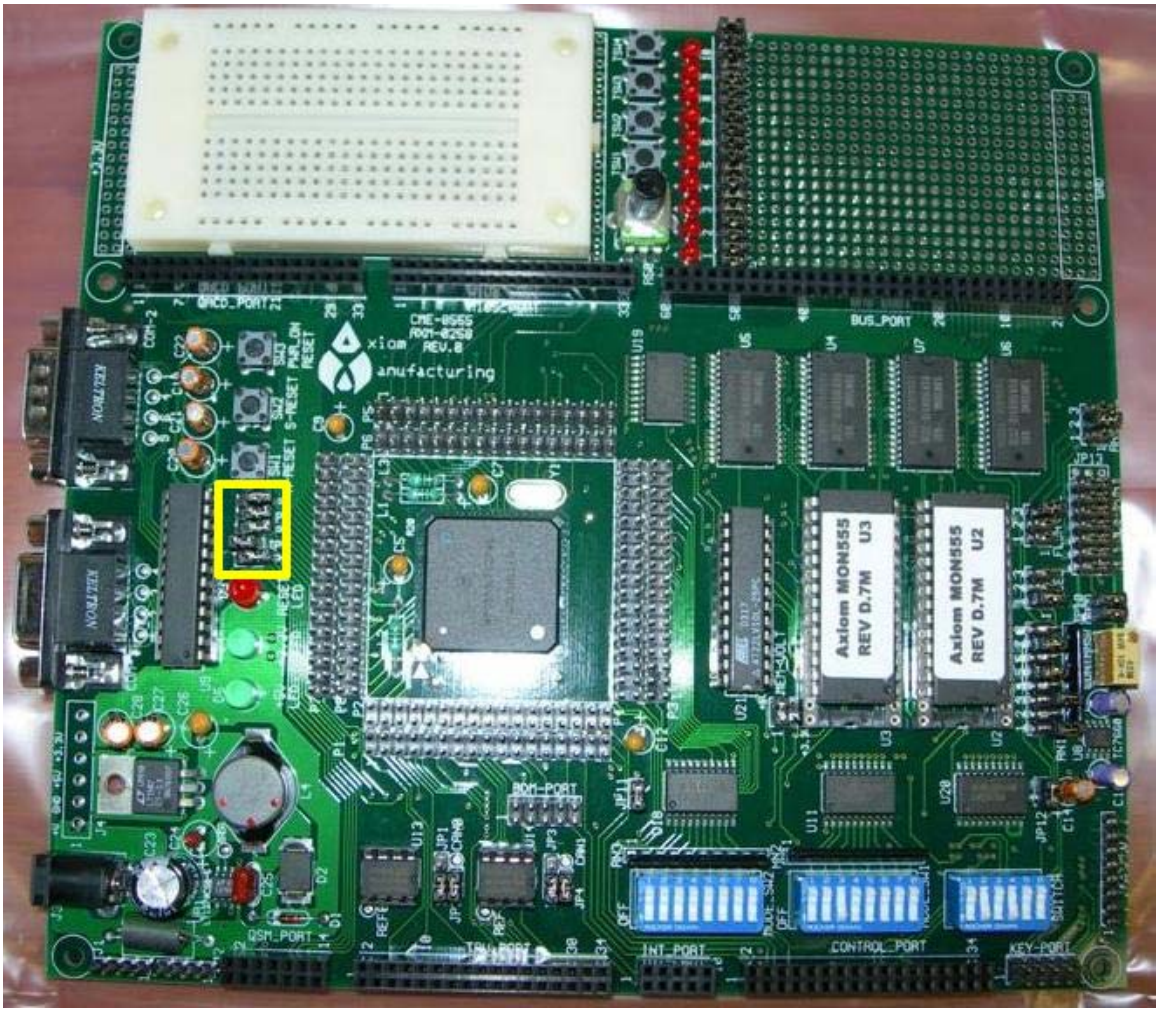

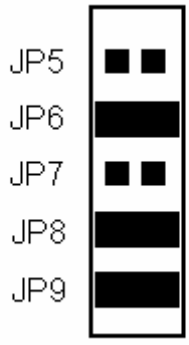

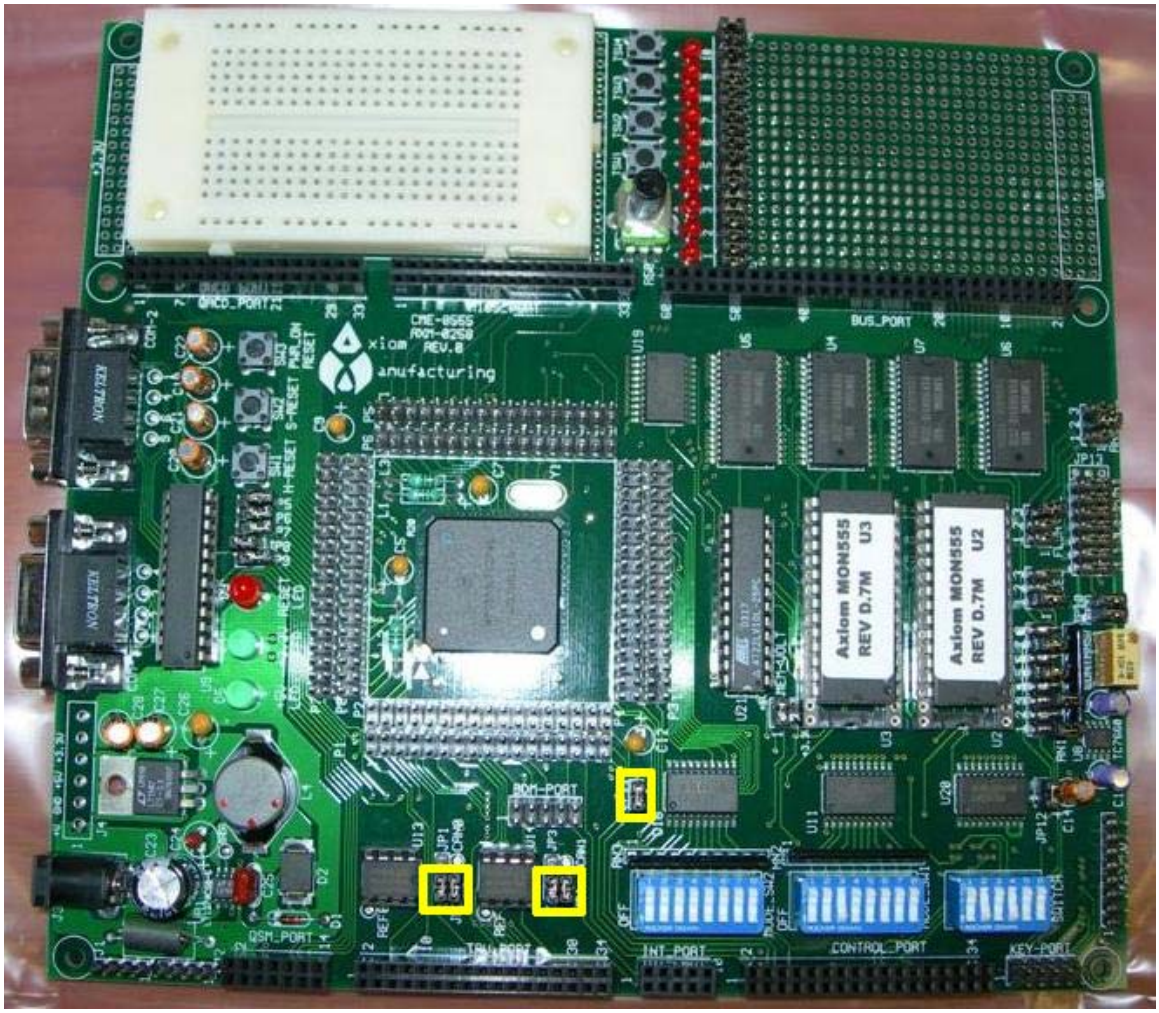
BUS_PORT
Axiom MON555
REV 0.7M U3
Axiom MON555
REV 0.7M U2
ROM-PORT
QSM_PORT
INT_PORT
CONTROL_PORT
KEY-PORT

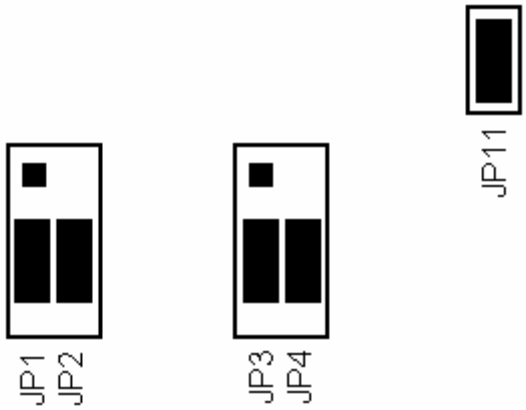
JP11
JP1
JP2
JP3
JP4

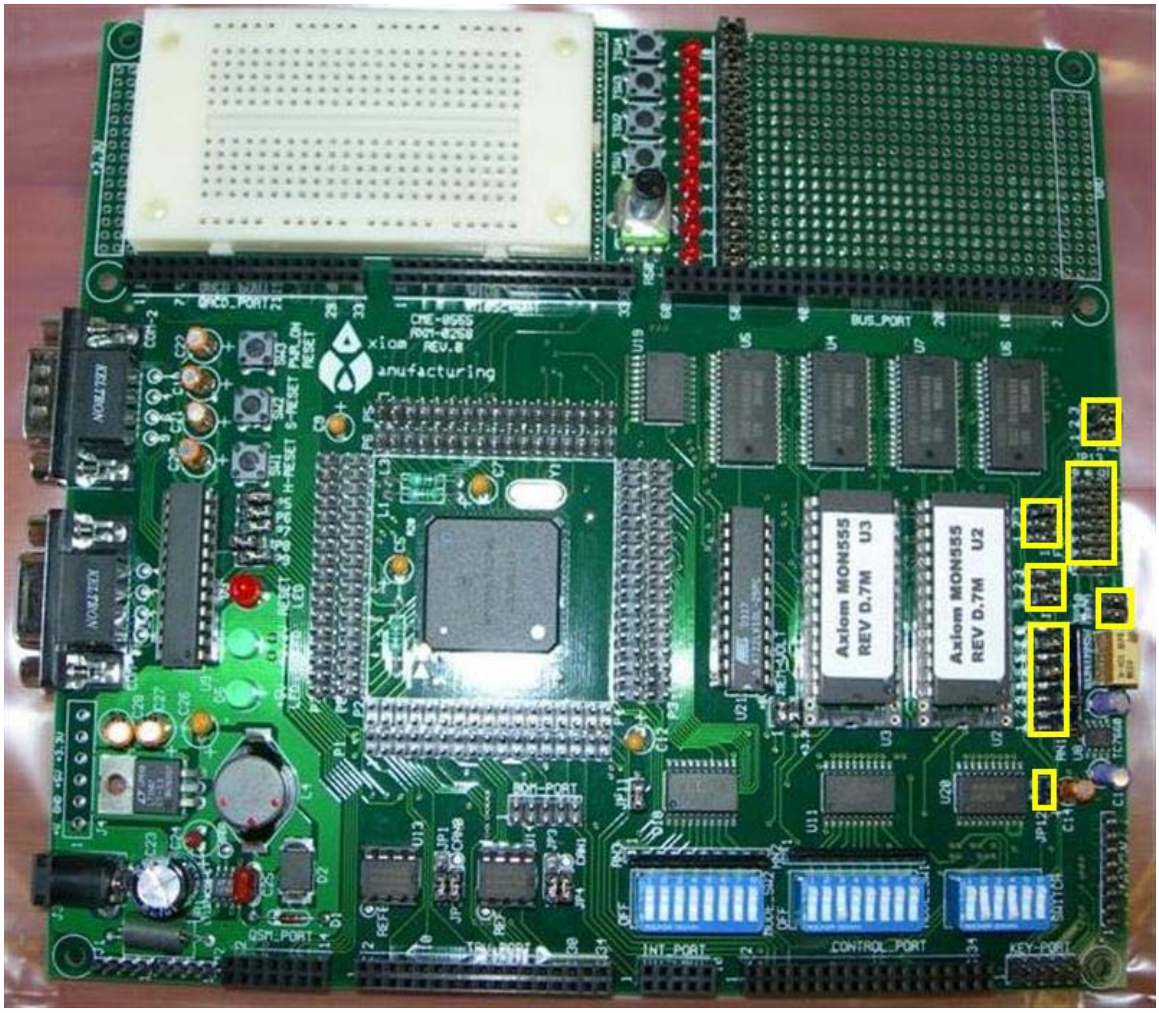
BUS_PORT
Axiom MON555
REV 0.7M U3
Axiom MON555
REV 0.7M U2
ROM-PORT
GSM_PORT
INT_PORT
CONTROL_PORT
KEY-PORT

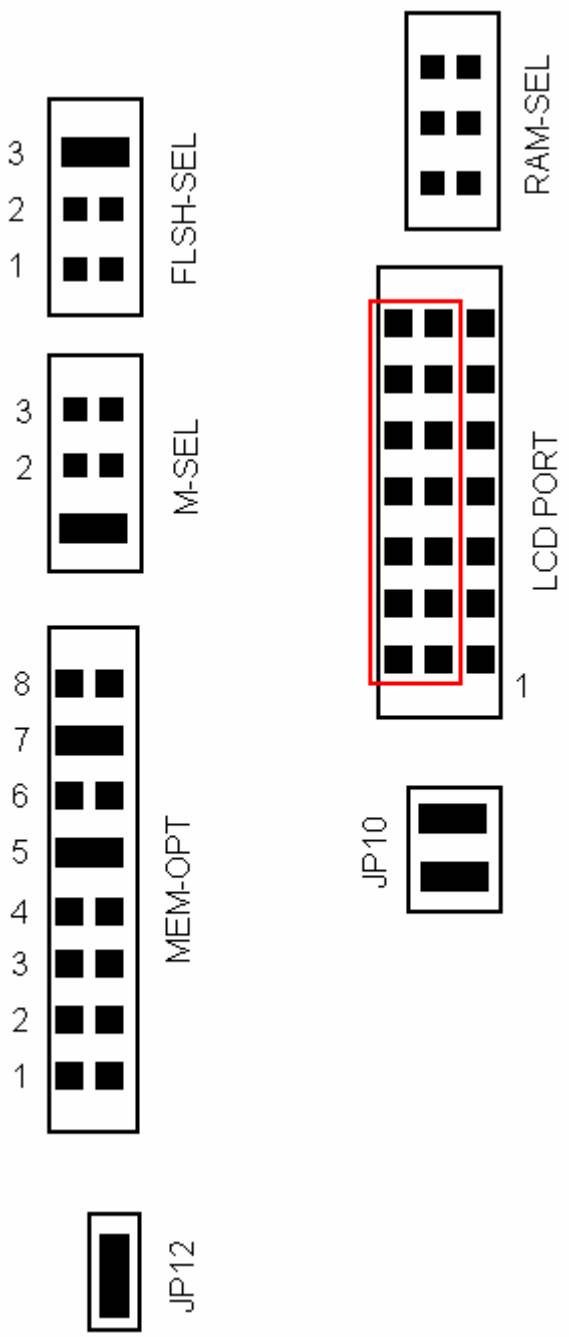
3
2
1
FLSH-SEL
3
2
M-SEL
8
7
6
5
4
3
2
1
MEM-OPT
JP12
RAM-SEL
LCD PORT
1
JP10

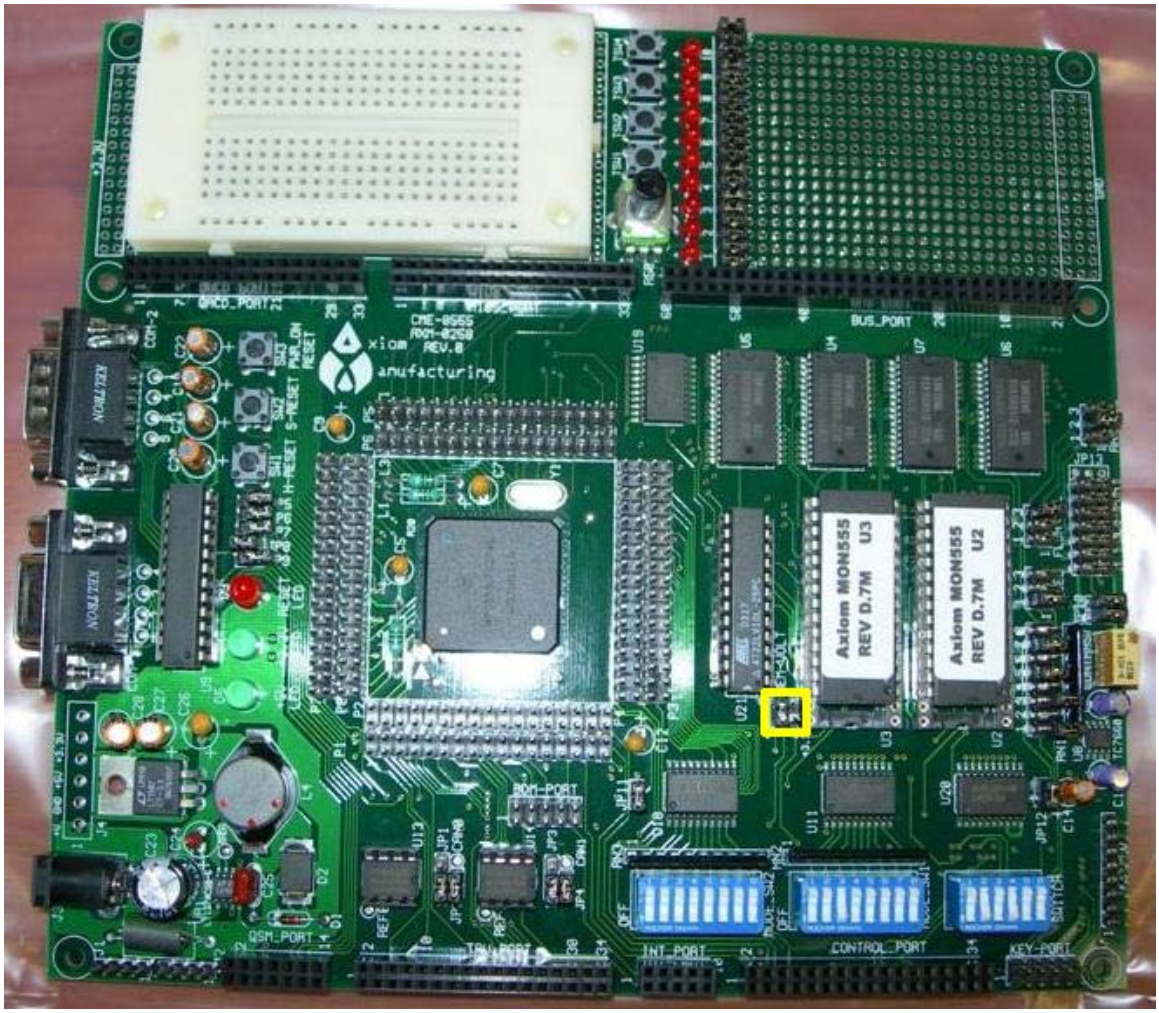
BUS_PORT
Axiom MON555
REV 0.7M U3
Axiom MON555
REV 0.7M U2
ROM-PORT
INT_PORT
CONTROL_PORT
KEY-PORT
+5V
MEM VOLT

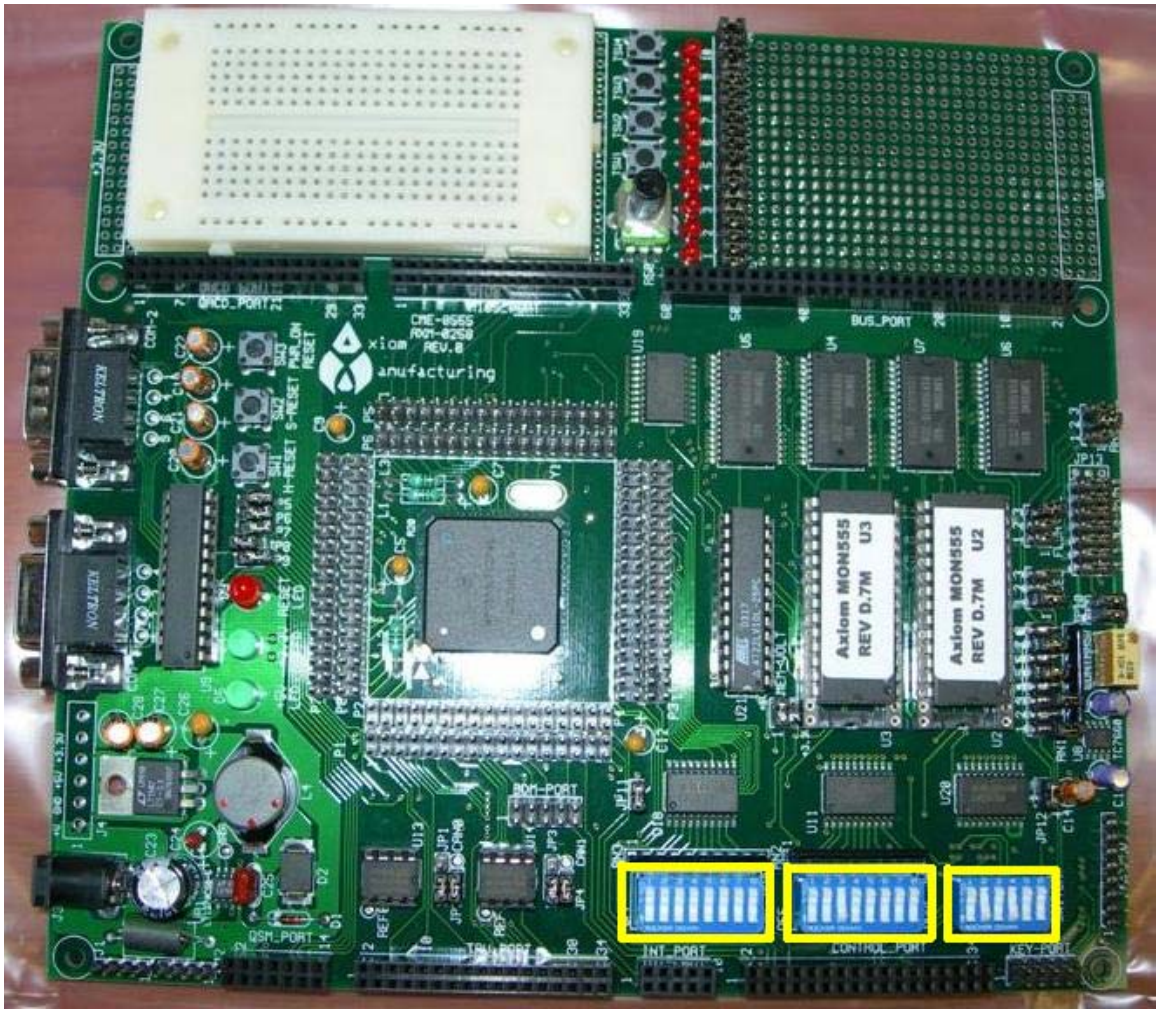

Left Group

- Switch 1 ON
- Switches 2-8 OFF

Center Group

- Switches 1-8 OFF

Right Group

- Switches 2, 4, 5, 6 ON
- Switches 1, 3 OFF

9) Finishing Touches

- Mount LCD to case cover using super glue
- Use ribbon cable to connect LCD to CME555. Make sure that the cable is connected properly. The pin marked "1" on the LCD should match up with the red wire on the ribbon cable. Connecting the LCD incorrectly will destroy the LCD.
- Cover case openings with metal plates (drill hole for GPS antenna)

10) Preliminary Tests

- Verify that all electrical connections are solid (including soldered connections)
- Verify 12V on CME555 and GPS power cords
- Make sure fans work
- Download code to CME555
- Plug into wall and verify correct operation (using LCD, GPS status lights)

Appendix V

PMU Frequency Data Plots

Courtesy of TVA

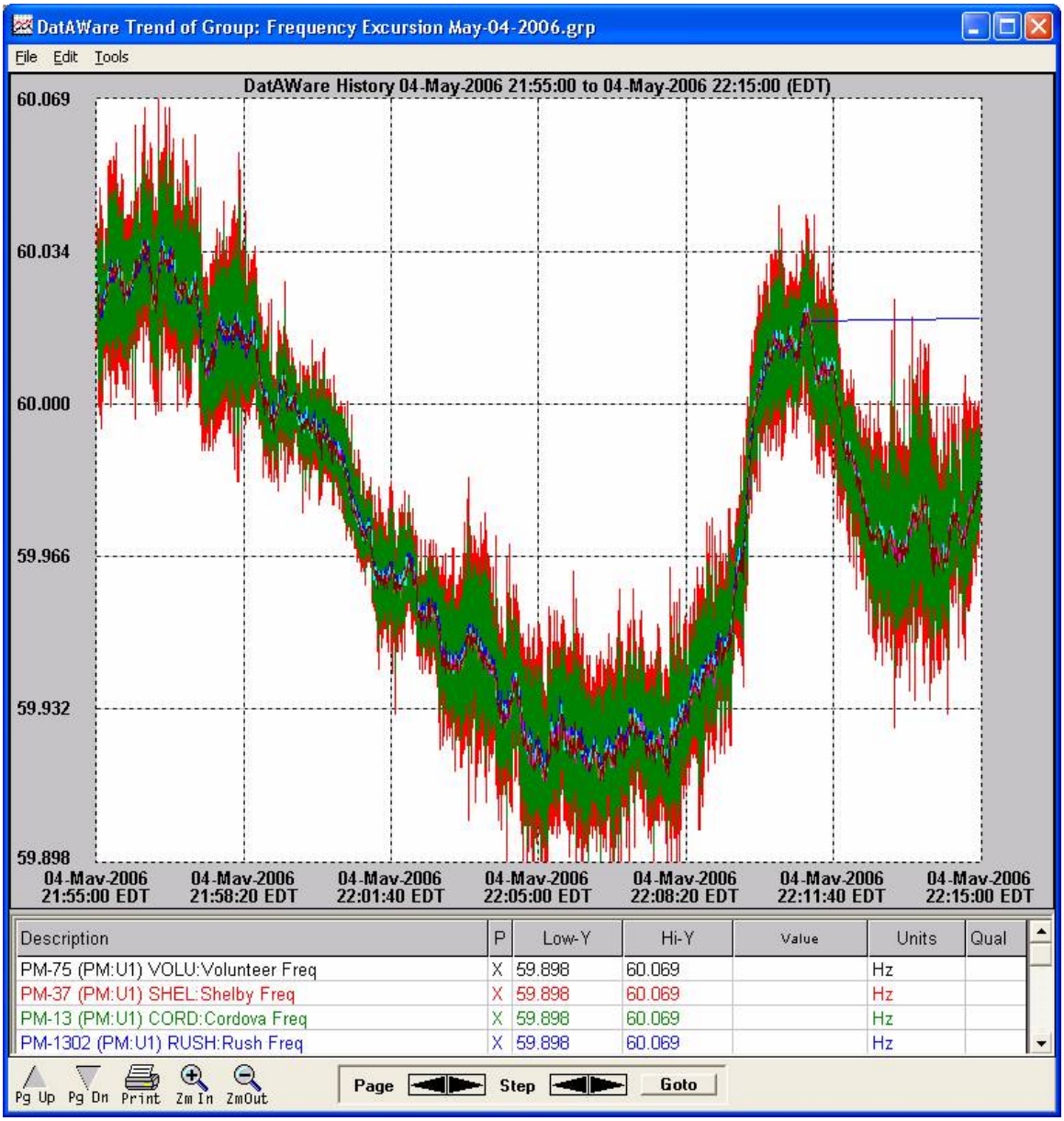

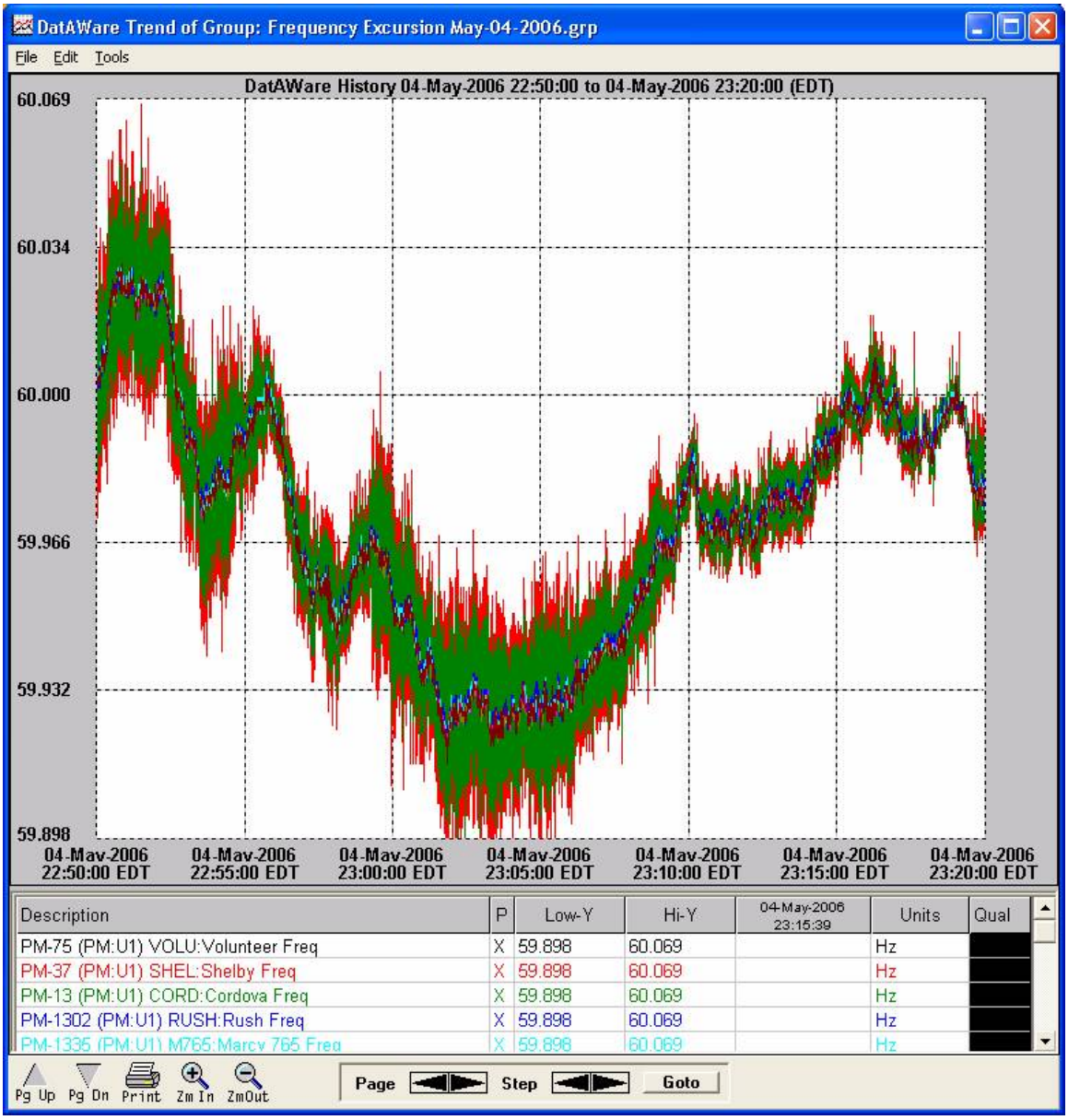
DatAWare Trend of Group: Frequency Excursion May-04-2006.grp
File Edit Tools
DatAWare History 04-May-2006 22:50:00 to 04-May-2006 23:20:00 (EDT)
60.069
60.034
60.000
59.966
59.932
59.898
04-May-2006 22:50:00 EDT
04-May-2006 22:55:00 EDT
04-May-2006 23:00:00 EDT
04-May-2006 23:05:00 EDT
04-May-2006 23:10:00 EDT
04-May-2006 23:15:00 EDT
04-May-2006 23:20:00 EDT
Description | P | Low-Y | Hi-Y | 04-May-2006 23:15:39 | Units | Qual
PM-75 (PM:U1) VOLU:Volunteer Freq | X | 59.898 | 60.069 | | Hz
PM-37 (PM:U1) SHEL:Shelby Freq | X | 59.898 | 60.069 | | Hz
PM-13 (PM:U1) CORD:Cordova Freq | X | 59.898 | 60.069 | | Hz
PM-1302 (PM:U1) RUSH:Rush Freq | X | 59.898 | 60.069 | | Hz
PM-1335 (PM:U1) M765:Marcy 765 Freq | X | 59.898 | 60.069 | | Hz
Pg Up
Pg Dn
Print
Zm In
ZmOut
Page
Step
Goto

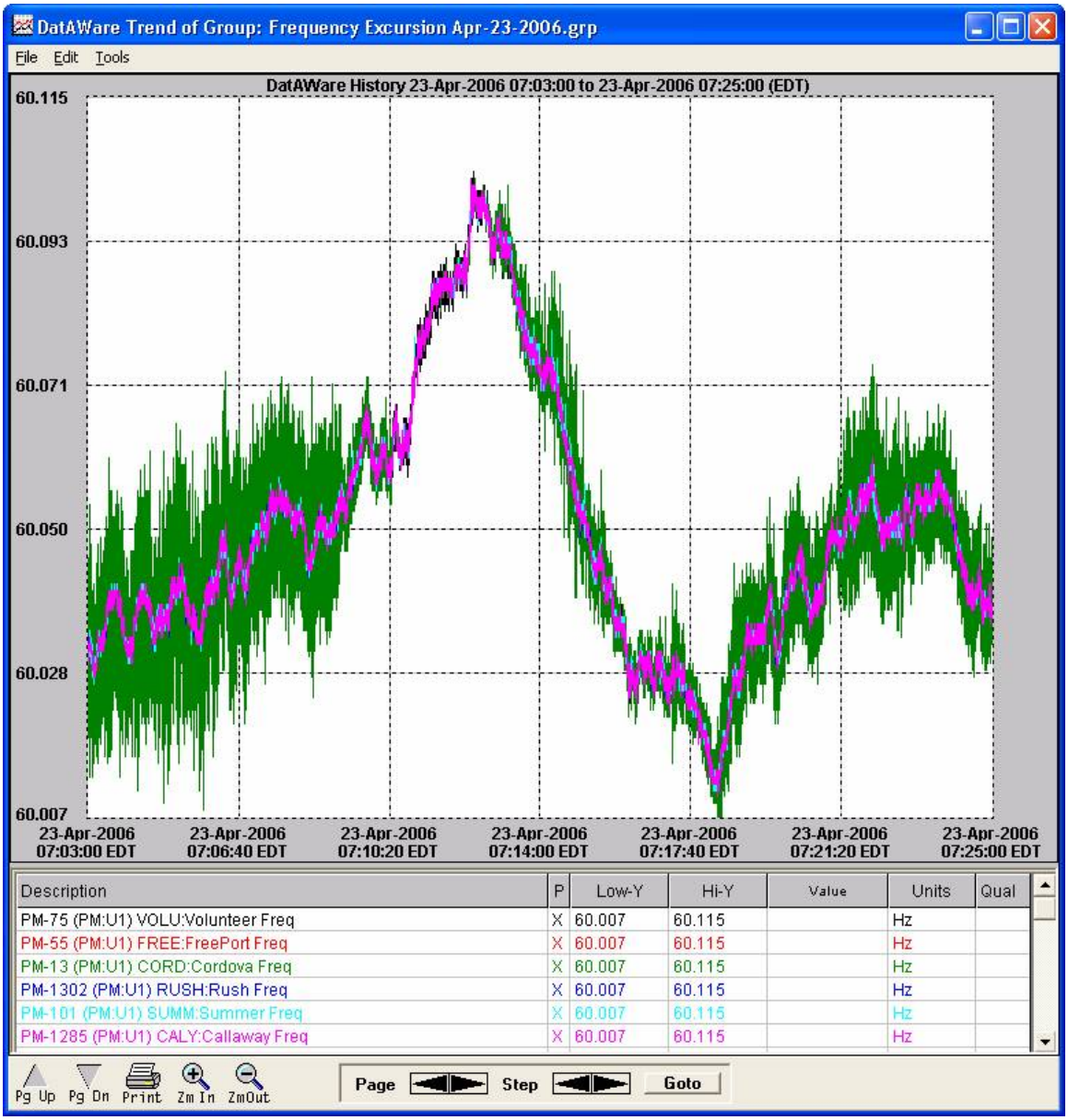
DatAWare Trend of Group: Frequency Excursion Apr-23-2006.grp
File Edit Tools
DatAWare History 23-Apr-2006 07:03:00 to 23-Apr-2006 07:25:00 (EDT)
60.115
60.093
60.071
60.050
60.028
60.007
23-Apr-2006 07:03:00 EDT
23-Apr-2006 07:06:40 EDT
23-Apr-2006 07:10:20 EDT
23-Apr-2006 07:14:00 EDT
23-Apr-2006 07:17:40 EDT
23-Apr-2006 07:21:20 EDT
23-Apr-2006 07:25:00 EDT
Description | P | Low-Y | Hi-Y | Value | Units | Qual
PM-75 (PM:U1) VOLU:Volunteer Freq | X | 60.007 | 60.115 | | Hz
PM-55 (PM:U1) FREE:FreePort Freq | X | 60.007 | 60.115 | | Hz
PM-13 (PM:U1) CORD:Cordova Freq | X | 60.007 | 60.115 | | Hz
PM-1302 (PM:U1) RUSH:Rush Freq | X | 60.007 | 60.115 | | Hz
PM-101 (PM:U1) SUMM:Summer Freq | X | 60.007 | 60.115 | | Hz
PM-1285 (PM:U1) CALY:Callaway Freq | X | 60.007 | 60.115 | | Hz
Pg Up
Pg Dn
Print
Zm In
ZmOut
Page
Step
Goto